Elucidation of the Molecular Genetic Basis of Inherited Hearing Impairment

Mirjam W.J. Luijendijk

Mirjam W.J. Luijendijk, 2006
Elucidation of the molecular genetic basis of inherited hearing impairment

Publication of this thesis was financially supported by the Department of Human Genetics, Radboud University Medical Centre.

Cover design: Tanno F. Weeda
Layout: Mirjam W.J. Luijendijk
Printed by: Print Partners Ipskamp, Enschede

ISBN-10: 90-9020488-1
ISBN-13: 978-90-9020488-8

Elucidation of the Molecular Genetic Basis of Inherited Hearing Impairment

een wetenschappelijke proeve op het gebied van de

Medische Wetenschappen

Proefschrift

ter verkrijging van de graad van doctor

aan de Radboud Universiteit Nijmegen

op gezag van de Rector Magnificus prof. dr. C.W.P.M. Blom,

volgens besluit van het College van Decanen

in het openbaar te verdedigen op dinsdag 4 april 2006

des namiddags om 1.30 precies

door

Mirjam Wilhelmina Johanna Luijendijk

geboren op 22 mei 1976

te Bleiswijk

Promotores:
Prof. dr. F.P.M. Cremers
Prof. dr. H.G. Brunner

Co-promotor:
Dr. H. Kremer

Manuscriptcommissie:
Prof. dr. B. Wieringa, voorzitter
Prof. dr. J. Schalkwijk
Prof. dr. G. Van Camp (Universiteit van Antwerpen, België)

Table of Contents

Abbreviations **7**

Chapter 1: General Introduction **9**
1.1 The ear 11
1.2 Inner ear development 16
1.3 Hearing loss 31
1.4 Strategies to identify hearing loss genes 45
1.5 Outline of this thesis 48
1.6 Electronic database information 50
1.7 References 50

Chapter 2: Cloning, characterization, and mRNA expression analysis of novel human fetal cochlear cDNAs **61**
2.1 Abstract 63
2.2 Introduction 63
2.3 Results 64
2.4 Discussion 73
2.5 Materials and methods 75
2.6 Acknowledgments 77
2.7 References 77

Chapter 3: A Novel Mutation Identified in the DFNA5 Gene in a Dutch Family: A Clinical and Genetic Evaluation **81**
3.1 Abstract 83
3.2 Introduction 83
3.3 Results 85
3.4 Discussion 94
3.5 Patients and methods 96
3.6 Acknowledgments 99
3.7 References 99

Chapter 4: Identification and molecular modelling of a mutation in the motor head domain of myosin VIIA in a family with autosomal dominant hearing impairment (DFNA11) **101**
4.1 Abstract 103
4.2 Introduction 103
4.3 Results 104
4.4 Discussion 108
4.5 Patients and methods 110
4.6 Acknowledgments 113
4.7 References 113

Chapter 5: Mutations in the VLGR1 gene implicate G-protein signalling in the pathogenesis of Usher syndrome type II **115**
5.1 Abstract 117
5.2 Introduction, results, discussion, materials, and methods 117
5.3 Acknowledgments 128
5.4 Electronic database information 129
5.5 References 129

Chapter 6: General discussion **133**
6.1 The value of a subtracted cochlea cDNA library 135
6.2 Molecular mechanisms underlying DFNA5 137
6.3 The DFNA11 phenotype is caused by mutations in different functional domains of myosin VIIa 138
6.6 References 140
6.4 VLGR1 involvement in Usher syndrome type II 140
6.5 General conclusion 140

Chapter 7: Summary **143**
7.1 Summary 145
7.2 Samenvatting 147

Chapter 8: Appendices **149**
8.1 Appendix 1: Table of gene expression in the developing inner ear 151
8.2 References 162
8.3 Appendix 2: full colour figures 166

Dankwoord **169**

List of publications **173**

Curriculum vitae **177**

Abbreviations

ADP	adenosine diphosphate
AHL	age-related hearing loss
ARMS	amplification refractory mutation system
ARTA	age-related typical audiogram
ATP	adenosine triphosphate
BOR	brancio-oto-renal
bp	base pairs
cDNA	complementary deoxyribonucleic acid
dB	decibel
DFN	X-linked nonsyndromic hearing loss
DFNA	autosomal dominant nonsyndromic hearing loss
DFNB	autosomal recessive nonsyndromic hearing loss
DHPLC	denaturing high-performance liquid chromatography
DNA	deoxyribonucleic acid
ENU	N-ethyl-N-nitrosurea
EST	expressed sequence tag
HC	hair cell
Hz	hertz
IHC	inner hair cell
kHz	kilo hertz
LNB	large N-terminal family B
mRNA	messenger ribonucleic acid
ncRNA	noncoding ribonucleic acid
NMD	nonsense mediated decay
OHC	outer hair cell
PCR	polymerase chain reaction
PTA	pure-tone average
RA	retinoic acid
RP	retinitis pigmentosa
RT-PCR	reverse transcriptase polymerase chain reaction
SAGE	serial analysis of gene expression
TH	thyroid hormone
TM	transmembrane
USH	Usher syndrome

Chapter 1

General Introduction

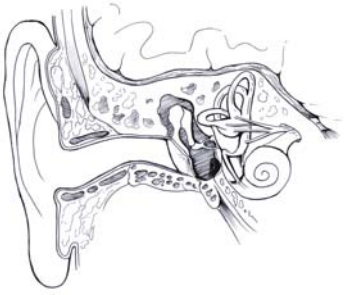

1.1 The ear

The ear converts the energy of pressure waves travelling through air into nerve impulses that the brain perceives as sound. The ear can be divided into three regions. The outer ear consists of the external pinna and the auditory canal, which collect sound waves and channel them to the tympanic membrane (eardrum) that marks the division between the outer and the middle ear (fig. 1). There, the vibrations are conducted through three small bones (the auditory ossicles), the malleus (hammer), incus (anvil), and stapes (stirrup), to the inner ear. These bones are attached to the wall of the middle ear chamber by ligaments and muscles. The “footplate” of the stapes is attached to the membrane covering the oval window. The middle ear also opens into the auditory (Eustachian) tube, which connects with the pharynx and equalizes pressure between the middle ear and the atmosphere. The inner ear consists of a labyrinth of channels, the membranous labyrinth, within the temporal bone, the hardest bone in the body, which is fused with the skull. These channels are lined by a membrane and contain fluid that moves in response to sound or movement of the head. The inner ear is divided into two separate sense organs; the organ of hearing, the cochlea, and that of equilibrium, or balance, consisting of the semicircular canals, the utricule, and the saccule (fig. 1).

1.1.1 The inner ear

The sensory organs in the inner ear differ in their function, and in the fine details of their cellular architecture, but they all conform to the same basic plan. They are relatively simple epithelia composed of two basic cell types, the sensory hair cells and their surrounding, non-sensory supporting cells (fig. 2). These epithelia lie upon a sheet of extracellular matrix, a basal lamina. The lateral membranes of the supporting cells surround the hair cells that do not contact the basal lamina, and they are isolated from one another by the supporting cells. At the apical surface of the epithelium, the supporting cell processes form tight and adherens junctions with each other and with the hair cells. The hair cells have a highly specialized bundle of modified microvilli called stereocilia, on their apical surface and it is this feature that enables them to detect mechanical stimuli and transduce them into electrical signals.

The vestibular system

The utricular and saccular hair cells are arranged in clusters, and all hairs project into the otoconial membrane, a gelatinous material containing many small calcium carbonate particles called otoliths (“ear stones”). Because this material is heavier than the endolymph within the utricle and saccule, gravity is always pulling downward on the hairs of the receptor cells, sending a constant train of action potentials along the sensory neurons of the vestibular branch of the auditory nerve. When the position of the head changes with respect to gravity (as when the head bends forward), the force on the hair cells changes, and increases or decreases its output of neurotransmitter. The brain interprets the resulting change in impulse production by the sensory neurons to determine the position of the head.

Within the three semicircular canals the cristae harbour the sensory cells. The sensory cells contain about 50 stereocilia and one kinocilium, a primary cilium that protrudes into a gelatinous mass, the cupula. During movement of the head the fluid in the semicircular canals lags behind creating a relative fluid flow causing the hair bundles to bend. This results in a change in the output of neurotransmitters. The sensory input from the utricule, saccule and semicircular canals is integrated with the input from the eyes, from the receptors in the muscles, joints and skin, to initiate reflexes that maintain the normal orientation.

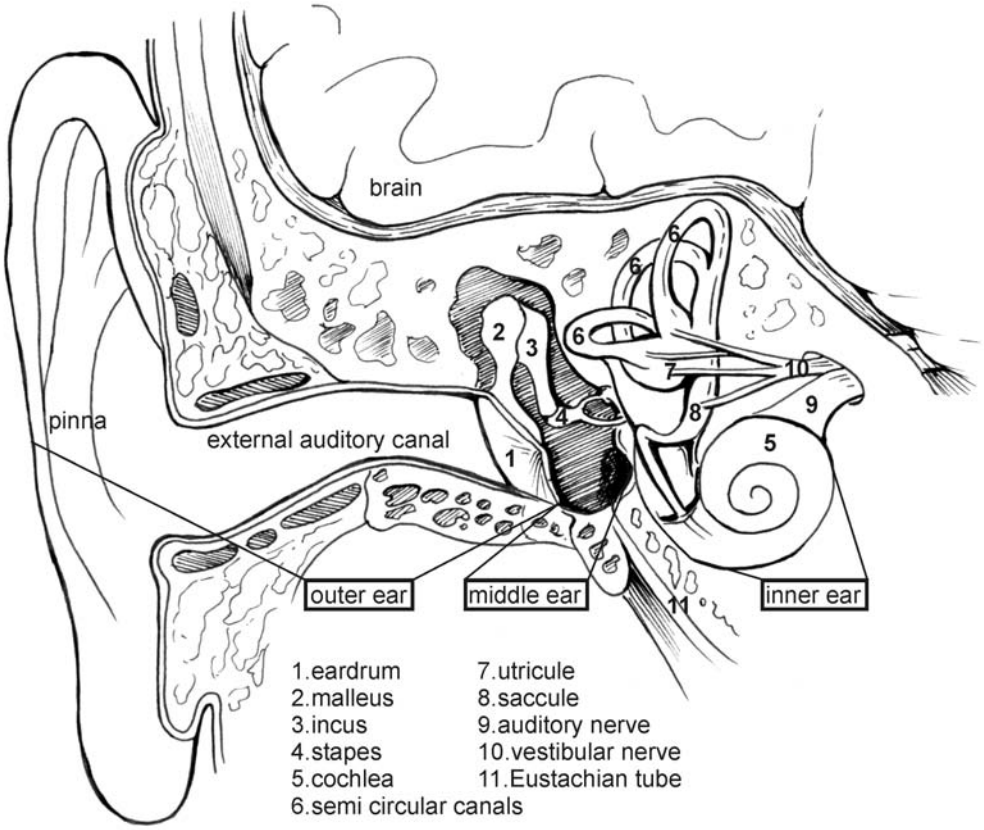

Figure 1. Schematic drawing of the outer, middle and inner ear

The cochlea

The modiolus, a long cartilaginous process, forms the central axis of the cochlea. Spiralling around the modiolus from the base to the apex, the interior of the cochlea is partitioned into three tubes or spaces (scalae) (fig. 2). The upper space (scala vestibuli) is separated from the middle (scala media) by Reissner´s membrane (fig. 2). The scala media is separated from the lower space (scala tympani) by parts of the osseous spiral lamina and the basilar membrane. The scala tympani and scala vestibuli are actually continuous at the apical tip of the cochlea, connected by a narrow opening called the

helicotrema. The stapes is attached to the membrane covering the oval window of the cochlea at a hole in the otic capsule over the scala vestibuli. At the base of the cochlea, the scala tympani ends at the membrane-covered round window (fig. 2).

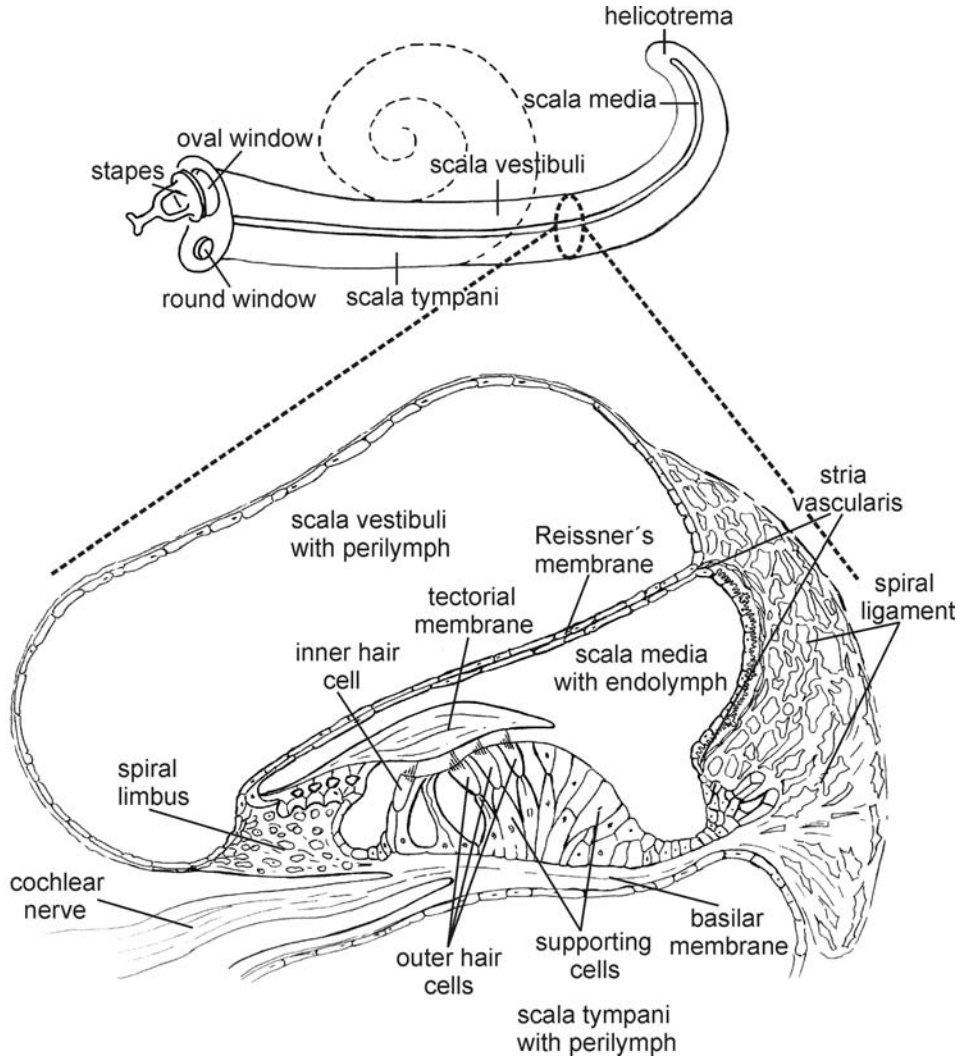

Figure 2. The cochlea and the organ of Corti

The organ of Corti, which harbours the sensory cells, spirals along the basilar membrane from the apex to the base of the cochlea (fig. 2). It is loosely structured to permit movement of the sensory epithelium in response to mechanical stimuli, yet it is rigid enough to transmit vibrations from the basilar membrane to the stereocilia. Along the spiral, the sensory epithelium contains approximately 20,000 sensory hair cells in humans (Dallos et al. 1996). In radial terms, sensory cells are either inner hair cells (IHCs), which form one row along the length of the sensory epithelium, or outer hair cells (OHCs), which form three rows. The hair cells each develop 10 to 50 stereocilia.

The stereocilia of the IHCs are arranged in a “U” shape, the stereocilia of the OHCs are arranged in a “W” shape. The tips of the stereocilia are embedded in the tectorial membrane, a fibrillar gelatinous substance that is carried by the spiral limbus whilst the bases of the hair cells make synaptic contact with dendritic endings of the cochlear nerve. Hair cells contact both afferent and efferent nerve fibres to permit transfer of information to the central nervous system and feedback to the periphery. The hair cells are separated from each other in a regular manner by various types of supporting cells that are specialised for mechanical and metabolic support. On the endolymphatic side of the spiral limbus, cells appear to have a secretory function and to be responsible for the formation of the tectorial membrane. Some cells separate the compartments containing the endolymph and perilymph, whereas others transport ions and may participate in the formation and maintenance of these two fluids.

The scala tympani and scala vestibuli are filled with perilymph, a high-sodium low-potassium solution resembling extracellular fluids and the scala media is filled with endolymph, a low-sodium high potassium solution resembling intracellular fluids. Tight junctions between the cells of Reissner´s membrane separate the endolymph from the perilymph of the scala vestibuli. Tight junctions at the apical surface of the sensory and supporting cells make up a second boundary. Thus, perilymph in the scala tympani can diffuse beyond the basilar membrane, and perilymph-like fluid bathes the cell bodies of the sensory and supporting cells of the organ of Corti. The stria vascularis, a complex vascularised epithelium located along the lateral wall of the cochlea is responsible for the production and maintenance of the endolymphatic potassium concentration. The stria vascularis is composed of three cell types; the marginal cells which line the endolymphatic compartment, the intermediate cells in a discontinuous layer enclosed entirely within the body of the epithelium, and the basal cells that separate the stria vascularis from the underlying spiral ligament. Tight junctions between adjacent marginal cells keep the endolymph from entering the stria vascularis. Within the lateral wall, adjacent cells coupled by tight junctions also form an intrastrial compartment. Thus, it appears that perilymph diffuses freely through the spiral ligament, but the stria vascularis is contained in a compartment that is formed and maintained by tight junctions among marginal cells on the endolymphatic side and among basal cells on the perilymphatic side.

1.1.2 The process of hearing

Vibrating objects, such as the reverberating strings of a guitar or the vocal cords of a speaking person, create percussion waves in the surrounding air. These waves cause the tympanic membrane to vibrate with the same frequency as the sound. The three bones of the middle ear transmit the mechanical movements to the cochlea. The stapes vibrating against the oval window creates a travelling pressure wave in the fluid of the cochlea that passes into the scala vestibuli. Reissner´s membrane is forced down and this increases pressure in the scala media until it is released by a downward movement of the basilar membrane. The resulting increase in pressure in the scala tympani is finally released by a bowing outward of the membrane covering the round window. The tectorial membrane, unlike Reissner´s membrane and the basilar membrane, floats

freely in the endolymph. In response to incoming sound the basilar membrane vibrates, but the tectorial membrane remains stationary. Therefore pressure changes will not cause it to move up and down in unison with the two other membranes. As the basilar membrane vibrates in response to the pressure waves, it alternatively presses the hair cells into and draws them away from the tectorial membrane. The stereocilia of the hair cells are thus subject to mechanical distortion. Movement of the hair cell stereocilia in the direction of the taller stereocilia opens transduction ion channels, allowing entry of potassium and calcium ions from the endolymph and generating a transduction current. This alters the hair cell resting electrical potential and leads to depolarisation of the hair cell. The depolarisation activates voltage sensitive calcium channels along the lateral wall and base of IHC as well as calcium-activated potassium channels. The end result is release of neurotransmitter at the hair cell base onto the auditory nerve endings. The signal is then transmitted to the brain where it is further processed. The apical influx of potassium ions in the stereocilia is coupled with a potassium efflux across the basolateral membrane. Potassium ions efflux to the supporting cells of the organ of Corti and through a mechanism of gap junctions and ion pumps, potassium is recycled back to the endolymph. This efflux is necessary to prevent cytotoxic accumulation of potassium in the hair cells and to maintain the correct potassium concentration in the endolymph. The efflux also serves to repolarise the cell by restoring the electronegativity of the cytoplasm. Movement of stereocilia in the opposite direction closes the stereocilia-related channels and stops the release of neurotransmitter. In the “resting” position of stereocilia (upright) the transduction channels are partially open, leading to a small release of transmitter. This in turn generates spontaneous activity in the auditory nerve and the ascending auditory pathways, even in the absence of sound. The frequency of movement of stereocilia matches the frequency of the sound stimulus (Raphael and Altschuler 2003). Hair cells are thus mechanotransducers converting a mechanical stimulus into an electrical signal.

Two important aspects of sound are volume and pitch. Volume (loudness) is determined by the amplitude, or height, of the sound wave. The greater the amplitude of a sound wave, the more vigorous the vibrations of fluid in the cochlea, the greater the bending of the stereocilia, and the more action potentials generated in the sensory neurons. Pitch is a function of the frequency of sound waves and is usually expressed in hertz (Hz). Short, high-frequency waves produce high-pitched sound, while long, low-frequency waves generate low-pitched sound. Healthy young humans can hear sounds in the range of 40 to 20,000 Hz, and a trained ear can discriminate between frequencies of 1000 Hz and 1002 Hz. Pitch can be distinguished by the cochlea because the basilar membrane is not uniform along its length. The proximal end near the oval window is relatively narrow and stiff, while the distal end near the tip is wider and more flexible. Each region of the basilar membrane is most affected by a particular frequency of vibrations, and the region vibrating most vigorously at any instant sends the most action potentials along the auditory nerve.

1.2 Inner ear development

The inner ear is structurally complex. A molecular description of its architecture, development and homeostasis is now emerging from the use of contemporary methods of cell and molecular biology. In addition the application of clinical and molecular genetics is providing new insights into the pathogenesis of a range of inner ear disorders.

1.2.1 Embryology of the human inner ear

The vertebrate inner ear develops from the embryonic ectoderm. The first sign of the developing ear in humans can be found in embryos of approximately 22 days as a thickening of the surface ectoderm on each side of the rhombencephalon close to the hindbrain (O´Rahilly 1963) (fig. 3) (table 1). These thickenings, the otic placodes, invaginate rapidly and form the otic cup and otic vesicles (otocysts), an ellipsoid shaped structure lined by pseudo-stratified epithelium (fig. 3). Later in development, each vesicle divides into a ventral component, which gives rise to the saccule and the cochlea, and a dorsal component, which forms the utricule and the semicircular canals (fig. 4) (Sadler 2004).

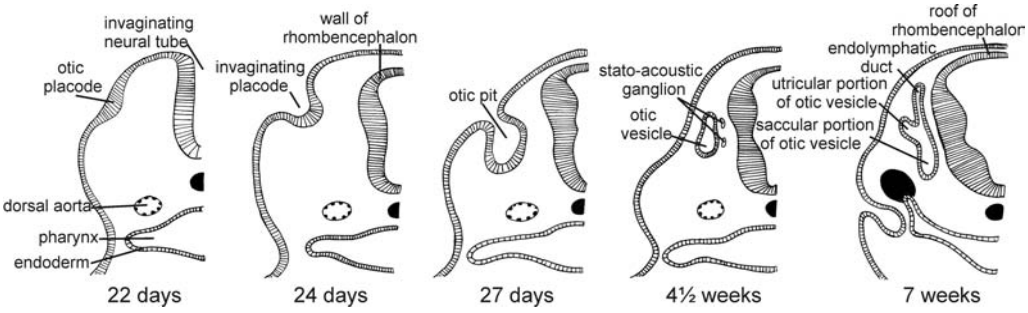

Figure 3. Schematic transverse sections through the region of the rhombencephalon of a human embryo

In the sixth week of development, the saccule forms a tubular-shaped outpocketing at its lower pole (fig. 4). This outgrowth, the cochlear duct, penetrates the surrounding mesenchyme in a spiral fashion until, at the end of the eighth week, it has completed 2½ turns (fig. 4) (table 1). The mesenchyme surrounding the cochlear duct soon differentiates into cartilage. In the tenth week, this cartilaginous shell undergoes vacuolisation and the scala vestibuli and scala tympani, are formed. The cochlear duct (scala media) is then separated from the scala vestibuli by Reissner´s membrane, and from the scala tympani by the basilar membrane (Sadler 2004). The lateral wall of the scala media remains attached to the surrounding cartilage by the spiral ligament, whereas its median angle is connected to, and partly supported by the modiolus. The epithelial cells of the cochlear duct are initially all alike. With further development, however, they form two ridges: the inner ridge (the future spiral limbus) and the outer ridge. The latter forms one row of IHCs and three rows of OHCs (Sadler 2004).

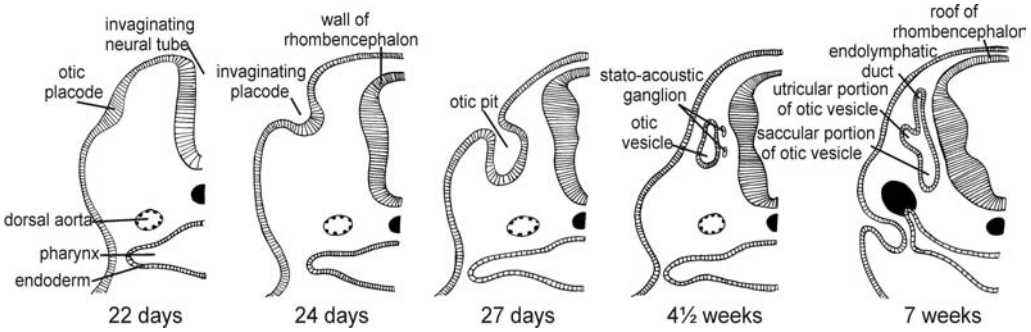

Figure 4. Schematic representation of the development of the otocyst showing a dorsal utricular portion with the endolymphatic sac and duct, and a ventral saccular portion and the cochear duct at 6, 7, and 8 weeks, respectively.

During the sixth week of development, the semicircular canals appear as flattened outpocketings of the utricular part of the otic vesicle (fig. 5) (Sadler 2004). The central portions of the walls of these outpocketings eventually disappear, thus giving rise to the three semicircular canals positioned in the three dimensions of space (fig. 5) containing the sensory cells that have evolved during the eighth week and detect angular accelerations of the head. At eight weeks the sensory areas have also developed in the walls of the utricule and the saccule (table 1) that respond to changes in head position with respect to gravity and movement in one direction.

The neurons that innervate the hair cells in each organ of the ear are derived from the otocyst, by a process of delamination, prior to the formation of the sensory organs (Rubel and Fritzsch 2002). Initially they form a single structure, the statoacoustic ganglion, which splits into the cochlear and vestibular ganglia as development proceeds (Politzer 1956).

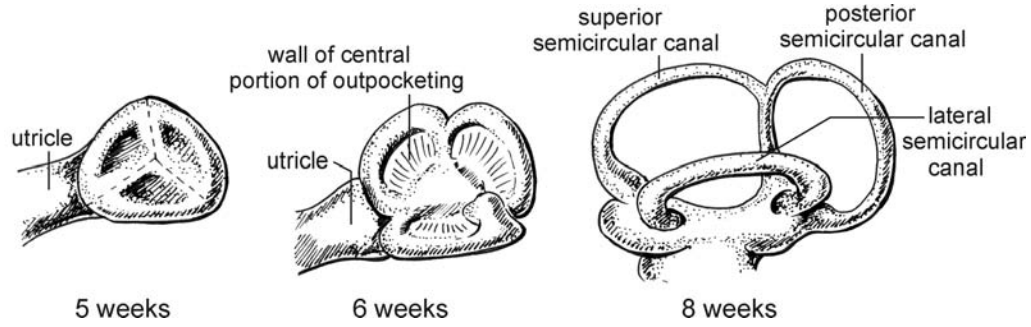

Figure 5. Schematic representation of the development of the semicircular canals in humans

Table 1. Timetable of inner ear development

Mouse	*Human*	*Description*
12-13 somites (9 days)	23 days	Otic placode evident
	24 days	Otic pit present
17 somites		Placode epithelium just starting to thicken, all ectoderm around placode thins
17-19 somites	26 days	Otic placode transforms into otic vesicle; ventral wall of otocyst contributes to statoacoustic ganglion
22-24 somites		Otocyst detached from the surface
27 somites (10 days)	4 weeks	Otocyst is a closed sac; medial wall is pseudostratified 2-3 layers of nuclei
12 days	5 weeks	Otocyst elongates and endolymphatic duct buds off the medial wall; otic capsule represented by condensed mesenchyme
13 days	7 weeks	½ Coil of cochlear duct; otic capsule is cartilaginous and in direct contact with epithelial portions of the labyrinth; HCs differentiated in the utricle and saccule
14 days	7 weeks	Cochlea at 1¼ turns; first definitive HCs
15 days	7 weeks	Tectorial membrane has started to form (mouse)
16 days	8 weeks	Cochlea has 1½ turns; perilymphatic spaces develop; many HCs differentiate in utricle, saccule, and semicircular canals
18 days	9 weeks	1¾ Turns (full number in mouse); 2½ turns (full number in human) but not full length in either; cochlear HCs identifiable in mouse; development of cuticular plate in mouse
	9-10 weeks	Tectorial membrane is starting to form; vestibular HCs
	11-12 weeks	IHC visible throughout the cochlea; OHC indistinguishable; stereocilia present on OHC and IHC; some cuticular plates identifiable; synaptic specializations present on HC; perilymphatic spaces begin to develop in human
6 DAB	4 months (16 weeks)	Tunnel of Corti appears in the basal coil (mouse); membranous labyrinth has adult dimensions
10 DAB	4.5 months	Tunnel of Corti formation complete (mouse)
16 DAB	5 months (20-22 weeks)	Adult stereocilia configuration on both OHC and IHC, but some kinocilia remain; tunnel of Corti appears in basal coil of human cochlea; periotic spaces fully formed; ossicles have adult configuration
20 DAB	8 months	Cochlear structure essentially similar to adult, including formation of Nuel spaces

Adapted from: Sulik K.K. 1995, DAB: days after birth

1.2.2 Gene expression during early inner ear development

The embryonic development of the inner ear is a very complex process and much research has been done to uncover all genes involved. It is impossible to include all these results here, however, the data presented below give a summary of what is known about the genes and signalling pathways involved in the most important developmental steps.

Despite its complexity and multiple functions, the origin of the inner ear epithelium is simple. All cellular components of the otic epithelium, including the neurons of the cochlear and vestibular ganglia, derive from the embryonic otic vesicle. Therefore, the unravelling of the development of the inner ear is largely dependent on studying the development of the otic vesicle. The lateral edges of the hindbrain have long been considered a source of otic vesicle-inducing activity (Groves and Bronner-Fraser 2000).

However, studies by Jacobson (1966) indicate that signals from the hindbrain and mesoderm are both needed for optimal induction and normal development of the inner ear. In the otic vesicle cell-to-cell communication and cell exchange are restricted so that the otic vesicle is functionally isolated from the surrounding ectoderm (Vazquez et al. 1996). The first indication of regional and cell fate specification of the development of the inner ear coincides with the earliest stage of regional gene expression and to the first events of cell differentiation, respectively. Both events begin around the otic placode stage and extend through the whole embryonic development until the early post-natal stage. Genes expressed during early otic development encode transcription factors, diffusible molecules, receptors, and cell adhesion proteins.

In the otic placode the earliest-expressed genes include several homeobox genes including those of the *distal-less* family, genes related to *Drosophila muscle segment homeobox* genes and NK-related homeobox genes, as well as LIM-homeodomain and paired-box transcription. Secreted factors like the BMP-family of TGFß-like polypeptides, and receptor molecules are also expressed at the placodal stage (reviewed by Torres and Giraldez 1998, Noramly and Grainger 2002). Most of the genes expressed at the otic placode stage maintain their expression in the otic vesicle, but typically restrict their expression domain, suggesting a role in the regional patterning of the otic vesicle. In the absence of available references to compartments or functional domains within the otic vesicle, genes expressed at this stage can be grouped as dorso-lateral on one side, and medial-ventral on the other (reviewed by Torres and Giraldez 1998, Represa et al. 2000) (Appendix 1).

As development progresses, groups of different genes are expressed in parallel to the generation of sensory and non-sensory patches in the auditory and vestibular sensory organs. Several classes of genes are expressed: (i) genes encoding transcription factors, (ii) genes encoding secreted factors, and (iii) genes encoding receptor tyrosine kinases. Some of these genes are specific for putative sensory epithelium while other genes are expressed in non-sensory areas.

Because a highly conserved *Pax-Six-Eya-Dach* synergistic regulatory genetic network is involved in the development of a number of organs, it was suggested that a *Pax-Six-Eya-Dach* synergistic regulatory network may be involved in the formation of the ear and may be among the first genes activated in response to inducing signals. This is indeed the case and the interactions among the genes in this complex network have been worked out in most detail for *Drosophila* and vertebrate eye development (for a review see Wawersik and Maas 2000). Specificity is conferred by differences in which family members are expressed (Appendix 1).

1.2.3 Differentiation of hair cells and supporting cells

Hair and supporting cells in the mammalian ear are born in a small developmental time window after the sensory patches have been specified (Sans and Chat 1982). In the cochlea of the mouse, the cyclin dependent kinase inhibitor, $p27^{Kip1}$ is expressed by cells of the organ of Corti as soon as they withdraw from the cell cycle (Chen and Segil 1999). The pattern of $p27^{Kip1}$ expression precisely delineates the region of the cochlear

duct within which the hair and supporting cells will differentiate. The expression of $p27^{Kip1}$ is down regulated in hair cells as they begin overt differentiation, but in supporting cells expression persists into adulthood (Chen and Segil 1999). In *$p27^{Kip1-/-}$* mice, cell proliferation within the organ of Corti continues and an excess of hair and supporting cells is found (Chen and Segil 1999, Lowenheim et al. 1999). These data indicate that $p27^{Kip1}$ negatively regulates cell proliferation in the organ of Corti.

Hair and supporting cells are born simultaneously and there is evidence that hair- and supporting-cell lineages arise from a common progenitor and do not segregate until very late in development. It has been shown that the potential to become either a hair or supporting cell is retained by a progenitor cell until it has passed through its final mitotic division. In mature sensory organs, hair cells are isolated from one another by the processes of supporting cells. This arrangement implicates an inhibitory mechanism of cell fate determination for these two cell types, a process named lateral inhibition. A few scattered cells commit to the primary fate, the hair cell fate. A committed hair cell then prevents every cell in contact with it from becoming a hair cell; the inhibited neighbours commit to the secondary fate, the supporting cell fate. Other cells contacting these committed supporting cells can, in turn, assume a hair cell fate. Thus, a pattern is propagated in which hair cells alternate with supporting cells in all directions around the seeding site of a committed hair cell.

Lateral inhibition is usually mediated by Notch signalling, and a number of studies have now shown that the Notch signalling pathway plays a key role in mediating the differentiation of hair and supporting cells in the inner ear (Adam et al. 1998, Haddon et al. 1998, Lanford et al. 1999, Eddison et al. 2000, Zine et al. 2000).

Notch1 and its ligands *Delta1*, *Jagged1* and *Jagged2* are expressed in the developing inner ear (Adam et al. 1998, Morrison et al. 1999). All progenitor cells initially express low levels of *Delta1* and *Notch1* and thereby mutually inhibit each other's differentiation. Emerging hair cells strongly upregulate *Delta1* expression, which elevates Notch activity in neighbouring cells. *$Notch1^{-/-}$* mice are early embryonic lethals, but in heterozygotes with presumably reduced levels of Notch1, a significant increase is observed in the numbers of regions along the cochlea where there are four instead of three rows of OHCs (Zhang et al. 2000). In *$Jagged2^{-/-}$* mice, there is an increase in the linear density of IHCs and OHCs in the cochlea, with a nearly complete duplication of the normal, single row of IHCs, and many stretches where there are four instead of three rows of OHCs (Lanford et al. 1999). Disruption of another gene, *Lunatic fringe* (*Lfng*), suppresses the *$Jagged2^{-/-}$* phenotype (Zhang et al. 2000). *Lfng* in mouse is expressed throughout the region of the ear that gives rise to sensory epithelia. The expression of *Delta1* and *Jagged2* in hair cells, and the overproduction of hair cells seen in the corresponding mutants, indicates that the hair cells use Notch signalling to laterally inhibit their neighbouring cells. *Jagged1* is expressed throughout the pro-sensory patch initially but becomes progressively restricted to the supporting cells as they differentiate (Morrison et al. 1999, Cole et al. 2000). The expression of *Jagged1* by supporting cells may not appear to be consistent with the idea that hair cells inhibit their neighbours. However there is evidence from the chick inner ear that the expression of *Jagged1* in supporting cells is positively regulated by Notch signalling via lateral induction (fig.

6) (Eddison et al. 2000). This would ensure that they do not differentiate as hair cells. Hair cells are unresponsive to Jaggged1 because *Notch* expression is down-regulated during initial stages of hair cell differentiation (Lanford et al. 1999), and hair cells also express Numb, an intracellular antagonist of Notch activity (fig. 6) (Eddison et al. 2000). Homozygous loss of *Jagged1* kills mouse embryos prior to the stage when hair cells differentiate, but *Jagged1* heterozygotes show a modest increase in production of IHCs in the cochlea (Kiernan et al. 2001). In humans mutations in *JAG1* are responsible for Alagille syndrome (Li et al. 1997, Oda et al. 1997). The overproduction of hair cells in the late embryonic rat cochlear cultures caused by *Jagged1* antisense oligonucleotides (Zine et al. 2000) is consistent with this, as reduced Notch activation should lead to an excess of hair cells. Jagged1 appears to be signalling in the opposite direction as Jagged2. It has been proposed from gene reporter studies that Notch3 acts by interfering with Notch1 signalling, possibly by blocking Notch1-mediated *Hes1* transcription in supporting cells (fig. 6) (Beatus et al. 1999). It is possible that Notch3 expression in hair cells may act as an antagonist of Notch1 expression in supporting cells, mediating an instructive signal for hair cells differentiation rather than inhibitory signal for supporting cell differentiation. Rivolta et al. (2002) propose that Jagged1 could have an inductive effect on hair cell differentiation mediated by Notch3.

Atoh1, a mouse homologue of the *Drosophila* proneural gene *atonal*, encodes a basic helix-loop-helix (bHLH) transcription factor. It is expressed in the primordium of the organ of Corti after the cells in this region have withdrawn from the cell cycle and have begun to express $p27^{Kip1}$, but before hair cells have started to express myosin VIIA, a marker for overt differentiation (Chen et al. 2002). Initially, Atoh1 is expressed by a thin band of epithelial cells that span the entire thickness of the epithelium and expression becomes restricted to the hair cells as they differentiate (Lanford et al. 2000, Chen et al. 2002). Hair cells are absent from the inner ears of *Atoh1*$^{-/-}$ mice by birth; instead a uniform sheet of supporting cells is formed (Bermingham et al. 1999). Overexpression of *Atoh1* results in the formation of supernumerary hair cells (Zheng and Gao 2000). Early markers of overt hair cell differentiation, myosin VI and calretinin, are never expressed during inner ear development in *Atoh1*$^{-/-}$ mice (Bermingham et al. 1999). These results indicate that Atoh1 is both necessary and sufficient for hair cell differentiation. Further research has shown that the hair cells may be produced, but fail to express any known markers of differentiation, and then die (Chen et al. 2002). *Delta1* and *Jagged2* are expressed by hair cells in the mouse cochlea approximately one day after the onset of *Atoh1* expression (Morison et al. 1999, Lanford et al. 2000).

The transcription factors *Hes1* and *Hes5*, mammalian homologues of the *Drosophila hairy* and *enhancer of Split* genes, are expressed in patterns that are both complementary and overlapping in the developing cochlea and act downstream of Notch (fig. 6) (Zheng et al. 2000a, Zine et al. 2001). Expression of *Hes5* is first observed in the supporting cells of the organ of Corti after the expression of A*toh1* has begun in differentiating hair cells, and probably slightly after the onset of expression of *Delta1* and *Jagged2* (Lanford et al. 2000). The expression of *Hes5* may be positively regulated by Notch activation as it is much reduced in the supporting cells of *Jagged2*$^{-/-}$ mice (Lanford et al. 2000). Additional IHCs are observed in *Hes1*$^{-/-}$ mutant mice, and

additional OHCs are observed in *Hes5*$^{-/-}$ mutants (Zheng et al. 2000a, Zine et al. 2001) these phenotypes indicate that these genes are regulators of hair cell differentiation. Hes1 overexpression blocks the ability of Atoh1 to induce hair cell formation (Zheng et al. 2000a). This suggests that these genes act antagonistically such that Atoh1 promotes hair cell differentiation and Hes1 prevents it.

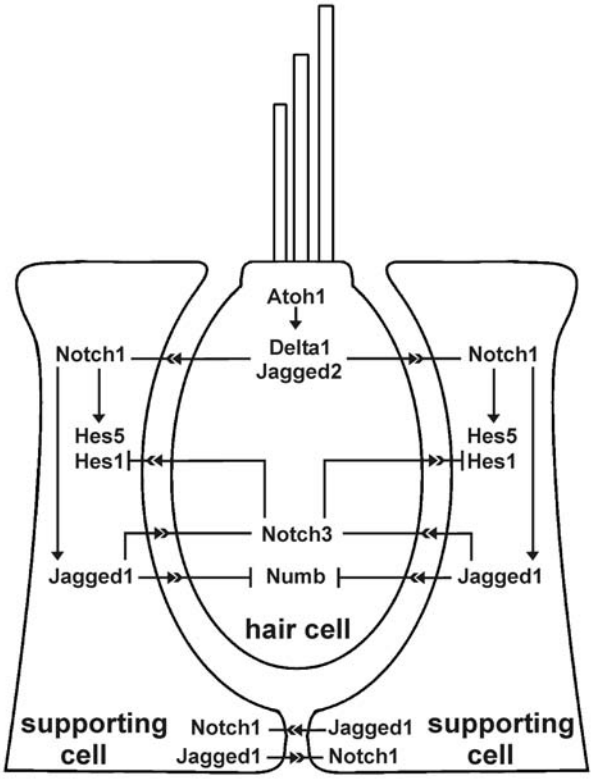

Figure 6. Diagram illustrating a model for lateral inhibition occurring between components of the Notch signalling pathway that lead to the differentiation of hair and supporting cells

Pou4f3 is a POU domain transcription factor that is expressed in all sensory areas of the otocyst and specifically by hair cells within the adult mouse inner ear (Erkman et al. 1996, Xiang et al. 1997). Pou4f3 is expressed by hair cells at approximately the same time as Jagged2 and Delta1, one day before the hair cell markers myosin VI and myosin VIIA (Xiang et al. 1997). *Pou4f3*$^{-/-}$ mice display a *shaker*/*waltzer* behavioural phenotype of circling and hyperactivity and are also completely deaf (Erkman et al. 1996). Hair cells are generated and express myosin VI, myosin VIIA and calretinin, but they never develop sensory hair bundles and are lost from the inner ear by P14 due to apoptosis. This shows that *Pou4f3* expression constitutes a requirement for the survival of the newly generated hair cells (Erkman et al. 1996, Xiang et al. 1997). Maturation of the supporting cells also appears to be impaired in the inner ears of these *Pou4f3*$^{-/-}$ mice, suggesting that active hair cell-supporting cell interactions are required for the survival of the supporting cell lineage. The ectopic overexpression of *Pou4f3* does not

lead to the production of supernumerary hair cells (Zheng and Gao 2000), indicating that Pou4f3 is only required for the later aspects of hair cell differentiation. In humans mutations in *POU4F3* are associated with nonsyndromic hearing loss, DFNA15 (Vahava et al. 1998).

Gfi1 encodes a zinc finger transcription factor that controls slightly later stages of hair cell differentiation than *Brn3C* (Wallis et al. 2003). *Gfi1* is related to *Drosophila senseless*, which is induced by proneural basic helix-loop-helix proteins and is required for development of the peripheral nervous system. In mice, *Gfi1* is expressed in the early otic vesicle and is later restricted to differentiating hair cells. Hair cells are produced in *Gfi1* mutants but show aberrant patterning and morphology. While mutant hair cells express most hair cell markers, including *Brn3c*, they also inappropriately express some neural markers. Hair cells in the cochlea die during early postnatal development, followed by death of cochlear neurons. Vestibular hair cells survive but are highly disorganised, and mutant mice exhibit ataxia and circling due to loss of vestibular function.

1.2.4 Roles of thyroid hormone and retinoic acid in hair cell differentiation

Nuclear receptors for thyroid hormone (TH) and retinoic acid (RA) are expressed in the developing sensory epithelia of the inner ear and their respective ligands are known to play a role in hair cell development. RA is produced by embryonic but not adult, organ of Corti. Treating cochlear cultures from early embryonic stages of development with RA leads to the production of extra rows of IHCs and OHCs (Kelley et al. 1993). The RARα/RXRα heterodimer is the most likely hair cell receptor for RA. The presence of RA has been documented in the developing inner ear (Kelley et al. 1993, Choo et al 1998). Embryos deficient in RA synthesis or reception show severe defects in morphogenesis and patterning of the otic vesicle, as do embryos treated with exogenous RA (Dupe et al. 1999, Romand et al. 2002) (appendix 1).

Experimental hypothyroidism in rodents has revealed that the cochlea is a major site of TH action and has shown that cochlear maturation and the onset of auditory function around postnatal day 14 (P14) require TH during a critical period between the late embryonic stage and the second postnatal week (Deol 1973, Uziel et al. 1983). Chemically induced hypothyroidism results in a delay in the maturation of most elements in the organ of Corti such as the tectorial membrane, hair cells (Deol 1973), synapse formation (Uziel et al. 1983), and myelination (Knipper et al 1998). The temporal TH dependency may be delineated by several factors, including the expression of the thyroid hormone receptor (TR) genes in the cochlea (Bradley et al. 1994, Forrest et al. 1996) and the increasing serum levels of L-thyronine (T4) and L-triiodothyronine (T3) during development. The study performed by Campos-Barros et al. (2000) demonstrates that type 2 iodothyoninedeiodinase (DIO2), which converts T4 into T3, the ligand for TR, exhibits a marked activity peak in the cochlea around P7 and suggests that DIO2 is likely to play a key role as a temporal trigger of the TR pathway required for cochlear development. *DIO2* mRNA was localized in the connective tissue that gives rise to the bony labyrinth and periodically along the spiral lamina. This pattern suggests that DIO2-containing cells in the connective tissue take up T4 from the circulatory system, convert

T4 to T3, and then release T3 to responsive cells in the sensory epithelium and spiral ganglion. This invokes a local release of T3 to stimulate nearby TR-expressing cells, suggestive of a paracrine rather than endocrine mode of signalling in the cochlea.

Two functional thyroid hormone receptors, TRα1 and TRß, and the non-ligand binding TRα2 are expressed in the sensory epithelia of the inner ear from early stages. TRα1 and TRß are expressed in the cochlea with TRß mRNA being prominent both in the embryonic otic vesicle and in the postnatal sensory epithelium and spiral ganglion (Bradley et al. 1994, Lauterman and Ten Cate 1997). The expression of TRß is restricted to the cochlear epithelium (Bradley et al. 1994). *TRß*-deficient mice and humans are severely deaf, as assessed by defective auditory-evoked brainstem responses (Refetoff 1967, Forrest et al. 1996), whereas *TRα1*-deficient mice have a normal auditory-evoked brainstem response (Rüsch et al. 1998). Mice that lack all known thyroid receptors show the same deficiencies as those with hypothyroidism (Rüsch et al. 2001). A recent study has shown that the gene encoding prestin that is associated with hearing loss in humans (Liu et al. 2003) is regulated by thyroid hormone (Weber et al. 2002).

1.2.5 Development of the sensory hair bundle

Following their specification hair cells undergo a series of morphological transformations leading to the development of a specialized cytoskeleton. At their apical surface, hair cells develop 10 to 50 actin-rich stereocilia, which are specialized derivatives of actin-based microvilli. Microtubules project from the cytoplasm into the cuticular plate and serve as connectors to the hair cell cytoskeleton (Jaeger et al. 1994). The apical domain of the hair cell also contains the zonula adherens (adherens junction), a ring of mixed polarity actin fibres running in a circumferential belt parallel to the plasma membrane forming focal contacts, containing α-actinin and tropomyosin, with supporting cells (Tilney et al. 1992a). A coherent adherens junction might provide tension across the apical hair cell surface to stabilize the cuticular plate.

Hair cell stereocilia cytoskeleton

The structure of the hair cell stereocilia cytoskeleton is mostly dominated by actin assemblies (fig. 7) (Tiley et al. 1992a). The extraordinary stability of a stereocilium was attributed long ago to the remarkable paracrystalline structure of its actin core (DeRosier et al. 1980, Tilney et al. 1980). The filaments are unidirectionally aligned with their barbed end — the site of high-affinity actin polymerisation — oriented away from the surface of the cell (Tilney et al. 1980). Growth of stereocilia therefore occurs by the addition of new actin monomers to their tips (Schneider et al. 2002). The main constituent of the stereocilia actin bundles is β-actin. Several dominant missense alleles of *ACTG1* that encode γ-actin have been described that result in hearing loss in humans (DFNA20/26) (van Wijk et al. 2003, Zhu et al. 2003), suggesting there is also a requirement for γ-actin in hair cell stereocilia. In auditory hair cells γ-actin is found in the stereocilia, the cuticular plate, and adherens junctions (Khaitlina 2001). The actin filaments are held together by actin-bundling proteins, such as espin and fimbrin/plastin (fig. 7) (Bartles 2000). L-plastin, a homologue of the actin-bundling protein fimbrin, is transiently present

during mammalian stereocilia bundle formation, but not in mature bundles (Daudet and Lebart 2002). A characteristic property of espins is that they bind to and cross-link actin filaments with a 10-100 fold higher affinity than the other actin bundling proteins. Espins are believed to derive actin-bundling activity from two F-actin binding sites disposed roughly at opposite ends of the actin-bundling molecule (Bartles et al. 1998, Chen et al. 1999). Results from Loomis et al. (2003) suggest that espins increase parallel actin bundle length by causing a net barbed-end elongation of the treadmilling actin filaments. In both the cochlea and the vestibule of the mouse inner ear, espin is localized mostly to the stereocilia of hair cells (Zheng et al. 2000b). A recessive mutation of the espin gene in the deaf *jerker* mouse results in failure to accumulate detectable amounts of this protein in the hair bundle, which leads to shortening, loss of mechanical stiffness and eventual disintegration of stereocilia. Abnormalities in the deaf *jerker* mouse coincided with onset of auditory function (Zheng et al. 2000b). In humans, recessive mutations of *ESPN* at the DFNB36 locus cause profound prelingual hearing loss and peripheral vestibular areflexia (Naz et al. 2004).

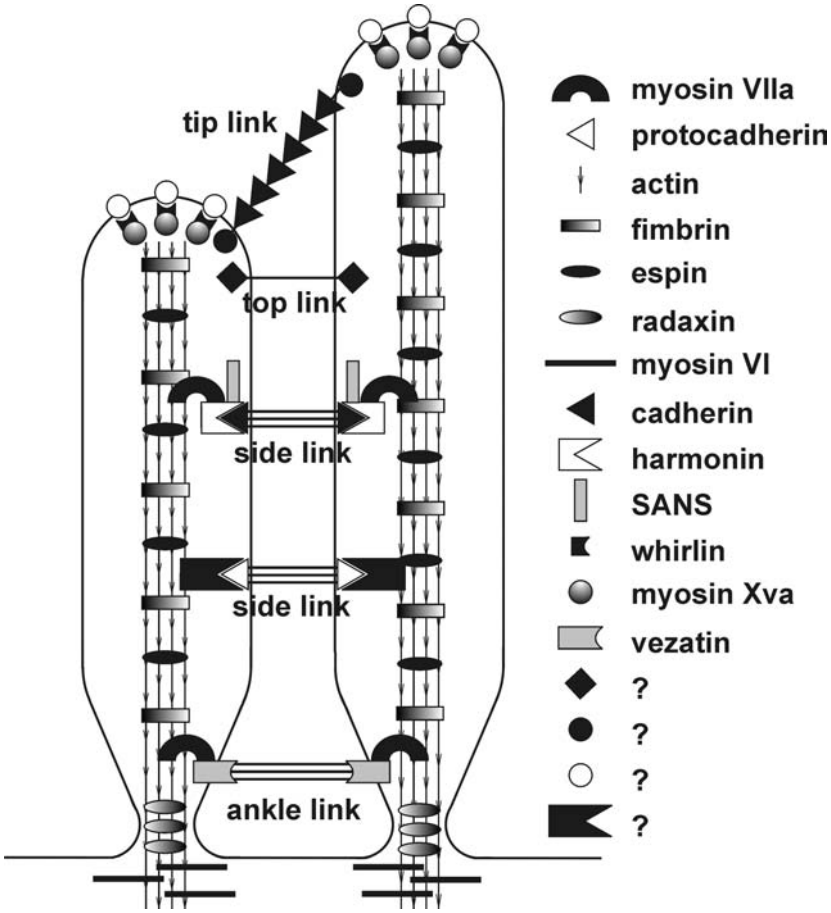

Figure 7: Schematic illustration of proteins that constitute adhesion complexes on the plasma membrane of the stereocilia.

Several other proteins have been implicated in the actin cytoskeleton dynamics of stereocilia. Stereocilia develop in close apposition to extracellular matrix receptors of the integrin family. Integrins are cell surface receptors for extracellular matrix molecules that activate pathways that regulate actin cytoskeletal dynamics and cell motility, proliferation and survival (Giancotti and Ruoslahti 1999). Therefore, they could affect many aspects of hair cell differentiation, including stereocilia formation. One integrin, α8β1, is localized to the apical surface during formation of the stereocilia. In α8β1$^{-/-}$ mice, stereocilia start to develop, but they deteriorate in a subpopulation of hair cells. Focal adhesion kinase, a key component of integrin-activated signalling pathways, is recruited to the apical cell surface during stereocilia formation. This recruitment is defective in the integrin α8β1 mutants (Littlewood-Evans and Müller 2000), which suggests that α8β1 integrin and focal adhesion kinase are in a molecular pathway that regulates the assembly or maintenance of the stereocilia cytoskeleton. Key downstream targets for integrins and other cell-surface receptors include small GTPases of the Rho family such as RHO, RAC and CDC42 (Hall and Nobes 2000). Rho GTPases regulate many aspects of cytoskeleton dynamics in different cell types. Control of actin polymerisation in the hair bundle by Rho GTPases is suggested to be mediated by profilins and formin homology proteins. Profilins are localized at sites of actin polymerisation *in vivo*, bind stoichiometrically to actin monomers, and greatly increase the polymerisation rate at the barbed end of actin filaments (Schluter et al. 1997). Studies of the *Diaphanous* gene, which was originally isolated from the fruit-fly, have established a link between profilin, Rho GTPases, and the inner ear (Lynch et al. 1997, Watanabe et al. 1997). Diaphanous belongs to the family of formin homology proteins which appear to function as platforms directing actin polymerisation to local sites within the cell (Wasserman 1998) and accelerate actin nucleation while interacting with the barbed end of actin filament (Higashida et al. 2004). The murine diaphanous protein binds to profilin as well as activated RhoA (Watanabe et al. 1997). A mutation in a human homologue of the *D. melanogaster* gene *diaphanous* is responsible for hearing loss at the *DFNA1* locus (Lynch et al. 1997). In mammalian cells, DIAPH1 cooperates with the RHO-activated kinase ROCK in the assembly of actin stress fibres that terminate at the cell membrane in local attachment points containing integrins and focal adhesion kinase (Nakano et al. 1999, Watanabe et al. 1999, Tominaga et al. 2000). DIAPH1 apparently helps to determine nucleation sites for actin filaments, whereas ROCK activates the actin-based molecular motor myosin II to exert tension force on actin filaments during stress fibre formation (Schoenwaelder and Burridge 1999). Taken together this suggests that a RHO-DIAPH1-activated signalling pathway regulates the assembly or maintenance of the hair cell cytoskeleton.

The tips of stereocilia might also contain an actin-binding protein, kaptin, which is recruited to the leading edge of lamellipodia of motile fibroblasts (Bearer and Abraham 1999). Another actin-binding protein, radixin, was detected at the taper of the hair cell stereocilium in chick, frog, mouse and zebrafish (fig. 7) (Pataky et al. 2004). Proteins of the ezrin/radixin/moesin (ERM) family crosslink actin filaments to plasma membranes and are involved in organising the cortical cytoskeleton, especially in the formation of microvilli (Tsukita and Yonemura 1999). So far, there are no reports of hair-bundle

abnormalities associated with mutations of genes that encode ERM proteins. However, these proteins might interact with unconventional myosins VIIa or XV which have FERM (band4.1, ezrin, radixin, moesin) binding domains (Oliver 1999), are specifically expressed in hair cells (Hasson et al. 1997, Belyantseva et al. 2003a), and have mutant allele products that are known to disrupt formation of the hair bundle (Probst et al. 1998, Self et al. 1998). Another unconventional myosin, myosin VI, is also involved in stereocilium formation. Myosin VI is a 'backward-stepping' actin-based motor that moves towards the pointed (minus) end of actin filaments (Wells et al. 1999, Nishikawa et al. 2002). In humans, dominant and recessive mutations in the *MYO6* gene can cause hearing loss (DFNA22 and DFNB37) (Melchionda et al. 2001, Ahmed et al. 2003a). Myosin VI is involved in many processes, including membrane trafficking and recycling, cell movement, and endocytosis (Mermall et al. 1998, Buss et al. 2001). In mammalian hair cells myosin VI has not been observed in stereocilia, but instead, is localized at the base of the hair bundle (fig. 7) within the cuticular plate that is thought to provide mechanical stability to the apex of the hair cell (Hasson et al. 1997). The *Snell's waltzer* (*sv*) mouse is deaf and has no detectable myosin VI protein in any tissues (Avraham et al. 1995). Stereocilia of the *Myo6*$^{sv/sv}$ mouse are fused at their bases, indicating that myosin VI is required to link the apical plasma membrane to the base of stereocilia and/or anchor stereocilia rootlets (Self et al. 1999, Altman et al. 2004).

Orientation and elongation of stereocilia

The evolutionary conservation of a precise arrangement of stereocilia rows in a staircase-like pattern indicates that this unique organization is required for mechanotransduction (Manley 2000). The orientation and overall arrangement of the stereocilia bundles indicates the presence of a mechanism that stabilizes the overall orientation of the cuticular plate and hair bundle as an integrated complex. This mechanism might involve myosin VIIa that is expressed in the stereocilia of the cochlea and vestibular epithelia as well as in the retina and several other tissues (El-Amraoui et al. 1996, Weil et al. 1996). Anchored by vezatin to a cadherin–catenin complex, myosin VIIa could link the cortical cytoskeleton to the adhesion junctions between hair cells and neighbouring supporting cells (fig. 7) (Kussel-Andermann et al. 2000). Consistent with this hypothesis mutations in myosin VIIa and cadherin 23 result in loss of the V/W configuration and disorientation of the bundle, respectively (Self et al. 1998, Di Palma et al. 2001). Mutations in several other genes are also known to cause hearing loss by disrupting bundle morphogenesis. Mutations in *MYO15,* which encodes myosin XV, cause non-syndromic sensorineural deafness (*DFNB3*) in humans as well as deafness and vestibular disorders in the *shaker-2* mouse (Probst et al. 1998, Wang et al. 1998b). Hair cell stereocilia in homozygous *shaker-2* mice are present and properly positioned, but are much shorter than wild-type stereocilia and there is no staircase organization of the mature hair bundle (Probst et al. 1998). Myosin XV transcripts are observed within areas corresponding to the sensory epithelia of the cochlea and vestibular systems in the developing mouse inner ear. In the adult mouse organ of Corti the protein is concentrated within the cuticular plate and at the tip of every stereocilium in wild-type auditory and vestibular hair cells

(fig. 7). Myosin XV appears just before the staircase emerges, which indicates that it is required for the elongation and formation of the stereocilia-bundle staircase (Probst et al. 1998, Belyantseva et al. 2003a). In a hair bundle, longer stereocilia have more myosin XV at their tips compared with the adjacent row of shorter stereocilia (Belyantseva et al. 2003a). Localization of myosin XV to the extreme tips of stereocilia raises the possibility that it is tethered there by integral membrane proteins. Although the proteins that interact with myosin XV are not known, it has two predicted FERM domains that could mediate interactions with ERM proteins. Perhaps more interestingly, myosin XV has a PDZ ligand sequence that could interact with PDZ domain-containing proteins to coordinate a macromolecular complex at the tips of stereocilia. PDZ scaffold proteins serve as organizing centres of macromolecular functional complexes (Harris and Lim 2001). Recessive mutations in one such PDZ domain-containing gene, *WHRN* (which encodes whirlin) cause deafness in humans (DFNB31) and in *whirler* mice (Mburu et al. 2003). Stereocilia of *whirler* mice are arrayed in a near-normal configuration on the apical hair cell surface but are abnormally short (Mburu et al. 2003). IHCs and OHCs of *whirler* mice eventually degenerate. The overall inner ear phenotype of *whirler* mice is strikingly similar to that of *shaker-2* mice. Whirlin also has a C-terminal PDZ ligand sequence that could interact with one of the PDZ domains of another whirlin protein to organize their multimerisation into a higher-order structure (Belyantseva et al. 2003b). Indeed, Delprat et al. (2005) have recently shown that myosin XVa and whirlin are both located at the tips of the stereocilia and interact directly. In addition, Belyantseva et al. (2005) have shown that myosin XVa is the motor protein that delivers whirlin to the tips of the stereocilia.

Links between stereocilia

Ultrastructural studies have revealed four different types of links between stereocilia that provide cohesiveness to the stereocilia bundle and might mediate signalling events during morphogenesis. From the top to the base of the stereocilia, these links are designated: tip-links, top-links, shaft connections or side-links, and ankle-links (fig. 7). Tip-links are present in mature hair cells and are believed to be crucial in mechanotransduction (Assad et al. 1991). They might serve as a gating spring that regulates the opening and closing of mechanically gated ion channels (Gillespie and Corey 1997). One component of the side links is a receptor protein tyrosine phosphatase (Müller and Littlewood-Evans 2001), suggesting that linkages might fulfil not only adhesive but also regulatory functions during bundle development. Ankle-links are located at the beginning of the steoreocilia taper and might determine the precise positioning and concomitant growth of individual stereocilia within a bundle (Tilney et al. 1992b).

Intercellular adhesion is a key signalling process that initiates cytoskeleton rearrangement during morphogenesis (McNeill 2000, Jamora and Fuchs 2002). The genetic investigations in type 1 Usher syndrome (USH1) in humans that is characterized by inherited hearing loss in combination with retinitis pigmentosa, and the characterization of corresponding mouse models has revealed that hair cells might use analogous adhesion mechanisms to control the morphogenesis of the hair bundle. On

the basis of similar mutant phenotypes, as well as *in vitro* protein-interaction studies, it was suggested that the protein products of genes that are involved in USH1 might form a macromolecular complex that provides cohesiveness to the stereocilia bundles (Boëda et al. 2002, Siemens et al. 2002, Weil et al. 2003) (table 2).

Table 2. Human Usher syndrome type 1 loci, genes, proteins and mouse models

Usher syndrome locus	*Gene*	*Protein*	*Mouse model*
USH1A	-	-	-
USH1B	*MYO7A*	myosin VIIa	*shaker-1*
USH1C	*USH1C*	harmonin	-
USH1D	*CDH23*	cadherin 23	*waltzer*
USH1E	-	-	-
USH1F	*PCDH15*	protocadherin 15	*ames waltzer*
USH1G	*USH1G*	SANS	*jackson shaker*

The protein encoded by *USH1C*, harmonin, has many tissue-specific isoforms in human (Scanlan et al. 1999). The predicted isoforms have two or three PDZ domains, one or two coiled-coil regions, and a PST (proline, serine, threonine) domain (Verpy et al. 2000). The harmonin b isoforms are found only in the inner ear and the eye, whereas the other isoforms are broader expressed (Verpy et al. 2000). In the inner ear, harmonin is found in the organ of Corti as well as in the five sensory areas of the vestibule (Verpy et al. 2000); in the eye harmonin b is found in the light sensitive rod outer segment (Reiners et al. 2003). An interaction has been shown between the first PDZ domain of harmonin and the second FERM and MyTh4 domain of myosin VIIa, while the second PDZ domain binds the cytoplasmic domain of cadherin 23, and the third PDZ domain along with the PST domain might interact with F-actin (fig. 7) (Boëda et al. 2002, Siemens et al. 2002). The three proteins form a transmembrane complex essential for the organisation and stabilisation of the stereocilia. SANS has also been implicated in an interaction with harmonin (fig. 7) (Weil et al. 2003). SANS and harmonin might act as cytoplasmic scaffold organizers of proteins. Cadherin 23 and protocadherin 15 are members of the cadherin superfamily of integral membrane proteins that are responsible for intercellular adhesion as well as signalling (Nelson and Nusse 2004). Interaction of these proteins might form links that interconnect stereocilia within a bundle. Protocadherins represent a large family of non-classical cadherins that are structurally and functionally divergent from the classic cadherins (Angst et al. 2001). Expression of *Pcdh15* is found in the developing sensory epithelia of the inner ear, the developing eye, the central nervous system, and epithelia of the kidney, lung and gastrointestinal tract (Murcia and Woychik 2001). Ahmed et al. (2003b) further localized the protein to the inner ear hair cell stereocilia, and to retinal photoreceptors. Both the IHC and OHC stereocilia of *Pcdh15*$^{-/-}$ mice were disorganised and associated with degeneration of the inner ear neuroepithelia (Alagramam et al. 2001). The OHCs did not display the characteristic “U” configuration found in wild-type mice. Protocadherin 15 appears in the stereocilia of developing mammalian hair cells and persists in adult hair cells along the length of stereocilia, indicating that it might be important for the long-term

maintenance of lateral connections (side-links) between stereocilia (fig. 7) (Ahmed et al. 2003b). In mice, cadherin23 is found specifically in the stereocilia of the IHCs and OHCs (Boëda et al. 2002, Siemens et al. 2002). During development in mammals, cadherin23 and harmonin transiently appear together in stereocilia, and have been reported to diminish to undetectable amounts in adult stereocilia (Boëda et al. 2002). Söllner et al. (2004) show that the defects in zebrafish *sputnik* mutants are caused by mutations in *Cdh23*. In *sputnik* mutants, stereociliary bundles are splayed to various degrees, with mutants displaying reduced or absent mechanotransduction (Nicolson et al. 1998). In zebrafish Cdh23 protein is concentrated near the tips of stereocilia bundles and tip links are absent in homozygous Cdh23 mutant *sputnik* (Söllner et al. 2004). Cdh23 is large enough to be the tip link and has biochemical properties similar to those of the tip link. Although Cdh23 has been shown to have a role in the development of hair bundles (Di Palma et al. 2001), the findings of Siemens et al. (2004) suggest that its role in adult hair cells is to form tip links, which transmit force to mechanically gated ion channels. Moreover, Cdh23 forms a complex with myosin 1c, the only known component of the mechanotransduction apparatus (Holt et al. 2002), suggesting that Cdh23 and myosin 1c cooperate to regulate the activity of mechanically gated ion channels in hair cells (fig. 7).

At least some hair-bundle adhesion complexes seem to be linked by unconventional myosin VIIa to the actin core at sites of links between stereocilia (fig. 7). At the lateral surface, myosin VIIa probably links USH1 macromolecular complexes (harmonin–cadherin23–SANS-protocadherin15) to the actin filaments during hair-bundle maturation (Boëda et al. 2002, Siemens et al. 2002, Weil et al. 2003). At the base of the stereocilium, myosin VIIa interacts with a novel transmembrane protein, vezatin, and could comprise part of an adhesion complex that is associated with ankle-links (fig. 7) (Kussel-Andermann et al. 2000). The unique location and putative composition of ankle-links are consistent with an additional role: an adhesion complex that regulates actin–myosin-based trafficking through the taper of a stereocilium (Frolenkov et al. 2004).

Hair cell maintenance

Barhl1 is a mammalian homolog of the *Drosophila BarH1* and *BarH2* genes, which encode homeodomain proteins that are required for determination of sensory organs and for normal eye morphogenesis (Higashijima et al. 1992a, Higashijima et al. 1992b, Bulfone et al. 2000). In the developing nervous system, *Barhl1* is primarily expressed in migrating neurons that settle in specific domains within the diencephalon, rhombencephalon and spinal cord (Bulfone et al. 2000). In the inner ear, *Barhl1* is expressed in all hair cells during inner ear development but it is more abundant in the adult cochlear OHCs. Targeted deletion of *Barhl1* causes degeneration of cochlear hair cells that is progressive and severe to profound hearing loss (Li et al. 2002). The onset of degeneration of cochlear IHCs was delayed for more than half a year relative to that of the OHCs, suggesting that IHCs and OHCs are differentially maintained. In fact, these two hair cell types appear to require different levels of *Barhl1* for their maintenance as a significantly higher level of *Barhl1* expression is seen in the OHCs. Data from Li et

al. (2002) indicate that *Barhl1* not only plays an essential role in the maintenance of cochlear hair cells but also in terminal differentiation of cochlear hair cells.

Caspase-3 has also been shown to play a role in inner ear hair cell maintenance (Takahashi et al. 2001). Caspases are cystein proteases that normally mediate apoptotic cell death. In developing *Caspase 3*$^{-/-}$ mice sensory epithelia initially appear normal, although maturation of the organ of Corti is slightly delayed. By five weeks, mutants show hyperplasia of supporting cells and significant loss of inner and outer hair cells (Takahashi et al. 2001). The few hair cells that survive show morphological abnormalities including loss of ciliary bundles or fusion of bundles between adjacent hair cells. Cochlear neurons also undergo significant degredation during this time (Takahashi et al. 2001). While production of supernumary supporting cells could result from inhibition of apoptosis, the cause of hair cell degeneration is not clear. Loss of hair cells could be an indirect effect of altering the balance of signals from supporting cells. Another possibility is that Caspase 3 plays a direct role in the differentiation or maintenance of hair cells.

1.3 Hearing loss

Hearing loss is the most common sensory disorder in the human population. One in 1000 children is born deaf and a similar number of children develop a hearing impairment during early childhood (Morton 1991, Gorlin et al. 1995, Fortnum et al. 2001). As age increases so does the prevalence of hearing impairment; by the age of 40-50 years, 2.3% of the population experience a hearing loss of greater than 40 dB, which increases to nearly 30% after the age of 70 years (Davis 1995).

1.3.1 Nonsyndromic hearing loss

Approximately equal numbers of cases of prelingual early childhood hearing loss are attributed to environmental and genetic factors. Of the cases attributed to genetic factors, about 70% are classified as nonsyndromic, i.e. hearing loss without other obvious clinical features, and 30% are classified as syndromic. Nonsyndromic hearing impairment can be further subdivided based on the mode of inheritance: ~77% of the cases are autosomal recessive, ~22% are autosomal dominant and ~1% are X-linked. Autosomal dominant loci are designated DFNA, autosomal recessive loci are designated DFNB and X-linked loci, DFN. The loci are numbered according to the order in which they were identified. Up to now, 39 autosomal dominant loci (DFNA), 37 autosomal recessive loci (DFNB) and 4 X-linked loci (DFN) have been described and 38 genes underlying nonsyndromic hearing impairment have been identified (table 3) (Van Camp G. and Smith R.J.H. Hereditary hearing loss homepage [http://www.uia.ac.be/DNAlab/hhh/]). In addition to nuclear genes some mitochondrial genes have been associated with hearing loss. As mitochondria have a crucial function in nearly every cell, it is not unexpected that mitochondrial DNA mutations mainly cause systemic diseases, including hearing impairment. Surprisingly, some mitochondrial mutations cause nonsyndromic hearing impairment in less than 1% of the cases (reviewed by Fischel-Ghodsian 2003).

Table 3. Genes involved in nonsyndromic hearing impairment

Gene	*Locus*	*Reference*
CRYM		Abe et al. 2002
GJA1 (Cx43)		Liu et al. 2001
PRES (Prestin)		Liu et al. 2003
ACTG1	DFNA20/26	van Wijk et al. 2003, Zhu et al. 2003
CDH23	DFNB12	Bork et al. 2001
CLDN14	DFNB29	Wilcox et al. 2001
COCH	DFNA9	Robertson et al. 1998, de Kok et al. 1999
COL11A2	DFNA13	McGuirt et al. 1999
DFNA5	DFNA5	Van Laer et al. 1998
DIAPH1	DFNA1	Lynch et al. 1997
ESPN	DFNB36	Naz et al. 2004
EYA4	DFNA10	Wayne et al. 2001
GJB2 (Cx26)	DFNA3/DFNB1	Kelsell et al. 1997
GJB3 (Cx31)	DFNA2	Xia et al. 1998
GJB6 (Cx30)	DFNA3/DFNB1	Grifa et al. 1999, Del Castillo et al. 2002
KCNQ4	DFNA2	Kubisch et al. 1999
MYH9	DFNA17	Lalwani et al. 2000
MYH14	DFNA4	Donaudy et al. 2004
MYO1A	DFNA48	Donaudy et al. 2003
MYO3A	DFNB30	Walsh et al. 2002
MYO6	DFNA22/DFNB37	Melchionda et al. 2001, Ahmed et al. 2003a
MYO7A	DFNA11/DFNB2	Liu et al. 1997a, b, Weil et al. 1997
MYO15	DFNB3	Wang et al. 1998b
OTOA	DFNB22	Zwaenepoel et al. 2002
OTOF	DFNB9	Yasunaga et al. 1999
PCDH15	DFNB23	Ahmed et al. 2003b
POU3F4	DFN3	De Kok et al. 1995
POU4F3	DFNA15	Vahava et al. 1998
SLC26A4	DFNB4	Li et al. 1998a
STRC	DFNB16	Verpy et al. 2001
TECTA	DFNA8/DFNA12/DFNB21	Verhoeven et al. 1998, Mustapha et al. 1999
TFCP2L3	DFNA28	Peters et al. 2002
TMC1	DFNA36/DFNB7/DFNB11	Kurima et al. 2002
TMIE	DFNB6	Naz et al. 2002
TMPRSS3	DFNB8/DFNB10	Scott et al. 2001
USHC1	DFNB18	Ahmed et al. 2002, Ouyang et al. 2002
WFS1	DFNA6/DFNA14	Bespalova et al. 2001, Young et al. 2001
WHRN	DFNB31	Mburu et al. 2003

Recessive nonsyndromic hearing loss

Most of the recessively inherited forms of hearing impairment cause a phenotypically identical bilateral severe to profound, prelingual hearing loss that is stable and affects all frequencies. However, mutations at a few loci, DFNB2 (*MYO7A*) (Liu et al. 1997b), DFNB8/10 (*TMPRSS3*) (Veske et al. 1996), and DFNB16 (*STRC*) (Verpy et al. 2001),

cause delayed, childhood-onset hearing impairment. Also of note is that hearing loss caused by mutations at DFNB4 (*SLC6A4*) may be associated with dilated vestibular aquaducts and endolymphatic sacs (Phelps et al. 1998), and there may be an associated auditory neuropathy with mutations in *OTOF* (DFNB9) (Varga et al. 2003). In addition, vestibular symptoms have been noted in DFNB2 (*MYO7A*), DFNB4 (*SLC6A4*) and DFNB12 (*CDH23*).

Although recessive nonsyndromic hearing impairment shows a very high degree of genetic heterogeneity mutations in the *GJB2* gene were shown to account for 50% of this type of hearing impairment in Caucasian populations (Denoyelle et al. 1997, Zelante et al. 1997, Morell et al. 1998). In European, North American and Mediterranean populations the most common mutation is a deletion of a single guanine nucleotide in a series of six guanines known as 35delG (Gasparini et al. 1997, Green et al. 1999). This mutation may account for 70% of mutant alleles of *GJB2* and the carrier frequency of this mutation alone on average is estimated 1 in 51 in Europe, but is considerably higher in Mediterranean populations (Zelante et al. 1997, Gasparini et al. 2000). At present it is not known whether this high carrier frequency is to be explained by genetic drift or by increased reproductive fitness.

Dominant nonsyndromic hearing loss

Autosomal dominant nonsyndromic hearing impairment is generally less severe than the autosomal recessive types. Most forms of autosomal dominant nonsyndromic hearing impairment are difficult to distinguish phenotypically. The majority of autosomal dominantly inherited types of hearing loss are associated with hearing impairment that is postlingual in onset, often beginning before the age of 20 years, and mostly affecting the high frequencies. Some forms, however, notably DFNA4 (Chen et al. 1995), DFNA9 (Manolis et al. 1996) and DFNA10 (O' Neil et al. 1996), are associated with hearing impairment starting somewhat later, during the third and fourth decades. Mutations at the DFNA6/14/38 locus (Lesperance et al. 1995, Van Camp et al. 1999) as well as those associated with the DFNA9 (Manolis et al. 1996) locus tend to have distinguishable clinical phenotypes, because they are associated with low frequency hearing loss and vestibular symptoms respectively. DFNA8/12 (Verhoeven et al. 1997, Kischhofer et al. 1998), DFNA13 (Brown et al. 1997) and DFNA21 (Kunst et al. 2000) can be discriminated by mid-frequency hearing impairment. All DFNA types of hearing impairment are sensorineural, except in a single family linked to DFNA23 in which a conductive component is present in approximately 50% of the affected persons (Salam et al. 2000).

In general, if more than one family has been linked to the same locus, the phenotypic characteristics of the hearing loss segregating in these families are comparable. Statistical analysis of audiometric data of large families can be used to construct age-related typical audiograms (ARTA) (Huygen et al. 2003), which often clearly characterize the hearing loss associated with the locus or gene. This type of analysis was recently performed for several autosomal dominant forms of nonsyndromic hearing impairment associated with mutations in the following genes: *COCH* (Kemperman et al.

2002), *COL11A2* (De Leenheer et al. 2002a), *DFNA5* (De Leenheer et al. 2002b), *EYA4* (De Leenheer et al. 2002c), *KCNQ4* (De Leenheer et al. 2000d), *POU4F3* (Gottfried et al. 2002) and loci for which causative genes not yet have been cloned (Huygen et al. 2002). The use of ARTAs can greatly facilitate the identification of deafness causing genetic defects, as described in this thesis in chapters three and four.

1.3.2 Syndromic hearing loss

There are many different syndromes that include an auditory phenotype as a prominent feature. Approximately 30% of individuals with prelingual hereditary hearing loss also have abnormalities of other organ systems. The accompanying abnormalities range from subtle to severe and may be congenital or delayed in appearance. The majority of these syndromes are inherited as monogenic disorders. Some of the genes involved in these syndromes have been mapped to chromosomal regions and a subset of these has been identified. A number of genes are involved in syndromic as well as nonsyndromic forms of hearing loss.

Table 4. Usher syndrome loci

Usher locus	*Chromosomal location*	*Gene*	*Overlapping NSHL locus*
USH1A	14q32		
USH1B	11q13.5	*MYO7A*	DFNB2, DFNA11
USH1C	11p15.1	*USH1C*	DFNB18
USH1D	10q22.1	*CDH23*	DFNB12
USH1E	21q21		
USH1F	10q21.1	*PCDH15*	DFNB23
USH1G	17q25.1	*SANS*	
USH2A	1q41	*USH2A*	
USH2B	3p23-p24.2		
USH2C	5q14.3-q21.3	*VLGR1*	
USH3A	3q25.1	*USH3A*	
USH3B	20q		

Adapted from Ahmed et al. 2003c Clin Genet 63: 431-444

Usher syndrome

Usher syndrome is characterized by various degrees of hearing loss and a progressive retinal dystrophy (retinitis pigmentosa [RP]) and is the most common form of deaf-blindness (50%[Boughman et al. 1983]). Its prevalence is currently estimated between 2-6.3 per 100,000 live births based on studies in Scandanavia (Hallgren 1959, Nuutila 197, Grondahl 1987, Rosenberg et al. 1997), Colombia (Tamayo et al. 1991), the United Kingdom (Hope et al. 1997), and the United States (Boughman et al. 1983). Three distinct phenotypes have been described. Usher syndrome type 1 is the most severe, patients have congenital severe to profound hearing loss and absence of vestibular function, whereas patients with Usher syndrome type 2 have congenital moderate-to-severe hearing loss and normal vestibular function. The onset of RP is prepuberal in patients with Usher syndrome type 1 and occurs during the second decade of life in

patients with Usher syndrome type 2 (Smith et al. 1994). Patients with Usher syndrome type 3 have postlingual, progressive hearing loss, and the onset of RP symptoms usually occurs by the second decade of life (Pakarinen et al. 1996). Some patients cannot be easily categorized into one of three subtypes and are designated atypical (Otterstedde et al. 2001). Usher syndrome is a genetically heterogeneous disorder, at least twelve loci account for subtypes of Usher syndrome, and eight genes have so far been identified (table 4).

1.3.3. Molecular genetics of hearing loss in humans

The great clinical heterogeneity seen in heritable deafness suggests the involvement of many genes in hearing. The identification of genes involved in hearing loss has enabled geneticists to offer DNA diagnostic tests for many types of nonsyndromic hearing loss. Moreover, it holds the promise to significantly improve the molecular knowledge on the auditory and vestibular organs and on the pathological mechanisms leading to hearing loss. This opens perspectives for future therapeutic and/or preventive measures for hearing loss. Genes that have been found to be responsible for nonsyndromic hearing loss can be classified by their function.

Components of the extracellular matrix

To date four genes encoding extracellular matrix components have been identified as being involved in nonsyndromic hearing impairment: *COCH*, *COL11A2*, *TECTA*, and *OTOA*.

The extracellular matrix protein COCH (Coagulation factor C Homologue) was isolated from a human fetal cochlea cDNA library by Robertson et al. (1994, 1997). Mutations in *COCH* are responsible for DFNA9, a form of autosomal dominant hearing loss that is associated with vestibular dysfunction (Robertson et al. 1998, de Kok et al. 1999). The COCH protein is ubiquitously present in the inner ear, and might even be the most abundant inner ear protein (Ikezono et al. 2000). Robertson et al. (2001) performed inmmunohistochemistry with an antibody raised against COCH and showed staining predominantly in the regions of the fibrocytes of the spiral limbus and of the spiral ligament in mouse and in human fetal ad adult tissue sections. High expression of *COCH* is unique to the cochlea, but the exact function of the protein is unknown. Grabski et al. (2003) showed that wild-type Coch accumulates in extracellular deposits that closely parallel the matrix component fibronectin, whereas mutant Coch varies in the amount and pattern of extracellular material. Whereas some mutants exhibited an almost normal deposition pattern, some showed a complete lack of deposition. These data suggest that DFNA9 results from gene products that fail to integrate correctly into the extracellular matrix. As symptoms of Menière's disease (including vertigo, tinnitus and a pressure feeling in the ear) were found in about 25% of patients with a *COCH* mutation, a putative role for COCH in Menière's disease was suggested (Fransen et al. 1999, Usami et al. 2003) but never confirmed.

One of the most prominent structures of the organ of Corti, the tectorial membrane, is composed of extracellular matrix molecules. It consists of collagen fibres

and a non-collagenous matrix. The major collagen in the tectorial membrane is collagen type II. Human type XI collagen is a quantitatively minor collagen that is composed of 3 α-chain polypeptide subunits: type XI collagen α1, α2, and α3. Mutations in *COL11A2* cause DFNA13, a mid-frequency hearing loss with no significant progression (McGuirt et al. 1999, De Leenheer et al. 2001), as well as two syndromic forms of hearing loss (Stickler syndrome type III and OSMED, Vikkula et al. 1995). In hearing impaired *Col11a2*$^{-/-}$ mice the tectorial membrane appeared to be thicker and less compacted than normal, due to disorganization of the type 2 collagen fibrils, which were not arranged in their usual parallel, evenly spaced manner (McGuirt et al. 1999). It was therefore hypothesized that the type XI collagen is needed in the tectorial membrane for even spacing of the type II collagen fibrils.

Three noncollagenous glycoproteins have been identified thus far that are components of the tectorial membrane (Cohen-Salmon et al. 1997, Legan et al. 1997). These are α-tectorin, β-tectorin, and otogelin. Up to 50% of the total protein content of the tectorial membrane consists of α- and β-tectorin (Goodyear and Richardson 2002). Mutation analysis of the gene encoding α-tectorin, *TECTA,* has revealed mutations associated with DFNA8/12 (Verhoeven et al. 1998) and DFNB21 (Mustapha et al. 1999). Dominantly inherited DFNA8/12 is a prelingual, moderate to severe, progressive type of hearing loss, whereas recessively inherited DFNB21 is characterized by prelingual, severe to profound hearing loss. The normal auditory function in carriers of recessive mutations implies that half the normal amount of α-tectorin is sufficient to maintain mechanical properties of the tectorial membrane. This implies that dominant mutations have a dominant negative effect, probably by interaction of mutant α-tectorin with wild type α-tectorin, β-tectorin, or collagen. In mice with a targeted deletion in the entactin G1-like domain of α-tectorin, the tectorial membrane lacks all noncollagenous matrix and is completely detached from the cochlear epithelium, but the architecture of the organ of Corti is otherwise normal (Legan et al. 2000).

The third component of the tectorial membrane, otogelin, is encoded by the gene *OTOG*. In *Otog*$^{-/-}$ mice, both the vestibular and the auditory functions were impaired (Simmler et al. 2000). Histological analysis of these mutants demonstrated that in the vestibule, otogelin is required for the anchoring of the otoconial membrane and cupulae to the neuroepithelia. No gross morphological anomalies were found in the tectorial membrane, however, ultrastructural analysis indicated that otogelin is involved in the organization of its fibrillar network. Otogelin could, therefore, be involved in the interaction or stabilization of this network, thus contributing to the mechanical stability, ductile capacity and tensile strength of the tectorial membrane.

The inner ear-specific protein otoancorin is defective in nonsyndromic recessive deafness DFNB22 (Zwaenepoel et al. 2002). In the cochlea otoancorin is located along the interface between the apical surface of the hair cells and the tectorial plama membrane and remains attached to the apical plasma membrane of epithelial cells in the absence of a tectorial membrane. In the vestibule, otoancorin is present on the apical surface of sensory cells, where they contact the otoconial membranes and cupulae. Sequence data have shown that otoancorin is probably a membrane-bound protein that is predicted to be a glycosyl-phosphatidylinositol-anchored protein, shares

weak homology with megakaryocyte potentiating factor/mesothelin precursor.

That mutations in *COL11A2* (collagen type XI polypeptide subunit 2), *OTOA* (otoancorin), and *TECTA* (alpha-tectorin) lead to either recessive or dominant nonsyndromic or syndromic hearing loss in humans emphasizes the importance of a structurally intact and firmly attached tectorial membrane.

Cytoskeletal proteins

Mutations in many cytoskeletal components result in nonsyndromic hearing loss. To date 15 such genes have been described. Several of these have been extensively discussed in the previous paragraph: *ACTG1*, *CDH23*, *DIAPH1*, *ESPN*, *PCDH15*, *USH1C*, and *WHRN* (table 3).

When analysing expression profiles of human inner ear tissues on a cDNA microarray, Abe et al. (2002) identified a gene, which was especially abundant in the inner ear, *CRYM*. Mutations in *CRYM* have been found to be responsible for nonsyndromic hearing loss (Abe et al. 2002). CRYM is one of the taxon-specific crystallins, also called “μ-crystallin” (Kim et al. 1992). *CRYM* transcription in fetal cochlea has been demonstrated in the Morton cochlear EST database. CRYM is thought to be a cytosolic NADP-regulated thyroid hormone-binding protein, a member of a group of molecular entities responsible for most of the intracellular high affinity binding of T3 and T4 (Vie et al. 1997). Thyroid hormone binding proteins are involved in sequestration and release of intracellular thyroid hormones. Whereas the cytosolic binding sites for T3 and T4 are similar to those of thyroid hormone receptors, the binding affinity of thyroid hormone binding proteins is 100 times greater than that of thyroid hormone receptors (Vie et al 1997). It is therefore speculated that the mutant CRYM could abrogate the affinity for thyroid hormone, which is essential for developmental periods as described in paragraph 2.2.6. Such deficiency results in defective morphological differentiation and maturation in the organ of Corti (Uziel 1986). *Crym* mRNA is localized in two distinct regions of the mouse cochlea, the lateral fibrocytes of the spiral ligament and the spiral limbus fibrocytes. The postulated role for these cells is potassium recycling (Spicer and Schülte 1996), suggesting that CRYM dysfunction interferes with potassium ion recycling and thus disturbs the maintenance of potassium-rich endolymph and a positive electrical potential.

Using a candidate gene approach Yasunaga et al. (1999) identified *OTOF*, the second member of a mammalian gene family related to *C. elegans fer-1*. It encodes otoferlin, a predicted cytosolic protein with six C2 domains and a single carboxy-terminal transmembrane domain (Yasunaga et al. 1999). C2 domain proteins are known to interact with phospholipids and proteins (Rizo and Südhof 1998). In mice, *Otof* is mainly expressed in cochlear inner hair cells and vestibular sensory cells (Yasunaga et al. 1999) and it has been suggested that OTOF plays a role in Ca^{2+} triggered fusion of synapse vesicles with the plasma membrane or generation of the lipid secondary messengers involved in transduction pathways (Yasanuaga et al. 2000). Mutations in otoferlin cause autosomal recessive, nonsyndromic, severe to profound, prelingual hearing impairment (DFNB9) (Yasunaga et al. 1999, Yasunaga et al. 2000, Houseman

et al. 2001). Varga et al. (2003) have also identified mutations in the *OTOF* gene in patients suffering from nonsyndromic recessive auditory neuropathy, in which patients have a hearing loss based on pure tone audiometry and auditory brain stem response, but with normal otoacoustic emissions.

Myosins

Myosins are molecular motor proteins that bind to actin and hydrolyse ATP to generate the force to move across actin filaments. Myosins consist of a head and a tail connected by a flexible neck region. The myosin superfamily consists of 15 branches, 14 of which are composed of unconventional myosins and one of conventional myosins. Two heavy chain myosins of the class II conventional nonmuscle myosins have so far been implicated in nonsyndromic hearing loss. *MYH9* is involved in DFNA17 (Lalwani et al. 1999, Lalwani et al. 2000). Within the rat cochlea, *MYH9* was localised throughout the outer hair cells, the subcentral region of the spiral ligament, and Reissner´s membrane (Lalwani et al. 2000). *MYH14* is localised within the DFNA4 critical region (Chen et al. 1995a, Mirghomizadeh et al. 2002) and in 2004 Donaudy et al. found mutations in MYH14 two large pedigrees linked to DFNA4 and in one sporadic case among 300 hearing-impaired individuals.. In human and mouse the gene is ubiquitously expressed at higher levels in adults than during development (Leal et al. 2003, Golomb et al. 2004). In the mouse cochlea (P0), with the exception of Reissner´s membrane, the protein is localised in all cells of the scala media wall, with relatively higher levels in the organ of Corti and the stria vascularis (Donaudy et al. 2004).

Five unconventional myosin genes have been described to be involved in nonsyndromic hearing loss (*MYO1A*, *MYO3A*, *MYO6*, *MYO7A*, and *MYO15*). Mutations in *shaker-1* mutant mice and human Usher syndrome type 1B patients were identified in the *myosin VIIA* gene simultaneously (Gibson et al. 1995, Weil et al. 1995). Subsequently, dominant and recessive human hearing loss were found to be associated with *myosin VIIA* mutations (Liu et al 1997a, 1997b). Mutations in *MYO15* are responsible for congenital profound deafness DFNB3 in humans (Wang et al. 1998b). S*haker-2* mice show deafness and vestibular defects and carry a spontaneous mutation in the *Myo15* gene (Probst et al. 1998). Mutations in the *myosin VI* gene, *Myo6*, are associated with deafness and vestibular dysfunction in the *Snell´s waltzer* mouse (Avraham et al. 1995) and mutations in the human ortholog, *MYO6*, are associated with dominantly inherited DFNA22 (Melchionda et al. 2001) and rcessively inherited DFNB37 (Ahmed et al. 2003a). The function of myosin VIIa, myosin XV and myosin VI in the inner ear is extensively discussed in paragraph 2 of the introduction.

Walsh et al. (2002) have shown that normal hearing in humans requires myosin IIIA, the human homolog of *D. Melanogaster* NINAC. Progressive hearing loss DFNB30 is caused by mutations in *myosin IIIA*. In *Drosophila* rhabdomeres, NINAC interacts with actin filaments and with a PDZ scaffolding protein INAD to organize the phototransduction machinery into a signalling complex. Mutations in *Drosophila NINAC* lead to retinal degeneration (Li et al. 1998b, Wes et al. 1999). Expression of mammalian myosin IIIA is highly restricted, with the strongest expression in retina and cochlea

(Walsh et al. 2002).

Donaudy et al. (2003) identified a nonsense mutation and six missense mutations in *MYO1A*, in DFNA48 patients suffering from sensorineural bilateral hearing loss of variable degree, usually ranging from moderate to severe hearing loss. Myosin I has been implicated in various processes involving motility, including organelle translocation, ion-channel gating and cytoskeleton reorganization. Besides in the cochlea (Donaudy et al. 2003) myosin 1a is present in the large and small instestine where it is a major component of the actin rich cytoskeleton of the brush border surface in intestinal epithelial cells (Skowron et al. 1998).

Molecules involved in ion homeostasis

Maintaining ion homeostasis within the cochlear duct, and in particular K^+ recycling, is of great importance for signal transduction involved in the hearing process. This is demonstrated by the number of genes involved in nonsyndromic hearing loss that are believed to play a role in ion homeostasis.

Mutations in the gene *CLDN14*, encoding tight junction claudin 14, cause autosomal recessive deafness DFNB29 (Wilcox et al. 2001). *CLDN14* is a member of the claudin gene family, which comprises the components of tight junctions. Tight junctions in the cochlear duct are thought to compartmentalize the endolymph and provide structural support for the auditory neuroepithelium. In mice *Cldn14* is expressed in the sensory epithelium of the organ of Corti and expression coincides with the development of the endocochlear potential during the first postnatal week, suggesting that *Cldn14* expression may be required for the development and maintenance of this latter process (Anniko and Bagger-Sjoback 1982, Souter and Forge 1998, Wilcox et al. 2001).

KCNQ4 is a member of the voltage-gated potassium channel gene family. The potassium channels are tetramers of identical or homologous subunits. Kubisch et al. (1999) found mutations in *KCNQ4* to be associated with DFNA2. Interestingly, otherpotassium channels have previously been associated with syndromic hearing loss. Mutations in *KCNQ1* or *KCNE1* cause the recessive Jervell/Lange-Nielsen syndrome characterized by hearing loss and cardiac rythm disturbances including a prolonged QT-interval (Neyroud et al. 1997, Schulze-Bahr et al. 1997). IN the mouse cochlea Kcnq4 is found in large amounts in the basal cell membrane of the OHCs (Kharkovets et al. 2000). In the mouse vestibular organs, *Kcnq4* expression is restricted to the hair cells and the afferent nerve endings ensheating these sensory cells. *Kcnq4* is also expressed in neurons of many, but not all, nuclei of the central auditory pathway (Kharkovets et al. 2000).

Liu et al. (2003) found that a mutation in the *prestin* gene, *PRES*, is responsible for recessive non-syndromic deafness in two families. Prestin is a member of the solute carrier (SLC) family 26 (SLC26A5), which constitute anion-transporter-related proteins. Like other members of this family, prestin has a highly hydrophobic core of 12 predicted transmembrane domains with the N- and C-termini located cytoplasmically (Dallos and Fakler 2002). Although prestin has not been shown to have any anion transport capability, it does appear to share the overall structure and specific protein domains

of the anion transporter family SLC26. The prestin gene (*Pres*) is highly expressed in outer hair cells and prestin lines the lateral wall of these cells in a close-packed array (Dallos and Fakler 2002). Prestin is necessary for fast electromotility and is likely to be the electromotility motor of cochlear OHCs (Zheng et al. 2000c, Dallos and Fakler 2002). Prestin is hypothesized to mediate the active amplification that boosts cochlear sensitivity by 100-1000 fold. A study of prestin knockout mice revealed hearing sensitivity that was reduced by 45-60 dB (Liberman et al. 2002). A recent study has shown that *PRES* expression is regulated by thyroid hormone (Weber et al. 2002).

SLC26A4 encodes pendrin, a chloride-iodide transporter (Scott et al. 1999). Yoshida et al. (2004) have shown that pendrin is important for chloride uptake and iodide efflux and that iodide and chloride activate the exchange activity of pendrin while they are transported. *SLC26A4* is expressed in the endolymphatic sac and duct and in limited cell types including the marginal cells of the stria vascularis from embryonic day 13 onwards and in non-sensory parts of the utricle, saccule and cochlea where it may be involved in regulation and resorption of endolymph (Everett et al. 1999, Everett et al. 2001). Yoshino et al. (2004) confirmed the expression pattern of pendrin in the mouse inner ear with immunohistochemical analysis. In addition pendrin was found in the apical membrane of the endolymphatic sac and duct, in the spiral ligament, the supporting cells, and the spiral ganglion of the cochlea. Individuals with mutations in *SLC26A4* have a variable clinical presentation ranging from full blown classical Pendred syndrome presenting with goitre and prelingual profound sensorineural hearing loss, to those without goitre in whom the hearing loss presents as nonsyndromic (Coyle et al. 1998, Campbell et al. 2001).

TMPRSS3 (transmembrane protease, serine 3) encodes a type II transmembrane serine protease that is mutated in both familial and sporadic cases of nonsyndromic autosomal recessive hearing loss (DFNB8/10) (Ben-Yosef et al. 2001, Masmoudi et al. 2001, Scott et al. 2001, Wattenhofer et al. 2002). The mouse and rat cochlea *Tmprss3* gene is expressed in the spiral ganglion, the supporting cells of the organ of Corti and the stria vascularis (Guipponi et al. 2002). TMPRSS3 is anchored in the endoplasmatic reticulum membranes and may play a role in the processing of epithelial amiloride-sensitive sodium channel, which is present in many sodium-reabsorbing tissues including the inner ear (Vallet et al. 1997, Vuagniaux et al. 2000). Recently, it has been suggested that EnaC plays a role in the establishment and maintenance of the remarkably low sodium concentration of the endolymph (Couloigner et al. 2001, Grunder et al. 2001). Guipponi et al. (2002) show that Tmprss3 co-localizes with EnaC in the spiral ganglion, the stria vascularis and in the supporting cells of the organ of Corti.

Connexins

Connexins connect adjacent cells and facilitate the exchange of ions, secondary messengers and other small molecules in the cochlea (Kikuchi et al 1995). The numbers assigned to the various connexins refer to their approximate molecular weight. Connexins form a family of more than 13 membrane proteins that can be classified into subgroups: α, β, and γ, based on similarities at the nucleotide and amino acid level. Six

connexin molecules assemble to form a half-channel or connexon, which docks with its counterpart in an adjacent cell to form a complete intercellular channel or gap junction. In the rodent auditory organ, gap junction channels contribute to two independent intercellular networks (Lautermann et al 1999, Xia et al. 1999). The epithelial gap junction system forms around embryonic day 16 and connects all supporting cells of the cochlear neurosensory epithelium as well as adjacent epithelial cells. No gap junctional communication has been found between the hair cells and the adjacent supporting cells. The gap junction system between connective tissue cells starts to develop around birth; this gap junction system is composed of fibrocytes in the spiral ligament and spiral limbus, and also includes basal, intermediate and marginal cells of the stria vascularis. It is thought that these gap junctions facilitate the recycling of K^+ from the hair cells back into the cochlear endolymph during auditory transduction, the K^+-recycling pathway (Kikuchi et al. 1995). To date, expression of at least four different connexins has been reported in the inner ear, connexin 26 (*GJB2*), connexin 30 (*GJB6*), connexin 31 (*GJB3*), and connexin 43 (*GJA1*). The fact that mutations in these four genes can cause hearing loss shows the functional importance of these gap junction networks in man (Kelsell et al. 1997, Grifa et al. 1999, Lerer et al. 2001, Liu et al. 2001, Del Castillo et al. 2002).

As described in paragraph 3.1.1, mutations in *GJB2* are responsible for DFNA3. Mutations in *GJB3* have been pathogenically linked to erythrokeratodermia variabilis (Richard et al. 1998), nonsyndromic autosomal dominant (DFNA2) (Xia et al. 1998) and recessive hereditary hearing impairment (Liu et al. 2000).

GJB6 mutations lead to a middle/high-frequency hearing loss (DFNA3/DFNB1) (Grifa et al. 1999, Lerer et al. 2001, Del Castillo et al. 2002, Pallares-Ruiz et al. 2002), hidrotic ectodermal dysplasia (Lamartine et al. 2000) and Clouston syndrome (Smith et al. 2002). Homozygous mouse mutants exhibit a severe constitutive hearing impairment (Teubner et al. 2003). A 342-kb deletion encompassing part of *GJB6* is the second most frequent mutation causing prelingual hearing loss, DFNB1, in the Spanisch population (Del Castillo et al. 2002). This deletion also causes hearing loss when present heterozygously in combination with a heterozygous mutation in *GJB2*, which suggests a digenic pattern of inheritance (Lerer et al. 2001).

Liu et al. (2001) have found that alterations in *GJA1* (Cx43) cause nonsyndromic autosomal recessive deafness. They show that connexin 43 is expressed in the cochlea in the non-sensory epithelial cells and in fibrocytes of the spiral ligament and the spiral limbus.

Transcription factors

So far four transcription factors have been implicated in nonsyndromic hearing loss. Interestingly, three of these are involved in autosomal dominant progressive hearing loss, while, given their expression during embryogenesis, one intuitively would expect a congenital hearing loss. Two of the transcription factors, POU4F3 and POU3F4, belong to the POU-domain containing family of transcription factors. These transcription factors play an important role in tissue-specific gene expression.

Mutations in *POU3F4* are responsible for X-linked mixed hearing loss that is characterized by temporal bone abnormalities, conductive hearing loss resulting from stapes fixation and progressive sensorineural hearing loss (DFN3) (de Kok et al. 1995, Cremers et al. 2000). DFN3 patients suffer from an increased perilymphatic pressure causing the typical "gusher" that appears during stapes footplate surgery. Throughout the inner ear, *POU3F4* is expressed in the mesenchyme of both the cochlear and vestibular aspects but not in tissues derived from neuroepithelial or neuronal cells, including the organ of Corti (McEvilly et al. 1996). Minowa et al. (1999) found expression of *Pou3f4* to be highest in the spiral ligament. In a study by Phippard et al. (1996) Pou3f4 was localized in the nucleus of ventral mesenchymal cells in the earliest developmental stages of the otic capsule. Pou3f4 remains nuclear in those regions of the otic capsule that give rise to the cellular regions of the mature bony labyrinth, while it shifts to perinuclear/ cytoplasmic localisation in those regions of the otic capsule that will cavitate to form acellular regions in the temporal bone such as the scala tympani, scala vestibuli and the inner auditory canal. *Pou3f4*-deficient mice were found to exhibit profound deafness but normal vestibular function (Minowa et al. 1999). The flexibility of auditory ossicle junctions and the mobility of stapes footplates of the mutant mice were indistinguishable from those of wild-type mice, but there was a dramatic reduction in endocochlear potential. Electron microscopy revealed severe ultrastructural alterations in cochlear spiral ligament fibrocytes. Because the number of fibrocytes in *Pou3f4*-deficient mice is similar to that in wild-type mice, *Pou3f4* may be essential for the differentiation or function of fibrocytes but not for their survival.

A mutation in *POU4F3* is responsible for DFNA15 (Vahava et al. 1998). Mutant POU4F3 loses most of its transcriptional activity and most of its ability to bind DNA (Weiss et al. 2003). *Pou4f3* is uniquely and strongly expressed in cochlear and vestibular hair cells. Whereas wild-type POU4F3 is found exclusively in the nucleus, the mutant protein is localized both to the nucleus and the cytoplasm (Weiss et al. 2003). Targeted deletion of *Pou4f3* in mice results in profound deafness and impaired balance due to complete loss of auditory and vestibular hair cells that is followed by a partial secondary loss of spiral and vestibular ganglion neurons (Xiang et al. 1995, Erkman et al. 1996, Xiang et al. 1997). Pou4f3 is required for the final differentiation and survival of hair cells (Xiang et al. 1998).

Borsani et al. (1999) characterized *EYA4* that is homologous to *Drosophila* '*eyes absent*' (*eya*). In *Drosophila*, eya is known to be a key regulator of ocular development and to mediate developmentally important protein-protein interactions. The Eya family members are transcriptional activators and in the developing mouse embryo, *Eya4* is expressed primarily in the cranofacial mesenchyme, the dermamyotome, and the limb. Wayne et al. (2001) identified mutations in *EYA4* that were responsible for the postlingual, progressive hearing loss, DFNA10. Just as EYA proteins interact with members of the SIX and DACH protein families during early embryonic development, the authors hypothesize that EYA4 is also important post-developmentally for continued function of the mature organ of Corti. Mutations in another member of this family, *EYA1*, are associated witht two forms of syndromic hearing loss, BOR (branchio-oto-renal) syndrome (Abdelhak et al. 1997a, Abdelhak et al. 1997b) and BO (branchio-oto)

syndrome (Vincent et al. 1997).

In 2000 Peters et al. studied a family with progressive sensorineural hearing loss, DFNA28 and found a mutation in the gene *TFCP2L3* (transcription factor cellular promoter 2-like gene 3). *TFCP2L3* is a member of the family of transcription factors that are homologous to the *Drosophila* gene *grainyhead*. The TFCP2 protein family shares a novel DNA-binding domain that is distinct from previously described DNA-binding domains (Johnson and McKnight 1989). The mouse gene *Tfcp2l3* is expressed in many epithelial tissues, including cells lining the cochlear duct. Expression is most abundant during embryonic development, and less so during early postnatal stages. In the cochlea, Tfcp2l3 expression appears to be restricted to the epithelial cells of placodal origin, which line the endolymph-containing scala media (Peters et al. 2000).

Genes with an unknown function

For several genes involved in nonsyndromic hearing loss the function remains unknown and one of these genes is *DFNA5*. To date three families have been described with DFNA5 that have mutations in the *DFNA5* gene (Van Laer et al. 1998, Yu et al. 2003, Bischoff et al. 2004 [chapter 3]). As there is no indication for the function of this gene and no significant homology with any other protein could be detected it was called *DFNA5* by default (Van Laer et al. 1998). Yu et al. (2003) used yeast as a model organism for studying the function of DFNA5. Yeast cells tolerated the expression of wild-type *DFNA5*, while expression of the mutant *DFNA5* led to cell cycle arrest. There are some other clues that DFNA5 might be involved in the regulation of apoptosis. Lage et al. (2001) reported that decreased *DFNA5* mRNA levels in cultured melanoma cells are associated with a decrease in apoptotic events after exposure to the drug etoposide. It appears that increased *DFNA5* mRNA levels are associated with increased cellular disposition to programmed cell death mediated by activation of caspase 3.

In 2001 Verpy et al. reported the isolation of a mouse transcript that is almost exclusively expressed in the inner ear. The gene *Strc*, encoding stereocilin was isolated from a mouse inner ear cDNA library (Cohen-Salmon et al. 1997) created by using subtractive amplification based on representational difference analysis (RDA) (Hubank and Schatz 1994). Genetic analysis shows that mutations in the human ortholog *STRC* are associated with the DFNB16 locus in two families. Stereocilin shows no significant homology to any other known protein. In the mouse inner ear *Strc* is only expressed in the sensory hair cells and the protein is associated with the stereocilia. In the developing cochlea, stereocilin appears in the hair bundle of the inner hair cells before it appears in the hair budle of the outer hair cells. The precise function of stereocilin however, is unknown.

Kurima et al. (2002) identified eight mutations in a new gene, transmembrane cochlear expressed gene 1, *TMC1*, associated with DFNA36 and DFNB7/11. In addition, a deletion was detected in *Tmc1* in a mouse model with recessive deafness, which lacks auditory responses and has hair cell degeneration (Bock and Steel 1983). The dominant mouse phenotype *Beethoven* is caused by a missense mutation in *Tmc1* indicating that dominant and recessive mutations in *TMC1* can cause progressive postlingual hearing

loss and profound prelingual deafness, in humans and mice respectively (Vreugde et al. 2002). *TMC1* is a member of a gene family predicted to encode transmembrane proteins with an unknown function. A model of six to ten membrane-spanning regions and cytoplasmic N- and C-termini is predicted for TMC1. This model is similar to those observed in ion channels or transporters, especially the superfamily cation channels with six transmembrane segments (Clapham et al. 2001). *Tmc1* mRNA is present in hair cells of the postnatal mouse cochlea and vestibular organs and inner and outer hair cells degenerate during the postnatal period in mice with a deletion in *Tmc1* (Bock and Steel 1983).

Naz et al. (2002) have identified five homozygous recessive mutations in a novel gene *TMIE* (transmembrane inner ear expressed gene), in patients suffering from DFNB6. *TMIE* encodes a protein that exhibits no significant nucleotide or deduced amino acid sequence similarity to any other protein. TMIE has a predicted intracellular amino terminus, two transmembrane regions separated by an extracellular loop, and an intracellular carboxy terminus and shares 92% identity with mouse Tmie. *TMIE* is expressed in many human tissues. Two independent recessive mutations were demonstrated to be responsible for hearing loss and vestibular dysfunction in the *spinner* mouse due to neuroepithelial defects in the inner ear (Mitchem et al. 2002). Loss of function of Tmie results in postnatal alterations of sensory hair cells in the cochlea, including severely shorter stereocilia. No obvious defects in gross inner ear morphogenesis or neuroepithelial cell patterning were noted. Later defects that were found included degeneration of the sensory cells in the cochlea and auditory nerve cells. The inner ear pathology in *spinner* mice suggests that *Tmie* is required for normal postnatal maturation of sensory hair cells in the cochlea (Mitchem et al. 2002).

Dominantly inherited progressive hearing loss DFNA6/14/38 is caused by a mutation in *WFS1*, the gene for recessively inherited Wolfram syndrome (Bespalova et al. 2001, Young et al. 2001,). Hearing loss in the DFNA6/14/38 families affects the low frequencies first and worsens over time without progressing to profound deafness. *WFS1,* encoding wolframin, is a member of a novel gene family with orthologs in several other organisms. Results from Osman et al. (2003) indicate that wolframin is an endoglycosidase H-sensitive multispanning membrane glycoprotein confined to the endoplasmic reticulum, where the protein is also predominantly localised (Takeda et al. 2001, Cryns et al. 2003). Wolframin appears to be important in the regulation of intracellular calcium homeostasis and may serve directly as an endoplasmic reticulum calcium channel or, alternatively, as a regulator of endoplasmic reticulum calcium channel activity. Given that regulation of the calcium concentration in the cytoplasm by the endoplasmic reticulum is prominent in cellular apoptosis, these data suggest that wolframin may be indirectly involved in the regulation of endoplasmic reticulum-mediated cellular mortality. Wolframin is N-glycosylated during maturation, which appears to be essential for the biogenesis and stability of the protein (Hofmann et al. 2003). Structural analysis by Hofmann et al. (2003) indicates that wolframin is organised in higher molecular weight complexes in which the protein is suggested to homo-oligomerise to a tetramer. *WFS1* was found to be ubiquitously expressed (Hofmann et al. 2003, Cryns et al. 2003) and the inner ear wolframin was found in the vestibular hair cells, inner and

outer hair cells, Dieters cells, Hensen cells, Claudius cells, interdental cells, pillar cells, external and internal sulcus cells, marginal cells of the stria vascularis and Reissners membrane (Cryns et al. 2003). Ishihara et al. (2004) generated mice with a disrupted *Wfs1* gene that develop glucose intolerance or overt diabetes due to insufficient insulin secretion. The defective insulin secretion was accompanied by reduced cellular calcium responses. Results from Ishihara et al. (2004) indicate that wolframin plays an important role in both stimulus-secretion coupling for insulin exocytosis, and regulation of calcium homeostasis, deterioration of which leads to impaired glucose homeostasis and diabetes. The progressive nature of the hearing loss suggests a role for wolframin in maintenance of sound transduction, but the function in hearing is still unknown.

Mitochondrial hearing loss

In addition to nuclear genes two mitochondrial genes have been associated with nonsyndromic hearing loss. Mutations in the *12S rRNA* gene lead to nonsyndromic hearing loss and aminoglycoside-induced hearing loss (Prezant et al. 1993). The second gene is the *tRNASer* (*UNC*) gene, in which four different mutations are known to cause nonsyndromic hearing loss (reviewed by Fishel-Ghodsian 2003). It is not unexpected that mitochondrial DNA mutations mainly cause multisystemic disease, but it is difficult to understand why these mutations only affect the inner ear, while a mutation in a mitochondrial tRNA gene would be expected to lead to aberrant mitochondrial protein synthesis and general dysfunction.

1.4 Strategies to identify hearing loss genes

Characterisation of genes and proteins that are important for proper development and homeostasis of the inner ear is central to understanding the molecular basis of hearing. The identification of these genes and their corresponding proteins largely depends on the identification of genes involved in hearing loss. The general approach for identifying these genes involves genetic linkage studies in families with hereditary hearing loss and subsequent positional cloning. However, a candidate gene approach, based on the identification of genes uniquely or preferentially expressed in the inner ear has produced additional human hearing loss genes (Robertson et al. 1998, Yasunaga et al. 1999, Verpy et al. 2001, Zwaenepoel et al. 2002). In addition to studying the genetic causes for hearing loss in humans, many model organisms are used to find the origins of genetic hearing and balance disorders. The most important model organism used for this purpose is the mouse. In most cases however, the combination of more than one strategy is the most successful in identifying genes involved in the processes of hearing. Table 5 summarises the methods used to identify nonsyndromic hearing loss genes. Below, the different approaches are outlined in further detail.

1.4.1. Positional cloning

Positional cloning of hearing impairment genes first involves localisation of the genetic defect(s) by linkage analysis or the fine mapping of structural rearrangements (e.g. deletions, duplications, translocations). The candidate region resulting from linkage

analysis can vary greatly in size depending on the number of individuals included in the study. The identification of disease associated chromosomal rearrangements, can rapidly result in the localisation of the causal gene.

Up to a couple of years ago, when a good candidate region was identified, a physical map of the region was constructed with overlapping genomic DNA clones spanning the critical region. Subsequently, a cDNA expression map was created. With the completion of the sequence of the human genome, defining a candidate region and identifying expressed sequences within that candidate region has become much easier. By using internet tools for instance the genome browser (http://genome.cse.ucsc.edu), all genes, expressed sequence tags (ESTs) and predicted genes in a candidate region can be found.

After the identification of expressed sequences in the candidate region, mutation analysis can be initiated. Depending on the number of genes present in the candidate region, and the size of genes, mutation analysis can be very laborious and expensive. An educated guess based on the predicted functional characteristics and available expression data of the most promising candidates, can limit the number of genes.

Table 5. Nonsyndromic hearing loss genes and the method with which they were identified.

Strategy	*Gene*
Positional cloning	*ACTG1*, *CLDN14*, *COL11A2*, *DFNA5*, *DIAPH1*, *EYA4*, *GJB2*, *GJB6*, *MYH9*, *MYO1A*, *MYO3A*, *OTOF*, *POU3F4*, *POU4F3*, *SLC26A4*, *TECTA*, *TFCP2L3*, *TMPRSS3*, *WFS1, WHRN*
Positional cloning/cDNA library	*USH1C*
Mouse model/positional cloning	*CDH23*, *MYO15*, *MYO6*, *MYO7A*, *PCDH15*, *TMC1*, *TMIE*
Mouse model/candidate gene approach	*ESPN*
Candidate gene approach	*GJA1*, *GJB3*, *KCNQ4*, *MYH14*, *PRES*
cDNA library analysis	*COCH*, *OTOA*, *STRC*
DNA microarray	*CRYM*

1.4.2 cDNA libraries

One of the most valuable tools to identify inner ear genes is a collection of cDNA libraries. High-quality inner ear cDNA libraries are the foundation of successful identification and cloning of inner ear-specific transcripts. cDNA libraries have been successfully constructed from the inner ears of a variety of species, including zebrafish (Coimbra et al. 2002), bullfrog (Chen et al. 1995b), chicken (Killick and Richardson 1997, Heller et al. 1998), guinea pig (Wilcox and Fex 1994), gerbil (Zheng et al. 2000c), mouse (Cohen-Salmon et al. 1997, Crozet et al. 1997), rat (Ryan et al. 1993, Soto-Prior et al. 1997, Harter et al. 1999) and human (Robertson et al. 1994, Jacob et al. 1998, Luijendijk et al. 2003). In order to create an inner ear specific cDNA library a widely used technique is cDNA subtraction. Subtraction techniques are based on the comparison of two cDNA preparations isolated from different tissues or cell types, called driver and tester. Sequences present in both populations are selectively removed, and the remaining cDNAs, enriched for transcripts specific to the tester population, are retained (Luijendijk

et al. 2003). This strategy led to the identification of the outer hair cell protein prestin in a library constructed with cDNA that was enriched by subtracting an inner hair cell cDNA driver from an outer hair cell tester cDNA (Zheng et al. 2000c).

The techniques that can be used to select inner ear-specific clones from cDNA libraries are manifold. Two approaches that are commonly used for this selection are EST analysis and serial analysis of gene expression (SAGE). Comparison of ESTs derived from an inner ear cDNA library with ESTs from libraries of other organs can indicate whether individual ESTs are expressed only in inner ear tissues. The use of this method has led to the identification of several novel inner ear genes (Jacob et al. 1998, Cohen-Salmon et al. 2000, Robertson et al. 2000). SAGE is a high-throughput method for assessing gene expression (Velculescu et al. 1995). It is based on creating double-stranded cDNA that is biotin labelled at its polyA tail from mRNA of the experimental tissue. Digestion with the frequent cutting restriction enzyme *Nla*III and affinity-purification using the biotin label results in enrichment of 3´-parts of cDNAs. High-throughput analysis is achieved by ligation of these short cDNA fragments to form long concatemers that are subcloned into plasmids to create a SAGE library. Sequencing of the library concatemers results in a collection of SAGE tags. These short tags are sufficient to identify specific transcripts because of their defined positions within known mRNA sequences. SAGE libraries can be analysed for multiple occurrences of individual tags, resulting in semi-quantitative information of specific transcripts. Comparison of SAGE tags from different libraries can reveal organ specific tags.

Although the discussed techniques are valid for the identification of genes that are restrictively expressed in the inner ear, they do not provide definite proof that an individual gene is specifically expressed in the inner ear. This requires other methods such as Northern blot analysis and reverse transcription PCR (RT-PCR) and in addition *in situ* hybridisation and immunocytochemistry allow visualization of mRNA or protein abundance, respectively, in individual cell types within the inner ear.

1.4.3 Mouse models

In the field of hearing research, recent advances using the mouse as a model for human hearing loss have brought insights into the molecular pathways involved in normal hearing and the mechanisms that are disrupted once a mutation occurs in one of the critical genes. The mouse, with its advantages of short gestation time, ease of selective matings, and similarity of the genome and the anatomy of the inner ear to humans, is a remarkable resource for knowledge on the human inner ear.

There is already an impressive collection of mouse mutants with hearing and/or vestibular dysfunction available. Defects in the vestibular system, often associated with hearing loss, are more severe in mice. The defects cause a phenotype of head bobbing or circling making deaf mice easily recognizable. There are three major ways in which mouse mutants are obtained; spontaneous, radiation or chemically induced, and transgenic or gene-targeted knockouts. Approximately 60 spontaneous mouse mutants have arisen in mouse facilities throughout the world over many years. Some of the mouse mutants suffering from hearing and/or vestibular dysfunction were by-products

of large-scale mutagenesis experiments designed to study the effects of radiation on the germline (Russel 1971). Mouse spermatogenesis cells are particularly susceptible to mutagenesis by chemicals such as N-ethyl-N-nitrosoura (ENU) and chlorambucil. Recently, several large ENU-mutagenesis screens have been initiated (Justice et al. 1999) leading to a large number of mouse models for hearing and balance disorders (Kiernan et al. 2001, Tsai et al. 2001, Vreugde et al. 2002). In 1980 the first transgenic mouse was made by microinjection of a foreign gene directly into a mouse embryo (Gordon et al. 1980). Since then, the advances in this area have been spectacular, culminating in the ability to conditionally knock-out a gene in a specific tissue (Kuhn et al. 1995).

One of the advantages of the use of mice in inner ear research is the ability to study the expression of a gene or protein during embryonic development and hair cell differentiation, as well as morphology. Visualization of the morphology of hair cells can provide valuable information about hair cell structure and loss. The morphology and physiology of the mouse inner ear can be studied using techniques such as scanning electron microscopy, patch clamping on individual hair cells (Kros et al. 1992), immunohistochemistry, *in situ* hybridisation, and culturing of the organ of Corti (Sobkowicz et al. 1993).

1.4.3. Gene expression arrays

Gene expression microarrays contain either large numbers of cDNA sequences representing known genes or uncharacterised sequences or oligonucleotides that represent specific genes. This allows fast simultaneous assessment of expression of multiple genes using very little material. Commercial high-throughput cDNA or oligonucleotide arrays representing up to 30.000 known human genes and EST clusters, a large fraction of the human genome, can reveal gene expression in a specific tissue, differential gene expression between tissues as well as changes in gene expression under changing experimental conditions or due to a particular disease.

Analysis of gene expression data from the inner ear obtained with cDNA arrays can reveal transcripts that appear or disappear during development, damage, recovery from damage, or ageing of the inner ear. This type of analysis has already proven to be successful. Chen and Corey (2001) have used oligonucleotide arrays to profile gene expression in the mouse cochlea (http://www.mgh.harvard.edu/depts/coreylab/index.html) and Cho et al. (2001) used a cDNA array to characterize and compare normal gene expression patterns in several regions of the auditory pathway of the rat. In 2003, Hawkins et al. used a set of custom microarrays to investigate differences in gene expression between constantly regenerating chick utricle and the mitotically quiescent cochlea. In addition, Abe et al. (2003) identified *CRYM*, a gene involved in nonsyndromic hearing loss through cDNA microarray analysis of human cochlear and vestibular tissues

1.5 Outline of this thesis

Identification of genes and proteins that are crucial for proper development and homeostasis of the inner ear is essential to understanding the molecular basis of hearing. The characterisation of these genes and their corresponding proteins largely depends on the identification of genes involved in hearing loss. A candidate gene approach, based on the identification of genes uniquely or preferentially expressed in the inner ear has been successful in characterising human hearing loss genes. Chapter 2 describes the construction and characterisation of a human foetal cochlear cDNA library. Novel cochlea cDNA clones expressed preferentially in the cochlea may represent genes important for the development and homeostasis of the cochlea. These genes are also good candidate genes for hereditary hearing loss.

Hearing loss is the most common sensory defect in the human population. Children can be born deaf or acquire hearing loss during their lifetime and as age increases so does the prevalence of hearing impairment. Approximately equal numbers of cases of prelingual early childhood hearing loss are attributed to environmental and genetic factors. Of the cases attributed to genetic factors, about 70% are classified as nonsyndromic, i.e. hearing loss without other obvious clinical features, and 30% are classified as syndromic. Up to now for nonsyndromic hearing loss, 39 autosomal dominant loci (DFNA), 37 autosomal recessive loci (DFNB) and 4 X-linked loci (DFN) have been described and 38 genes underlying nonsyndromic hearing impairment have been identified. Chapter 3 and 4 describe the identification of mutations in nonsyndromic hearing loss genes in two Dutch families. The identification of a novel mutation in the *DFNA5* gene in a five-generation family is described in chapter 3. A nucleotide substitution in the splice acceptor site of intron 7, leads to skipping of exon 8 and the formation of an aberrant protein in part of the transcripts. Chapter 4 describes the identification and molecular modelling of a novel mutation in the motor head domain of myosin VIIA in a family with autosomal dominant hearing impairment. The amino acid substitution is predicted to lead to disruption of the ATP/ADP binding and impair the myosin power-stroke, which would have a severe effect on the function of the myosin VIIA protein.

There are many different syndromes that include an auditory phenotype as a prominent feature. Approximately 30% of individuals with prelingual hereditary hearing loss also have abnormalities of other organ systems. The accompanying abnormalities range from subtle to severe and may be congenital or delayed in appearance. Some of the genes involved in these syndromes have been mapped to chromosomal regions and a subset of these has been identified. Usher syndrome is characterized by various degrees of hearing loss and of loss of eyesight and is the most common form of deaf-blindness (50%). Three distinct Usher syndrome phenotypes have been described. Usher syndrome type II patients have a moderate-to-severe sensorineural hearing loss that is stable in most cases, normal vestibular function, and retinitis pigmentosa. In chapter 5 mutations in *VLGR1* are shown to be involved Usher syndrome type IIc. This implicates G-protein signalling in the pathogenesis of Usher syndrome type II.

1.6 Electronic database information

URLs for data presented herein are as follows:

Genome browser: http://genome.cse.ucsc.edu

Gene expression profile of mouse cochlea generated with oligonucleotide arrays: http://www.mgh.harvard.edu/depts/coreylab/index.html

Hereditary hearing loss homepage: http://www.uia.ac.be/DNAlab/hhh/

1.7 References

Abe S., Katagiri T., Saito-Hisaminato A., et al., Identification of CRYM as a candidate responsible for nonsyndromic deafness, through cDNA microarray analysis of human cochlear and vestibular tissues. Am J Hum Genet 2002 72: 73-82.

Abdelhak S., Kalatzis V., Heilig R., et al., A human homologue of the Drosophila eyes absent gene underlies branchio-oto-renal (BOR) syndrome and identifies a novel gene family. Nat Genet 1997a 15: 157-64 .

Abdelhak S., Kalatzis V., Heilig R., et al., Clustering of mutations responsible for branchio-oto-renal (BOR) syndrome in the eyes absent homologous region (eyaHR) of EYA1. Hum Mol Genet 1997b 6: 2247-55.

Adam J., Myat A., Le Roux I., et al., Cell fate choices and the expression of Notch, Delta and Serrate homologues in the chick inner ear: parallels with Drosophila sense-organ development. Development 1998 125: 4645-4654.

Ahmed Z.M., Smith T.N., Riazuddin S., et al., Nonsyndromic recessive deafness DFNB18 and Usher syndrome type IC are allelic mutations of USHIC. Hum Genet 2002 110: 527-531.

Ahmed Z.M., Morell R.J., Riazuddin S., et al., Mutations of MYO6 are associated with recessive deafness, DFNB37.Am J Hum Genet 2003a 72: 1315-1322.

Ahmed Z.M., Riazuddin S., Ahmad J., et al., PCDH15 is expressed in the neurosensory epithelium of the eye and ear and mutant alleles are responsible for both USH1F and DFNB23. Hum Mol Genet 2003b 12: 3215-3223.

Ahmed Z.M., Riazuddin S., Riazuddin S., et al., The molecular genetics of Usher syndrome. Clin Genet 2003c 63: 431-444.

Alagramam K.N., Murcia C.L., Kwon H.Y., et al., The mouse Ames waltzer hearing-loss mutant is caused by mutation of Pcdh15, a novel protocadherin gene. Nat Genet 2001b 27: 99-102.

Altman D., Sweeney H.L., and Spudich J.A., The mechanism of myosin VI translocation and its load-induced anchoring. Cell 2004 116: 737-749.

Angst B.D., Marcozzi C., and Magee A.I., The cadherin superfamily. J Cell Sci 2001 114: 629-641.

Anniko M. and Bagger-Sjoback D., Maturation of junctional complexes during embryonic and early postnatal development of inner ear secretory epithelia. Am J Otolaryngol 1982 3: 242-253.

Assad J.A., Shepard G.M., and Corey D.P., Tip-link integrity and mechanical transduction in vertebrate hair cells. Neuron 1991 7: 985-994.

Avraham K.B., Hasson T., Steel K.P., et al., The mouse Snell's waltzer deafness gene encodes an unconventional myosin required for structural integrity of inner ear hair cells. Nat Genet 1995 11: 369-375.

Bartles J.R., Zheng L., Li A., et al., Small espin: a third actin-bundling protein and potential forked protein ortholog in brush border microvilli. J Cell Biol 1998 143: 107-119.

Bartles J.R., Parallel actin bundles and their multiple actin-bundling proteins. Curr Opin Cell Biol 2000 12: 72-78.

Bearer E.L. and Abraham M.T., 2E4 (kaptin): a novel actin-associated protein from human blood platelets found in lamellipodia and the tips of the stereocilia of the inner ear. Eur J Cell Biol 1999 78: 117-126.

Beatus P., Lundkvist J., Oberg C., et al., The notch 3 intracellular domain represses notch 1-mediated activation through Hairy/Enhancer of split (HES) promoters. Mech Dev 1999 126: 3925-3935.

Belyantseva I.A., Boger E.T., and Friedman T.B., Myosin XVa localizes to the tips of inner ear sensory cell stereocilia and is essential for staircase formation of the hair bundle. Proc Natl Acad Sci USA 2003a 100: 13958-13963.

Belyantseva I.A., Labay V., Boger E.T., et al., Stereocilia: the long and the short of it. Trends Mol Med 2003b 9: 458-461.

Belyantseva I.A., Boger E.T., Naz S., et al., Myosin-XVa is required for tip loalization of whirlin and differential elongation of hair cell stereocilia. Nat Cell Biol 2005 7: 148-156.

Ben-Yosef T., Wattenhofer M., Riazuddin S., et al., Novel mutations of TMPRSS3 in four DFNB8/B10 families segregating congenital autosomal recessive deafness. J Med Genet 2001 38: 396-400.

Bermingham N.A., Hassan B.A., Price S.D., et al., Math1: an essential gene for the generation of inner ear hair cells. Science 1999 284: 1837-1841.

Bespalova I.N., Van Camp G., Bom S.J., et al., Mutations in the Wolfram syndrome 1 gene (WFS1) are a common cause of low frequency sensorineural hearing loss. Hum Mol Genet 2001 10: 2501-2508.

Bock G.R. and Steel K.P., Inner ear pathology in the deafness mutant mouse. Acta Otolaryngol 1983 96: 39-47.

Boëda B., El-Amraoui A., Bahloul A., et al., Myosin VIIa, harmonin and cadherin23, three Usher I gene prodcts that cooperate to shape the sensory hair cell bundle. EMBO J 2002 21: 6689-6699.
Bork J.M., Peters L.M., Riazuddin S., et al., Usher syndrome 1D and nonsyndromic autosomal recessive deafness DFNB12 are caused by allelic mutations of the novel cadherin-like gene CDH23. 2001 Am J Hum Genet 68: 26-37.
Borsani G., DeGrandi A., Ballabio A., et al., EYA4, a novel vertebrate gene related to Drosophila eyes absent. Hum Mol Genet 1999 8: 11-23.
Boughman J.A., Vernon M., and Shaver K.A., Usher syndrome: definition and estimate of prevalence from two high-risk populations. J Chronic Dis 1983 36: 595-603.
Bradley D.J., Towle H.C., and Young W.S. 3rd, Alpha and beta thyroid hormone receptor (TR) gene expression during auditory neurogenesis: evidence for TR isoform-specific transcriptional regulation in vivo. Proc Natl Acad Sci USA 1994 91: 439-443.
Bulfone A., Menguzzato E., Broccoli V., et al., Barhl1, a gene belonging to a new subfamily of mammalian homeobox genes, is expressed in migrating neurons of the CNS. Hum Mol Genet 2000 9: 1443-1452.
Buss F., Arden S.D., Lindsay M., et al., Myosin VI isoform localized to clathrin-coated vesicles with a role in clathrin-mediated endocytosis. EMBO J 2001 20: 3676-3684.
Campbell C., Cucci R.A., Prasad S., et al., Pendred syndrome, DFNB4, and PDS/SLC26A4 identification of eight novel mutations and possible genotype-phenotype correlations. Hum Mut 2001 17: 403-411.
Campos-Barros A., Amma L.L., Faris J.S., et al., Type 2 iodothyronine deiodinase expression in the cochlea before the onset of hearing. Proc Natl Acad Sci USA 2000 97: 1287-1292.
Chen Z.Y. and Corey D.P., An inner ear gene expression database. J Ass Res Otorhynolaryngol 2001 3: 140-148.
Chen P. and Segil N., p27(Kip1) links cell proliferation to morphogenesis in the developing organ of Corti. Development 1999 126: 1581-1590.
Chen A.H., Ni L., Fukushima K., et al., Linkage of a gene for dominant non-syndromic deafness to chromosome 19. Hum Mol Genet 1995a 4: 1073-1076.
Chen H., Thalmann I., Adams J.C., et al., cDNA cloning, tissue distribution, and chromosomal localization of Ocp2, a gene encoding a putative transcription-associated factor predominantly expressed in the auditory organs. Genomics 1995b 27: 389-398.
Chen B., Li A., Wang D., et al., Espin contains an additional actin-binding site in its N terminus and is a major actin-bundling protein of the Sertoli cell-spermatid ectoplasmic specialization junctional plaque. Mol Biol Cell 1999 10: 4327-4339.
Chen P., Johnson J.E., Zoghbi H.Y., et al., The role of Math1 in inner ear development: Uncoupling the establishment of the sensory primordium from hair cell fate determination. Development 2002 129: 2495-2505
Cho Y., Gong T.-W.L., Ströver T. et al., Gene expression profiles of the rat cochlea, chochlear nucleus, and inferior colliculus. J Ass Res Otorhynolaryngol 2001 3: 54-67.
Choo D., Sanne J.-L., and Wu D.K., The differential sensitivities of inner ear structures to retinoic acid during development. Dev Biol 1998 204: 136-150.
Clapham D.E., Runnels L.W., and Strubing C., The TRP ion channel family. Nat Rev Neurosci 2001 2: 387-396.
Cohen-Salmon M., El-Amraoui A., Leibovici M., et al., Otogelin: a glycoprotein specific to the acellular membranes of the inner ear. Proc Natl Acad Sci USA 1997 94: 14450-14455.
Coimbra R.S., Weil D., Brottier P., et al., A subtracted cDNA library from the zebrafish (Danio rerio) embryonic inner ear. Genome Research 2002 12: 1007-1011.
Cole L.K., Le Roux I., Nunes F., et al., Sensory organ generation in the chicken inner ear: contributions of bone morphogenetic protein 4, serrate1, and lunatic fringe. J Comp Neurol 2000 424: 509-520.
Couloigner V., Fay M., Djelidi S., et al., Location and function of the epithelial Na channel in the cochlea. Am J Physiol Renal Physiol 2001 280: F214-222.
Coyle B., Reardon W., Herbrick J.A., et al., Molecular analysis of the PDS gene in Pendred syndrome. Hum Mol Genet 1998 7: 1105-1112.
Cremers F.P., Cremers C.W., and Ropers H.H., The ins and outs of X-linked deafness type 3. Adv Otorhinolaryngol 2000 56: 184-195
Crozet F., El-Amraoui A., Blanchard S., et al., Cloning of the genes encoding two murine and human cochlear unconventional type I myosins. Genomics 1997 40: 332-341.
Cryns K., Thys S., Van Laer L., et al., The WFS1 gene, responsible for low frequency sensorineural hearing loss and Wolfram syndrome, is expressed in a variety of inner ear cells. Histochem Cell Biol 2003 119: 247-256.
Dallos P. and Fakler B., Prestin, a new type of motor protein. Nat Rev Mol Cell Biol 2002 3: 104-111.
Dallos P., Popper A.N., and Fay R.R., The cochlea. 1996 Springer, New York.
Daudet N. and Lebart M.C. Transient expression of the t-isoform of plastins/fimbrin in the stereocilia of developing auditory hair cells. 2002 Cell Motil Cytoskeleton 53: 326-336.
Davis A.C., Hearing in adults. 1995 Whurr. London.
de Kok Y.J., van der Maarel S.M., Bitner-Glindzicz M., et al., Association between X-linked mixed deafness and mutations in the POU domain gene POU3F4. Science 1995 267: 685-688.
de Kok Y.J., Bom S.J., Brunt T.M., et al., A Pro51Ser mutation in the COCH gene is associated with late

onset autosomal dominant progressive sensorineural hearing loss with vestibular defects. Hum Mol Genet 1999 8: 361-366.
De Leenheer E.M., Kunst H.P., McGuirt W.T., et al., Autosomal dominant inherited hearing impairment caused by a missense mutation in COL11A2 (DFNA13). Arch Otolaryngol Head Neck Surg 2001 127: 13-17.
De Leenheer E.M., McGuirt W.T., Kunst H.P., et al., The phenotype of DFNA13/COL11A2. Adv Otorhinolaryngol 2002a 61: 85-91.
De Leenheer E.M., van Zuijlen D.A., Van Laer L., et al., Clinical features of DFNA5. Adv Otorhinolaryngol 2002b 61: 53-59.
De Leenheer E.M., Huygen P.L., Wayne S., et al., DFNA10/EYA4--the clinical picture. Adv Otorhinolaryngol 2002c 61: 73-78.
De Leenheer E.M., Ensink R.J., Kunst H.P., et al., DFNA2/KCNQ4 and its manifestations. Adv Otorhinolaryngol 2002d 61: 41-46.
del Castillo I., Villamar M., Moreno-Pelayo M.A., et al., A deletion involving the connexin 30 gene in nonsyndromic hearing impairment. New Engl J Med 2002 346: 243-249.
Delprat B., Michel V., Goodyear R., et al., Myosin XVa and whirlin, two deafness gene products required for hair bundle growth, are located at the stereocilia tips and interact directly. Hum Mol Genet 2005 14: 401-410.
Denoyelle F., Weil D., Maw M.A., et al., Prelingual deafness: high prevalence of a 30delG mutation in the connexin 26 gene. Hum Mol Genet 1997 6: 2173-2177.
Deol M.S., An experimental approach to the understanding and treatment of hereditary syndromes with congenital deafness and hypothyroidism. J Med Genet 1973 10: 235-242.
DeRosier D.J., Tilney L.G., and Egelman E., Actin in the inner ear: the remarkable structure of the stereocilium. Nature 1980 287: 291-26.
Di Palma F., Holme R.H., Bryda E.C., et al., Mutations in Cdh23, encoding a new type of cadherin, cause stereocilia disorganization in waltzer, the mouse model for Usher syndrome type 1D. Nat Genet 200127: 103-107.
Donaudy F., Ferrara A., Esposito L., et al., Multiple mutations of MYO1A, a cochlear-expressed gene, in sensorineural hearing loss. Am J Hum Genet 2003 72: 1571-1577.
Donaudy F., Snoeckx R., Pfister M., et al., Nonmuscle myosin heavy -chain gene MYH14 is expressed in cochlea and mutated in patients affected by autosomal dominant hearing impairment (DFNA4). Am J Hum Genet 2004 74: 770-776.
Dupe V., Ghyselinck N.B., Wendling O., et al., Key roles of retinoic acid receptors alpha and beta in the patterning of the caudal hindbrain, pharyngeal arches and otocyst in the mouse. Development 1999 126: 5051-5059.
Eddison M., Le Roux I., and Lewis J., Notch signaling in the development of the inner ear: lessons from Drosophila. Proc Natl Acad Sci USA 2000 97: 1692-1699.
El-Amraoui A., Sahly I., Picaud S., et al., Human Usher 1B/mouse shaker-1: the retinal phenotype discrepancy explained by the presence/absence of myosin VIIA in the photoreceptor cells. Hum Mol Genet 1996 5: 1171-1178.
Erkman L., McEvilly R.J., Luo L., et al., Role of transcription factors Brn-3.1 and Brn-3.2 in auditory and visual system development. Nature 1996 381: 603-606.
Everett L.A., Morsli H., Wu D.K., et al., Expression pattern of the mouse ortholog of the Pendred's syndrome gene (Pds) suggests a key role for pendrin in the inner ear. Proc Natl Acad Sci USA 1999 96: 9727-9732.
Everett L.A., Belyantseva I.A., Noben-Trauth K., et al., Targeted disruption of mouse Pds provides insight about the inner-ear defects encountered in Pendred syndrome. Hum Mol Genet 2001 10: 153-161.
Fischel-Ghodsian N., Mitochondrial deafness. Ear Hear 2003 24: 303-313.
Forrest D., Erway L.C., Ng L., et al., Thyroid hormone receptor beta is essential for development of auditory function. Nat Genet 1996 13: 354-357.
Fortnum H.M., Summerfield A.Q., Marshall D.H., et al., Prevalence of permanent childhood hearing impairment in the United Kingdom and implications for universal neonatal hearing screening: questionnaire based ascertainment study. Br Med J 2001 323: 536-540.
Frolenkov G.I., Belyantseza I.A., Friedman T.B., et al., Genetic insights into the morphogenesis of inner ear hair cells. Nat Genet Rev 2004 5: 489-498.
Gasparini P., Estivill X., Volpini V., et al., Linkage of DFNB1 to non-syndromic neurosensory autosomal-recessive deafness in Mediterranean families. Eur J Hum Genet 1997 5: 83-88.
Gasparini P., Rabionet R., Barbujani G., et al., High carrier frequency of the 35delG deafness mutation in European populations. Genetic Analysis Consortium of GJB2 35delG. Eur J Hum Genet 2000 8: 19-23.
Giancotti F.G. and Ruoslahti E., Integrin signalling. Science 1999 285: 1028-1032.
Gibson F., Walsh J., Mburu P., et al., A type VII myosin encoded by the mouse deafness gene shaker-1. Nature 1995 374: 62-64.
Gillespie P.G. and Corey D.P., Myosin and adaptation by hair cells. Neuron 1997 19: 955-958.
Golomb E., Ma X., Jana S.S., et al., Identification and characterization of nonmuscle myosin II-C, a new member of the myosin II family. J Biol Chem 2004 279: 2800-2808.
Goodyear R.J. and Richardson G.P., Extracellular matrices associated with the apical surfaces of sensory epithelia in the inner ear: molecular and structural diversity. J Neurobiol 2002 52: 212-227.

Gordon J.W., Scangos G.A., Plotkin D.J., et al., Genetic transformation of mouse embryo's by microinjection of purified DNA. Proc Natl Acad Sci USA 1980 77: 7380-7384.
Gorlin R.J., Toriello H.V., and Cohen M.M., Hereditary hearing loss and its syndromes. 1995 Oxford University Press, New York.
Gottfried I., Huygen P.L., and Avraham K.B., The clinical presentation of DFNA15/POU4F3. Adv Otorhinolaryngol 2002 61: 92-97
Grabski R., Szul T., Sasaki T., et al., Mutations in COCH that result in non-syndromic autosomal dominant deafness (DFNA9) affect matrix deposition of cochlin. Hum Genet 2003 113: 406-416.
Green G.E., Scott D.A., McDonald J.M., et al., Carrier rates in the midwestern United States for GJB2 mutations causing inherited deafness. JAMA 1999 281: 2211-2216.
Grifa A., Wagner C.A., D'Ambrosio L., et al., Mutations in GJB6 cause nonsyndromic autosomal dominant deafness at DFNA3 locus. Nat Genet 1999 23: 16-18.
Groves A.K. and Bonne-Fraser M., Competence, specification and commitment in otic placode induction. Development 2000 127: 3489-3499.
Grondahl J., Estimation of prognosis and prevalence of retinitis pigmentosa and Usher syndrome in Norway. Clin Genet 1987 31: 255-264.
Grunder S., Muller A., and Ruppersberg J.P., Developmental and cellular expression pattern of epithelial sodium channel alpha, beta and gamma subunits in the inner ear of the rat. Eur J Neurosci 2001 13: 641-648.
Guipponi M., Vuagniaux G., Wattenhofer M., et al., The transmembrane serine protease (TMPRSS3) mutated in deafness DFNB8/10 activates the epithelial sodium channel (ENaC) in vitro. Hum Mol Genet 2002 11: 2829-2836.
Haddon C., Jiang Y.J., Smithers L., et al., Delta-Notch signalling and the patterning of sensory cell differentiation in the zebrafish ear: evidence from the mind bomb mutant. Development 1998 125: 4637-4644.
Hall A. and Nobes C.D., Rho GTPases: molecular switches that control the organization and dynamics of the actin cytoskeleton. Philos Trans R Soc Lond B Biol Sci 2000 355: 965-970.
Hallgren B., Retinitis pigmentosa combined with congenital deafness with vestibulo-cerebellar ataxia and mental abnormality in a proportion of cases. A clinical and genetico-statistical study. Acta Psychiatry Scand Suppl 1959 138: 5-101.
Harris B.Z. and Lim W.A., Mechanism and role of PDZ domains in signaling complex assembly. J Cell Sci 2001 114: 3219–3231.
Harter C., Ripoll C., Lenoir M., et al., Expression pattern of mammalian cochlea outer hair cell (OHC) mRNA: screening of a rat OHC cDNA library. DNA Cell Biol 1999 18: 1-10.
Hasson T., Unconventional myosins in inner-ear sensory epithelia. J Cell Biol 1997 137: 1287-1307.
Hawkins R.D., Bashiardes S., Helms C.A., et al., Gene expression differences in quiescent versus regenerating hair cells of avian sensory epithelia: implications for human hearing and balance disorders. Hum Mol Genet 2003 12: 1261-1272.
Heller S., Sheane C.A., Javed Z., et al., Molecular markers for cell types of the inner ear and candidate genes for hearing disorders. Proc Natl Acad Sci USA 1998 95: 11400-11405.
Higashida C., Miyoshi T., Fujita A., et al., Actin polymerization-driven molecular movement of mDia1 in living cells. Science 2004 303: 2007-2010.
Higashijima S., Kojima T., Michiue T., et al., Dual Bar homeo box genes of Drosophila required in two photoreceptor cells, R1 and R6, and primary pigment cells for normal eye development.Genes Dev 1992a 6: 50-60.
Higashijima S., Michiue T., Emori Y., et al., Subtype determination of Drosophila embryonic external sensory organs by redundant homeo box genes BarH1 and BarH2. Genes Dev 1992b 6: 1005-1018.
Hofmann S., Philbrook C., Gerbitz K.D., et al., Wolfram syndrome: structural and functional analyses of mutant and wild-type wolframin, the WFS1 gene product. Hum Mol Genet 2003 12: 2003-2012.
Holt J.R., Gillespie S.K., Provance D.W., et al., A chemical-genetic strategy implicates myosin-1c in adaptation by hair cells. Cell 2002 108: 371-381.
Hope C.I., Bundey S., Proops D., et al., Usher syndrome in the city of Birmingham – prevalence and clinical classification. Br J Ophtalmol 1997 81: 46-53.
Houseman M.J., Jackson A.P., Al-Gazali L.I., et al., A novel mutation in a family with non-syndromic sensorineural hearing loss that disrupts the newly characterised OTOF long isoforms. J Med Genet 2001 38: E25.
Hubank M. and Schatz D.G., Identifying differences in mRNA expression by representational difference analysis of cDNA. Nucleic Acids Res 1994 22: 5640-5648.
Huygen P.L., Bom S.J., van Camp G., et al., Clinical presentation of the DFNA loci where causative genes have not yet been cloned. DFNA4, DFNA6/14, DFNA7, DFNA16, DFNA20 and DFNA21. Adv Otorhinolaryngol 2002 61: 98-106.
Huygen P.L., Pennings R.J., and Cremers C.W., Characterizing and distinguishing progressive phenotypes in non syndromic autosomal dominant hearing impairment. Audiol Med 2003 1:37-46.
Ikezono T., Omori A., Ichinose S., et al., Identification of the protein product of the Coch gene (hereditary deafness gene) as the major component of bovine inner ear protein. Biochim Biophys Acta 2001 1535: 258-265.
Ishihara H., Takeda S., Tamura A., et al., Disruption of the WFS1 gene in mice causes progressive beta-

cell loss and impaired stimulus-secretion coupling in insulin secretion. Hum Mol Genet 2004 13: 1159-1170.
Jacob A.N., Manjunath N.A., Bray-Ward P., et al., Molecular cloning of a zinc finger gene eZNF from a human inner ear cDNA library, and in situ expression pattern of its mouse homologue in mouse inner ear. Somat Cell Mol Genet 1998 24: 121-129.
Jacobson A.G., Inductive processes in embryonic development. 1966 Sciece 152:25-34.
Jamora C. and Fuchs E., Intercellular adhesion, signalling and the cytoskeleton. Nature Cell Biol 2002 4: E101–E108.
Jaeger R.G., Fex J., and Kachar B., Structural basis for mechanical transduction in the frog vestibular sensory apparatus: II. The role of microtubules in the organization of the cuticular plate. Hear Res 1994 77: 207-215.
Johnson P.F. and McKnight S.L., Eukaryotic transcriptional regulatory proteins. Annu Rev Biochem 1989 58: 799-839.
Justice M.J., Noveroske J.K., Weber J.S., et al., Mouse ENU mutagenesis. Hum Mol Genet 1999 8: 1955-63.
Kelley M.W., Xu X.M., Wagner M.A., et al., The developing organ of Corti contains retinoic acid and forms supernumerary hair cells in response to exogenous retinoic acid in culture. Development 1993 119: 1041-1053.
Kelsell D.P., Dunlop J., Stevens H.P., et al., Connexin 26 mutations in hereditary non-syndromic sensorineural deafness. Nature 1997 387: 80-83.
Kemperman M.H., Bom S.J., Lemaire F.X., et al., DFNA9/COCH and its phenotype.Adv Otorhinolaryngol 2002 61: 66-72.
Khaitlina S.Y., Functional specificity of actin isoforms. Int Rev Cytol 2001 202: 35-98.
Kiernan A.E., Ahituv N., Fuchs H., et al., The Notch ligand Jagged1 is required for inner ear sensory development. Proc Natl Acad Sci USA 2001 98: 3873-3878.
Kikuchi T., Kimura R.S., Paul D.L., et al., Gap junctions in the rat cochlea: immunohistochemical and ultrastructural analysis. Anat Embryol (Berl)1995 191: 101-118.
Killick R. and Richardson G., Isolation of chicken alpha ENaC splice variants from a cochlear cDNA library. Biochim Biophys Acta 1997 1350: 33-37.
Kim R.Y., Gasser R., and Wistow G.J., Mu-crystallin is a mammalian homologue of Agrobacterium ornithine cyclodeaminase and is expressed in human retina. Proc Natl Acad Sci USA 1992 89: 9292-9296.
Knipper M., Bandtlow C., Gestwa L., et al., Thyroid hormone affects Schwann cell and oligodendrocyte gene expression at the glial transition zone of the VIIIth nerve prior to cochlea function. Development 1998 125: 3709-3718.
Kros C.J., Rusch A., and Richardson G.P., Mechano-electrical transducer currents in hair cells of the cultured neonatal mouse cochlea. Proc Biol Sci 1992 249: 185-193.
Kubisch C., Schroeder B.C., Friedrich T., et al., KCNQ4, a novel potassium channel expressed in sensory outer hair cells, is mutated in dominant deafness.Cell 1999 96: 437-446.
Kuhn R., Schwenk F., Aguet M., et al., Inducible gene targeting in mice. Science 1995 269: 1427-1429.
Kurima K., Peters L.M., Yang Y., et al., Dominant and recessive deafness caused by mutations of a novel gene, TMC1, required for cochlear hair-cell function. Nat Genet 2002 30: 277-284.
Kussel-Andermann P., El-Amraoui A., Safieddine S., et al., Vezatin, a novel transmembrane protein, bridges myosin VIIA to the cadherin-catenins complex. EMBO J 2000 19: 6020-6029.
Lage H., Helmbach H., Grottke C., et al., DFNA5 (ICERE-1) contributes to acquired etoposide resistance in melanoma cells. FEBS Lett 2001 494: 54-59.
Lalwani A.K., Luxford W.M., Mhatre A.N., et al., A new locus for nonsyndromic hereditary hearing impairment, DFNA17, maps to chromosome 22 and represents a gene for cochleosaccular degeneration. Am J Hum Genet 1999 64: 318-323.
Lalwani A.K., Goldstein J.A., Kelley M.J., et al., Human nonsyndromic hereditary deafness DFNA17 is due to a mutation in nonmuscle myosin MYH9. Am J Hum Genet 2000 67: 1121-1128.
Lamartine J., Munhoz Essenfelder G., Kibar Z., et al., Mutations in GJB6 cause hidrotic ectodermal dysplasia. Nat Genet 2000 26: 142-144.
Lanford P.J., Lan Y., Jiang R., et al., Notch signalling pathway mediates hair cell development in mammalian cochlea. Nat Genet 1999 21: 289-292.
Lanford P.J., Shailam R., Norton C.R., et al., Expression of Math1 and HES5 in the cochleae of wildtype and Jag2 mutant mice. J Assoc Res Otolaryngol 2000 1: 161-171.
Sadler T.W., Langman´s embryology 2000 Lippincott, Williams and Wilkins, Philadelphia.
Lautermann J., and ten Cate W.J., Postnatal expression of the alpha-thyroid hormone receptor in the rat cochlea. Hear Res 1997 107: 23-28.
Lautermann J., Frank H.G., Jahnke K., et al., Developmental expression patterns of connexin26 and -30 in the rat cochlea. Devel Genet 1999 25: 306-311.
Leal A., Endele S., Stengel C., et al., A novel myosin heavy chain gene in human chromosome 19q13.3. Gene 2003 312: 165-171.
Legan P.K., Rau A., Keen J.N., et al., The mouse tectorins. Modular matrix proteins of the inner ear homologous to components of the sperm-egg adhesion system. J Biol Chem 1997 272: 8791-8801.
Legan P.K., Lukashkina V.A., Goodyear R.J., et al., A targeted deletion in alpha-tectorin reveals that the tectorial membrane is required for the gain and timing

of cochlear feedback. Neuron 2000 28: 273-285.
Lerer I., Sagi M., Ben-Neriah Z., et al., A deletion mutation in GJB6 cooperating with a GJB2 mutation in trans in non-syndromic deafness: A novel founder mutation in Ashkenazi Jews. Hum Mutat 2001 18: 460-469.
Li L., Krantz I.D., Deng Y., et al., Alagille syndrome is caused by mutations in human Jagged1, which encodes a ligand for Notch1. Nat Genet 1997 16: 243-251.
Li X.C., Everett L.A., Lalwani A.K., et al., A mutation in PDS causes non-syndromic recessive deafness. Nat Genet 1998a 18: 215-217.
Li H.S., Porter J.A., and Montell C., Requirement for the NINAC kinase/myosin for stable termination of the visual cascade. J Neurosci 1998b 18: 9601-9606.
Li S., Price S.M., Cahill H., et al., Hearing loss caused by progressive degeneration of cochlear hair cells in mice deficient for the Barhl1 homeobox gene. Development 2002b 129: 3523-3532.
Liberman M.C., Gao J., He D.Z., et al., Prestin is required for electromotility of the outer hair cell and for the cochlear amplifier. Nature 2002 419: 300-304.
Littlewood-Evans A. and Muller U., Stereocilia defects in the sensory hair cells of the inner ear in mice deficient in integrin alpha8beta1. Nat Genet 2000 24: 424-42.
Liu X.Z., Walsh J., Mburu P., et al., Mutations in the myosin VIIA gene cause non-syndromic recessive deafness. Nat Genet 1997a 16: 188-190.
Liu X.Z., Walsh J., Tamagawa Y., et al., Autosomal dominant non-syndromic deafness caused by a mutation in the myosin VIIA gene. Nat Genet 1997b 17: 68-269.
Liu X.Z., Xia X.J., Xu L.R., et al., Mutations in connexin31 underlie recessive as well as dominant non-syndromic hearing loss. Hum Mol Genet 2000 9: 63-67.
Liu X.Z., Xia X.J., Adams J., et al., Mutations in GJA1 (connexin 43) are associated with non-syndromic autosomal recessive deafness. Hum Mol Genet 2001 10: 2945-2951.
Liu X.Z., Ouyang X.M., Xia X.J., et al., Prestin, a cochlear motor protein, is defective in non-syndromic hearing loss. Hum Mol Genet 2003 12: 1155-1162.
Loomis P.A., Zheng L., Sekerkova G., et al., Espin cross-links cause the elongation of microvillus-type parallel actin bundles in vivo. J Cell Biol 2003 163: 1045–1055.
Lowenheim H., Furness D.N., Kil J., et al., Gene disruption of p27(Kip1) allows cell proliferation in the postnatal and adult organ of corti. Proc Natl Acad Sci USA 1999 96: 4084-4088.
Lynch E.D., Lee M.K., Morrow J.E., et al., Nonsyndromic deafness DFNA1 associated with mutation of a human homolog of the Drosophila gene diaphanous. Science 1997 278: 1315-1318.
Manley G.A., Cochlear mechanisms from a phylogenetic viewpoint. Proc Natl Acad Sci USA 2000 97: 11736–11743.
Masmoudi S., Antonarakis S.E., Schwede T., et al., Novel missense mutations of TMPRSS3 in two consanguineous Tunisian families with non-syndromic autosomal recessive deafness. Hum Mutat 2001 18: 101-108.
Mburu P., Mustapha M., Varela A., et al., Defects in whirlin, a PDZ domain molecule involved in stereocilia elongation, cause deafness in the whirler mouse and families with DFNB31. Nat Genet 2003 34: 421-428.
McEvilly R.J., Erkman L., Luo L., et al., Requirement for Brn-3.0 in differentiation and survival of sensory and motor neurons. Nature 1996 384: 574-577.
McGuirt W.T., Prasad S.D., Griffith A.J., et al., Mutations in COL11A2 cause non-syndromic hearing loss (DFNA13). Nat Genet 1999 23: 413-419.
McNeill H., Sticking together and sorting things out: adhesion as a force in development. Nature Rev Genet 2000 1: 100–108.
Melchionda S., Ahituv N., Bisceglia L., et al., MYO6, the human homologue of the gene responsible for deafness in Snell's waltzer mice, is mutated in autosomal dominant nonsyndromic hearing loss. Am J Hum Genet 2001 69: 635-640.
Mermall V., Post P.L., and Mooseker M.S., Unconventional myosins in cell movement, membrane traffic, and signal transduction. Science 1998 279: 527-533.
Minowa O., Ikeda K., Sugitani Y., et al., Altered cochlear fibrocytes in a mouse model of DFN3 nonsyndromic deafness. Science 1999 285: 1408-1411.
Mitchem K.L., Hibbard E., Beyer L.A., et al., Mutation of the novel gene Tmie results in sensory cell defects in the inner ear of spinner, a mouse model of human hearing loss DFNB6. Hum Mol Genet 2002 11: 1887-1898.
Morell R.J., Kim H.J., Hood L.J., et al., Mutations in the connexin 26 gene (GJB2) among Ashkenazi Jews with nonsyndromic recessive deafness. N Engl J Med 1998 339: 1500-1505.
Morrison A., Hodgetts C., Gossler A., et al., Expression of Delta1 and Serrate1 (Jagged1) in the mouse inner ear. Mech Dev 1999 84: 169-172.
Morton N.E., Genetic epidemiology of hearing impairment. Ann. N. Y. Acad. Sci. 1991 630: 16-31.
Müller U. and Littlewood-Evans A., Mechanisms that regulate mechanosensory hair cell differentiation. Trends Cell Biol 2001 11: 334-342.
Murcia C.L. and Woychik R.P., Expression of Pcdh15 in the inner ear, nervous system and various epithelia of the developing embryo. Mech Dev 2001 105: 163-166.
Mustapha M., Weil D., Chardenoux S., et al., An alpha-tectorin gene defect causes a newly identified autosomal recessive form of sensorineural pre-lingual non-syndromic deafness, DFNB21. Hum Mol

Genet 1999 8: 409-412.
Nakano K., Takaishi K., Kodama A., et al., Distinct actions and cooperative roles of ROCK and mDia in Rho small G protein-induced reorganization of the actin cytoskeleton in Madin-Darby canine kidney cells. Mol Biol Cell 1999 10: 2481-2491.
Naz S., Giguere C.M., Kohrman D.C., et al., Mutations in a novel gene, TMIE, are associated with hearing loss linked to the DFNB6 locus. Am J Hum Genet 2002 71: 632-636.
Naz S., Griffith A.J., Riazuddin S., et al., Mutations of ESPN cause autosomal recessive deafness and vestibular dysfunction. J Med Genet 2004 41: 591-595.
Nelson W.J. and Nusse R., Convergence of Wnt, beta-catenin, and cadherin pathways. Science 2004 303: 1483–1487.
Neyroud N., Tesson F., Denjoy I., et al., A novel mutation in the potassium channel gene KVLQT1 causes the Jervell and Lange-Nielsen cardioauditory syndrome. Nat Genet 1997 15: 186-189.
Nicolson T., Rusch A., Friedrich R.W., et al., Genetic analysis of vertebrate sensory hair cell mechanosensation: the zebrafish circler mutants. Neuron 1998 20: 271-283.
Nishikawa S., Homma K., Komori Y., et al., Class VI myosin moves processively along actin filaments backward with large steps. Biochem Biophys Res Comm 2002 290: 311-317.
Noramly S. and Grainger R.M., Determination of the embryonic inner ear. J Neurobiol 2002 53: 100-128.
Nuutila A., Dystrophia retinae pigmentosa-dysacusis syndrome (DRD): a study of the Usher or Hallgren syndrome. J Hum Genet 1970 18: 57-88.
O´Rahilly R., The early development of the otic vesicle in staged human embryos. J Embryol Exp Morphol 1963 11: 741.
Oda T., Elkahloun A.G., Pike B.L., et al., Mutations in the human Jagged1 gene are responsible for Alagille syndrome. Nat Genet 1997 16: 235-242.
Oliver T.N., Berg J.S., and Cheney R.E., Tails of unconventional myosins. Cell Mol Life Sci 1999 56: 243–2457.
Osman A.A., Saito M., Makepeace C., et al., Wolframin expression induces novel ion channel activity in endoplasmic reticulum membranes and increases intracellular calcium. J Biol Chem 2003 278: 52755-52762.
Otterstedde C.R., Spandau U., Blankenagel A., et al., A new clinical classification for Usher's syndrome based on a new subtype of Usher's syndrome type I. Laryngoscope 2001 111: 84-86.
Ouyang X.M., Xia X.J., Verpy E., et al., Mutations in the alternatively spliced exons of USH1C cause non-syndromic recessive deafness. Hum Genet 2002 111: 26-30.
Pakarinen L., Tuppurainen K., Laippala P., et al., The ophthalmological course of Usher syndrome type III. Intl Ophtalmol 1996 19: 307-311.
Pallares-Ruiz N., Blanchet P., Mondain M., et al., A large deletion including most of GJB6 in recessive nonsyndromic deafness: a digenic effect? Eur J Hum Genet 2002 10: 72-76.
Pataky F., Pironkova R., and Hudspeth A.J., Radixin is a constituent of stereocilia in hair cells. Proc Natl Acad Sci USA 2004 101: 2601–2606.
Peters L.M., Anderson D.W., Griffith A.J., et al., Mutation of a transcription factor, TFCP2L3, causes progressive autosomal dominant hearing loss, DFNA28. Hum Mol Genet 2002 11: 2877-2885.
Phelps P.D., Coffey R.A., Trembath R.C., et al., Radiological malformations of the ear in Pendred syndrome. Clin Radiol 1998 53: 268-273.
Politzer G., The formation of the austic ganglion in humans. Acta Anat (Basel) 1956 6: 1.
Prezant T.R., Agapian J.V., Bohlman M.C., et al., Mitochondrial ribosomal RNA mutation associated with both antibiotic-induced and non-syndromic deafness. Nat Genet 1993 4: 289-294.
Probst F.J., Fridell R.A., Raphael Y., et al., Correction of deafness in shaker-2 mice by an unconventional myosin in a BAC transgene.Science 1998 280: 1444-1447.
Raphael Y. and Altschuler R.A., Structure and innervation of the cochlea. Br Res Bull 2003 60: 397-422.
Refetoff S., DeWind L.T., and DeGroot L.J., Familial syndrome combining deaf-mutism, stuppled epiphyses, goiter and abnormally high PBI: possible target organ refractoriness to thyroid hormone. J Clin Endocrinol Metab 1967 27:279-294.
Reiners J., Reidel B., El-Amraoui A., et al., Differential distribution of harmonin isoforms and their possible role in Usher-1 protein complexes in mammalian photoreceptor cells. Invest Ophthalmol Vis Sci 2003 44: 5006-5015.
Represa J., Frenz D.A., and Van De Water T.R., Genetic patterning of embryonic inner ear development. Acta Otolaryngol 2000 120: 5-10.
Richard G., Smith L.E., Bailey R.A., et al., Mutations in the human connexin gene GJB3 cause erythrokeratodermia variabilis. Nat Genet 1998 20: 366-369.
Rivolta M.N., Halsall A., Johnson C.M., et al., Transcript profiling of functionally related groups of genes during conditional differentiation of a mammalian cochlear hair cell line. Genome Res 2002 12; 1091-1099.
Rizo J. and Südhof T.C., Mechanics of membrane fusion. Nat Struc Biol 1998 5: 839-842.
Robertson N.G., Khetarpal U., Gutierrez-Espeleta G.A., et al., Isolation of novel and known genes from a human fetal cochlear cDNA library using subtractive hybridization and differential screening. Genomics 1994 23: 42-50.
Robertson N.G., Skvorak A.B., Yin Y., et al., Mapping and characterization of a novel cochlear gene in human and in mouse: a positional candidate gene

for a deafness disorder, DFNA9. Genomics 1997 46: 345-354.
Robertson N.G., Lu L., Heller S., et al., Mutations in a novel cochlear gene cause DFNA9, a human nonsyndromic deafness with vestibular dysfunction. Nat Genet 1998 20: 299-303.
Robertson N.G., Heller S., Lin J.S., et al., A novel conserved cochlear gene, OTOR: identification, expression analysis, and chromosomal mapping. Genomics 2000 66: 242-248.
Robertson N.G., Resendes B.L., Lin J.S., et al., Inner ear localisation of mRNA and protein products of COCH, mutated in the sensorineural deafness ad vestibular disorder DFNA9. Hum Mol Genet 2001 10: 2493-2500.
Romand R., Hashino E., Dolle P., et al., The retinoic acid receptors RARalpha and RARgamma are required for inner ear development. Mech Dev 2002 119: 213-223.
Rosenberg T., Haim M., Hauch A.M., et al., The prevalence of Usher syndrome and other retinal dystrophy-hearing impairment associations. Clin Genet 1997 51: 314-321.
Rubel E.W. and Fritzsch B., Auditory system development: primary auditory neurons and their targets. Annu Rev Neurosci 2002 25: 51-101.
Rusch A., Erway L.C., Oliver D., et al., Thyroid hormone receptor beta-dependent expression of a potassium conductance in inner hair cells at the onset of hearing. Proc Natl Acad Sci USA 1998 95: 15758-15762.
Rusch A., Ng L., Goodyear R., et al., Retardation of cochlear maturation and impaired hair cell function caused by deletion of all known thyroid hormone receptors. J Neurosci 2001 21: 9792-9800.
Russel L.B., Definition of functional units in a small chromosomal segment of the mouse and its use in interpreting the nature of radiation-induced mutations. Mut Res 1971 11: 107-123.
Ryan A.F., Batcher S., Brumm D., et al., Cloning genes from an inner ear cDNA library. Arch Otolaryngol Head Neck Surg 1993 19: 1217-1220.
Salam A.A., Hafner F.M., Linder T.E., et al., A novel locus (DFNA23) for prelingual autosomal dominant nonsyndromic hearing loss maps to 14q21-q22 in a Swiss German kindred. Am J Hum Genet 2000 66: 1984-1988.
Sans A. and Chat M., Analysis of temporal and spatial patterns of rat vestibular hair cell differentiation by tritiated thymidine radioautography. J Comp Neurol 1982 206: 1-8.
Scanlan M.J., Williamson B., Jungbluth A., et al., Isoforms of the human PDZ-73 protein exhibit differential tissue expression. Biochim Biophys Acta 1999 1445: 39-52.
Schluter K., Jockusch B.M., and Rothkegel M., Profilins as regulators of actin dynamics. Biochim Biophys Acta 1997 1359: 97-109.
Schneider M.E., Belyantseva I.A., Azevedo R.B., et al., Rapid renewal of auditory hair bundles. Nature 2002 418: 837–838.
Schoenwaelder S.M. and Burridge K., Bidirectional signaling between the cytoskeleton and integrins. Curr Opin Cell Biol 1999 11: 274-286.
Schulze-Bahr E., Haverkamp W., Wedekind H., et al., Autosomal recessive long-QT syndrome (Jervell Lange-Nielsen syndrome) is genetically heterogeneous. Nat Genet 1997 17: 267-268.
Scott D.A., Wang R., Kreman T.M., et al., The Pendred syndrome gene encodes a chloride-iodide transport protein. Nat Genet 1999 21: 440-443.
Scott H.S., Kudoh J., Wattenhofer M., et al., Insertion of beta-satellite repeats identifies a transmembrane protease causing both congenital and childhood onset autosomal recessive deafness. Nat Genet 2001 27: 59-63.
Self T., Mahony M., Fleming J., et al., Shaker-1 mutations reveal roles for myosin VIIA in both development and function of cochlear hair cells. Development 1998 125: 557–566.
Self T., Sobe T., Copeland N.G., et al., Role of myosin VI in the differentiation of cochlear hair cells. Dev Biol 1999 214: 331–341.
Siemens J., Kazmierczak P., Reynolds A., et al., The Usher syndrome proteins cadherin 23 and harmonin form a complex by means of PDZ-domain interactions. Proc Natl Acad Sci USA 2002 99: 14946–14951.
Siemens J., Lillo C., Dumont R.A., et al., Cadherin 23 is a component of the tip link in hair-cell stereocilia. Nature 2004 428: 950–955.
Simmler M.C., Cohen-Salmon M., El-Amraoui A., et al., Targeted disruption of otog results in deafness and severe imbalance. Nat Genet 2000 24:139-143.
Skowron J.F., Bement W.M., and Mooseker M.S., Human brush border myosin-I and myosin-Ic expression in human intestine and Caco-2BBe cells. Cell Motil Cytoskeleton 1998 41: 308-324.
Smith R.J., Berlin C.I., Hejtmancik J.F., et al., Clinical diagnosis of the Usher syndromes. Usher Syndrome Consortium. Am J Med Genet 1994 50: 32-38.
Smith F.J., Morley S.M., and McLean W.H., A novel connexin 30 mutation in Clouston syndrome. J Invest Dermatol 2002 118: 530-532.
Sobkowicz H.M., Loftus J.M., and Slapnick S.M., Tissue culture of the organ of Corti. Acta Otolaryngol 1993 502: 3-36.
Sollner C., Rauch G.J., Siemens J., et al., Tubingen 2000 Screen Consortium. Mutations in cadherin 23 affect tip links in zebrafish sensory hair cells. Nature 2004 428: 955-959.
Soto-Prior A., Lavigne-Rebillard M., Lenoir M., et al., Identification of preferentially expressed cochlear genes by systematic sequencing of a rat cochlea cDNA library. Brain Res Mol Brain Res 1997 47: 1-10.
Souter M. and Forge A., Intercellular junctional maturation in the stria vascularis: possible association with onset and rise of endocochlear potential. Hear

Res 1998 119: 81-95.
Spicer S.S. and Schülte B.A., The fine structure of spiral ligament cells relates to ion return to the stria and varies with place-frequency. Hear Res 1996 100: 80-100.
Sulik K.K., Embryology of the ear. In Gorlin R.J., Toriello H.V., and Cohen M.M., Hereditary hearing loss and its syndromes. 1995 Oxford University Press, New York.
Takahashi K., Kamiya K., Urase K., et al., Caspase-3-deficiency induces hyperplasia of supporting cells and degeneration of sensory cells resulting in the hearing loss. Brain Res 2001 894: 359-357.
Takeda K., Inoue H., Tanizawa Y., et al., WFS1 (Wolfram syndrome 1) gene product: predominant subcellular localization to endoplasmic reticulum in cultured cells and neuronal expression in rat brain. Hum Mol Genet 2001 10: 477-484.
Tamayo M.L., Bernal J.E., Tamayo G.E., Frias J.L. Alvira G., Vergara O., Rodriguez V., Uribe J.I., and Silva J.C., Usher syndrome: results of a screening program in Colombia. Clin Genet 1991 40: 304-311.
Teubner B., Michel V., Pesch J., et al., Connexin30 (Gjb6)-deficiency causes severe hearing impairment and lack of endocochlear potential. Hum Mol Genet 2003 12: 13-21.
Tilney L.G., Derosier D.J., and Mulroy M.J., The organization of actin filaments in the stereocilia of cochlear hair cells. J Cell Biol 1980 86: 244–259.
Tilney L.G., Tilney M.S., and DeRosier D.J., Actin filaments, stereocilia, and hair cells: how cells count and measure. Annu Rev Cell Biol 1992a 8: 257-274.
Tilney L.G., Cotanche D.A., and Tilney M.S., Actin filaments, stereocilia and hair cells of the bird cochlea. VI. How the number and arrangement of stereocilia are determined. Development 1992b 116: 213–226.
Tominaga T., Sahai E., Chardin P., et al., Diaphanous-related formins bridge Rho GTPase and Src tyrosine kinase signaling. Mol Cell 2000 5: 13-25.
Torres M. and Giráldez F., The development of the vertebrate inner ear. Mech Dev 1998 71: 5-21.
Tsai H., Hardisty R.E., Rhodes C., et al., The mouse slalom mutant demonstrates a role for Jagged1 in neuroepithelial patterning in the organ of Corti. Hum Mol Genet 2001 10: 507-512.
Tsukita S. and Yonemura S., Cortical actin organization: lessons from ERM (ezrin/radixin/moesin) proteins. J Biol Chem 1999 274: 34507–34510.
Usami S., Takahashi K., Yuge I., et al., Mutations in the *COCH* gene are a frequent cause of autosomal dominant progressive cochlea-vestibular dysfunction, but not of Meniere's disease. Eur J Hum Genet 2003 11: 744-478.
Uziel A., Pujol R., Legrand C., et al., Cochlear synaptogenesis in the hypothyroid rat. Brain Res 1983 7: 295-301.
Uziel A., Periods of sensitivity to thyroid hormone during the development of the organ of Corti. Acta Otolaryngol Suppl 1986 429: 23-27.
Vahava O., Morell R., Lynch E.D., et al., Mutation in transcription factor POU4F3 associated with inherited progressive hearing loss in humans. Science 1998 279: 950-1953.
Vallet V., Chraibi A., Gaeggeler H.P., et al., An epithelial serine protease activates the amiloride-sensitive sodium channel. Nature 1997 389: 607-610.
Van Laer L., Huizing E.H., Verstreken M., et al., Nonsyndromic hearing impairment is associated with a mutation in DFNA5. Nat Genet 1998 20: 194-197.
van Wijk E., Krieger E., Kemperman M.H., et al., A mutation in the gamma actin 1 (ACTG1) gene causes autosomal dominant hearing loss (DFNA20/26). J Med Genet 2003 40: 879–884.
Varga R., Kelley P.M., Keats B.J., et al., Non-syndromic recessive auditory neuropathy is the result of mutations in the otoferlin (OTOF) gene. J Med Genet 2003 40: 45-50.
Velculescu V.E., Zhang L., Vogelstein B., et al., Serial analysis of gene expression. Science 1995 270: 484-487.
Verhoeven K., Van Laer L., Kirschhofer K., et al., Mutations in the human alpha-tectorin gene cause autosomal dominant non-syndromic hearing impairment. Nat Genet 1998 19: 60-62.
Verpy E., Leibovici M., Zwaenepoel I., et al., A defect in harmonin, a PDZ domain-containing protein expressed in the inner ear sensory hair cells, underlies Usher syndrome type 1C. Nat Genet 2000 26: 51-55.
Verpy E., Masmoudi S., Zwaenepoel I., et al., Mutations in a new gene encoding a protein of the hair bundle cause non-syndromic deafness at the DFNB16 locus. Nat Genet 2001 29: 345-349.
Veske A., Oehlmann R., Younus F., et al., Autosomal recessive non-syndromic deafness locus (DFNB8) maps on chromosome 21q22 in a large consanguineous kindred from Pakistan. Hum Mol Genet 1996 5: 165-168.
Vie M.P., Evrard C., Osty J., et al., Purification, molecular cloning, and functional expression of the human nicodinamide-adenine dinucleotide phosphate-regulated thyroid hormone-binding protein. Mol Endocrinol 1997 11: 1728-1736.
Vikkula M., Mariman E.C., Lui V.C., et al., Autosomal dominant and recessive osteochondrodysplasias associated with the COL11A2 locus. Cell 1995 80: 431-437.
Vincent C., Kalatzis V., Abdelhak S., et al., BOR and BO syndromes are allelic defects of EYA1. Eur J Hum Genet 1997 5: 242-6.
Vreugde S., Erven A., Kros C.J., et al., Beethoven, a mouse model for dominant, progressive hearing loss DFNA36. Nat Genet 2002 30: 257-258.
Vuagniaux G., Vallet V., Jaeger N.F., et al., Activation of the amiloride-sensitive epithelial sodium channel by the serine protease mCAP1 expressed in a mouse

cortical collecting duct cell line. J Am Soc Nephrol 2000 11: 828-834.
Wallis D., Hamblen M., Zhou Y., et al., The zinc finger transcription factor Gfi1, implicated in lymphomagenesis, is required for inner ear hair cell differentiation and survival. Development 2003 130: 221-232.
Walsh T., Walsh V., Vreugde S., et al., From flies' eyes to our ears: mutations in a human class III myosin cause progressive nonsyndromic hearing loss DFNB30. Proc Natl Acad Sci USA 2002 99: 7518-7523.
Wang A., Liang Y., Fridell R.A., et al., Association of unconventional myosin MYO15 mutations with human nonsyndromic deafness DFNB3. Science 1998b 280: 1447–1451.
Wasserman S., FH proteins as cytoskeletal organizers. Trends Cell Biol 1998 8: 111-115.
Watanabe N., Madaule P., Reid T., et al., p140mDia, a mammalian homolog of Drosophila diaphanous, is a target protein for Rho small GTPase and is a ligand for profilin. EMBO J 1997 16: 3044-3056.
Watanabe N., Kato T., Fujita A., et al., Cooperation between mDia1 and ROCK in Rho-induced actin reorganization. Nat Cell Biol 1999 1: 136-143.
Wattenhofer M., Di Iorio M.V., Rabionet R., et al., Mutations in the TMPRSS3 gene are a rare cause of childhood nonsyndromic deafness in Caucasian patients. J Mol Med 2002 80: 124-131.
Wayne S., Robertson N.G., DeClau F., et al., Mutations in the transcriptional activator EYA4 cause late-onset deafness at the DFNA10 locus. Hum Mol Genet 2001 10: 195-200.
Weber T., Zimmermann U., Winter H., et al., Thyroid hormone is a critical determinant for the regulation of the cochlear motor protein prestin. Proc Natl Acad Sci USA 2002 99: 2901-2906.
Weil D., Blanchard S., Kaplan J., et al., Defective myosin VIIA gene responsible for Usher syndrome type 1B. Nature 1995 374: 60-61.
Weil D., Levy G., Sahly I., et al., Human myosin VIIA responsible for the Usher 1B syndrome: a predicted membrane-associated motor protein expressed in developing sensory epithelia. Proc Natl Acad Sci USA 1996 93: 3232-3237.
Weil D., Kussel P., Blanchard S., et al., The autosomal recessive isolated deafness, DFNB2, and the Usher 1B syndrome are allelic defects of the myosin-VIIA gene. Nat Genet 1997 16: 191-3.
Weil D., El-Amraoui A., Masmoudi S., et al., Usher syndrome type I G (USH1G) is caused by mutations in the gene encoding SANS, a protein that associates with the USH1C protein, harmonin. Hum Mol Genet 2003 12: 463–471.
Weiss S., Gottfried I., Mayrose I., et al., The DFNA15 deafness mutation affects POU4F3 protein stability, localization, and transcriptional activity. Mol Cell Biol 2003 23: 7957-7964.
Wells A.L., Lin A.W., Chen L.Q., et al., Myosin VI is an actin-based motor that moves backwards. Nature 1999 401: 505–508.
Wes P.D., Xu X.Z., Li H.S., et al., Termination of phototransduction requires binding of the NINAC myosin III and the PDZ protein INAD. Nat Neurosci 1999 25: 447-453.
Wilcox E.R. and Fex J., Construction of a cDNA library from microdissected guinea pig crista ampullaris. Hear Res 1994 73: 65-66.
Wilcox E.R., Burton Q.L., Naz S., et al., Mutations in the gene encoding tight junction claudin-14 cause autosomal recessive deafness DFNB29. Cell 2001 104: 165-172.
Xia J.H., Liu C.Y., Tang B.S., et al., Mutations in the gene encoding gap junction protein beta-3 associated with autosomal dominant hearing impairment. Nat Genet 1998 20: 370-373.
Xia A., Kikuchi T., Hozawa K., et al., Expression of connexin 26 and Na,K-ATPase in the developing mouse cochlear lateral wall: functional implications. Brain Res 1999 846: 106-111.
Xiang M., Maklad A., Pirvola U., et al., Brn3c null mutant mice show long-term, incomplete retention of some afferent inner ear innervation. BMC Neurosci 1995 4: 2.
Xiang M., Gan L., Li D., et al., Essential role of POU-domain factor Brn-3c in auditory and vestibular hair cell development. Proc Natl Acad Sci USA 1997 94: 9445-9450.
Xiang M., Gao W.Q., Hasson T., et al., Requirement for Brn-3c in maturation and survival, but not in fate determination of inner ear hair cells. Development 1998 125: 3935-3946.
Yasunaga S., Grati M., Cohen-Salmon M., et al., A mutation in OTOF, encoding otoferlin, a FER-1-like protein, causes DFNB9, a nonsyndromic form of deafness. Nat Genet 1999 21: 363-369.
Yasunaga S., Grati M., Chardenoux S., et al., OTOF encodes multiple long and short isoforms: genetic evidence that the long ones underlie recessive deafness DFNB9. Am J Hum Genet 2000 67: 591-600.
Yoshida A., Hisatome I., Taniguchi S., et al., Mechanism of iodide/chloride exchange by pendrin. Endocrinology 2004 145: 4301-4308.
Yoshino T., Sato E., Nakashima T., et al., The immunohistochemical analysis of pendrin in the mouse inner ear. Hear Res 2004 195: 9-16.
Young T.L., Ives E., Lynch E., et al., Non-syndromic progressive hearing loss DFNA38 is caused by heterozygous missense mutation in the Wolfram syndrome gene WFS1. Hum Mol Genet 2001 10: 2509-2514.
Yu C., Meng X., Zhang S., et al., A 3-nucleotide deletion in the polypyrimidine tract of intron 7 of the DFNA5 gene causes nonsyndromic hearing impairment in a Chinese family. Genomics 2003 82: 575-579.
Zelante L., Gasparini P., Estivill X., et al., Connexin26

mutations associated with the most common form of non-syndromic neurosensory autosomal recessive deafness (DFNB1) in Mediterraneans. Hum Mol Genet 1997 6: 1605-1609.
Zhang N., Martin G.V., Kelley M.W., et al., A mutation in the Lunatic fringe gene suppresses the effects of a Jagged2 mutation on inner hair cell development in the cochlea. Curr Biol 2000 10: 659-662.
Zheng J.L. and Gao W.Q., Overexpression of Math1 induces robust production of extra hair cells in postnatal rat inner ears. Nat Neurosci 2000 3: 580-586.
Zheng J.L., Shou J., Guillemot F., et al., Hes1 is a negative regulator of inner ear hair cell differentiation. Development 2000a 127: 4551-60.
Zheng L., Sekerkova G., Vranich K., et al., The deaf jerker mouse has a mutation in the gene encoding the espin actin-bundling proteins of hair cell stereocilia and lacks espins. Cell 2000b 102: 377-85.
Zheng J., Shen W., He D.Z., et al., Prestin is the motor protein of cochlear outer hair cells. Nature 2000c 405: 149-55.
Zhu M., Yang T., Wei S., et al., Mutations in the gamma-actin gene (ACTG1) are associated with dominant progressive deafness (DFNA20/26). Am J Hum Genet 2003 73: 1082–1091.
Zine A., Van De Water T.R., and de Ribaupierre F., Notch signaling regulates the pattern of auditory hair cell differentiation in mammals. Development 2000 127: 3373-3383.
Zine A., Aubert A., Qiu J., et al., Hes1 and Hes5 activities are required for the normal development of the hair cells in the mammalian inner ear. J Neurosci 2001 21: 4712-4720.
Zwaenepoel I., Mustapha M., Leibovici M., et al., Otoancorin, an inner ear protein restricted to the interface between the apical surface of sensory epithelia and their overlying acellular gels, is defective in autosomal recessive deafness DFNB22. Proc Natl Acad Sci USA 2002 99: 6240-624.

Chapter 2

Cloning, characterization, and mRNA expression analysis of novel human fetal cochlear cDNAs

M.W.J. Luijendijk[a], T.J.R. van de Pol[a], G. van Duijnhoven[a], A.I. den Hollander[a], J. ten Caat[a], V. van Limpt[a], H.G. Brunner[a], H. Kremer[b], and F.P.M. Cremers[a]

[a] Department of Human Genetics, University Medical Centre Nijmegen, P.O. Box 9101, 6500 HB Nijmegen, The Netherlands
[b] Department of Otorhinolaryngology, University Medical Centre Nijmegen, P.O. Box 9101, 6500 HB Nijmegen, The Netherlands

Published in: Genomics 2003 82: 480-490

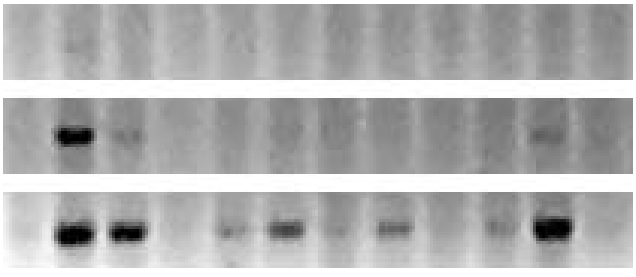

2.1 Abstract

To identify novel genes that are expressed specifically or preferentially in the cochlea, we constructed a cDNA library enriched for human cochlear cDNAs using a suppression subtractive hybridisation technique. We analysed 2640 clones by sequencing and BLAST similarity searches. One hundred and fifty-five different cDNA fragments mapped in nonsyndromic hearing impairment loci for which the causative gene has not been cloned yet. Approximately 30% of the clones show no similarity to any known human gene or expressed sequence tag (EST). Clones mapping in nonsyndromic deafness loci and a selection of clones that represent novel ESTs were analysed by reverse transcriptase-polymerase chain reaction (RT-PCR) of RNA derived from 12 human fetal tissues. Our data suggest that a quarter of the novel genes in our library are preferentially expressed in fetal cochlea. These may play a physiologically important role in the hearing process and represent candidate genes for hereditary hearing impairment.

Keywords: Cochlea; cDNA subtraction; Hearing impairment; mRNA expression profiling

2.2 Introduction

Hearing is a complex process requiring highly specialized structures and mechanisms. The most intricate structure involved in hearing is the cochlea, which processes mechanical sound waves into a signal that can be perceived by the brain. Over the past years, many discoveries have been made regarding the structure and function of the cochlea by studying the molecular defects underlying hearing impairment and deafness (Morton 2002). Still, many gaps remain in our understanding of the molecular processes involved in hearing.

Hearing loss is the most common sensory disorder in the human population. One in 1000 children is born deaf and approximately equal numbers of cases are attributed to environmental and genetic factors (Morton 1991, Gorlin et al. 1995). Of the cases attributed to genetic factors, about 70% are classified as nonsyndromic, i.e., deafness without other obvious clinical features. Nonsyndromic hearing impairment can be further subdivided based on the mode of inheritance: ~77% of the cases are autosomal recessive, ~22% are autosomal dominant, ~1% are X-linked, and ~1% are due to mitochondrial inheritance. Up to now, 39 autosomal dominant loci (DFNA), 33 autosomal recessive loci (DFNB), and 5 X-linked loci (DFN) have been described and 31 genes underlying nonsyndromic hearing impairment have been identified (http://www.uia.ac.be/DNAlab/hhh/) (Morton 2002). Very few of these genes show expression that is restricted to the cochlea (Verpy et al. 2001, Zwaenepoel et al. 2002). It is possible that cochlea-specific genes have been refractory to cloning because their mRNA is present at very low levels, present only in specific cell types of the inner ear, e.g., inner or outer hair cells, or present in very small developmental time windows. In view of the complex nature of the process of hearing, it can be expected that the identification of novel genes expressed exclusively or predominantly in the cochlea will contribute greatly to the understanding of cochlear development and homeostasis and the pathogenesis of

hearing impairment.

To identify genes underlying hereditary hearing impairment, the most common approach involves genetic linkage studies in families with hearing impairment and subsequent positional cloning of the mutated gene. However, the candidate gene approach could facilitate this kind of research greatly. This is especially true for small families and sporadic patients in which linkage analysis cannot be performed.

To isolate novel cochlear-expressed genes, we constructed a cochlea-enriched complementary DNA (cDNA) library. We used a polymerase chain reaction (PCR)-based suppression subtractive hybridisation technique (Diatchenko et al. 1996). This normalizes sequence abundance and achieves enrichment for differentially expressed cDNAs by a single round of suppression subtractive hybridisation. Subtraction was performed against a mixture of cDNAs from several tissues. This method has already proven its strength in research of retinal disorders (den Hollander et al. 1999). Here we describe the sequence analysis and mapping of 2640 cDNAs. In addition, we performed semiquantitative reverse transcriptase polymerase chain reaction (RT-PCR) to evaluate mRNA expression levels of selected clones in a panel of human fetal tissues.

2.3 Results

2.3.1. Subtraction efficiency analysis

Successful suppression subtractive hybridisation decreases the prevalence of ubiquitously expressed (housekeeping) genes and increases the prevalence of tissue-specific genes in a cDNA library. The effectiveness of the technique was tested by RT-PCR of *GAPDH*, *TECTA*, and C1B10 on subtracted and unsubtracted cDNA, taking samples after 23, 28, and 33 cycles of PCR. The housekeeping gene *GAPDH* displays a significant decrease in the amount of transcript present after subtraction compared to before subtraction (fig. 1). In contrast, the amount of transcript of *TECTA*, a gene previously described to be expressed specifically in the cochlea (Legan et al. 1997), increased after subtraction. After subtraction, a *TECTA* cDNA product is clearly visible after 28 and 33 cycles of PCR, whereas before subtraction, no band is visible even after 33 cycles of PCR. As a control, we also used clone C1B10, which was isolated during this study and showed preferential expression in the cochlea. Before subtraction, C1B10 cDNA product is only detectable after 33 cycles of PCR. After subtraction a product is clearly visible after 28 and 33 cycles.

2.3.2 Sequence analysis of cDNAs

The sequences of 2640 clones from the cochlea-enriched cDNA library were determined and the clones were shown to be represented by 1944 unique sequences. Clones were sequenced in one direction. Some clones contained a stretch of A's or T's that disturbed the sequencing process. In these cases the clones were sequenced in both directions. Often the full insert sequence could be determined by sequencing in one direction, but several insert sequences are not complete. The length of the sequences ranged from 59 to 699 bases with an average of 324 bases. These sequences were analysed by

comparing them to GenBank, EMBL, and human EST databases and nonhuman EST databases, using BLAST-analysis. The results of this analysis enabled localization of the majority of the clones in the human genome.

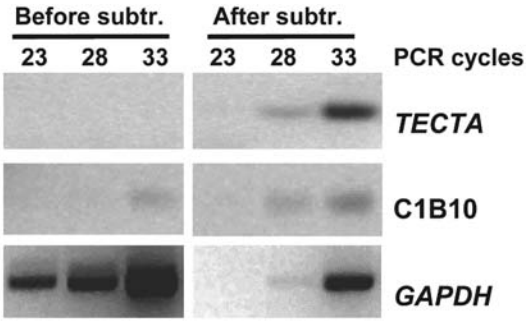

Figure 1. PCR of the subtracted and unsubtracted cochlea cDNA as a control for the suppression subtractive hybridisation technique. Control PCR products of *TECTA* and C1B10, a clone showing preferential expression in cochlea isolated from the human fetal cochlea cDNA library, as positive controls for enrichment, and *GAPDH*, as a positive control for subtraction, are shown. The control PCRs were performed on cDNA samples of human fetal cochlea. The left panel shows samples taken before cDNA subtraction; the right panel shows samples taken after subtraction. Samples were taken after the indicated number of PCR cycles.

Table 1. Results of BLAST-analysis of 2640 sequences derived from the cDNA library

Sequence analysis[a]	*Number of clones*	*Percentage of clones*	*Number of unique sequences*	*Percentage of unique sequences*
Similarity to known gene	784	29.7	424	21.8
Similarity to predicted gene	106	4.0	82	4.2
Similarity to EST(s) Unigene cluster	551	20.9	386	19.9
Similarity to other EST(s)	31	1.2	26	1.3
Similarity to sequence non-human organism	309	11.7	269	13.8
Novel ESTs[b]	788	29.8	691	35.5
Novel sequences[c]	71	2.7	66	3.4
Total	**2640**		**1944**	

[a]Clones were subdivided into seven categories as indicated.
[b]Clones have similarity to genomic DNA sequences but not to any other sequence.
[c]Clones have no similarity to any sequence.

BLAST-analysis showed that 29.7% of the clones (table 1) had significant similarity to a total of 330 different known human genes. Of these known genes, 92 were found in the library more than once and 46 were found more than twice (table 2). The gene most highly represented in the cDNA library is *osteoglycin* (*OGN*; also named *osteoinductive factor* (*OIF*)) (table 2). Eighty-nine clones from the cDNA library are derived from *OGN*, the protein product of which is known to induce ectopic bone formation in conjunction with the transforming growth factor TGFB1 or TGFB2. The next most frequently found genes are *COL1A2* (46 clones), *COL2A1* (39 clones), *DIO2* (31 clones), and *COL9A1* (26 clones). Among the 22 most highly represented genes, 2 are known to be involved in hereditary nonsyndromic hearing impairment. *COCH*

is involved in DFNA9 (Robertson et al. 1998) and *POU3F4* is involved in DFN3 (de Kok et al. 1995). *OTOR* (Robertson et al. 2000), a gene that was recently identified because of its presence in a human fetal cochlear cDNA library, was also among the 22 most prevalent genes. Other deafness-associated genes represented in our library are *COL1A1* (15 clones), *COL11A1* (13 clones), *COL3A1* (9 clones), *SOX9* (3 clones), *KCNQ1* (potassium voltage-gated channel, KQT-like subfamily member 1, NM_000218) (2 clones), and *MANBA* (mannosidase, βA, lysosomal, NM_005908) (1 clone).

Table 2. Known human genes represented more than twice in the human fetal cochlear cDNA library

GenBank ID	*Gene*	*Protein description*	*Frequency*
AF202167	*OGN/OIF*	osteoglycin / osteo inductive factor / mimecan	89
NM000089	*COL1A2*	collagen 1A2	46
NM001844	*COL2A1*	collagen 2A1	39
AF093774	*DIO2*	deiodinase iodothyronine type 2	31
NM001851	*COL9A1*	collagen 9A1	26
AF193855	*ZIC2*	zinc finger protein of cerebellum	22
NM00307	*POU3F4*	POU domain transcription factor 3F4	16
NM000088	*COL1A1*	collagen 1A1	15
NM001854	*COL11A1*	collagen 11A1	13
NM000090	*COL3A1*	collagen 3A1	9
NM000618	*IGF1*	insulin-like growth factor 1	8
NM012431	*SEMA3E*	sema domain immunoglobulin domain secreted 3E	7
NM003107	*SOX4*	SRY (sex determining region 4) box 4	7
NM001852	*COL9A2*	collagen 9A2	6
NM004967	*IBSP*	integrin-binding sialoprotein, bone sialoprotein II	6
NM002356	*MARCKS*	myristoylated alanine-rich protein kinase C substrate	6
AF217500	*MORF*	histone acetyltransferase	6
NM020157	*OTOR*	Otoraplin	6
NM004086	*COCH*	coagulation factor C, cochlin	5
NM014483	*RBMS3*	RNA binding motif single stranded interacting protein 3	5
NM004598	*SPARC/ SPOCK*	secreted protein, acidic, cysteine-rich (osteonectin)	5
NM003380	*VIM*	vimentin, cytoskeletal element	5
NM000484	*APP*	amyloid beta protein	4
U85962	*CREBBP*	cAMP responsive element binding protein binding protein	4
NM006597	*HSPA8*	heat shock 70kD protein	4
NM000304	*PMP22*	peripheral myelin protein 22	4
NM007168	*ABCA8*	ATP-binding cassette, subfamily 1 member 8	3
NM001614	*ACTG1*	actin gamma 1	3
NM015928	*AS3*	androgen-induced prostate proliferative shutoff associated protein	3
AB018321	*ATP1A2*	ATPase, Na^+/K^+ transporting, alpha 2 polypeptide	3
NM022845	*CBFB*	core binding factor beta	3
NM001892	*CSNK1A1*	casein kinase 1 alpha 1	3

AF042345	*EVI5*	ecotropic viral integration site 5	3
NM000146	*FTL*	ferritin L chain	3
NM005348	*HSPCA*	heat shock 90kD protein 1 alpha	3
NM014333	*IGSF4*	immunoglobulin superfamily member 4	3
NM016269	*LEF1*	lymhoid enhancer binding factor-1	3
NM006791	*MRG15*	MORF related gene 15	3
NM005385	*NKTR*	cyclophilin related protein, natural killer tumor recognition sequence	3
NM006206	*PDGFRA*	platelet-derived growth factor receptor alpha	3
NM000021	*PSEN1*	presenilin 1	3
NM003017	*SFRS3*	splicing factor arginine/serine-rich	3
NM000345	*SNCA*	alpha-synuclein; precursor of non-A beta component of Alzheimer's disease amyloid	3
NM000346	*SOX9*	SRY (sex-determining region Y)-box 9	3
AB038518	*SRCL*	scavenger receptor with C-type lectin type I	3
NM003257	*TJP1*	tight junction protein 1 (zona occludens 1)	3

The cDNA fragments resulting from the suppression subtractive hybridisation cloning procedure are *Rsa*I restriction fragments. The first-strand cDNA was synthesized using an oligo(dT) primer, which could possibly result in an overrepresentation of cDNA fragments from the 3' end of the cochlear genes. To obtain an impression of the distribution and size of *Rsa*I cDNA fragments, we analysed the 22 most frequently found genes. Multiple *Rsa*I cDNA fragments can be derived from one gene. The gene represented by the highest number of different *Rsa*I fragments is *OGN* (fig. 2). All six *OGN Rsa*I cDNA fragments longer than 100 bp were each found at least six times. The *Rsa*I fragments shorter than 100 bp were not found (four fragments) or found only once (one fragment). This absence of *Rsa*I fragments from the library is due to the purification protocol (Advantage cDNA Pure) used after cDNA digestion in which fragments shorter than 200 bp are lost.

The longest mRNA transcript that can be reconstructed by sequence comparison of the *Rsa*I fragments was 2575 bp long and derived from the *OGN* gene. The average length of the *Rsa*I fragments in this study was 347 bp. The longest fragment measured 1280 bp and was derived from *COL1A2*; the shortest fragment measured 59 bp and was derived from *COL2A1*.

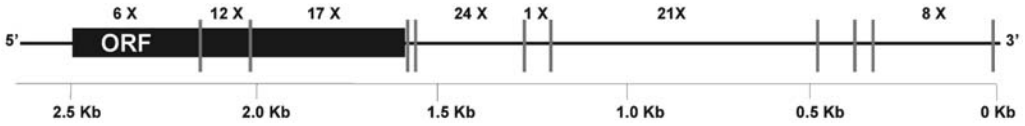

Figure 2. *Rsa*I cDNA fragment representation of the *OGN* gene. The distribution of *Rsa*I restriction sites (vertical bars) is shown along the sequence of *OGN* and the number of clones representing each *Rsa*I fragment is shown above each fragment. The open reading frame (ORF) is shown as a black box.

Table 3. The number of clones and unique sequences mapping in known nonsyndromic deafness loci for which the causative gene is not known

Deafness locus	*Map location*[a]	*Flanking markers*[a]	Interval size[a]	*Number of clones*	*Number of unique sequences*
DFNA4	19q13	D19S208-ApoC2	~9.8 Mb	4	4
DFNA7	1q21-q23	D1S104-D1S466	~18.6 Mb	17	15
DFNA16	2q24	D2S2380-D2S335	~8.7 Mb	20	16
DFNA23	14q21-q22	D14S980-D14S1046	~8.0 Mb	6	6
DFNA25	12q21-q22	D12S327-D12S84	~13.8 Mb	13	5
DFNA26	17q25	D17S784-D17S970	~8.5 Mb	8	5
DFNA27	4q12	D4S428-D4S392	~14.6 Mb	10	7
DFNA30	15q26	D15S130-D15S127	~3.6 Mb	4	4
DFNA34	1q44	D1S102-D1S3739	~4.7 Mb	7	5
DFNB5	14q12	D14S253-D14S79	~5.6 Mb	3	3
DFNB13	7q34-q36	D7S2468-D7S2439	~12.1 Mb	6	6
DFNB14	7q31	D7S527-D7S3074	~11.9 Mb	7	7
DFNB17	7q31	D7S486-D7S2529	~6.5 Mb	3	2
DFNB19	18p11	D18S62-D18S378	~5.3 Mb	16	11
DFNB23	10p11.2-q21	D10S220-D10S1652	~12.0 Mb	4	4
DFNB24	11q23	D11S2017-D11S1992	~8.3 Mb	17	14
DFNB25	4p15.3-q12	D4S1632-D4S428	~25.3 Mb	14	11
DFNB26	4q31	D4S424-D4S1604	~1.8 Mb	6	4
DFNB27	2q23-q31	D2S2157-D2S2273	~18.5 Mb	7	7
DFNB28	22q13	D22S1045-D22S282	~3.8 Mb	6	5
DFN4	Xp21.2	DXS992-DXS1068	~7.8 Mb	10	7
DFN6	Xp22	DXS7108-DXS7105	~12.1 Mb	5	4
DFNM1	1q24	D1S2658-D1S2790	~4.7 Mb	4	3
Total				**197**	**155**

[a]Because of sequence gaps and rearrangements in the human genome sequence the positions of markers and clones may vary.

2.3.3 Expression profile analysis of clones located in known nonsyndromic deafness loci using semiquantitative RT-PCR

Clones were mapped in the human genome using the results of BLAST-analysis and several databases. We compared the map location of the clones with the location of known nonsyndromic deafness loci for which the gene responsible has not yet been identified (http://www.uia.ac.be/ dnalab/hhh/). In total, 197 clones from our library representing 155 unique sequences were found to be located within known nonsyndromic deafness loci (table 3). Of the 155 unique sequences, 72 (46.5%) showed similarity to a genomic sequence but not to any other sequence and are therefore considered novel ESTs, 52 (33.5%) showed similarity to a human EST and 30 (19.3%) showed similarity to a known or predicted gene (table 4).

Semiquantitative RT-PCR was used to investigate if a sequence was specifically or preferentially expressed in human fetal cochlea. All cDNA was tested for genomic DNA contamination with primers for the housekeeping genes *GAPDH* and *GUSB* spanning

one or more introns. No contamination was detected, and equal expression was found across all tissues tested. To test the effectiveness of the semiquantitative RT-PCR, we determined the expression pattern of three genes that are involved in nonsyndromic hearing impairment and/or known to show a distinctive expression pattern, *POU3F4* (de Kok et al. 1995), *TECTA* (Verhoeven et al. 1998), and *OTOR* (Robertson et al. 2000).

Table 4. Results of sequence analysis of clones located in nonsyndromic deafness loci

Sequence analysis[a]	*Number of clones*	*%*	*Number of unique sequences*	*%*	*Number of clones preferentially expressed in cochlea*
Similarity to known gene	44	22.3	25	16.1	5
Similarity to predicted gene	5	2.5	5	3.2	-
Similarity to EST(s) from Unigene cluster	44	22.3	36	23.2	8
Similarity to other EST(s)	18	9.1	16	10.3	3
Similarity to sequence non-human organism	1	0.5	1	0.6	-
Novel ESTs	85	43.1	72	46.5	29
Total	**197**		**155**		**45**

[a]Clones located in nonsyndromic deafness loci were subdivided into seven categories as indicated.

POU3F4 shows distinctive expression in fetal cochlea, fetal spinal cord, fetal brain, and fetal kidney after 25 and 30 cycles of PCR (fig. 3A). After 35 cycles, expression can also be detected in other tissues. This is in accordance with what has been found in the developing rat embryo by in situ hybridisation (Le Moine and Young 1992). Expression was present in the brain, the central nervous system, and the otic vesicles. There is no evidence that in rat *POU3F4* is expressed in the developing kidney. However, expression of *POU3F4* in human fetal kidney and human fetal brain has been shown by Northern blot analysis (personal communication, Y.J.M. de Kok, and F.P.M.C., unpublished data). *TECTA* shows highest expression in fetal cochlea after 25, 30, and 35 cycles of PCR, but expression can also be detected in fetal spinal cord and fetal tongue after 25 cycles (fig. 3A). These results can be compared to what has been found by Northern blot analysis of tissues from 2- to 3-dayold mice (Legan et al. 1997). Expression of the *TECTA* gene was shown to be restricted to cochlea; no transcripts could be detected in any of the other tissues tested, which did not include spinal cord or tongue. *OTOR* shows a very distinct expression pattern. The expression in fetal cochlea is clearly the highest after 30 and 35 cycles of PCR, however, a band can also be detected in fetal brain and fetal tongue after 30 cycles and in fetal colon, fetal stomach, fetal lung, and fetal skeletal muscle after 35 cycles of PCR (fig. 3A). The expression of *OTOR*, found with semiquantitative RT-PCR of human fetal tissues as described, is similar to what has been published. With Northern blot analysis of human fetal tissues, expression could clearly be seen in cochlea, however, expression could not be detected in brain or tongue (Robertson et al. 2000). Using 35 cycles of semiquantitative RT-PCR on mouse tissues, expression of *OTOR* could also clearly be detected in cochlea (Cohen-Salmon et al. 2000).

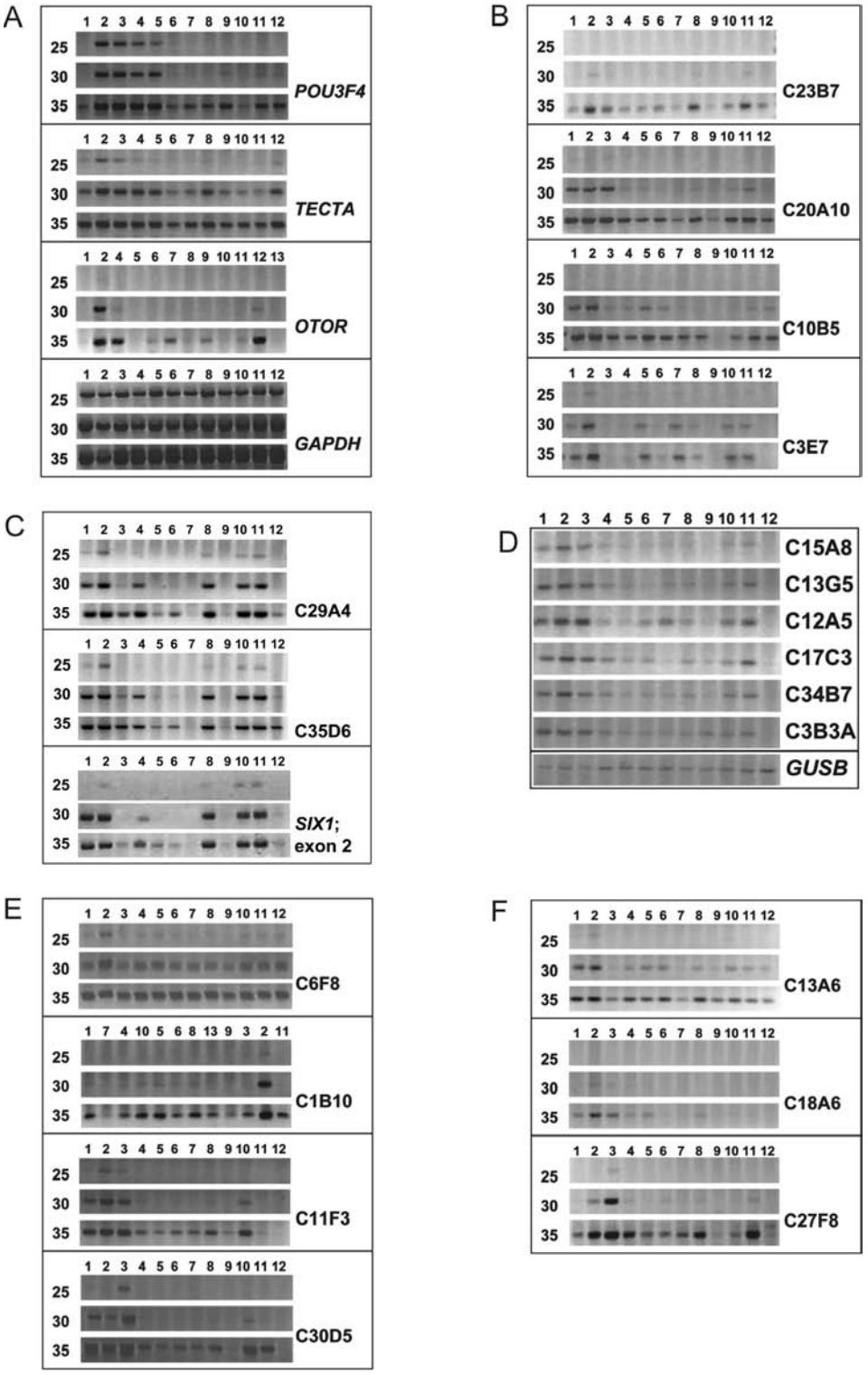
A
1 2 3 4 5 6 7 8 9 10 11 12
25
30
35
POU3F4
TECTA
1 2 4 5 6 7 8 9 10 11 12 13
OTOR
GAPDH
B
C23B7
C20A10
C10B5
C3E7
C
C29A4
C35D6
SIX1; exon 2
D
C15A8
C13G5
C12A5
C17C3
C34B7
C3B3A
GUSB
E
C6F8
1 7 4 10 5 6 8 13 9 3 2 11
C1B10
C11F3
C30D5
F
C13A6
C18A6
C27F8

Figure 3. Semiquantitative RT-PCR analysis of known genes and clones isolated from the cochlea-enriched cDNA library. Samples were taken after 25, 30, and 35 cycles of PCR, except for (D), in which samples were only taken after 25 cycles. The mRNA employed for RT-PCR analysis was isolated from the following human tissues: (A) (1) fetal eye, (2) fetal cochlea, (3) fetal spinal cord, (4) fetal brain, (5) fetal kidney, (6) fetal colon, (7) fetal stomach, (8) fetal heart, (9) fetal lung, (10) fetal liver, (11) fetal skeletal muscle, (12) fetal tongue, and (13) placenta. (B through F) (1) fetal eye, (2) fetal cochlea, (3) fetal brain, (4) fetal kidney, (5) fetal colon, (6) fetal stomach, (7) fetal heart, (8) fetal lung, (9) fetal liver, (10) fetal skeletal muscle, (11) fetal tongue, and (12) placenta. (A) Known genes *POU3F4, TECTA, OTOR,* and *GAPDH.* (B) Four clones localized in nonsyndromic deafness loci. (C) Exon 2 of the *SIX1* gene and two colocalizing clones in the DFNA23 locus. (D) Six clones that form a cluster derived from chromosome 21q21.1. As a positive control RT-PCR analysis of *GUSB* was performed. (E) Four clones that have similarity to up to five ESTs preferentially derived from brain or cochlea. (F) Three novel clones. Clone C13A6 has overlap with a predicted exon in the Human Genome Project Working Draft (June 2002 freeze) and clones C18A6 and C27F8 are represented by more than two sequences.

Expression could also be detected in brain and some other tissues that were not tested in our study. Interestingly, expression of *OTOR* in the eye cannot be detected with RT-PCR in human, but could be detected with RT-PCR in mouse. In summary, our results show that the expression patterns of these genes in human fetal tissues determined by semiquantitative RT-PCR are comparable with previously published expression data for these genes.

Semiquantitative RT-PCR analysis was performed for the 155 unique sequences mapping in known nonsyndromic deafness loci. Forty-five of these sequences (29%) showed preferential expression as either their cDNA PCR product is more abundant in fetal cochlea than in other fetal tissues analysed or their cDNA PCR product is more abundant in fetal cochlea and a small subset of other tissues than in other fetal tissues analysed (table 4). Representative results are shown for four of these clones (fig. 3B). Clone C23B7 is localized in the DFNB5 locus (Fukushima et al. 1995) and shows weak expression in fetal cochlea, fetal lung, and fetal tongue after 30 cycles of PCR. After 35 cycles of PCR, this clone is preferentially expressed in fetal cochlea, fetal lung, and fetal tongue. Clone C20A10, localized in the DFNB14 locus (Mustapha et al. 1998), shows preferential expression in fetal eye, fetal cochlea, and fetal brain after 30 cycles of PCR. After 30 cycles of PCR, clone C10B5, localized in the DFNB27 region (Pulleyn et al. 2000), shows preferential expression in fetal cochlea and to a lesser degree in fetal eye and fetal colon. C3E7 is derived from the DFN6 interval (Del Castillo et al. 1996) on the X chromosome. After 25 cycles of PCR, a vague band can already be seen in fetal cochlea. After 30 cycles of PCR, the clone shows preferential expression in fetal cochlea, but bands are also clearly visible in fetal eye, fetal colon, fetal heart, fetal skeletal muscle, and fetal tongue.

Expression profiling of two clones colocalizing in the DFNA23 region, C29A4 and C35D6, yielded very similar patterns of expression (fig. 3C). After 25 cycles of PCR, expression is shown in fetal eye, fetal cochlea, fetal lung, fetal skeletal muscle, and fetal tongue, with most pronounced expression in fetal cochlea. After 30 cycles, both clones show expression in fetal eye, fetal cochlea, fetal kidney, fetal lung, fetal skeletal muscle, and fetal tongue. These clones were found to be located 3' of the *SIX1* gene at 750 bp

from the last coding exon. To investigate whether the clones are part of the *SIX1* gene, a pattern of expression of exon 2 of the *SIX1* gene was determined (fig. 3C). *SIX1* shows expression in the same tissues as the cDNA clones, which strongly suggests that the clones indeed belong to the transcriptional unit of the *SIX1* gene. These results render *SIX1* a good candidate gene for DFNA23.

2.3.4. Expression profile analysis of clones that form a cluster

The cDNA cloning procedure used to construct the cDNA library yields nonoverlapping RsaI cDNA fragments. Therefore cluster-analysis could not be performed by analysing sequence overlap between clones. This complicates the assessment of whether clones belong to the same gene.

To obtain more information about the relationship between the clones located near each other, we performed expression pattern analysis for several of these clusters. This is exemplified by the analysis of a cluster of RsaI fragments that was localized on chromosome 21q21.1 (fig. 3D). The cluster consists of 20 sequences from which six representative RsaI fragments were selected for semiquantitative RT-PCR. All selected clones clearly show preferential expression in fetal eye, fetal cochlea, fetal brain, and fetal tongue after 25 cycles of PCR, indicating that these clones are either derived from the same gene or from closely related neighbouring genes with coordinate expression.

2.3.5 Expression profile analysis of clones that represent novel genes

The majority of clones that are not derived from a known gene (70.3%, 1856 clones) (table 1) are not located in a known locus for nonsyndromic deafness. These clones can be subdivided into two groups: (1) clones that show similarity to a coding sequence present in GenBank; predicted genes, ESTs, and nonhuman coding sequences, and (2) clones that do not show similarity to any coding sequence present in GenBank; novel ESTs and novel sequences. To obtain more insight in the expression of these clones that are likely to represent novel genes, we performed mRNA expression profile analysis.

From the first group consisting of 763 unique sequences, we selected 60 clones that show similarity to up to five ESTs preferably derived from brain, fetal brain, or fetal cochlea. Twenty clones showed preferential expression in fetal cochlea and six clones showed preferential expression in fetal brain (table 5). Three clones with preferential expression in fetal cochlea and one with preferential expression in fetal brain are shown in figure 3E. After 35 cycles of PCR, clone C6F8 shows expression in all tissues tested. However, after 25 and 30 cycles, the clone clearly exhibits a much higher level of expression in fetal cochlea compared to the other tissues. Clone C1B10 shows highest expression in fetal cochlea after 30 and 35 cycles of PCR. After 35 cycles, expression is also seen in other tissues. The expression of clone C11F3 is highest in fetal cochlea and fetal brain after 25 cycles. After 30 and 35 cycles, the clone is most highly expressed in fetal eye, fetal cochlea, fetal brain, and fetal skeletal muscle. Clone C30D5 is preferentially expressed in fetal brain after 25, 30, and 35 cycles of PCR. After 30 cycles, expression can also be detected in fetal eye, fetal cochlea, and fetal skeletal

muscle and expression can be seen in all other tissues except fetal liver and placenta after 35 cycles.

From the second group consisting of 757 unique clones, we selected 20 clones that either are represented by more than two clones or have overlap with an exon predicted in the Human Genome Project Working Draft (June 2002 freeze). Five clones showed preferential expression in fetal cochlea and two clones showed preferential expression in brain (table 5). Clone C13A6 has overlap with a predicted exon in the Human Genome Working Draft sequence and after 25, 30, and 35 cycles shows preferential expression in fetal cochlea and fetal eye (fig. 3F). The sequences of clone C18A6 and C27F8 are represented three times in the library. Clone C18A6 clearly shows preferential expression in fetal cochlea after 30 and 35 cycles of PCR (fig. 3F). However, after 35 cycles, expression can also be detected in other tissues. After 25 and 30 cycles, clone C27F8 is clearly preferentially expressed in fetal brain. After 30 cycles, expression can also be detected in fetal cochlea and fetal tongue and after 35 cycles, expression can be detected in almost all tissues (fig. 3F).

Of the 80 sequences representing novel genes in total, 25 (31.3%) showed preferential expression in fetal cochlea and 8 (10%) showed preferential expression in fetal brain (table 5).

Table 5. Results of expression profile analysis of clones that represent novel genes

Sequence analysis[a]	*Number of clones*	*%*	*Number of unique sequences*	*%*	*Number of clones preferentially expressed in cochlea*
Similarity to known gene	44	22.3	25	16.1	5
Similarity to predicted gene	5	2.5	5	3.2	-
Similarity to EST(s) from Unigene cluster	44	22.3	36	23.2	8
Similarity to other EST(s)	18	9.1	16	10.3	3
Similarity to sequence non-human organism	1	0.5	1	0.6	-
Novel ESTs	85	43.1	72	46.5	29
Total	**197**		**155**		**45**

2.4 Discussion

The aim of this study was to identify novel ESTs that are specifically or preferentially expressed in the human cochlea. Using fetal cochlear cDNA as tester and driver cDNAs derived from several other tissues, the suppression subtractive hybridisation technique resulted in a highly complex cDNA library, as evidenced by the fact that we isolated 1944 different cDNA clones among 2640 analysed. Cochlear cDNA libraries were previously constructed for rat (Ryan et al. 1993, Soto-Prior et al. 1997, Harter et al. 1999) and guinea pig (Wilcox and Fex 1992) and using a subtraction protocol for mouse (Cohen-Salmon et al. 1997), chicken (Killick et al. 1997, Heller et al. 1998), gerbil (Zheng et al. 2000), and zebrafish (Coimbra et al. 2002). Human cochlear cDNA libraries have been generated only without suppression subtractive hybridisation (Robertson et al. 1994, Jacob et al. 1998). In contrast to conventional subtraction methods and differential

hybridisation techniques previously used to isolate cochlea-specific genes (Robertson et al. 1994, Skvorak et al. 1999), suppression subtractive hybridisation allows the isolation of tissue-specific transcripts expressed at moderate or low levels in the tissue of interest. This has been demonstrated by the isolation of *PRES*, the motor protein of the cochlear outer hair cells (Zheng et al. 2000), from gerbil outer hair cells using a cDNA library constructed using suppression subtractive hybridisation (Zheng et al. 2000). Such transcripts are underrepresented in the collection of ESTs deposited in public databases.

About one-third of the cDNA clones of our library were novel and therefore not present among 14,850 ESTs derived from the fetal cochlear cDNA library constructed by Robertson et al. (1994) (http://hearing.bwh.harvard.edu/estinfo. HTM). Some of the novel ESTs may be the result of genomic DNA contamination. We have found that 1 of 13 novel ESTs selected for expression profile analysis was not expressed in any of the tissues in our panel. Since the absence of an RT-PCR product could be due to a very low transcript level in the tissues tested, our most pessimistic estimate is therefore that of the 691 unique novel EST sequences we have identified, 53 will be the result of genomic DNA contamination. However, according to semiquantitative RT-PCR analysis of a subset of clones representing novel genes, 31% are preferentially expressed in fetal cochlea. Hence, our library potentially contains a high number of novel cochlear cDNAs, a substantial fraction of which might have an important function in the cochlea.

2.4.1 Subtraction efficiency and evaluation of the cDNA library

The efficiency of cDNA suppression was clearly shown by the considerable decrease in the abundance of cDNA of the housekeeping gene *GAPDH* after subtraction. Enrichment for cochlea-specific genes is more difficult to evaluate because of the scarcity of cochlea-specific genes. Both *TECTA*, which by Northern blot analysis could be detected only in the inner ear (Legan et al. 1997), and C1B10, a cDNA clone isolated from the library showing preferential expression in cochlea, showed increased abundance of cDNA after the suppression subtraction procedure. Additional evidence for enrichment of cochlear clones is provided by the presence in our library of genes known to be involved in hearing impairment, e.g., *COCH*, *POU3F4*, and *KCNQ1*. Not unexpectedly, several other important deafness genes known to be expressed in many noncochlear tissues, such as *CX26* (Zhang and Nicholson 1989), *MYO7A* (Gibson et al. 1995), and *MYO15* (Wang et al. 1998), are not represented in the library. Collagen genes are highly represented in our library. Collagen molecules are synthesized in the developing cochlea and defects in, e.g., *COL1A2* (Pentinnen et al. 1975), *COL2A1* (Ahmed et al. 1991), *COL11A1* (Richards et al. 1996), and *COL11A2* (McGuirt et al. 1999), have been associated with deafness. The high abundance of collagen cDNA fragments in our library probably also is due to the absence of driver mRNAs derived from noncochlear bony tissues.

2.4.2 Expression profile analysis

To analyse the expression characteristics of a selected number of clones, we have used

a semiquantitative RT-PCR method, which is sensitive, fairly fast, and in our hands reproducible. Alternative high-throughput or more global analyses methods, such as cDNA microarray analysis, might not be sensitive enough to detect transcripts of genes expressed only in a subset of cochlear cells.

The majority of the 31 known genes mutated in inherited deafness is expressed either ubiquitously or in several (fetal) human tissues. At the onset of this study we speculated that the scarcity of cochlea-specific genes might be due to their under representation in commonly used cDNA libraries. Our results suggest, but do not prove, that true cochlea-specific genes may be very rare. Due to illegitimate transcription with little functional meaning, it is possible that some cochlea-specific clones appear to be preferentially expressed only in fetal cochlea in our study. Given this limitation, we find that no cDNA clones are exclusively expressed in the (developing) inner ear. In contrast many clones show preferential expression in the cochlea. RT-PCR analysis of 256 unique sequences selected based on their location in hereditary deafness linkage intervals (155 sequences), their location in a cluster of clones (21 sequences), their similarity to a maximum of five ESTs preferably from (fetal) brain or fetal cochlea (60 sequences), or their novelty and overlap with a predicted exon (20 sequences) resulted in the identification of 70 clones with preferential expression in fetal cochlea. The expression of these clones will be analysed in more detail in the future by Northern blot analysis and mRNA in situ hybridisation. The semiquantitative nature of our expression analysis cautions us to draw definite conclusions. Nevertheless, our data suggest that at least a quarter of the novel genes in our library are preferentially expressed in fetal cochlea. Hence, over 250 such clones may be present in our collection.

In conclusion, this study resulted in a valuable collection of novel cDNA fragments that will form the basis for more detailed spatial and temporal expression analysis (e.g., mRNA in situ hybridisation), characterization of the corresponding genes, and future investigations into their putative roles in hearing and/or hereditary deafness.

2.5 Materials and methods

2.5.1 Suppression subtractive hybridisation

For suppression subtractive hybridisation, poly(A)$^+$ RNA from five human adult tissues (brain, kidney, liver, heart, skeletal muscle) and total RNA from placenta were purchased from Clontech. Total RNA from fetal brain, tongue, kidney, adrenal gland, lung, and liver was isolated with RNAzol B (Campro Scientific). Total fetal cochlear RNA of 16- to 22-week-old fetuses was kindly provided by Dr. C.C. Morton. The RNA was isolated as described elsewhere (Robertson et al. 1994). Complementary DNA (cDNA) was synthesized using the SMART PCR cDNA Synthesis Kit (Clontech). First-strand synthesis was performed with 1.0 µg total RNA using an oligo(dT) primer. Single-stranded cDNA was amplified by long-distance PCR with the Advantage cDNA PCR Kit (Clontech). Prior to subtraction, cDNA was size fractionated with Chroma Spin-1000 columns (Clontech), digested by *Rsa*I, and purified with the Advantage PCRPure Kit (Clontech).

Subtraction of the cochlear RNA was performed with the PCR-Select cDNA

Subtraction Kit (Clontech) according to the method described by Diatchenko et al. (Diatchenko et al. 1996). Tester cDNA consisted of cochlear cDNA. Driver cDNA consisted of a mixture of cDNAs from fetal tissues (brain, tongue, kidney, adrenal gland, lung, and liver) and adult tissues (brain, heart, skeletal muscle, kidney, and liver). Tester cDNA was divided into two portions and ligated to two different adaptors. In the first hybridisation step, an excess of denatured driver (450 ng) was added to each sample of denatured tester (12 ng). In the second hybridisation step, the two primary hybridisation samples were mixed, and freshly denatured cDNA (300 ng) was added. Differentially expressed cDNAs were amplified by two suppression PCR amplifications with the Advantage cDNA PCR Kit (Clontech).

2.5.2 Cloning and analysis of the subtracted cDNA

Subtracted PCR products were ligated into plasmid vector pCRII, using a T/A cloning kit (Invitrogen). The resulting constructs were transformed to TOP10F' competent cells (Invitrogen) and selected by blue/white screening. Approximately 3000 clones from the cochlea-enriched library were picked manually and grown for 16 h in 100 µL LB containing ampicillin (50 µg/ml) in 96-well tissue culture plates. After the addition of 100 µL 30% (w/v) glycerol, the plates were stored at -80°C.

Inserts from cDNA clones were recovered by direct PCR amplification of the culture using the vector primers T7 and M13 Reverse. Insert PCR products were isolated from an agarose gel with the Qiaquick Gel Extraction Kit (Qiagen) and sequenced with the Thermo Sequenase Dye Terminator Cycle Sequencing Pre-mix Kit (Amersham), using an automated DNA sequencer (Applied Biosystems, Inc., Model 3700). The clones were sequenced using the vector primers. Nucleic acid similarity searches were performed using the BLAST program (Altschul et al. 1997) against the GenBank, EMBL, and EST databases at the Centre for Molecular Bioinformatics (http://www.cmbi.kun.nl/). Sequence data have been deposited with GenBank under Accession Nos. CB831773-CB831790 and CB410624-CB410971.

Subtraction efficiency was tested with PCR according to the protocol provided with the PCR-Select cDNA Subtraction Kit (Clontech).

2.5.3 Mapping and analysis of clones

In the early phase of the project, radiation hybrid mapping was performed with the Stanford G3 Radiation Hybrid Panel (Research Genetics) for a number of clones. PCRs were performed in a volume of 10 µL using 25 ng DNA of each hamster/human cell line, 4 pmol of each primer, 10 mM Tris-HCl, pH 8.3, 50 mM KCl, 1.5 mM $MgCl_2$ (for most primer sets), 5 mM DTT, 200 µM of each dNTP, and 0.4 U Taq DNA polymerase (Invitrogen). Amplification was performed for 35 cycles at 94°C for 1 min, 60°C for 1 min (for most primer sets), and 72°C for 1 min in a microtiter PCR machine (MG Research). The localization of the cDNA fragments with the Stanford G3 Radiation Hybrid Map was determined at the Stanford Human Genome Centre Web site (http://www-shgc.stanford.edu).

Most of the clones were mapped using the results of BLAST-analysis using

publicly available programs UCSC Human Genome Project Working Draft, http://genome.cse.ucsc.edu; NCBI Mapviewer, http://www.ncbi.nlm. nih.gov/cgi-bin/Entrez/hum_srch; and Unigene at the NCBI, http://www.ncbi.nlm.nih.gov/UniGene/). Other programs used to analyze the clones were the Celera database (http://cds.celera.com) and Vector NTI 7.1 (InforMax, http://www.informaxinc.com).

2.5.4 Expression profile analysis by semiquantitative RT-PCR

For semiquantitative RT-PCR, total RNA was isolated from nine human fetal tissues (eye, cochlea, spinal cord, heart, kidney, colon, stomach, lung, tongue, and skeletal muscle) (Chirgwin et al. 1979). Total RNA from three human tissues (fetal brain, fetal liver, and placenta) was purchased from Clontech. Total RNA was treated with DNase I (Invitrogen). Random-primed RNA was synthesized in a volume of 250 µL from 3.1 µg total RNA using 4 pmol random hexanucleotides ($pd(N)_6$; Pharmacia), 10 mM Tris-HCl, pH 8.3, 50 mM KCl, 0.01% (v/w) gelatin, 5 mM $MgCl_2$, 1 mM DTT, 95 U RNAguard (Pharmacia), and 2500 U MMLV reverse transcriptase (Invitrogen). All cDNA was tested for genomic DNA contamination by performing a PCR on the cDNA, using primers spanning an intron of the housekeeping genes *GAPDH* (5'-ACCACAGTCCATGCCATCAC-3' and 5'-TCCACCACCCTGTTGCTGTA-3', spanning intron 8) and *GUSB* (3'-ACTATCGCCATCAACAACACACTGACC-3' and 5'-GTGACGGTGATGTCATCGAT-5', spanning introns 3 and 4). Primer sets were designed with the Primer 3 program (http://www-genome.wi.mit.edu/cgi-bin/primer/primer3_www.cgi) (Rozen and Skaletsky 2000) to amplify products of 100 to 250 bp. The primer sets were first tested on genomic DNA for the optimal annealing temperature and $MgCl_2$ concentration of the PCR. Semiquantitative RTPCRs were performed in a volume of 35 µL using 87 ng randomly primed cDNA, 11.2 pmol each primer, 10 mM Tris-HCl, pH 8.3, 50 mM KCl, 0.01% gelatin, the optimal concentration of $MgCl_2$, 160 µM of each dNTP, and 1.75 U Taq DNA polymerase (Invitrogen). For the majority of the primer sets amplification was performed at 94°C for 1 min, 60°C for 1 min, and 72°C for 1 min in a Peltier thermal cycler (PTC-200; MJ Research). Samples of 10 µL were taken from the PCRs after 25, 30, and 35 cycles.

2.6 Acknowledgments

We thank Cynthia C. Morton for kindly providing us the total human fetal cochlear RNA. This work was supported by The Netherlands Organization for Scientific Research (NWO), Grant 901-04-205; the Heinsius-Houbolt Foundation; and the Nijmegen ORL Research Foundation.

2.7 References

Ahmad N.N., Ala-Kokko L., Knowlton R.G., et al., Stop codon in the procollagen II gene (COL2A1) in a family with the Stickler syndrome (arthro-ophthalmopathy). Proc Natl Acad Sci USA 1991 88: 6624-6627.

Altschul S.F., Madden T.L., Schaffer A.A., et al., Gapped BLAST and PSI-BLAST: a new generation of protein database search programs. Nucleic Acids Res 1997 25: 3389-3402.

Chirgwin J.M., Przybyla A.E., MacDonald R.J., et al., Isolation of biologically active ribonucleic acid from sources enriched in ribonuclease, Biochemistry 1979 18: 5294-5299.

Cohen-Salmon M., El Amraoui A., Leibovici M., et al., Otogelin: a glycoprotein specific to the acellular membranes of the inner ear. Proc Natl Acad Sci USA 1997 94: 14450-14455.
Cohen-Salmon M., Frenz D., Liu W., et al., Fdp, a new fibrocyte-derived protein related to MIA/CD-RAP, has an in vitro effect on the early differentiation of the inner ear mesenchyme. J Biol Chem 2000 275: 40036-40041.
Coimbra R.S., Weil D., Brottier P., et al., A subtracted cDNA library from the zebrafish (Danio rerio) embryonic inner ear. Genome Research 2002 12: 1007-1011.
de Kok Y.J., van der Maarel S.M., Bitner-Glindzicz M., et al., Association between X-linked mixed deafness and mutations in the POU domain gene POU3F4. Science 1995 267: 685-688.
Del Castillo I., Villamar M., Sarduy M., et al., A novel locus for non-syndromic sensorineural deafness (DFN6) maps to chromosome Xp22. Hum Mol Genet 1996 5: 1383-1387.
den Hollander A.I., van Driel M.A., de Kok Y.J., et al., Isolation and mapping of novel candidate genes for retinal disorders using suppression subtractive hybridization. Genomics 1999 58: 240-249.
Diatchenko L., Lau Y.F., Campbell A.P. et al., Suppression subtractive hybridization: a method for generating differentially regulated or tissue-specific cDNA probes and libraries. Proc Natl Acad Sci USA 1996 93: 6025-6030.
Fukushima K. Ramesh A., Srisailapathy C.R., et al., Consanguineous nuclear families used to identify a new locus for recessive non-syndromic hearing loss on 14q. Hum Mol Genet 1995 4: 1643-1648.
Gibson F., Walsh J., Mburu P., et al., A type VII myosin encoded by the mouse deafness gene shaker-1. Nature 1995 374: 62-64.
Gorlin R.J., Toriello H.V., and Cohen M.M., Hereditary hearing loss and its syndromes. 1995 Oxford University Press, New York.
Harter C., Ripoll C., Lenoir M., et al., Expression pattern of mammalian cochlea outer hair cell (OHC) mRNA: screening of a rat OHC cDNA library. DNA Cell Biol 1999 18: 1-10.
Heller S., Sheane C.A., Javed Z., et al., Molecular markers for cell types of the inner ear and candidate genes for hearing disorders. Proc Natl Acad Sci USA 1998 95: 11400-11405.
Jacob A.N., Manjunath N.A., Bray-Ward P., et al., Molecular cloning of a zinc finger gene eZNF from a human inner ear cDNA library, and in situ expression pattern of its mouse homologue in mouse inner ear. Somatic Cell Mol Genet 1998 24: 121-129.
Killick R. and Richardson G., Isolation of chicken alpha ENaC splice variants from a cochlear cDNA library. Biochim Biophys Acta 1997 1350: 33-37.
Le Moine C. and Young III W.S., RHS2, a POU domain-containing gene, and its expression in developing and adult rat. Proc Natl Acad Sci USA 1992 89: 3285-3289.
Legan P.K., Rau A., Keen J.N., et al., The mouse tectorins, modular matrix proteins of the inner ear homologous to components of the sperm-egg adhesion system. J Biol Chem 1997 272: 8791-8801.
McGuirt W.T., Prasad S.D. Griffith A.J., et al., Mutations in COL11A2 cause non-syndromic hearing loss (DFNA13). Nat Genet 1999 23: 413-419.
Morton C.C., Genetics, genomics and gene discovery in the auditory system. Hum Mol Genet 2002 11: 1229-1240.
Morton N.E., Genetic epidemiology of hearing impairment. Ann N Y Acad Sci 1991 630: 16-31.
Mustapha M., Salem N., Weil D., et al., Identification of a locus on chromosome 7q31, DFNB14, responsible for prelingual sensorineural non-syndromic deafness. Eur J Hum Genet 1998 6: 548-551.
Pentinnen R.P., Lichtenstein J.R., Martin G.R., et al., Abnormal collagen metabolism in cultured cells in osteogenesis imperfecta. Proc Natl Acad Sci USA 1975 72: 586-586.
Pulleyn L.J., Jackson A.P., Roberts E., et al., A new locus for autosomal recessive non-syndromal sensorineural hearing impairment (DFNB27) on chromosome 2q23-q31. Eur J Hum Genet 2000 8: 991-993.
Richards A.J., Yates J.R., Williams R., et al., A family with Stickler syndrome type 2 has a mutation in the COL11A1 gene resulting in the substitution of glycine 97 by valine in alpha 1 (XI) collagen. Hum Mol Genet 1996 5: 1339-1343.
Robertson N.G., Khetarpal U., Gutiérrez-Espeleta G.A., et al., Isolation of novel and known genes from a human fetal cochlear cDNA library using subtractive hybridization and differential screening. Genomics 1994 23: 42-50.
Robertson N.G., Lu L., Heller S., et al., Mutations in a novel cochlear gene cause DFNA9, a human nonsyndromic deafness with vestibular dysfunction. Nat Genet 1998 20: 299-303.
Robertson N.G., Heller S., Lin J.S., et al., A novel conserved cochlear gene, OTOR: identification, expression analysis, and chromosomal mapping. Genomics 2000 66: 242-248.
Rozen S. and Skaletsky H., Primer3 on the WWW for general users and for biologist programmers. Methods Mol Biol 2000 132: 365-386.
Ryan A.F., Batcher S., Brumm D., et al., Cloning genes from an inner ear cDNA library. Arch Otolaryngol Head Neck Surg 1993 119: 1217-1220.
Skvorak A.B., Weng Z., Yee A.J., et al., Human cochlear expressed sequence tags provide insight into cochlear gene expression and identify candidate genes for deafness. Hum Mol Genet 1999 8: 439-452.
Soto-Prior A., Lavigne-Rebillard M., Lenoir M., et al., Identification of preferentially expressed cochlear genes by systematic sequencing of a rat cochlea

cDNA library. Brain Res Mol Brain Res 1997 47: 1-10.
Verhoeven K., Van Laer L., Kirschhofer K., et al., Mutations in the human alpha-tectorin gene cause autosomal dominant non-syndromic hearing impairment. Nat Genet 1998 19: 60-62.
Verpy E., Masmoudi S., Zwaenepoel I., et al., Mutations in a new gene encoding a protein of the hair bundle cause non-syndromic deafness at the DFNB16 locus. Nat Genet 2001 29: 345-349.
Wang A., Liang Y., Fridell R.A., et al., Association of unconventional myosin MYO15 mutations with human nonsyndromic deafness DFNB3. Science 1998 280: 1447–1451.
Wilcox E.R.and Fex J., Construction of a cDNA library from microdissected guinea pig organ of Corti. Hear Res 1992 62: 124-126.
Zhang J.T. and Nicholson B.J., Sequence and tissue distribution of a second protein of hepatic gap junctions, Cx26, as deduced from its cDNA. J Cell Biol 1989 109: 3391-3401.
Zheng J., Shen W., He D.Z., et al., Prestin is the motor protein of cochlear outer hair cells. Nature 2000 405: 149-55.
Zwaenepoel I., Mustapha M., Leibovici M., et al., Otoancorin, an inner ear protein restricted to the interface between the apical surface of sensory epithelia and their overlying acellular gels, is defective in autosomal recessive deafness DFNB22. Proc Natl Acad Sci USA 2002 99: 6240-624.

Chapter 3

A Novel Mutation Identified in the DFNA5 Gene in a Dutch Family: A Clinical and Genetic Evaluation

A.M.L.C. Bischoff[a], M.W.J. Luijendijk[b], P.L.M. Huygen[a], G. van Duijnhoven[b], E.M.R. De Leenheer[a], G.G. Oudesluijs[a], L. Van Laer[c], F.P.M. Cremers[b], C.W.R.J. Cremers[a] and H. Kremer[a]

A.M.L.C.B. and M.W.J.L. contributed equally to this work.

[a] Department of Otorhinolaryngology, University Medical Centre Nijmegen, P.O. Box 9101, 6500 HB Nijmegen, The Netherlands
[b] Department of Human Genetics, University Medical Centre Nijmegen, P.O. Box 9101, 6500 HB Nijmegen, The Netherlands
[c] Department of Medical Genetics, University of Antwerp, Belgium

Published in: Audiol. Neurootol. 2004 9: 34-46

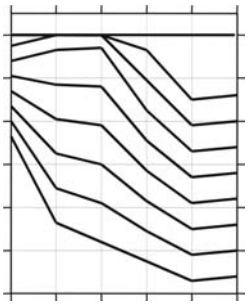

3.1 Abstract

A novel *DFNA5* mutation was found in a Dutch family, of which 37 members were examined. A nucleotide substitution was identified in the splice acceptor site of intron 7, leading to skipping of exon 8 in part of the transcripts. The mutation was found in 18 individuals. Sensorineural hearing impairment was non-syndromic and symmetric. In early life, presumably congenitally, hearing impairment amounted to 30 dB in the high frequencies. Progression was most pronounced at 1 kHz (1.8 dB/year). Speech recognition was relatively good with a phoneme score of about 50% at the age of 70. Onset age was 37 years, and recognition deteriorated by 1.3% per year. The recognition score deteriorated by 1.0% per decibel threshold increase from a mean pure-tone average (PTA at 1, 2 and 4 kHz) of 63 dB onwards. Vestibular function was generally normal. The second mutation identified in the *DFNA5* gene results in hearing impairment, similar to that in the original DFNA5 family in terms of pure-tone thresholds, but with more favourable speech recognition.

Keywords: *DFNA5* gene; Hearing impairment, progressive; High frequency; Splicing defect

3.2 Introduction

Since the early nineties, gene linkage and mutation analysis have been applied to increase our knowledge of hereditary non-syndromic hearing impairment. At the moment about 75 genetically different types of non-syndromic hearing impairment have been identified (Van Camp G. and Smith R.J.H. Hereditary hearing loss homepage [http://www.uia.ac.be/DNAlab/hhh/]). Knowledge of hereditary hearing impairment at a molecular level is still limited but can be enhanced by studies on genotype-phenotype correlations in families with hearing impairment (Huygen et al. 2003). This is especially true for autosomal dominant types, which display the largest phenotypic variation. The results of such family studies are also of value for genetic counselling purposes.

Up to now, only 1 DFNA5 family has been described (Huizing et al. 1965, Huizing et al. 1966a, Huizing et al. 1966b, Huizing et al. 1972, Huizing et al. 1983, van den Wijngaard et al. 1985a, van de Wijngaart et al. 1985b). In this family, non-syndromic symmetric hearing impairment was severest at the high frequencies, and progression was most distinct in the first three decades of life. In 1995, the responsible gene was localized to a region on chromosome 7p15. The locus was designated DFNA5 (Van Camp et al. 1995). After sequencing of the *DFNA5* gene, a complex insertion/deletion mutation was found in intron 7, causing skipping of exon 8 and leading to premature termination of the encoded protein. As there was no indication for its function, the gene was called *DFNA5* by default (Van Laer et al. 1998). The DFNA5 protein is not homologous to any other human protein described up to now. Also no information is available about the structure or the subcellular localization
of the protein.

In this report we describe a second mutation in the *DFNA5* gene, in a Dutch family with autosomal dominant sensorineural hearing impairment. A nucleotide substitution

was identified in the splice acceptor site of intron 7, which leads to alternative splicing. This results in skipping of exon 8 in part of the transcripts. Pure-tone and speech audiometric data were analysed and compared to the results in the previously described DFNA5 family (De Leenheer et al. 2002a). Although a larger part of the transcripts is normal in comparison to the original DFNA5 family, the severity of hearing impairment is fairly similar in terms of pure-tone hearing thresholds.

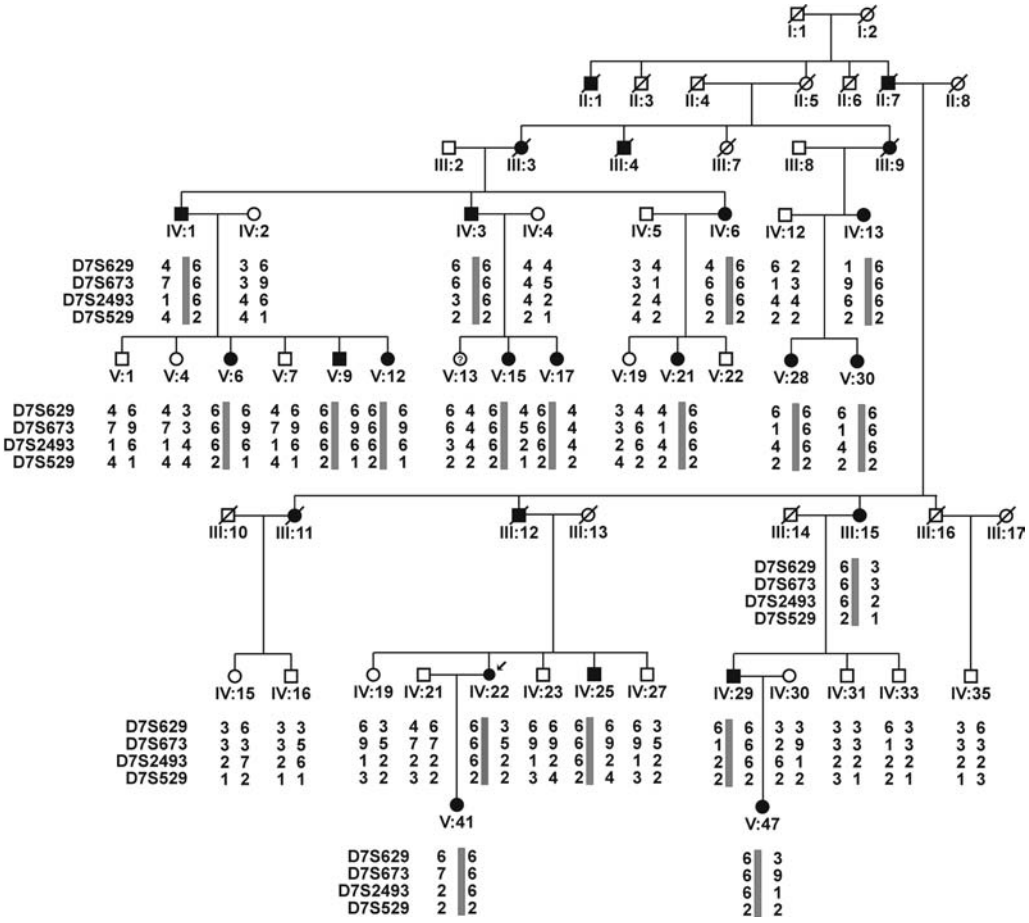

Figure 1. Pedigree of family W00-212 and genotypic data for markers flanking the *DFNA5* gene, listed in centromere-to-telomere order. The most likely haplotypes are shown. A bar indicates the haplotype that is associated with the affected status. The marker order is in agreement with the most recent freeze (June 2002) of the Human Genome Working Draft (http://genome.ucse.edu). Men are indicated with a square, women are indicated with a circle and filled symbols indicate affected persons. The proband is indicated with an arrow. Haplotype reconstruction for the individuals III:2 and III:3 suggests the presence of 5 alleles. However, assuming one allele change for marker D7S2493 for either individual IV:3 or IV:6 can explain this.

3.3 Results

The pedigree (fig. 1) comprised 27 affected family members, 18 of whom were still alive and participated in this study. The pattern of inheritance is clearly autosomal dominant. Affected persons showed no evidence of other causes of hearing impairment than otitis in the past, except for case V:21, who had a cholesteatoma in the right ear at 14 years of age that required surgery. The data for the right ear in this individual were therefore excluded from the present analysis. The first symptoms of hearing impairment were reported at ages ranging from 0 to 40 years. Vestibular symptoms were not reported. Otoscopy was generally normal. Pure-tone audiograms (fig. 2) showed a so-called Z shape curve; predominantly highfrequency hearing loss with a large drop for the mid frequencies and relatively sparing of the lower frequencies. The audiograms were fairly symmetric, except for cases V:21 and V:30.

3.3.1 Audiometric analysis

All available data, combining individual longitudinal (11 cases) and single snapshot (7 cases) measurements are shown in figure 3. As analysis of covariance indicated that pooling of regression lines was not allowed for any frequency, the trend lines were derived. At each frequency, it was checked that fairly similar numbers of individuals were represented by threshold values - either pertaining to longitudinal or snapshot observations - above and below the trend line. The annual threshold of deterioration increased from 0.7 dB/year at 0.25 kHz to 1.8 dB/year at 1 kHz and then decreased to 1.2 dB/year at 4-8 kHz.

The constructed ARTA (fig. 4) show a configuration with congenital high-frequency hearing impairment of about 30 dB and progression that was most pronounced at 0.5 and 1 kHz. To check whether the constructed ARTA was reliable, we plotted the thresholds predicted for minimum and maximum age, derived from the ARTA, in the original audiograms (fig. 2, dotted lines). This highlighted threshold variability, especially in the younger individuals, who seemed to be more severely affected than was indicated by their expected audiograms. Attempts to improve prediction for the younger patients only succeeded at the cost of the quality of prediction in the remaining cases and were therefore abandoned.

In figure 4, the ARTA published for the original DFNA5 family (De Leenheer et al. 2002a) is illustrated, in juxtaposition to the ARTA derived for the present family. For both families, we created a threshold features array as described elsewhere (Huygen et al. 2003). A χ^2 test did not detect a significant difference between the families, although in the first four decades the ARTA of the present family exhibited better thresholds at the speech frequencies.

We checked for the presence of phenotypic differences related to gender since the expression of *DFNA5*, also known as *ICERE-1*, is higher in oestrogen-receptor-negative than in oestrogen-receptor-positive breast carcinomas (Thompson and Weigel 1998); none were found.

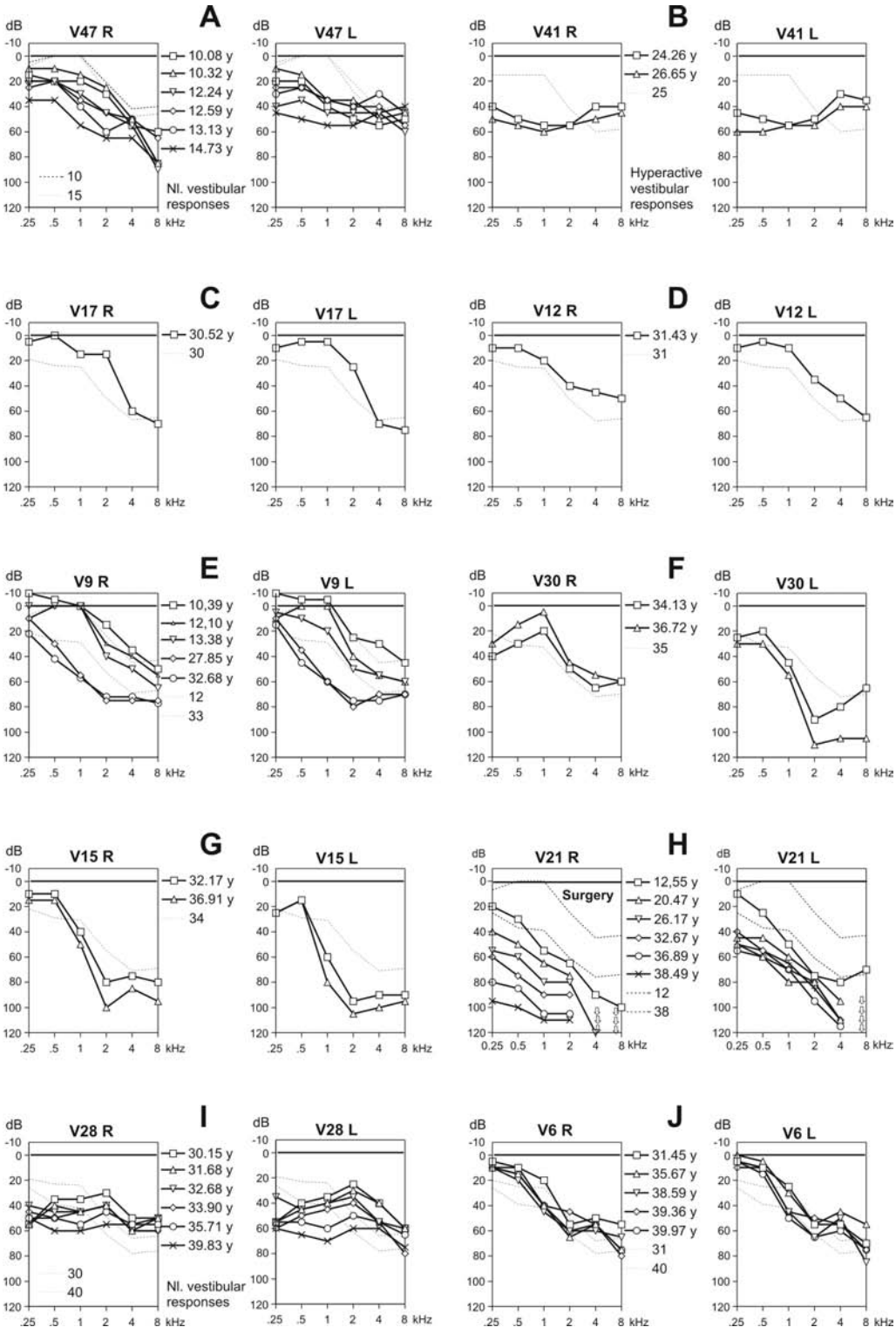
A
V47 R
V47 L
10.08 y
10.32 y
12.24 y
12.59 y
13.13 y
14.73 y
10
15
Nl. vestibular responses
B
V41 R
V41 L
24.26 y
26.65 y
25
Hyperactive vestibular responses
C
V17 R
V17 L
30.52 y
30
D
V12 R
V12 L
31.43 y
31
E
V9 R
V9 L
10,39 y
12,10 y
13.38 y
27.85 y
32.68 y
12
33
F
V30 R
V30 L
34.13 y
36.72 y
35
G
V15 R
V15 L
32.17 y
36.91 y
34
H
V21 R
V21 L
Surgery
12,55 y
20.47 y
26.17 y
32.67 y
36.89 y
38.49 y
12
38
I
V28 R
V28 L
30.15 y
31.68 y
32.68 y
33.90 y
35.71 y
39.83 y
30
40
Nl. vestibular responses
J
V6 R
V6 L
31.45 y
35.67 y
38.59 y
39.36 y
39.97 y
31
40
dB
kHz
.25 .5 1 2 4 8
0.25 0.5 1 2 4 8

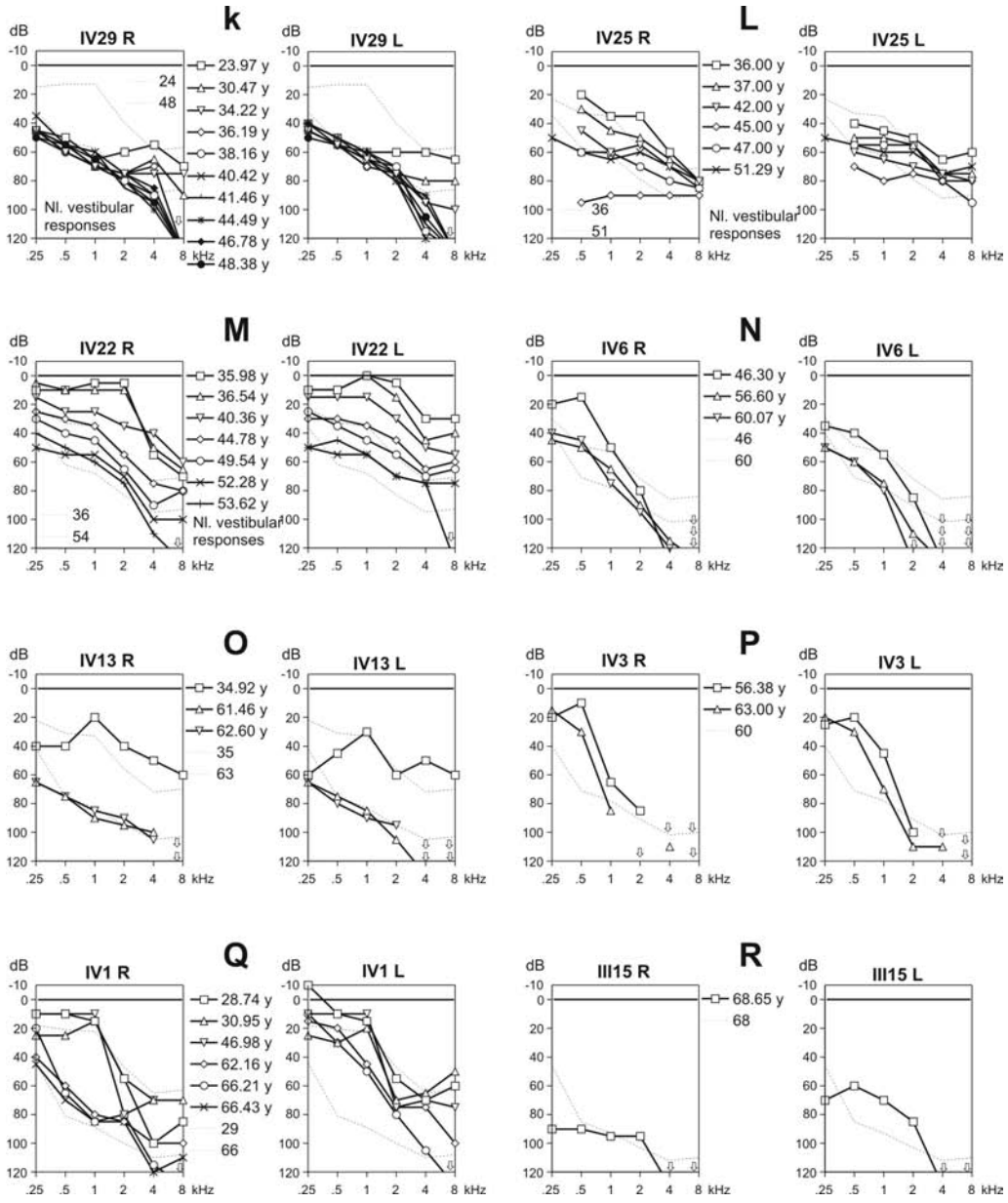

Figure 2. Audiograms of the 18 affected family members. Nl = Normal. The dotted lines represent the predicted thresholds at the ages specified, as derived from the ARTA. The results of the 6 vestibulo-ocular function tests are also indicated.

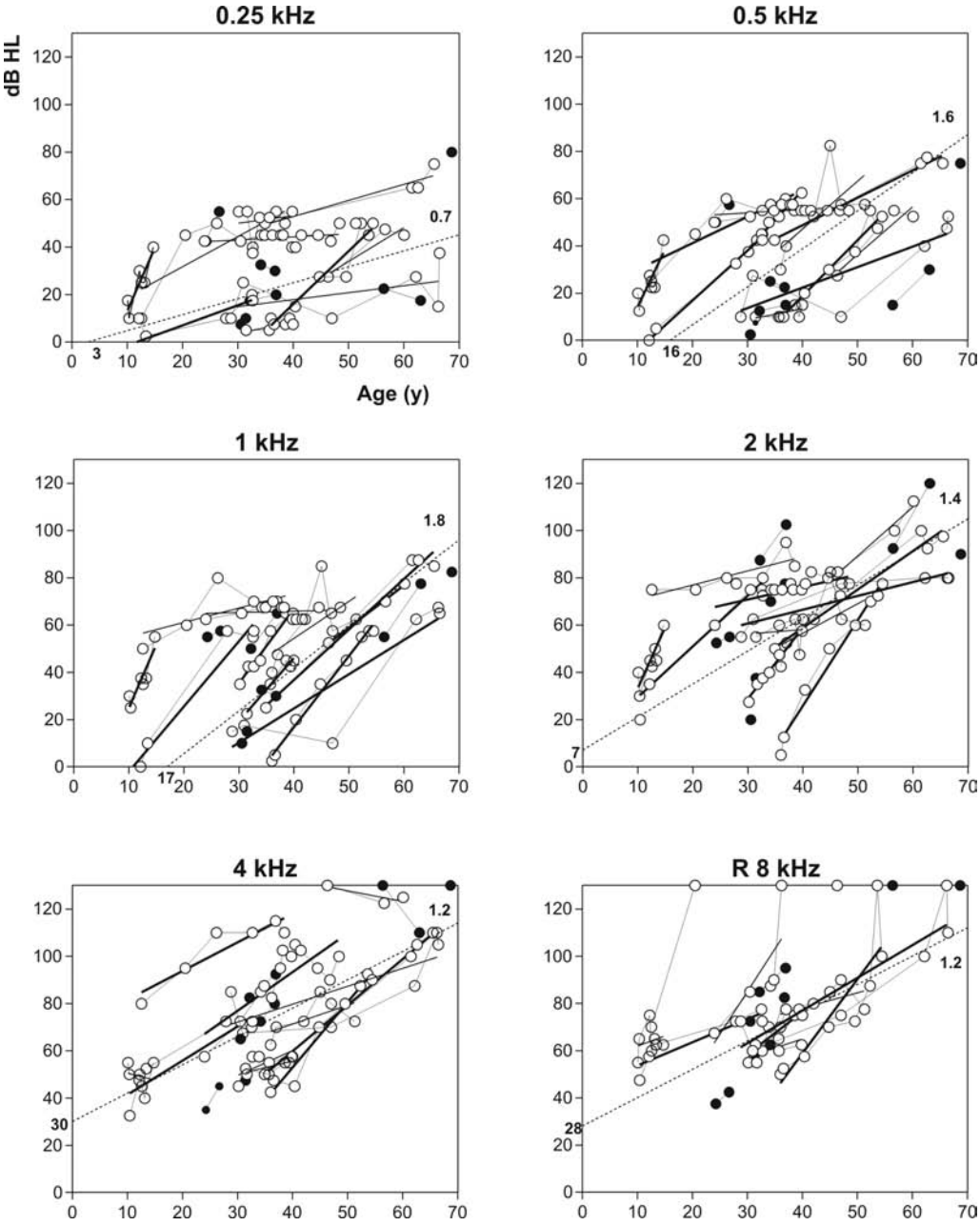

Figure 3. Longitudinal analysis (binaural air conduction threshold). Threshold data (in decibels hearing level) versus age (in years) for the frequencies from 0.25 to 8 kHz combining individual longitudinal data (open circles) with connecting hairlines and single snapshot measurements (filled circles) of the 18 mutation carriers. The regression lines fitted to the individual longitudinal measurements are included (a bold line indicates significant progression). The dotted line pertains to the trend line derived for the ensemble of these data points (see text). Slopes and intercepts are indicated in bold.

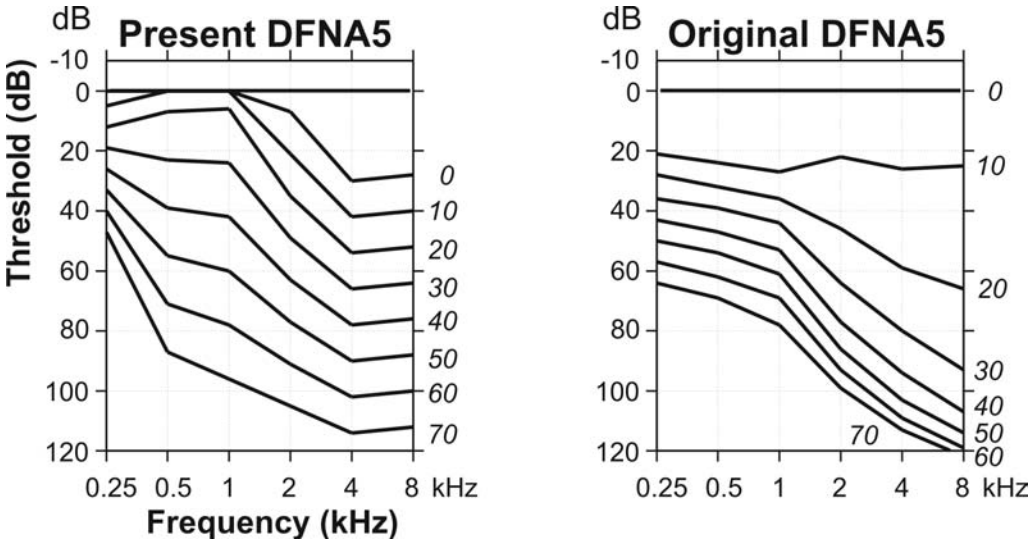

Figure 4. ARTA of the original and the present DFNA5 family from birth to the 7th decade. Italics indicate age (years) in decade steps.

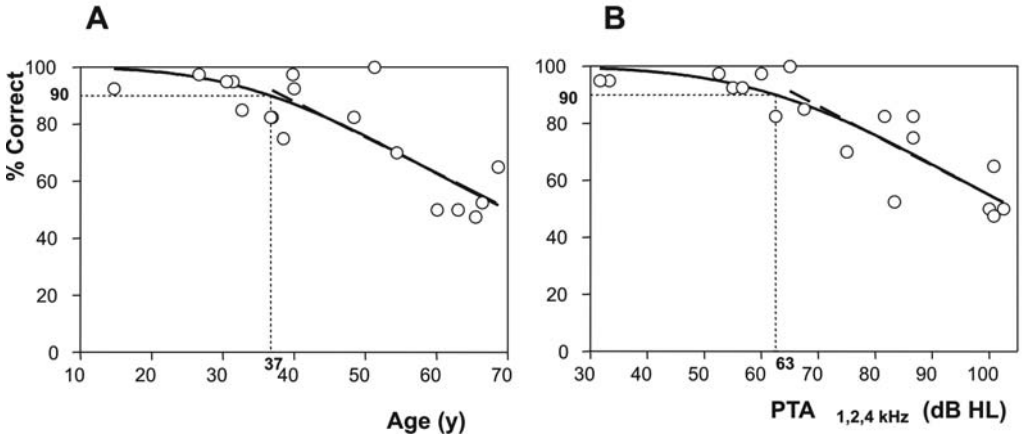

Figure 5. Cross-sectional binaural mean speech recognition scores at the last visit against age (A) and PTA at 1, 2 and 4 kHz (B). The continuous curve was fitted using a non-linear equation. A straight line (dashed) approximated the relevant part of this curve, see methods. The onset age and onset level were derived, using the non-linear curve.

3.3.2 Speech recognition

Speech recognition was relatively good, with scores still better than 50% at the age of 70. The recognition score (fig. 5A) declined substantially from onset at the age of 37 with a deterioration rate of 1.3% per year (table 1). The 90% recognition score was found at a PTA level of 63 dB HL and deteriorated by about 1.0% per decibel (fig. 5B).

The present findings were compared to and tested against the previously reported results for the original DFNA5 family (De Leenheer et al. 2002b). It appeared that onset age, onset level and deterioration gradient were significantly higher in the

present family (table 1, fig. 6). The deterioration rate of the present family, although substantially higher, did not differ significantly from the one derived for the original DFNA5 family. Figure 6 demonstrates that at an age of <65 years, our patients had better recognition scores than the patients from the original family, which could also be explained by their more favourable thresholds in the speech frequencies in the first four decades of life (fig. 4). Patients from the two DFNA5 families tended to develop similar poor phoneme scores at an advanced age (fig. 6A) and around a PTA level of about 85 dB at a score of about 75% (fig. 6B). Remarkably, figure 6B suggests the scores to diverge at higher PTA levels, with a relatively better performance in the original DFNA5 family (De Leenheer et al. 2002b).

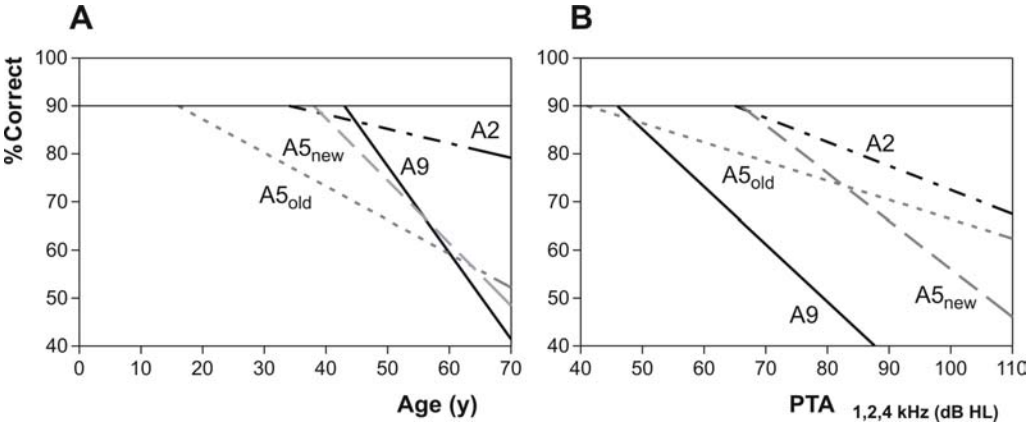

Figure 6. Comparison of performance versus age (A) and performance versus impairment level (B) plots pertaining to speech recognition scores of the present ($A5_{new}$, dashed line) and the original ($A5_{old}$, dotted line) DFNA5 patients. Linear plots ($X>X_{90}$) for the scores of DFNA2 (A2) and DFNA9 (A9) patients are included for comparison (see text).

3.3.3 Vestibular Function Tests and Computerized Tomography

Although no vestibular problems appeared to be present in this family, vestibular function was tested in 6 cases. Electronystagmography was normal in 5 cases (IV:22, IV:25, IV:29, V:28 and V:47) and revealed a hyperactive vestibulo-ocular reflex in 1 individual (V:41). Computerized tomography (case IV:22) showed a normal temporal bone configuration.

Table 1. Speech recognition scores

	Present DFNA5	*Original DFNA5*	*DFNA2*	*DFNA9*
Age, years				
n	12	33	43	41
Onset age	38 (28-49)S	16 (10-22)	34	43
SE	5	3		
Det. Rate	1.3 (0.5-2.0)NS	0.7 (0.4-0.9)	0.3	1.8
SE	0.3	0.1		
PTA, dB				
n	11	33	42	41
Onset level	66 (53-80)	41 (31-52)	65	46
SE	6	5		
Det. gradient	1.0 (0.5-1.6)S	0.4 (0.3-0.6)	0.5	1.2
SE	0.3	0.1		

Onset age (years), onset level (dB), deterioration (det.) rate (% per year) and deterioration gradient (% per dB) are shown for the original and the present DFNA5 families; figures in parentheses indicate 95% confidence intervals. n = Number of cases; SE = standard error; S = significantly different; NS = not significantly different. The data of the present family shown in the table were derived from the linear curve that approximates the most relevant part of the continuous curve. The two columns on the right show reference data of DFNA2 and DFNA9.

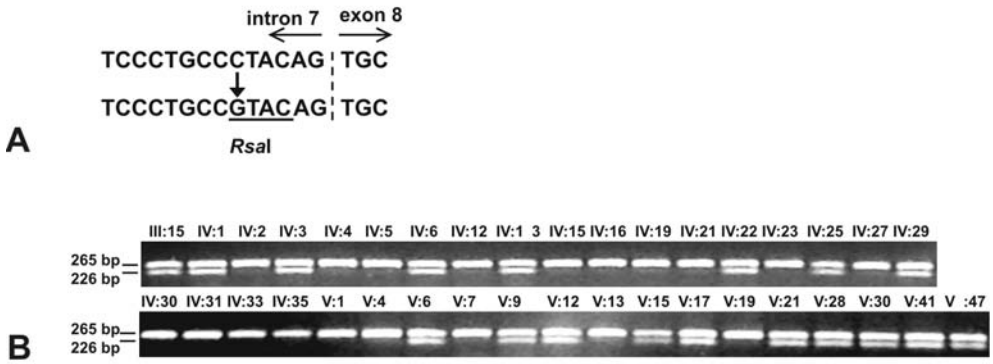

Figure 7. Restriction analysis. (A) Sequence of the boundary of intron 7 and exon 8 of the DFNA5 gene, showing that the mutation creates an *Rsa*I restriction site. (B) Restriction digestion with RsaI in 18 affected and 19 non-affected family members. The 265-bp fragment represents the wild-type allele, the 226-bp fragment the mutant allele.

3.3.4 Linkage analysis

Due to the similarity of the type of hearing loss in the present family as compared to that in the DFNA5 family described previously, linkage studies were initiated with markers flanking the *DFNA5* gene. The markers D7S629 and D7S673 are located telomeric to the *DFNA5* gene at 7p15.3, and D7S2493 and D7S529 are derived from the region centromeric to the gene. All markers are located within a distance of 2.5 cM from the

gene according to the Généthon genetic map (Dib et al. 1996). All affected individuals were included in the linkage analysis, as well as non-affected individuals from the age of 30 years onwards. As already suggested by the type of hearing loss, there was co-segregation of the disorder and a specific haplotype in the DFNA5 interval (fig. 1). A maximum lod score of 6.82 was calculated for marker D7S673. The maximum lod scores for markers D7S629, D7S2493 and D7S529 were 3.85, 2.34 and 5.09, respectively.

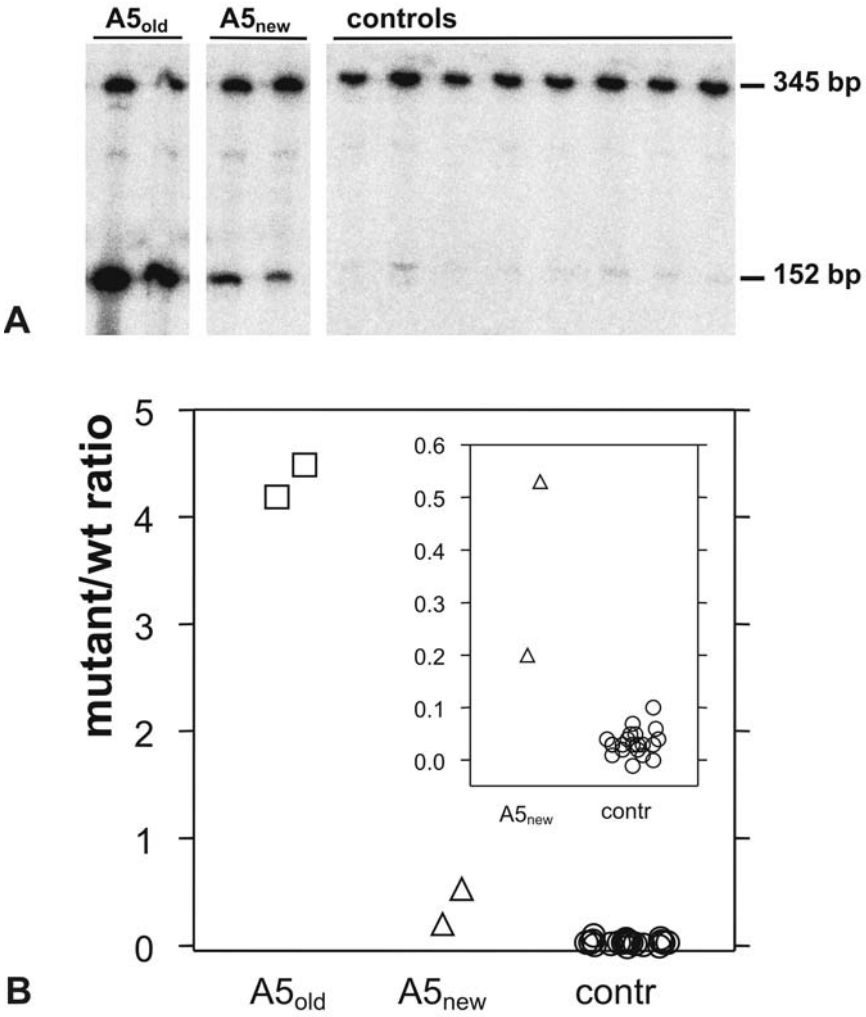

Figure 8. (A) Aberrant splicing of exon 8 of the *DFNA5* gene. Two affected persons from the original DFNA5 family ($A5_{old}$), 2 affected persons from the present DFNA5 family ($A5_{new}$) and 8 control individuals (control) are shown. The wild-type splice product is 345 bp long; the aberrant splice product in which exon 8 is skipped is 152 bp long. (B) Ratios of mutant versus wild type (wt) cDNA of 2 patients of the present family ($A5_{new}$), 2 patients of the original DFNA5 family ($A5_{old}$) and 22 control individuals. The inset shows part of the data on a different scale.

3.3.5 Mutation analysis

For 2 affected family members the coding region and the exon-intron boundaries of the *DFNA5* gene were analysed for the presence of a mutation by DNA sequencing. When compared to the published sequence, 2 changes were found. The first change was a C-to-G transversion in the splice acceptor site of intron 7 at position -6, which was heterozygously present. The second change was a c.1200 G>A transition in exon 9 (1257 G>A (Van Laer et al. 2002a)), which was homozygously present. This was a silent mutation that was also seen homozygously in patients from the original DFNA5 family and the majority of the control individuals. The C-to-G transversion created an *Rsa*I restriction site. The co-segregation of the mutation in the family could therefore be shown by restriction digestion of a 265-bp PCR fragment encompassing the mutated splice site, resulting in 2 fragments of 226 and 39 bp in length (fig. 7). The mutation was not present in 100 control individuals.

No deletions in any part of the gene could be detected by probing a Southern blot containing genomic DNA of 2 patients (III:15 and IV:1) and 2 control individuals with cDNA representing the entire protein-coding region (data not shown).

3.3.6 Effect of the splice site utation on splicing efficiency

Although the detected mutation in the splice acceptor site of intron 7 was not predicted (Shapiro and Senapathy 1987) to lead to a reduced splicing efficiency (86.25 vs. 85.00), mRNA derived from cultured lymphoblastoid cells was analysed for the presence of alternative splicing products. RT-PCR with primers located in exon 7 and exon 9 resulted in a fragment of 152 bp, which indicates skipping of exon 8 (fig. 8A). The absence of exon 8 in the fragment was confirmed by sequence analysis. Skipping of exon 8 causes a frame shift at amino acid 330. This leads to 41 aberrant codons followed by a premature stop codon. The amount of the short PCR product found in this study was lower than the amount found in patients from the original DFNA5 family, in which the mutation also affects splicing of intron 7 leading to skipping of exon 8 (Van Laer et al. 1998) (fig. 8A). A variable but low amount of the PCR fragment representing the alternatively spliced mRNA was also seen in some control individuals. Therefore, 22 control individuals, 2 patients of the present family and 2 patients of the original DFNA5 family were compared with regard to the ratio between RT-PCR products with and without exon 8 by phospho-imaging (fig. 8B). One control measurement was detected as an outlier because the background signal was higher than the signal from the alternatively spliced mRNA resulting in a negative measured ration. Therefore this measurement was excluded from the analysis. For the remaining control measurements, the mean was 0.034 and SD 0.024. Ninety-five percent tolerance limits, according to t statistics, ranged from -0.017 to 0.084. All DFNA5 patients had values above the upper tolerance limit. Skipping of exon 8 was therefore statistically significantly more frequent in patients of the present and the original family as compared to control individuals. Student's t test detected a significant difference ($p = 0.003$) between the original DFNA5 patients (mean 4.34) and the present DFNA5 patients (mean 0.365). Consequently, splicing in the patients of the present family was less severely disturbed than in the original DFNA5 family. The

presence of the C-to-G transversion in the splice acceptor site of intron 7 at position -6 was excluded in the 22 normal-hearing control individuals by restriction digestion with *Rsa*I and DNA sequencing.

To exclude that the difference in the amount of the long and the short splice product was a result of preferential degradation of the short splice form by NMD, we used the chemical cycloheximide to inhibit NMD in lymphoblastoid cell cultures of 2 affected individuals from the present family. We found a 1.36-fold increase in the average ratio when cycloheximide was added (data not shown). Because the amounts of long as well as short splice product were increased after treatment, 1.33- and 1.80-fold respectively, the increased ratio could only be attributed to the presence of an increased amount of short splice product.

To exclude additional intronic mutations that affect correct splicing of the *DFNA5* mRNA, RT-PCR was performed with mRNA derived from cultured lymphoblastoid cells of 2 patients and 2 control individuals. Six primer combinations were used, which amplify overlapping cDNA fragments, covering the entire coding region. There were no indications for additional alternative splicing (data not shown).

3.4 Discussion

We report the second family with a mutation in the *DFNA5* gene associated with hearing loss. Noticeable is the fact that the mutation in both families influences the splicing process resulting in skipping of exon 8, however to a different extent. The relatively fast elucidation of the molecular defect in this second DFNA5 family, based on a comparison of the type of hearing loss with that of a genetically elucidated type, illustrates the value of a detailed analysis of hearing loss in families.

Sensorineural hearing impairment in the present family was non-syndromic and symmetric with progression of 0.7-1.8 dB/year, depending on the frequency. Progression was fairly constant, in contrast with the original family, in which there was more rapid progression in the first 4 decades than at more advanced ages, especially in the high frequencies (about 1 dB/year at 0.25-1 kHz and 1-4 dB/year at 2-8 kHz) (De Leenheer et al. 2002a). The ARTA, however, were not significantly different. A large variation in audiogram types was found, which was also reported in the original family. There was severer hearing loss in the younger individuals than was predicted following the present procedures.

Speech recognition scores were relatively good with an onset age of 37 years and a deterioration rate of 1.3% per year. Recognition scores decreased by 1.0% per decibel threshold increase from a mean PTA (1, 2, 4 kHz) of 63 dB onwards. The difference in speech recognition between both families might be explained by the more favourable thresholds in the speech frequencies in the first four decades of life, demonstrated by the ARTA of the present family.

Table 1 and figure 6 include data derived from previous reports on DFNA2 and DFNA9 (Bom et al. 2001). Straight lines were fitted for $X>X_{90}$ to approximate the regression curves. The original DFNA5 patients tended to show similar phoneme scores as the DFNA9 patients, only at a more advanced age. The present DFNA5

patients showed this similarity already from a younger age onwards. At a given level of hearing impairment, DFNA5 patients of both families generally showed recognition scores that were better than those of DFNA9 patients but worse than those of DFNA2 patients. As previously described (Bom et al. 2001), the high-frequency sensorineural hearing impairment of DFNA2 may be attributed to lack of expression of potassium channels, especially in the inner hair cells of the lower turns in the cochlea. Relatively better speech recognition in DFNA2 was explained by relative sparing of outer hair cell function in this region preserving pre-amplification and fine-tuning mechanisms. The relatively goodspeech recognition performance in DFNA5 patients might be explained in a similar way.

The similarities in the type of hearing loss and a comparable effect of the mutations, namely skipping of exon 8 in both the present and the original DFNA5 family, indicate that the mutation in the present family indeed is the disease-causing genetic defect. Also, despite one silent mutation, no other mutations were found in the *DFNA5* gene in the present family. Although the transcript without exon 8 was also seen in control individuals, the relative amount was statistically significantly higher in the two patients from the present family than in the control individuals. Also, we have to note that the effect of the mutation on splicing might be different in the inner ear compared to lymphoblastoid cell lines. The 1200 G>A polymorphism has no major influence on the splicing efficiency of exon 8, because the disease-causing mutation in the present and the original family co-segregates with an A at position 1200. Also, the majority of the controls were homozygous A. Even though our results show that the ratio between the long and short splice form increases after treatment with cycloheximide, the lower amount of short splice product as compared to the amount of long splice product in the present family remains, indicating that this difference is not a result of NMD. Also, the low amount of short mRNA in the present family as compared to the previously described family cannot be explained by a higher rate of NMD in the present family.

The relatively low amount of the short transcript in the present family suggests that not haplo-insufficiency but a dominant negative effect of the mutant protein causes the hearing loss, which might be attributed to the relatively large stretch of 41 aberrant amino acids. Since the alternative splicing product is also seen in a variable but lower ratio to the normal mRNA in controls, there might be a critical threshold for the aberrant protein above which it becomes pathogenic. This is underlined by the fact that the mutations in the only two DFNA5 families known so far have the same effect on the mRNA and the putative protein but affect a different amount of the transcript. Unfortunately, nothing is known about either the wild type or the short protein. Both proteins have very different C termini and neither have similarity with any other protein or protein domain. Whether the differences in speech recognition between the two families are due to the different ratios of normal versus short protein remains to be elucidated. One might think about discrepancies in pathogenic thresholds in different parts of the cochlea. Alternatively, modifier genes might be involved. Findings in additional families with a mutation in the *DFNA5* gene may elucidate whether other mutations in the gene also lead to a similar type of hearing impairment or whether only the putative short protein causes hearing loss.

The function of the DFNA5 protein is still unknown, although there are some clues indicating that DFNA5, also designated ICERE-1, might be involved in the regulation of apoptosis. Recently, Lage et al. (Lage et al. 2001) reported that decreased *DFNA5* mRNA levels are associated with a decrease in apoptotic events after exposure to the drug etoposide. It appeared that increased *DFNA5* mRNA levels are associated with increased cellular disposition to programmed cell death mediated by activation of caspase 3. However, it has not yet been proven that there is a direct effect of DFNA5 on apoptosis. Interestingly, apoptosis is important in the development of the inner ear predominantly during the embryonic and early postnatal development of the cochlea (Jókay et al. 1998, Nishizaki et al. 1998, Nishikori et al. 1999, Nikolic et al. 2000). Two studies of *caspase 3* knockout mice have shown that caspase 3 deficiency results in severe hearing loss (Morishita et al. 2001, Takahashi et al. 2001). Hyperplasia of supporting cells and degeneration of sensory hair cells and cochlear neurons are seen in the inner ear of these mice (Morishita et al. 2001, Takahashi et al. 2001). In 5-week-old homozygous *caspase 3* knockout mice extensive loss of hair cells was observed in the basal and middle turns of the cochlea but not in the apical turns. Degeneration of the hair cells begins early, progressively worsens with age and spreads from the basal turns towards the apical turns. These findings might explain why DFNA5 is a progressive form of hearing loss that affects the higher and middle frequencies earlier and more severely than the lower frequencies. The ongoing characterization of mice in which the mutation in the original DFNA5 family is mimicked will elucidate whether the cochlear defects are similar to those in the caspase 3-deficient mice and thus whether DFNA5 might have a function in apoptosis in the inner ear (Van Laer et al. 2002b).

3.5 Patients and methods

A 5-generation pedigree was established for the present family (W00-212). Thirty-seven family members participated in this study. The medical history was taken and otological examination was performed. Attention was paid to the presence of any syndromic features. Non-hereditary causes of hearing loss were excluded, and written informed consent was obtained. All individuals included in this study underwent pure-tone audiometry; speech audiometry was performed in affected persons only. Vestibular function was tested in 6 cases. One affected person underwent computerized tomography of the temporal bones. Blood samples were obtained for linkage analysis from 18 presumably affected family members and 19 presumably unaffected persons.

3.5.1 Audiometric Analysis

Pure-tone and speech audiometry were performed in a soundtreated room, conforming to the International Standards Organisation (ISO) standards (ISO 389: Acoustics. Standard reference zero for the calibration of pure tone air conduction audiometers. Geneva, International Organisation for Standardization, 1985 and ISO 8253-1: Acoustics. Audiometric test methods. I. Basic pure tone air and bone conduction threshold audiometry. Geneva, International Organisation for Standrdization, 1989). The individual 95th percentile threshold values of presbyacusis in relation to the patient's

sex and age were derived for each frequency using the ISO 7029 method (ISO 7029: Acoustics. Threshold as hearing by air conduction as a function of age and sex for otologically normal persons. Geneva, International Organisation for Standardization, 1984). Persons were considered affected if the best hearing ear showed thresholds beyond this 95th percentile threshold of presbyacusis. Mean binaural threshold levels were used to perform longitudinal regression analyses. Analysis of covariance (Prism PC version 3.02; GraphPad, San Diego, Calif., USA) was performed to compare between slopes and intercepts of the regression lines pertaining to individual measurements per frequency. Where pooled regression was inappropriate, the median slope (called annual threshold deterioration, expressed in decibels per year) and intercept were calculated, following inspection of the corresponding frequency distributions. Outlying values were excluded, if necessary. The lines defined by the combination of the slope and intercept values thus obtained were called trend lines. These lines were used to construct age-related typical audiograms (ARTA). To compare the audiological data of the original (De Leenheer et al. 2002a) and the present DFNA5 family, we transformed the ARTA into a one dimensional threshold features array, which can be used for χ^2 analysis, as previously described (Huygen et al. 2003).

3.5.2 Speech audiometry

Speech audiometry was performed, using standard monosyllabic Dutch word lists. The maximum monaural phoneme score (percent correct recognition) was derived from a performance versus intensity plot. Cross-sectional binaural mean phoneme recognition scores were plotted for all mutation carriers against age and binaural mean PTA at 1, 2 and 4 kHz (pure-tone average in decibels hearing level). Non-linear regression analysis was used to fit sigmoidal doseresponse curves with variable slope, as previously described (Bom et al. 2001). Outlying values were excluded, if necessary. The age of onset and onset level were defined at a maximum phoneme recognition score of 90% in the performance versus age and performance versus impairment plots. The slope was called deterioration rate in the performance versus age plot, whereas it was called deterioration gradient in the performance versus impairment plot. To simplify the results and allow for additional testing, 'local average' slope (i.e. on a linear scale) for $X>X_{90}$ (X is either age or PTA level) was obtained by fitting a straight line as previously described (Bom et al. 2003), using a non-linear method to estimate X_{90} (De Leenheer et al. 2002b). Student's t test (with Welch correction if significantly unequal variance was detected by Bartlett's test) was employed to test age of onset, deterioration rate, onset level or deterioration gradient between the present and the original DFNA5 family (De Leenheer et al. 2002b).

3.5.3 Linkage analysis

DNA was isolated from peripheral blood according to Miller et al. (1988). Analysis of the microsatellite markers was performed as described by Kremer et al. (1996). Two-point lod scores were calculated with the MLINK subroutine of the LINKAGE package version 5.1 (Lathrop and Lalouel 1984, Lathrop et al. 1984, Lathrop et al. 1986). A

penetrance of 0.95, a disease allele frequency of 0.0001 and a phenocopy rate of 0.001 were assumed for the calculations.

3.5.4 Mutation analysis

Amplification of the protein-coding region from chromosomal DNA was performed using standard PCR conditions. Primer sequences have been described by Van Laer et al. (Van Laer et al. 2002a), except for amplification of exon 9 for which we used 5'-GGTCCCACCTGGGAGGTTGC-3' and 5'-CTGTGACTGTGATTTTTCTCTCC-3'. Prior to sequencing, PCR fragments were purified with the QIAquick gel extraction kit (Qiagen). Sequence analysis was performed using the ABI PRISM Big Dye Terminator cycle sequencing V2.0 ready reaction kit and an ABI PRISM 3700 DNA analyser (Applied Biosystems). For testing the segregation of the mutation in the family, genomic DNA was amplified with the primers 5'-GTCTCCAGCTGTGTCATGACC-3' and 5'-CCATTTCTTTCATTTTCTTTTCTCC-3'. PCR fragments were digested with *Rsa*I (Invitrogen) and separated on an agarose gel (Seakem agarose, FMC).

3.5.5 Reverse transcriptase polymerase chain reaction

Messenger RNA of lymphoblastoid cells cultured under standard conditions was isolated according to the RNA-Bee (Campro Scientific) protocol. To establish the effect of nonsense mediated RNA decay (NMD), lymphoblastoid cells were treated with cycloheximide (100 µg/ml cell culture medium) for 4.5 h. For the initial testing of skipping of exon 8 and detection of other alternative splicing products, cDNA was synthesized by random priming with MMLV reverse transcriptase (Invitrogen). Subsequently PCR was performed with the primers 5'-CCTGAGCCACAACAGACAGC-3' in exon 7 and 5'-GGCACAGTGTGGGAATGATCTG-3' in exon 9, and fragments were analysed on agarose gel. For the detection of alternative splicing in other parts of the mRNA, the following primers were used: 5'-AGAGGCCCCGACATCTCC-3' in exon 1, 5'-TCGACCTGCATGTGCTCAG-3' in exon 4, 5'-GGTGCTGGAAGGAAGGAATG-3' in exon 4, 5'-CAAATAGGACCGCCTGGAAG-3' in exon 7, 5'-TCTGCTGGGCACTTGCTG-3' in exon 9 and 5'-TCATCATGCAAAATGTCACCAC-3' in exon 10. For comparison of the ratio between the normal and the short *DFNA5* mRNA, cDNA synthesis was performed with the one-step RT-PCR kit (Qiagen). The ^{32}P-labelled primers given above for testing of exon 8 skipping were used, and 25 cycles of PCR were performed. After denaturation, fragments were separated on a denaturing acrylamide gel. Phospo-imaging was performed using the Gs-363 molecular imaging system (Biorad). The data were analysed, and the ratios between normal and short mRNA were determined with the molecular analyst software, version 1.5 (Biorad). As control samples for RT-PCR, mRNA was isolated from lymphoblastoid cells of 22 normal-hearing individuals. One individual was 15 years old, all others were between 20 and 83 years old.

3.5.6 Southern blot analysis

Chromosomal DNA (about 8 µg per lane) was digested with *Msp*I, *Eco*RI and *Taq*I and separated on a 0.8% agarose gel (Seakem agarose, FMC) and blotted onto GeneScreen

plus (NEN Life Science Products) by a standard dry blot transfer method. As probe, 40 ng of a cDNA encompassing the complete coding region was labelled with α[$_{32}$P]dCTP by random primer extension and hybridised under standard conditions.

3.6 Acknowledgments

We wish to thank the participating family. Dr. C.F.S. Schudel is acknowledged for the logistic support during the clinical study. Prof. Dr. E.H. Huizing is accredited for usage of previously published data. This study was supported by grants from the Heinsius Houbolt Foundation, the Nijmegen ORL Research Foundation and the Netherlands Organization for Scientific Research (grant 901-04-205). L.V.L. holds a research position with the Flemish Fonds voor Wetenschappelijk Onderzoek.

3.7 References

Bom S.J.H., De Leenheer E.M.R., Lemaire F.X., et al., Speech recognition scores related to age and degree of hearing impairment in DFNA2/*KCNQ4* and DFNA9/*COCH*. Arch Otolaryngol Head Neck Surg 2001 127: 1045-1048.

Bom S.J.H., Kemperman M.H., Huygen P.L.M., et al., Cross-sectional analysis of hearing threshold in relation to age in a large family with cochleovestibular impairment thoroughly genotyped for DFNA9/COCH. Ann Otol Rhinol Laryngol 2003 112: 280-286.

De Leenheer E.M.R., van Zuijlen D.A., Van Laer L., et al., Clinical features of DFNA5. in Cremers C.W.R.J., Smith R., Genetic Hearing Impairment: Its Clinical Presentations. Adv Otorhinolaryngol. 2002a Karger, Basel 61: 53-59.

De Leenheer E.M.R., van Zuijlen D.A., Van Laer L., et al., Further delineation of the *DFNA5* phenotype: Results of speech recognition tests. Ann Otol Rhinol Laryngol 2002b 111: 639-641.

Dib C., Faure S., Fizames C., et al., and Weissenbach J., A comprehensive genetic map of the human genome based on 5,264 microsatellites. Nature 1996 380: 152-154.

Huizing E.H., van Bolhuis A.H., and Odenthal D.W., Onderzoekingen over progressieve hereditaire perceptiedoofheid bij een uit 355 leden bestaande familie. Ned Tijdschr Geneesk 1965 109: 499-503.

Huizing E.H., van Bolhuis A.H., and Odenthal D.W., Studies on progressive hereditary perceptive deafness in a family of 335 members. I. Genetical and general audiologic results. Acta Otolaryngol 1966a 61: 35-41.

Huizing E.H., van Bolhuis A.H., and Odenthal D.W., Studies on progressive hereditary perceptive deafness in a family of 335 members. II. Characteristic pattern of hearing deterioration. Acta Otolaryngol 1966b 61: 161-167.

Huizing E.H., Odenthal D.W., and van Bolhuis A.H., Results of further studies on progressive hereditary sensorineural hearing loss. Audiology 1972 12: 261-263.

Huizing E.H., van den Wijngaart W.S.I.M., and Verschuure J., A follow-up study in a family with dominant progressive inner ear deafness. Acta Otolaryngol 1983 95: 620-626.

Huygen P.L.M., Pennings R.J.E., and Cremers C.W.R.J., Characterizing and distinguishing progressive

Jókay I., Soós G., Répássy G., et al., Apoptosis in the human inner ear: Detection by in situ end-labeling of fragmented DNA and correlation with other markers. Hear Res 1998 117: 131-139.

Kremer H., Kuyt L., van den Helm B., van Reen M., et al., Localization of a gene for Möbius syndrome to chromosome 3q by linkage analysis in a Dutch family. Hum Mol Genet 1996 5: 1367-1371.

Lage H., Helmbach H., Grottke C., et al., DFNA5 (ICERE-1) contributes to acquired etoposide resistance in melanoma cells. FEBS Lett 2001 494: 54-59.

Lathrop G. and Lalouel J., Easy calculations of lod scores and genetic risks on small computers. Am J Hum Genet 1984 36: 460-465.

Lathrop G., Lalouel J., Julier C., et al., Strategies for multilocus linkage analysis in humans. Proc Natl Acad Sci USA 1984 81: 3443-3446.

Lathrop G., Lalouel J., and White R., Construction of human linkage maps: Likelihood calculations for multilocus linkage analysis. Genet Epidemiol 1986 3: 39-52.

Miller S., Dykes D., and Polensky H., A simple salting out procedure for extracting DNA from human nucleated cells. Nucleic Acids Res 1988 16: 1215.

Morishita H., Makishima T., Kaneko C., et al.., Deafness due to degeneration of cochlear neurons in caspase-3-deficient mice. Biochem Biophys Res Commun 2001 284: 142-149.

Nikolic P., Järlebark L.E., Billett T.E., et al., Apoptosis in the developing rat cochlea and its related structures. Dev Brain Res 2000 119: 75-83.

Nishikori T., Hatta T., Kawauchi H., et al., Apoptosis during inner ear development in human and mouse

embryos: An analysis by computer- assisted three dimensional reconstruction. Anat Embryol 1999 200: 19-26.
Nishizaki K., Anniko M., Orita Y., et al., Programmed cell death in the developing epithelium of the mouse inner ear. Acta Otolaryngol 1998 18: 96-100.
phenotypes in nonsyndromic autosomal dominant hearing impairment. Audiol Med 2003 1: 37-46.
Shapiro M.B. and Senapathy P., RNA splice junctions of different classes of eukaryotes: Sequence statistics and functional implications in gene expression. Nucleic Acids Res 1987 15: 7155-7174.
Takahashi K., Kamiya K., Urase K., et al., Caspase-3-deficiency induces hyperplasia of supporting cells and degeneration of sensory cells resulting in hearing loss. Brain Res 2001 894: 359-367.
Thompson D.A. and Weigel R.J., Characterization of a gene that is inversely correlated with estrogen receptor expression (ICERE-1) in breast carcinomas. Eur J Biochem 1998 252: 169-177.
Van Camp G., Coucke P., Balemans W., et al., Localisation of a gene for non-syndromic hearing loss (DFNA5) to chromosome 7p15. Hum Mol Genet 1995 4: 2159-2163.
van den Wijngaart W.S.I.M., Verschuure J., Brocaar M.P., et al., Follow-up study in a family with dominant progressive hereditary sensorineural hearing impairment. I. Analysis of hearing deterioration. Audiology 1985a 24: 233-240.
van den Wijngaart W.S.I.M., Huizing E.H., Niermeijer M.F., et al., Follow-up study in a family with dominant progressive hereditary sensorineural hearing impairment. II. Clinical aspects. Audiology 1985b 24: 336-342.
Van Laer L., Huizing E.H., Verstreken M., et al., Nonsyndromic hearing impairment is associated with a mutation in DFNA5. Nat Genet 1998 20: 194-197.
Van Laer L., De Stefano A.L., Myers R.H., et al., Is *DFNA5* a susceptibility gene for age-related hearing impairment? Eur J Hum Genet 2002a 10: 883-886.
Van Laer L., Pfister M., Thys S., et al., The DFNA5 mouse: The first analysis of the phenotype (abstract). Acta Otorhinolaryngol Belg 2002b 56: 267.

Chapter 4

Identification and molecular modelling of a mutation in the motor head domain of myosin VIIA in a family with autosomal dominant hearing impairment (DFNA11)

M.W.J. Luijendijk[a], E. van Wijk[b], A.M.L.C. Bischoff[b], E. Krieger[c], P.L.M. Huygen[b], R.J.E. Pennings[b], H.G. Brunner[a], C.W.R.J. CremersF[b], F.P.M. Cremers[a] and H. Kremer[b]

[a] Department of Human Genetics, University Medical Centre Nijmegen, Nijmegen, The Netherlands
[b] Department of Otorhinolaryngology, University Medical Centre Nijmegen, Nijmegen, The Netherlands
[c] Center for Molecular and Biomolecular Informatics, University of Nijmegen, Nijmegen, The Netherlands

Published in: Hum. Genet. 2004 115: 149-156

4.1 Abstract

Myosin VIIA is an unconventional myosin that has been implicated in Usher syndrome type 1B, atypical Usher syndrome, non-syndromic autosomal recessive hearing impairment (DFNB2) and autosomal dominant hearing impairment (DFNA11). Here, we present a family with non-syndromic autosomal dominant hearing impairment that clinically resembles the previously published DFNA11 family. The affected family members show a flat audiogram at young ages and only modest progression, most clearly at the high frequencies. In addition, they suffer from minor vestibular symptoms. Linkage analysis yielded a maximum two-point lodscore of 3.43 for marker D11S937 located within 1 cM of the myosin VIIA gene. The myosin VIIA gene was sequenced and 11 nucleotide variations were found. Ten nucleotide changes represent benign intronic variants, silent exon mutations or nonpathologic amino acid substitutions. One variant, a c.1373A>T transversion that is heterozygously present in all affected family members and absent in 300 healthy individuals, is predicted to result in an Asn458Ile amino acid substitution. Asn458 is located in a region of the myosin VIIA motor domain that is highly conserved in different classes of myosins and in myosins of different species. To evaluate whether the Asn458Ile mutation was indeed responsible for the hearing impairment, a molecular model of myosin VIIA was built based on the known structure of the myosin II heavy chain from *Dictyostelium discoideum*. In this model, conformational changes in the protein caused by the amino acid substitution Asn458Ile are predicted to disrupt ATP/ADP binding and impair the myosin power-stroke, which would have a severe effect on the function of the myosin VIIA protein.

4.2 Introduction

Myosin VIIA is an unconventional myosin that has been implicated in recessively inherited Usher syndrome type 1B (Weil et al. 1995, Weston et al. 1996), recessively inherited atypical Usher syndrome (Liu et al. 1998, Zina et al. 2001), non-syndromic autosomal recessive hearing impairment (DFNB2; Liu et al. 1997a, Liu 2002) and autosomal dominant hearing impairment (DFNA11; Liu et al. 1997b). The myosin VIIA (*MYO7A*) gene consists of 49 exons and encodes a polypeptide of 2,215 amino acids. *MYO7A* is expressed in the inner ear, retina, testis, lung and kidney (Hasson et al. 1995). In the human retina *MYO7A* is expressed in the retinal pigment epithelium and in photoreceptor cells (El-Amraoui et al. 1996). In the inner ear, the gene is expressed in the inner and outer hair cells of the cochlea and in the type I and type II hair cells of the utricular and semicircular canal hair cells, in which it is found in the stereocilia, the cuticular plate and the cell body (Hasson et al. 1995, 1997).

Unconventional myosins are actin-based motor molecules that transduce chemical energy derived from ATP into a force enabling them to move along actin filaments, thereby transporting cargo along these filaments (see Hirokawa and Takemura 2003, and references therein). The structure of type VII myosin proteins is highly conserved in vertebrates and invertebrates (Oliver et al. 1999). The human myosin VIIA consists of a motor head domain (amino acids 1-729) containing ATP- and actinbinding motifs, a neck region composed of five isoleucine/glutamine (IQ) motifs (amino acids

730-855; expected to bind calmodulin) and a long tail (amino acids 856-2,215). The tail begins with a short coiled-coil domain (amino acids 848-1,095) shown to be involved in homodimer formation (Weil et al. 1997). This domain is followed by two large repeats of ~460 amino acids each containing a myosin tail homology 4 (MyTH4) and a 4.1, ezrin, radixin, moesin (FERM)-like domain, separated by a poorly conserved src homology type 3 (SH3) domain (fig. 4; Oliver et al. 1999). Previously, Liu et al. (1997b) have shown that an inframe 9-bp deletion in exon 22 of *MYO7A* causes DFNA11 in a Japanese family. The affected family members suffer from postlingual, bilateral, non-syndromic sensorineural hearing loss, with gradual progression at all frequencies and minor vestibular problems; no evidence has been found for retinitis pigmentosa (Tamagawa et al. 2002). The 9-bp deletion is predicted to result in a 3-amino-acid deletion in the coiled-coil region of the protein. The aberrant protein is thought to be able to interact with the wild-type protein, resulting in a dominant negative effect (Liu et al. 1997b).

Here, we present a second mutation in *MYO7A* found to be implicated in DFNA11. Affected family members suffer from bilateral non-syndromic hearing loss, which is most progressive at the higher frequencies, and minor vestibular problems. We have found a nucleotide change causal for the hearing impairment, viz. a transversion that is heterozygously present in all affected persons. This nucleotide change results in an Asn458Ile amino acid substitution. We present a molecular model of the motor head domain of the human myosin VIIA protein. In the model of the mutant protein, the isoleucine residue at position 458 probably disrupts ATP/ADP binding and impairs the myosin power-stroke. The c.1373A>T nucleotide change is therefore considered to underlie the hearing impairment in this family.

4.3 Results

4.3.1 Linkage analysis

The cross-sectional age-related typical audiograms combined with the minor vestibular problems suggested DFNA11 as the type of hearing loss segregating in family W02-011 (fig. 1). Therefore, a linkage study was initiated with the maker D11S937 located at 11q14.1 approximately 1 Mb telomeric of the causative gene for DFNA11, *MYO7A*. The distance between marker D11S937 and *MYO7A* is <1 cM according to the deCode genetic map (Kong et al. 2002). All affected and non-affected family members from the age of 30 years onwards were included in the linkage study. As suggested by the clinical data, the hearing loss completely co-segregated with one particular allele of D11S937 (fig. 2), with a maximum two-point lodscore of 3.43.

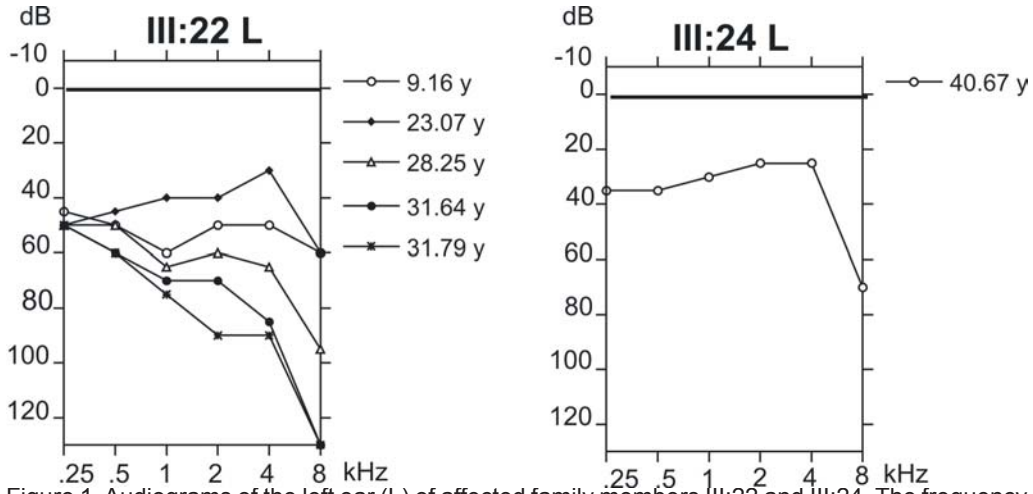

Figure 1. Audiograms of the left ear (L) of affected family members III:22 and III:24. The frequency is indicated on the X-axis in kilohertz (kHz). The hearing threshold is indicated on the Y-axis in decibels (dB). The ages at which audiograms are taken are given in years (y).

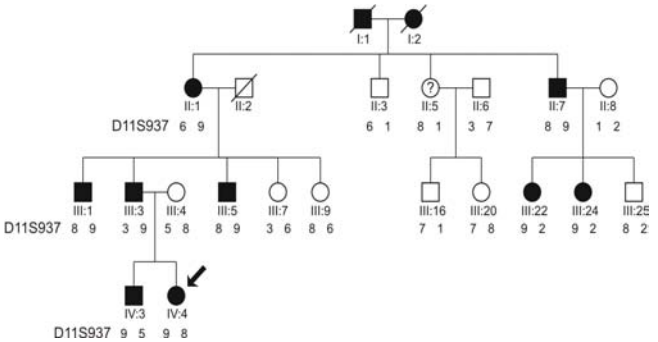

Figure 2. Pedigree of family W02-011 and D11S937 marker analysis. Square Men, circle women, filled symbols affected persons, arrow proband. Allele 9 co-segregates with the disease. The hearing status of person II:5 was unclear; she was therefore given an unknown status (?).

4.3.2 Mutation analysis

Only one other DFNA11 family has been described so far (Liu et al. 1997b) in which a 9-bp deletion in exon 22 of the MYO7A gene results in a 3-amino acid deletion (Lys888-Lys890del) in the coiled-coil region of the protein. Therefore, exon 22 was first analysed by DNA sequencing in the present family but no mutation was found. The remaining 48 exons of the gene were subsequently analysed by direct DNA sequencing of DNA from person III:3. Eleven sequence variations were found that were all present heterozygously, except for the homozygous change IVS41-12T>C (table 1). A total of four intronic nucleotide changes previously described as polymorphisms reside in or near splice sites. According to the “splice efficiency” calculation proposed by Shapiro and Senapathy (1987), these nucleotide changes are not predicted to have a negative effect on splicing efficiency.

Table 1. Polymorphisms found in the *MYO7A* DNA sequence in the DFNA11 family.

Exon	*Nucleotide change*	*Amino acid change*	*Reference*
8	c.783T>C	Gly261Gly	Weston et al. 1996; Lévy et al. 1997; Bharadwaj et al. 2000
10	c.1007G>A	Arg336His	This study
13	**c.1373A>T**	**Asn458Ile**	**This study**
27	IVS27+10del22	no effect on splicing[a]	Adato et al. 1997; Janecke et al. 1999)
30	IVS30+12C>T	no effect on splicing[a]	(Bharadwaj et al. 2000
35	c.4755C>T	Ser1585Ser	Lévy et al. 1997; Adato et al. 1997; Janecke et al. 1999; Bharadwaj et al. 2000
36	c.4996T>A	Cys1666Ser	Lévy et al. 1997; Janecke et al. 1999; Bharadwaj et al. 2000
41	c.5715G>A	Lys1905Lys	Lévy et al. 1997; Adato et al. 1997; Janecke et al. 1999; Bharadwaj et al. 2000
42	IVS41-12T>C[b]	no effect on splicing[a]	This study
43	c.5860A>C	Ile1954Leu	Adato et al. 1997; Janecke et al. 1999; Bharadwaj et al. 2000
43	IVS42-7A>T	no effect on splicing[a]	Lévy et al. 1997; Janecke et al. 1999; Bharadwaj et al. 2000

[a]According to Shapiro and Senapathy (1987)
[b]Homozygous sequence variant

Three previously described variants reside in the *MYO7A* open reading frame but do not lead to amino acid substitutions. Three other exonic changes result in amino acid changes. Cys1666Ser and Ile1954Leu are previously described polymorphisms (Lévy et al. 1997, Adato et al. 1997). Arg336His is a novel sequence variant that has been shown not to co-segregate with the hearing impairment in our family. We therefore assume that this is a rare polymorphism. A c.1373A>T transversion was found heterozygously in exon 13 (fig. 3A, B) in all affected, but in none of the unaffected, family members, as confirmed by direct sequencing. Individual II:5 did not carry the mutation. The nucleotide change is predicted to result in an Asn458Ile amino acid substitution. ARMS analysis showed that the c.1373A>T change was absent in 300 control individuals. In this analysis, we found one control individual with a c.1373A>G transversion, which leads to amino acid change Asn458Ser (data not shown).

4.3.3 Molecular modelling

Asn458 is located in a region of the myosin VIIA motor domain, which is highly conserved in different classes of myosins and myosins of different species (fig. 4). To evaluate whether the Asn458Ile mutation is indeed responsible for the hearing impairment in this DFNA11 family, a molecular model of myosin VIIA was built based on the known structure of the myosin II heavy chain from *D. discoideum* (Kliche et al. 2001). With 37% sequence identity and an alignment spanning 750 amino acid residues, both proteins are guaranteed to adopt the same fold (Rost 1999). In the model, Asn458 is a conserved residue that is part of the switch II α-helix and fulfils an important structural role by attaching the helix to the preceding switch II loop (fig. 3C). This is achieved via a strong hydrogen bond between its side-chain amino group and the backbone oxygen of

the Phe439 in the loop. The two conserved flanking residues, Ile438 and Gly440, have been shown to be of crucial importance for a conformational change of the myosin head. Depending on the ligand bound in the ATPase pocket, the two corresponding residues in *D. discoideum*, Ile455 and Gly457, undergo changes of the backbone torsion angles that are accompanied by a concerted rigid body movement of the Cterminal domain (Fisher et al. 1995). Whereas the precise mechanism of the myosin power-stroke is still a matter of debate, this domain movement clearly plays an important role.

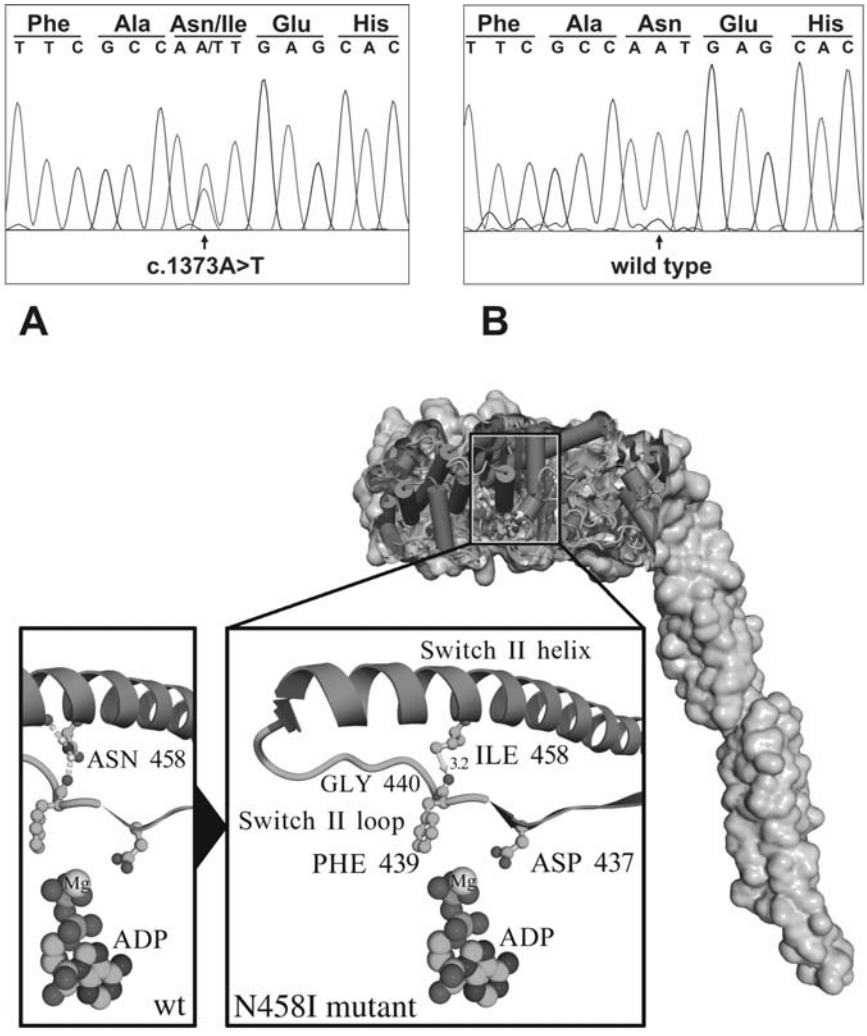

Figure 3. Identification of the Asn458Ile mutation and the predicted functional effect in the myosin VIIA model. (A) Sequence analysis of exon 13 of MYO7A reveals a heterozygous c.1373A>T (Asn458Ile) substitution. (B) Sequence analysis of exon 13 of MYO7A of an unaffected individual. (C) Molecular modelling of myosin VIIA. If isoleucine replaces asparagine at position 458, its larger side-chain collides with the backbone oxygen of phenylalanine 439 in the switch II loop (arrow), pushing the loop towards the ATPase pocket. This is assumed to negatively influence the sensing of the active site state (involving Asp437) and the reorientation in the switch II loop hinge region (Ile438 and Gly440, not shown).

In the model, the Asn458Ile mutation is predicted to have severe effects (fig. 3C). The differently shaped isoleucine side-chain collides with the backbone of Phe439 and pushes the entire switch II loop towards the ATPase pocket (arrow in fig. 3C). The connecting hydrogen bond is lost and, at the same time, the hydrophobic side chain of Ile458 covers the backbone oxygen of Phe439, adding an unsaturated hydrogen-bond acceptor to the energetic cost of the mutation.

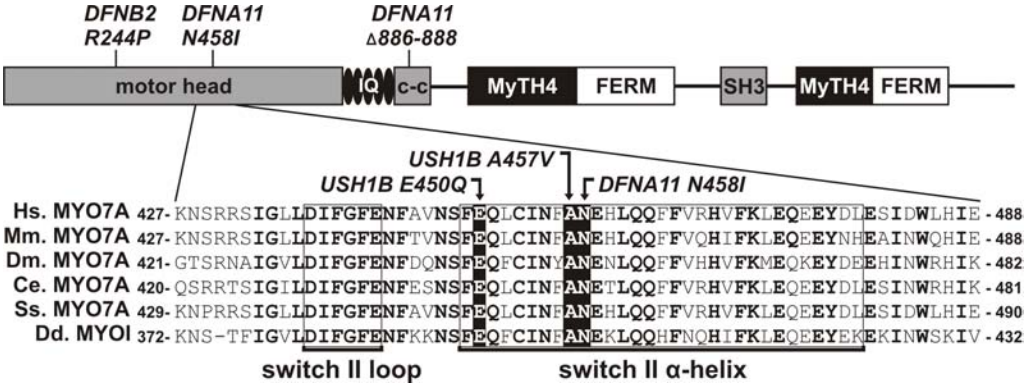

Figure 4. Myosin VIIA protein domain structure and amino-acid sequence alignment of myosin VIIA orthologues derived from six different species. Upper panel The various protein domains are indicated with different shades of grey. The motor head domain, 5 IQ regions, a coiled-coil domain (c-c), two MyTH4 domains, two FERM-like domains, and an SH3 domain are shown. The positions of two DFNA11 mutations and one DFNB2 mutation are also indicated. Lower panel Sequences of myosin VIIA protein orthologues from six species are compared: Homo sapiens (Hs.), Mus musculus (Mm.), Drosophila melanogaster (Dm.), Caenorhabditis elegans (Ce.), Sus scrofa (Ss.) and Dictyostelium discoideum (Dd.). Conserved residues are indicated in bold. The highly conserved switch II loop and switch II α-helix. The DFNA11 and USH1B mutations are indicated.

4.4 Discussion

Based on careful phenotypic analysis, we could identify a second family in which non-syndromic autosomal dominant hearing impairment segregates with the DFNA11 locus at 11q14.1. Sequence analysis revealed 11 sequence variations in the *MYO7A* gene. Only one nucleotide change, c.1373A>T, leading to an Asn458Ile amino acid change, was inherited with the hearing loss. Asn458 is fully conserved in all known myosin VIIA homologues. Computer modelling based on the known structure of the myosin II heavy chain of *D. discoideum* revealed that Asn458 has an important structural role. In the model of the aberrant protein, the differently shaped side chain of isoleucine at position 458 is predicted to cause important structural changes in the motor head domain of the protein. This will probably disrupt ATP/ADP binding and/or impair the myosin power-stroke. A putative Asn458Ser amino acid change found heterozygously in one out of 300 control persons tested was predicted by modelling to have little or no effect on the function of the protein (data not shown). We assume that Asn458Ser is a rare polymorphism or a rare recessive mutation.

In a previously described Japanese family (Liu et al. 1997b), a 9-bp deletion

was found in exon 22 encoding the coiled-coil region that is predicted to allow myosin VIIA to dimerise (Weil et al. 1997). The 3-amino-acid deletion in the coiled-coil region is presumed to have a dominant negative effect, because of the improper dimerisation of wild-type and mutant proteins and thus the impairment of the function of the wild-type protein. In contrast, in the family described here, the aberrant protein is expected to dimerise properly. However, since aberrant proteins can dimerise with wild-type proteins and thus also impair the function of wild-type proteins, this is presumed to give a dominant negative effect. The phenotypes in the Japanese and Dutch families are similar, suggesting similar disease mechanisms, despite the underlying mutations being different.

The main phenotypic variation caused by mutations in the *MYO7A* gene is the presence or absence of impaired visual function. The function of the protein therefore probably differs in the processes of hearing and vision. The recent finding of a protein (MyRIP) that binds myosin VIIA and Rab27a, a melanosome-binding G-protein, supports the idea that, in the eye, the myosin VIIA protein is involved in the short-range peripheral movement of melanosomes along the actin-rich microvilli of the retinal pigment epithelial cells (El-Amraoui et al. 2002). Wolfrum and Schmitt (2000) have demonstrated that myosin VIIA and rhodopsin are spatially co-localized at the membrane domain of the connecting cilium of the photoreceptor cells. Combined with the abnormally high amounts of opsin seen in the connecting cilia of shaker-1 mice (Liu et al. 1999), these results indicate the functional coupling of myosin VIIA motor function and the transport of opsin through the connecting cilium. In addition, Gibbs et al. (2003) have concluded that myosin VIIA is required for the normal processing of ingested disk membranes in the retinal pigment epithelium, primarily in the basal transport of the phagosomes into the cell body where they then fuse with lysosomes. From their recent studies, Kros et al. (2002) have suggested that, in the inner ear, myosin VIIA participates in the anchoring of membrane-bound elements to the actin core of the stereocilium and is required for the normal gating of transducer channels in the stereocilia. Boëda et al. (2002) have shown that myosin VIIA interacts directly with harmonin and may convey harmonin b along the actin core of the developing stereocilia where it anchors cadherin 23 to the actin filament core. Boëda et al. (2002) have postulated that myosin VIIA indirectly modulates the gating properties of the transducer channels in the stereocilia during development, by translocating the proteins that regulate the transduction process along the developing stereocilium. These findings are supported by studies on a mouse model for myosin VIIA mutations, shaker-1 (*sh1*; Self et al. 1998), which have revealed that severe mutations result in the disorganization of the normal pattern of stereocilia on the surface of the hair cells in the cochlea. Milder mutations do not cause changes in hair cell morphology, but affected animals are nevertheless deaf (Self et al. 1998), suggesting that myosin VIIA performs other functions in the hair cells in addition to ensuring the proper organization of the stereocilia. Apparently, the transversion of asparagine into isoleucine in the aberrant protein causes impaired inner ear function, whereas the function of the retina is not affected.

Alternatively, other complementary proteins might rescue the loss of function of myosin VIIA in the eye, whereas in the inner ear, the function of the protein is unique and

cannot be compensated for by other proteins. In addition, the residual wild-type dimers that can still be formed may suffice for proper visual function.

There appears to be no obvious correlation between the location of a missense mutation in the myosin VIIA protein and the resulting phenotype. For example, Asn458Ile causes DFNA11, whereas a change in the flanking amino acid, Ala457Val combined with Arg90Pro, can cause Usher syndrome type 1B (Bharadwaj et al. 2000), as does Glu450Gln in the same highly conserved switch II α-helix (Weston et al. 1996). In order to understand the disease mechanisms underlying these different phenotypes and to gain more insights into the function of individual amino acids in the protein, in vivo functional studies are essential. Of late, many functional studies of various model organisms, such as mice and zebra fish, have been published (Self et al. 1998, Ernest et al. 2000). A model organism that is frequently used for these investigations is *D. discoideum* (Sasaki and Sutoh 1998, Furch et al. 1999, Tsiavaliaris et al. 2002). Unfortunately, none of the many studies of mutations in the motor domain that have been undertaken to investigate myosin VIIA properties have, to our knowledge, included the mutation that we describe here. Further functional studies of the myosin VIIA protein, e.g. in *Dictyostelium*, should be carried out to provide further evidence that the amino acid change Asn458Ile is causative of the hearing impairment inherited in this family.

In conclusion, in this study, we have identified the first autosomal dominant hearing impairment mutation in the motor head domain of myosin VIIA and have provided a model for the functional consequences of the mutation. The phenotype in the first DFNA11 family is similar to that in the present family, although the mutation in the first DFNA11 family is in a different region of the protein and can be predicted to have a different effect. Our results also show that phenotypic characteristics in a family with hearing loss can lead to the rapid elucidation of the underlying genetic defect.

4.5 Patients and methods

4.5.1 Patients

A four-generation pedigree was established for a Dutch family (W02-011) with hearing impairment (fig. 2). Twenty-six family members from the youngest three generations participated in this study. The local ethics committee approved this study and written informed consent was obtained from all participating individuals. Blood samples were obtained for linkage and mutation analysis.

The genetic defect segregating in this family shows autosomal dominant inheritance (fig. 2). Affected family members present with a flat audiogram at young ages and there is only modest progression, most clearly at high frequencies, with increasing age (A.M.L.C. Bischoff et al., unpublished data). Two audiograms are given in figure 1. Vestibular examination in six affected individuals showed a variation in vestibular function from normal vestibular responses to areflexia. Four out of six affected individuals in whom vestibular examination was performed presented with vestibular symptoms such as vertigo and unsteady walking, especially in the dark. Five affected individuals underwent extensive ophthalmological examination. Minor abnormalities in electro-oculograms and electro-retinograms were found in some affected individuals.

The hearing status of person II:5 in the pedigree was unclear; she was therefore given an unknown status in the linkage analysis. Clinical details will be presented in a separate paper (A.M.L.C. Bischoff et al., unpublished data).

4.5.2 Linkage analysis

DNA was isolated from peripheral blood according to Miller et al. (1988). Analysis of microsatellite markers was performed as described by Kremer et al. (1996). Two-point lod scores were calculated with the MLINK subroutine of the LINKAGE package version 5.1 (Lathrop and Lalouel 1984, Lathrop et al. 1984, 1986). A penetrance of 0.95, a disease allele frequency of 0.0001 and a phenocopy rate of 0.001 were assumed for the calculations.

4.5.3 Mutation analysis

All 49 exons and exon-intron boundaries of the *MYO7A* gene were amplified by using standard polymerase chain reaction (PCR) conditions and were completely sequenced. The primer sequences are given in table 2 and the precise PCR conditions are available from the authors upon request. Prior to sequencing, PCR fragments were purified with the QIAquick gel extraction kit (Qiagen). Sequence analysis was performed with the ABI PRISM Big Dye Terminator cycle sequencing V2.0 ready reaction kit and an ABI PRISM 3700 DNA analyzer (Applied Bio systems). The sequences were compared with the known sequence (GenBank accession no. NM_000260). The presence of the mutation was tested in 300 ethnically matched control individuals with the amplificationrefractory mutation system (ARMS; Newton et al. 1989) and primers: 5′-TTGAGCAGCTCTGCATCAACTTCGCCGT-3′ (*MYO7A* mutant forward), 5′-TTGAGCAGCTCTGCATCAACTTCGCCGA-3′ (*MYO7A* wild-type forward) and 5′-acttgctctcctcatcgatgagggagat-3′ (*MYO7A* ARMS reverse). The ARMS reaction was performed with the standard protocol described by Newton et al. (1989), at an annealing temperature of 62°C and a final concentration of 2.5 mM $MgCl_2$.

4.5.4 Molecular modelling of human myosin VIIA

The sequence of human myosin VIIA (Swissprot ID MY7A_HUMAN) was submitted to the 3D-PSSM-fold recognition server (Kelley et al. 2000), which identified four homologues of known structure with E-values below 0.1 (PDB IDs 1BR1, 1I84, 1B7T and 1G8X). Molecular models for all four alignments were built with WHAT IF (Vriend 1990) and refined with YASARA (Krieger et al. 2002). Validation of the models with WHAT_CHECK (Hooft et al. 1996) identified template 1G8X, the myosin II heavy chain from *Dictyostelium discoideum* solved at a resolution of 2.8 Å (Kliche et al. 2001), as the best choice. The model covers the myosin head domain from residue Val2 to Gln752; a coordinate file is available from the authors upon request.

Table 1 Oligonucleotides flanking *MYO7A* exons. Sequences (5'-3') of forward and reverse primers.

Exon	*Forward primer Code*	*Sequence*	*Reverse primer Code*	*Sequence*
1	6889	GAGAAGGCTCTGGAGTGAGG	6890	GCAGAGGCTCTAGAGGTAGC
2	6891	CAAGGAGGGTTCCCTTGAG	6892	CATATGGATGAGGGGATATGG
3	6893	ATATAGGGCTGCCTGGAAGG	6894	TTCGATCATCTCCCTGCATC
4	6895	AGAGAGGTCGAGGCCCTTAC	6896	CACAGCGGACAAAGTCTCAG
5	6897	GTCTCCCACATGGAATCAGC	6898	CGCACAGTTGGAGCTCTAGG
6-7	6899	GAGTCCCTGTGGGTTGTGAC	6900	AGCAATACGGGCAGCAATAC
8	6901	TAGTTCCTGATGGCCTCCTC	6902	TAGCCAGCTCCCTACAATCC
9	6903	GGTACACTGACGTCCTCTTGC	6904	AAACTGAGCTGCCAATACCAC
10	6905	TCTTAGGACTGTCCCCTTGC	6906	CCCAGCAATGTGGTTCCTAC
11	6907	ATCCGGGTGTGGGTGGAG	6908	AACTTCCCAAGGGGTAGGG
12	6909	GTTCCACACAAGGGCTGGAG	6910	CTTATTTCCATATTGGGGAAGG
13	6911	CTTGCTAATGGCCATGCTG	6912	AAAGCAGGGAAGGAAGCTG
14	6913	GAGAGGGTGGGCTCACAG	6914	TATTCCTGGGCTGGAGCAG
15	6915	CCAGAGCTGGTGAGAGGTG	6916	GCTGAAGCTGTTGGACAAGG
16	6917	TCCTGGGACACTGGATGG	6918	CTCCACGTCACCCTAGCC
17	6919	GTGGACTTGGCCTTTCTGAG	6920	AAGAAAATTGGGACCCTTGC
18	6921	GAAGAGCCCTGCCTCTCAG	6922	GCCCACATCATGGGAATTTAC
19	6923	TCCCAGTGAAGGAAGAGCAG	6924	CCAAACACCACACGTACACC
20	6925	ATCCCAAACCCACCTGTACC	6926	AGCAAGGCTGGGTTCAAAG
21	6777	AGTCTGGAATGGGACAGCAG	6778	CTGTGGGTGCTATGGACTTG
22	6682	CCCTGCAACAACAGCTACAC	6683	ACCGGGTGACAGATGAGAAG
23	6779	GACCCCGTGTCTTCTGTGTC	6780	ACACAAGCGGTGTGTGTGG
24	6781	GATCCTCCCACCTGAGCTTC	6782	CCCACCACCCTCATCACTAC
25	6783	CGCCAGGTCATTTTGACAG	6784	GGGAGGGACATCATCCAGAG
26	6927	GCTTTCTGCTCAGCCACTTG	6928	AGTGTCCACTCCTGCTCCTG
27	6929	GGGAACACCCCTAACTTTACC	6930	TTGACAGAGGCACCACTCAG
28	6931	TTGGAGAGGACAGCTGTGTG	6932	ATGGGGCTCAGTAAGGAGTG
29	6933	GCTGCCCTCAAAATCCAC	6934	CACACACGCATTTACACACG
30	6935	AGCAGAGAGCCAAAGTCCAG	6936	GTGCTCAAGGGTGAATAGCC
31	6937	GTCCTTCCCTGACTCTGTGC	6938	CTCACAGAGGAGCACTCAGC
32	6939	AGCCTTTGGTGGTGTGGAAG	6940	TCAGGTCCACATCCCTTCTC
33	6941	GCAGCAGCAGCTGATTTTTAG	6942	GCTGGAGCTACAGAGCAAGG
34	6943	GAAATCAGTGTATTGCCACCTG	6944	CTCTCCTTCCCCTCTGTCTG
35	6945	ACTGGTTGGGGCATGACTG	6946	AGTCTGCATAACACCCTGACC
36	6947	TCCAACTCAGCCTGTCTCTG	6948	GGACAAAGAGGGGTCTAATGG
37	6949	TGGTGGCCACAGGTAGAGAG	6950	GACCAGACAGTAGCGGAAGC
38	6951	CACAACCTGGGGGTTTCTC	6952	AGGCAGTGTGCAGACGAAG
39	6953	CCAGTGCTCCCTCTATTCG	6954	TCACAGCAGGTGAGGTCTG
40	6955	AGGTCCTGTGACTCCCGATG	6956	AAGGGGCTCATCCCACAAG
41	6957	GGATCAGAACTGGGGTTGTC	6958	GAGGCTTAAGGCCACCTTTG
42	6959	ATAGGAGGCATAGCCAGAGG	6960	CCCCCAGTTCCTCTCTCTTC
43-44	6961	GGGAAGGTCAGAAAATGCAG	6962	TTTCAGGGCCAAAGTACAGC

45	6963	GTCTTGGTGTGGTGGGAAAG	6964	GCGGCCTCATCAAGTACAAG
46	6965	GGAGGTCGGGAGTCCATTAG	6966	TGCTTTATCAATGCCCTGTTC
47	6967	CCCAAATGCTTTTCTTGCTC	6968	TGTCTGTGGTTCAGGCAGAG
48	6969	CTTCTGTGAGGGCATGTGTG	6970	CGCACACTACTGTGTTTGTTCC
49	6971	CTGGGAGCTGTGCTATGGTC	6972	CAGTCCCTTCGGTTTCAGAG

4.6 Acknowledgments

This project has been supported by the Foundation “De Drie Lichten” in The Netherlands, the Heinsius-Houbolt Foundation, the Nijmegen ORL Research Foundation and ZonMW AGIKO-grant 920-03-222. We thank Henriëtte Weekamp for her contribution in gathering the patient material, and Prof. Dr. J.R.M. Cruysberg for performing the ophthalmological examination of the patients.

4.7 References

Adato A., Weil D., Kalinski H., et al., Mutation profile of all 49 exons of the human myosin VIIA gene, and haplotype analysis, in Usher 1B families from diverse origins. Am J Hum Genet 1997 61: 813-821.

Bharadwaj A.K., Kasztejna J.P., Huq S., et al., Evaluation of the myosin VIIA gene and visual function in patients with Usher syndrome type I. Exp Eye Res 2000 71: 173-181.

Boëda B., El Amraoui A., Bahloul A., et al., Myosin VIIa, harmonin and cadherin 23, three Usher I gene products that cooperate to shape the sensory hair cell bundle. EMBO J 2002 21: 6689-6699.

El-Amraoui A., Sahly I., Picaud S., et al., Human Usher 1B/mouse shaker-1: the retinal phenotype discrepancy explained by the presence/absence of myosin VIIA in the photoreceptor cells. Hum Mol Genet 1996 5: 1171-1178.

El-Amraoui A., Schonn J.S., Kussel-Andermann P., et al., MyRIP, a novel Rab effector, enables myosin VIIa recruitment to retinal melanosomes. EMBO Rep 2002 3: 463-470.

Ernest S., Rauch G.J., Haffter P., et al., Mariner is defective in myosin VIIA: a zebrafish model for human hereditary deafness. Hum Mol Genet 2000 9: 2189-2196.

Fisher A.J., Smith C.A., Thoden J.B., et al., X-ray structures of the myosin motor domain of *Dictyostelium discoideum* complexed with MgADP. BeFx and MgADP.AlF4-. Biochemistry 1995 34: 8960-8972.

Furch M., Fujita-Becker S., Geeves M.A., et al., Role of the salt-bridge between switch-1 and switch-2 of *Dictyostelium* myosin. J Mol Biol 1999 290: 797-809.

Gibbs D., Kitamoto J., and Williams D.S., Abnormal phagocytosis by retinal pigmented epithelium that lacks myosin VIIa, the Usher syndrome 1B protein. Proc Natl Acad Sci USA 2003 100: 6481-6486.

Hasson T., Heintzelman M.B., Santos-Sacchi J., et al., Expression in cochlea and retina of myosin VIIa, the gene product defective in Usher syndrome type 1B. Proc Natl Acad Sci USA 1995 92: 9815-9819.

Hasson T., Gillespie P.G., Garcia J.A., et al., Unconventional myosins in inner-ear sensory epithelia. J Cell Biol 1997 137: 1287-1307.

Hirokawa N. and Takemura R., Biochemical and molecular characterization of diseases linked to motor proteins. Trends Biochem Sci 2003 28: 558-565.

Hooft R.W., Vriend G., Sander C., et al., Errors in protein structures. Nature 1996 381: 272.

Janecke A.R., Meins M., Sadeghi M., et al., Twelve novel myosin VIIA mutations in 34 patients with Usher syndrome type I: confirmation of genetic heterogeneity. Hum Mutat 1999 13: 133-140.

Kelley L.A., MacCallum R.M., and Sternberg M.J., Enhanced genome annotation using structural profiles in the program 3D-PSSM. J Mol Biol 2000 299: 499-520.

Kliche W., Fujita-Becker S., Kollmar M., et al., Structure of a genetically engineered molecular motor. EMBO J 2001 20: 40-46.

Kong A., Gudbjartsson D.F., Sainz J., et al., A high-resolution recombination map of the human genome. Nat Genet 2002 31: 241-247.

Kremer H., Kuyt L.P., van den Helm B., et al., Localization of a gene for Mobius syndrome to chromosome 3q by linkage analysis in a Dutch family. Hum Mol Genet 1996 5: 1367-1371.

Krieger E., Koraimann G., and Vriend G., Increasing the precision of comparative models with YASARA NOVA—a self-parameterizing force field. Proteins 2002 47: 393-402.

Kros C.J., Marcotti W., van Netten S.M., et al., Reduced climbing and increased slipping adaptation in cochlear hair cells of mice with Myo7a mutations. Nat Neurosci 2002 5: 41-47 .

Lathrop G.M. and Lalouel J.M., Easy calculations of lod scores and genetic risks on small computers. Am J Hum Genet 1984 36: 460- 465.

Lathrop G.M., Lalouel J.M., Julier C., et al., Strategies for multilocus analysis in humans. Proc Natl Acad Sci USA 1984 81: 3443-3446.
Lathrop G.M., Lalouel J.M., and White R.L., Construction of human linkage maps: likelihood calculations for multilocus linkage analysis. Genet Epidemiol 1986 3: 39-52.
Lévy G., Levi-Acobas F., Blanchard S., et al., Myosin VIIA gene: heterogeneity of the mutations responsible for Usher syndrome type IB. Hum Mol Genet 1997 6: 111-116.
Liu X.Z., The clinical presentation of DFNB2. Adv Otorhinolaryngol 2002 61: 120-123.
Liu X.Z., Walsh J., Mburu P., et al., Mutations in the myosin VIIA gene cause non-syndromic recessive deafness. Nat Genet 1997a 16: 188-190.
Liu X.Z., Walsh J., Tamagawa Y., et al., Autosomal dominant non-syndromic deafness caused by a mutation in the myosin VIIA gene. Nat Genet 1997b 17: 268-269.
Liu X.Z., Hope C., Walsh J., et al., Mutations in the myosin VIIA gene cause a wide phenotypic spectrum, including atypical Usher syndrome. Am J Hum Genet 1998 63: 909-912.
Liu X.Z., Udovichenko I.P., Brown S.D., et al., Myosin VIIa participates in opsin transport through the photoreceptor cilium. J Neurosci 1999 19: 6267-6274.
Miller S.A., Dykes D.D., and Polesky H.F., A simple salting out procedure for extracting DNA from human nucleated cells. Nucleic Acids Res 1988 16: 1215.
Newton C.R., Graham A., Heptinstall L.E., et al., Analysis of any point mutation in DNA. The amplification refractory mutation system (ARMS). Nucleic Acids Res 1989 17: 2503-2516.
Oliver T.N., Berg J.S., and Cheney R.E., Tails of unconventional myosins. Cell Mol Life Sci 56:243-257
Rost B (1999) Twilight zone of protein sequence alignments. Protein Eng 1999 12: 85-94.
Sasaki N. and Sutoh K. Structure-mutation analysis of the ATPase site of *Dictyostelium discoideum* myosin II. Adv Biophys 1998 35: 1-24.
Self T., Mahony M., Fleming J., et al., Shaker-1 mutations reveal roles for myosin VIIA in both development and function of cochlear hair cells. Development 1998 125: 557-566.
Shapiro M.B. and Senapathy P., RNA splice junctions of different classes of eukaryotes: sequence statistics and functional implications in gene expression. Nucleic Acids Res 1987 15: 7155-7174.
Tamagawa Y., Ishikawa K., Ishikawa K., et al., Phenotype of DFNA11: a nonsyndromic hearing loss caused by a myosin VIIA mutation. Laryngoscope 2002 112: 292-297.
Tsiavaliaris G., Fujita-Becker S., Batra R., et al., Mutations in the relay loop region result in dominant-negative inhibition of myosin II function in Dictyostelium. EMBO Rep 2002 3: 1099-1105.
Vriend G., WHAT IF: a molecular modeling and drug design program. J Mol Graph 1990 8: 52-56.
Weil D., Blanchard S., Kaplan J., et al., Defective myosin VIIA gene responsible for Usher syndrome type 1B. Nature 1995 374: 60-61.
Weil D., Küssel P., Blanchard S., et al., The autosomal recessive isolated deafness, DFNB2, and the Usher 1B syndrome are allelic defects of the myosin-VIIA gene. Nat Genet 1997 16: 191-193.
Weston M.D., Kelley P.M., Overbeck L.D., et al., Myosin VIIA mutation screening in 189 Usher syndrome type 1 patients. Am J Hum Genet 1996 59: 1074-1083.
Wolfrum U. and Schmitt A. Rhodopsin transport in the membrane of the connecting cilium of mammalian photoreceptor cells. Cell Motil Cytoskeleton 2000 46: 95-107.
Zina Z.B., Masmoudi S., Ayadi H., et al., From DFNB2 to Usher syndrome: variable expressivity of the same disease. Am J Med Genet 2001 101: 181-183.

Chapter 5

Mutations in the VLGR1 gene implicate G-protein signalling in the pathogenesis of Usher syndrome type II

M.D. Weston[a,b], M.W.J. Luijendijk[d], K.D. Humphrey[c], Claes Möller[e], and W.J. Kimberling[a]

[a] Center for the Study and Treatment of Usher Syndrome, Department of Genetics, Boys Town National Research Hospital, Omaha
[b] Department of Biomedical Sciences, Creighton University, Omaha
[c] Departmentof Biology, Creighton University, Omaha
[d] Department of Human Genetics, University Medical Center Nijmegen, Nijmegen, The Netherlands
[e] Department of Audiology, Sahlgrenska University Hospital, Göteborg, Sweden

Am. J. Hum. Genet. 2004 74: 357-366

5.1 Abstract

Usher syndrome type II (USH2) is a genetically heterogeneous autosomal recessive disorder with at least three genetic subtypes (USH2A, USH2B, and USH2C) and is classified phenotypically as congenital hearing loss and progressive retinitis pigmentosa. The *VLGR1* (*MASS1*) gene in the 5q14.3-q21.1 *USH2C* locus was considered a likely candidate on the basis of its protein motif structure and expressed-sequence-tag representation from both cochlear and retinal subtracted libraries. Denaturing high-performance liquid chromatography and direct sequencing of polymerase-chain-reaction products amplified from 10 genetically independent patients with USH2C and 156 other patients with USH2 identified four isoform-specific *VLGR1* mutations (Q2301X, I2906FS, M2931FS, and T6244X) from three families with USH2C, as well as two sporadic cases. All patients with *VLGR1* mutations are female, a significant deviation from random expectations. The ligand(s) for the VLGR1 protein is unknown, but on the basis of its potential extracellular and intracellular protein-protein interaction domains and its wide mRNA expression profile, it is probable that VLGR1 serves diverse cellular and signalling processes. *VLGR1* mutations have been previously identified in both humans and mice and are associated with a reflex-seizure phenotype in both species. The identification of additional *VLGR1* mutations to test whether a phenotype/genotype correlation exists, akin to that shown for other Usher syndrome disease genes, is warranted.

5.2 Introduction, results, discussion, materials, and methods

Usher syndrome is a clinically and genetically heterogeneous recessive disease with three clinical subtypes. The subtypes are differentiated on the basis of the severity of hearing loss and presence or absence of vestibular abnormalities. Patients with Usher syndrome type I (USH1) present with profound congenital hearing loss, vestibular areflexia (in most cases), and a progressive retinal degeneration, with impaired night vision and decreased visual fields diagnosed as retinitis pigmentosa (RP). Usher syndrome type II (USH2 [MIM 276900]) have a moderate-to-severe sensorineural hearing loss that is stable in most cases, normal vestibular function, and RP, whereas patients with type III (USH3) present a moderate sensorineural hearing loss with progression to acquired deafness, progressive vestibular dysfunction, and RP. Currently, 11 loci have been identified for Usher syndrome (Kimberling et al. 1990, 1992, Kaplan et al. 1992, Smith et al. 1992, Sankila et al. 1995, Wayne et al. 1996, 1997, Chaib et al. 1997, Hmani et al. 1999, Pieke-Dahl et al. 2000, Mustapha et al. 2002); families that do not link to the known loci indicate additional genes exist. Of the 11 loci, 7 genes have been found with Usher syndrome mutations (Weil et al. 1995, 2003, Eudy et al. 1998, Bitner-Glindzicz et al. 2000, Verpy et al. 2000, Ahmed et al. 2001, Alagramam et al. 2001, Bolz et al. 2001, Bork et al. 2001, Joensuu et al. 2001).

Previously, we had localized the *USH2C* gene to a 20-cM region on chromosome 5q14.3-5q21.1 (Pieke-Dahl et al. 2000). Reference mRNAs in this linkage interval were obtained from the UCSC Genome BrowserWeb site and were prioritised for candidate-gene mutation screening. The very large G-coupled receptor gene (*VLGR1*) was considered a likely *USH2C* candidate (Burgess 2001, Staub et al. 2002), with EST

representation in both human fetal retina and cochlea (obtained from the National Eye Institute Gene Bank Web site) subtracted libraries. Use of the conserved domain architecture retrieval (CDART) tool on VLGR1 (Geer et al. 2002) revealed a motif architecture similar to the cadherin superfamily of integral membrane proteins. This superfamily includes *CDH23* and *PCDH15,* which are the genes mutated in USH1D (MIM 601067) and USH1F (MIM 602083), respectively. In addition, VLGR1 and the *USH2A* gene product usherin exhibit a high degree of similarity in their respective pentraxin (PTX) homology domains. On the basis of this evidence, we sought to implicate the *VLGR1* gene in the pathogenesis of USH2.

Denaturing high-performance liquid chromatography (DHPLC) and direct sequencing were used to detect mutations in PCR-amplified genomic DNA from 10 probands with USH2C (MIM 605472) for 90 *VLGR1* exons. The 10 affected probands were members of families consistent with genetic linkage to 5q14-21 (Pieke-Dahl et al. 2000). We had previously obtained informed consent and had extracted DNA from peripheral whole blood of the study subjects according to standard conditions (Puregene). Patients with a clinical diagnosis of USH2 were ascertained through physician referral and self-referral. The study was conducted with the approval of the Boys Town National Research Hospital (BTNRH) institutional review board and met all ethical requirements and Health Insurance Portability and Accountability Act (HIPAA) standards. DNAs from an additional 152 unrelated patients with USH2 without an identifiable *USH2A* mutation on chromosome 1q41 were used to screen for specific *VLGR1* mutations identified from either the mutation screen of the 10 probands with USH2C or from those *VLGR1* mutations reported elsewhere (Nakayama et al. 2002).

Genomic *VLGR1* PCR primer pairs were designed and synthesized commercially (sequences available upon request [Integrated DNA Technologies]). PCR used 20 ng genomic DNA, 0.2 µM primer, 2.5 mM $MgCl_2$, 200 µM dNTP, in 1X PCR buffer with 0.5 units AmpliTaqGold (PE Biosystems) in 25 µl total volume. The initial PCR cycle was 95ºC for 8 min and 30 sec, followed by 40 cycles of 95ºC for 30 sec, 55ºC for 30 sec, and 72ºC for 1 min, with a final step of 70ºC for 10 min. BAC clones spanning the *VLGR1* genomic interval (CTD-2034A10, exons 1-4; RP11-29K14, exons 2-42; RP11-62E10, exons 18-73; RP11-3B6, exons 51-83; CTD-2001K4, exons 84 and 85; CTD-2266L18, exons 86 and 87; RP11- 414H23, exons 88-90) were identified and used as a control template to evaluate PCR-product heteroduplexes that were separated by DHPLC; these clones were also used in direct PCR sequence analysis.

Table 2. VLGR1 DNA variants including pathologic USH2C mutations (italicized).

			BTNRH Frequency				
Exon	*Name*	*Codon*	*USH2C*	*USH2A*[a]	*Controls*	*SNP DB*	*Reference*
4	380T>G	L127R	1/20				
7	746G>A	R249K[b]	1/20		0/188		
9	IVS9+54C>T		4/20				
10	IVS10+53delA		4/20				
12-13	IVS11-19G>T		4/20			1344030	Nakayama et al. 2002
12-13	IVS12+8C>T		3/20			2366773	Nakayama et al. 2002

			BTNRH Frequency				
Exon	*Name*	*Codon*	*USH2C*	*USH2A*[a]	*Controls*	*SNP DB*	*Reference*
15	IVS14-34C>G		4/20				Nakayama et al. 2002
17	3141A>G	A1047A	3/20			950692	Nakayama et al. 2002
17	3279G>T	L1093F	5/20			2366777	Nakayama et al. 2002
22	IVS22+87T>A		6/20			1028191	
A[c]	IVS22 +234A>G		6/20			1028192	
A[c]	IVS22+244A>G		1/20				
24	5304G>A	E1768E	1/20		1/190		
B[c]	IVS25+780C>T		3/20				
28	IVS27-23T>C		5/20				Nakayama et al. 2002
28	5780C>T	T1927M	1/20				
28	5851A>G	I1951V	5/20				Nakayama et al. 2002
28	5953A>G	N1985D	3/20				Nakayama et al. 2002
28	5960C>T	P1987L	5/20				Nakayama et al. 2002
28	6012G>T	L2004F	3/20		20/170		Nakayama et al. 2002
30	6695A>G	Y2232C	6/20		36/144		Nakayama et al. 2002
31	*6901C>T*	*Q2301X*	*1/20*	*3/282*	*0/190*		
32	IVS31-10G>A		8/20				Nakayama et al. 2002
32	c.7034A>G	N2345S	8/20			2366926	Nakayama et al. 2002
33	7135G>A	G2379A	0/20		1/190		
33	7155G>T	L2385L	0/20		1/190		
33	7176C>T	S2392S[d]	1/20		0/190		
33	7179C>T	D2393D	0/20		2/190		
33	7206G>A	E2402E	5/20		69/190		Nakayama et al. 2002
33	7751G>A	S2584N	5/20			1878878	Nakayama et al. 2002
33	IVS33+27A>C		7/20				
34	IVS34+82T>C		6/20				
36	IVS35-60G>A		0/20		1/190		
36	8291C>T	S2764L	1/20		6/190		Nakayama et al. 2002
37	8495C>A	S2832X	0/20	0/276			Nakayama et al. 2002
37	8407G>A	A2803T	1/20		1/190		
37	8538T>G	L2846L	4/20		21/190		Nakayama et al. 2002
38	IVS37-60G>T		6/20			1160121	
38	IVS37-13C>T		0/20		1/28[e]		Nakayama et al. 2002
38	*8716-17insAACA*	*I2906FS*	*1/20*	*0/276*	*0/190*		
38	IVS38+10insT		6/20				
39	*8790delC*	*M2931FS*	*1/20*	*0/280*	*0/190*		
39	ISV39+50A>C		1/20		6/190		
41	IVS41+57C>T		2/20				
45	9650C>T	A3217V	1/20		3/190		
45	9743G>A	G3248D	4/20		21/190		
47	IVS46-35C>A		6/20				
47	9927T>G	P3309P	8/20				
48	IVS48+26G>T		6/20				
49	10411G>A	E3471K	3/20			2366928	
51	10577T>C	M3526T	1/20		3/182		
51	IVS51+9A>G		0/20		2/182		
56	IVS55-3insC		8/20		90/190		

			BTNRH Frequency				
Exon	*Name*	*Codon*	*USH2C*	*USH2A*[a]	*Controls*	*SNP DB*	*Reference*
56	11599G>A	E3867K	8/20		75/190		
56	11682C>T	P3894P	8/20		92/190	2438349	
59	12269C>A	T4090N[f]	1/20		0/166		
64	IVS63-36A>T		2/20		19/190		
64	IVS63-31C>T		2/20		6/190		
67	13590C>T	P4530P	2/20		3/158		
67	13599A>G	T4533T	3/20		29/158		
74	15987C>T	Y5329Y[g]	1/20		0/190		
74	16031G>A	G5344E	0/20		4/190	2438374	
76	IVS75-15G>A[h]		1/20		0/190		
76	16248C>T	V5416V	0/20		3/190		
76	16312A>G	T5438G	0/20		1/190		
82	17626A>G	I5876V	5/20			2247870	
88	IVS87 complex[i]		3/20		34/190		
C[c]	IVS24a+1G>A		6/20		50/192		
89	IVS88-7T>C		3/20		12/192		
89	*18732-18750del*[j]	*Y6244X*	*1/20*	*0/282*	*0/190*		
89	18741G>A	G6247G	0/20		23/192		
89	ISV89+44C>G		0/20		1/40[e]		

[a] Cohort of 152 USH2 patients negative for identified mutations in the USH2A gene, 11 samples failed amplification consistently due to poor template quality.
[b] Conservative missense mutation in cis (paternal) with Q2301X mutation in family 1848.
[c] Alternative exons based on EST evidence.
[d] Isocoding mutation in cis (maternal) with I2906FS mutation in family 1848.
[e] Variant frequency identified from direct sequence of PCR products chosen to identify a distinct DHPLC positive variant.
[f] Conservative missense mutation disrupts a potential N-glycosylation site within the 27th CalX-β motif.
[g] Isocoding mutation in cis (paternal) with Q2301X mutation in family 1848.
[h] IVS mutation increases the potential of a cryptic splice site donor cite. Pathology unknown. In cis (paternal) with an undetected USH2C mutation in family #964.
[i] IVS87 33:$(CTTTT)_4(T)_9$GCAG>IVS87-31$(CTTTT)_3(T)_{12}$GCAG.
[j] Deletion is TGGCCAGGGGTCACTGATA.

Three human *VLGR1* mRNA isoforms are expressed (VLGR1a, VLGR1b, and VLGR1c), of which only VLGR1b and VLGR1c isoforms are expressed in mouse (McMillan et al. 2002) (fig. 2). Of 72 nucleotide changes discovered in *VLGR1* (table 1), 4 mutations would prematurely terminate VLGR1a and VLGR1b protein translation (fig. 1). The *VLGR1* 6901C>T (Q2301X) and 8716-17insAACA (I2906FS) mutations were found in repulsion exclusively in the members of family 1848 who were affected with USH2C (fig. 1a and 1c). Family 964 (with USH2C) was found to segregate a maternal *VLGR1* 8790delC (M2931FS) mutation (fig. 1b). A paternal 19-bp deletion (18732-18750del19bp; T6244X) segregates appropriately with the phenotype in family 735 (fig. 1d). Families 735 and 964 have been shown elsewhere to genetically link to the 5q14.3-q21 region, with all affected siblings sharing family-specific 5q 14.3-q21 haplotypes

(Pieke-Dahl et al. 2000). No other potential *VLGR1* variant was found associated with the maternal allele of family 735; however, a paternal IVS75-15G>A mutation absent in 190 control chromosomes was found segregating with the phenotype in family 964 (data not shown). It remains to be determined whether and how IVS75-15G>A affects *VLGR1* expression. Screening for *USH2C* mutations in 152 patients with USH2 revealed the Q2301X mutation in two other unrelated patients with sporadic USH2. Table 2 presents a clinical summary of all patients with USH2C who harbour *VLGR1* mutations. A total of five independent probands with USH2 and eight affected siblings were found to bear pathological *VLGR1* mutations. Two probands have pathological mutations identified in both alleles; three occult mutant alleles either have escaped detection by the methodology employed, lie in unscreened regions of the gene, or have been detected but not appreciated as disease alleles. None of the four *VLGR1* mutations was observed in 190 control chromosomes. These results establish *VLGR1* as the USH2C gene and implicate the protein, which is the largest cell surface receptor known (McMillan et al. 2002), in the pathogenesis of USH2.

Because the USH2 phenotype manifests cochlear and retinal defects, we wanted to determine if any of the three VLGR1 isoforms were tissue specific in these organs (fig. 3a and 3b). We performed semiquantitative RT-PCR by use of total RNA isolated from nine human fetal tissues. Primer pairs for the human isoforms VLGR1a, VLGR1b, and VLGR1c have been described elsewhere (McMillan et al. 2002). Total RNA from three human tissues (fetal brain, fetal liver, and placenta) was purchased from Clontech. For cDNA synthesis, total RNA was treated with DNase I (Invitrogen), according to the manufacturer's conditions, and random-primed in a volume of 250 µl from 3.1 µg total RNA using 4 pmol random hexanucleotides, 10 mM Tris-HCl, pH 8.3, 50 mM KCl, 0.01% (v/w) gelatin, 5 mM $MgCl_2$, 1 mM DTT, 95 U RNAguard (Pharmacia), and 2,500 U MMLV reverse transcriptase (Invitrogen). Semiquantitative RT-PCRs were performed by sampling 50 µl RT-PCR reactions at the 25th, 30th, 35th, and 40th cycle. PCR reactions included 87 ng of randomly primed cDNA, 11.2 pmol of each primer, 10 mM Tris-HCl, pH 8.3, 50 mM KCl, 0.01% gelatin, 2.5-3 mM $MgCl_2$, 160 mM of each dNTP, and 1.75 U *Taq* DNA polymerase (Invitrogen) under the following conditions: 92ºC for 4 min, followed by 40 cycles of 95ºC for 30 sec, 50ºC / 55ºC for 30 sec, and 72ºC for 1 min, with a final step at 72ºC for 10 min. RT-PCR results show expression of all three VLGR1 isoforms from fetal retina and cochlea, confirming the EST expression profile of *VLGR1.* High relative expression in fetal brain and spinal cord confirms the neuronal expression of *VLGR1* (McMillan et al. 2002) (fig. 3a and 3b). Although there appears to be a consistent difference in the amount of VLGR1a, VLGR1b, and VLGR1c RT-PCR products amplified from different tissues, no apparent tissue-specific differences in the relative abundance between the three isoforms was seen in any of the fetal tissues tested (fig. 3a and 3b). In addition, we find the relative amount of the VLGR1a and VLGR1b isoforms to be roughly equal as judged by RT-PCR, which is in contrast to an approximately fourfold difference in expression of the VLGR1b isoform over the VLGR1a isoform previously observed in human fetal kidney, brain, and lung (McMillan et al. 2002). One explanation for this disparity could be the way the RT-PCR of the VLGR1a and VLGR1b isoforms was performed, as the study by McMillan et

al. (2002) amplified VLGR1a and VLGR1b in multiplex, whereas we chose to amplify them in separate reactions because of a significant difference in the TMs of the sense primers.

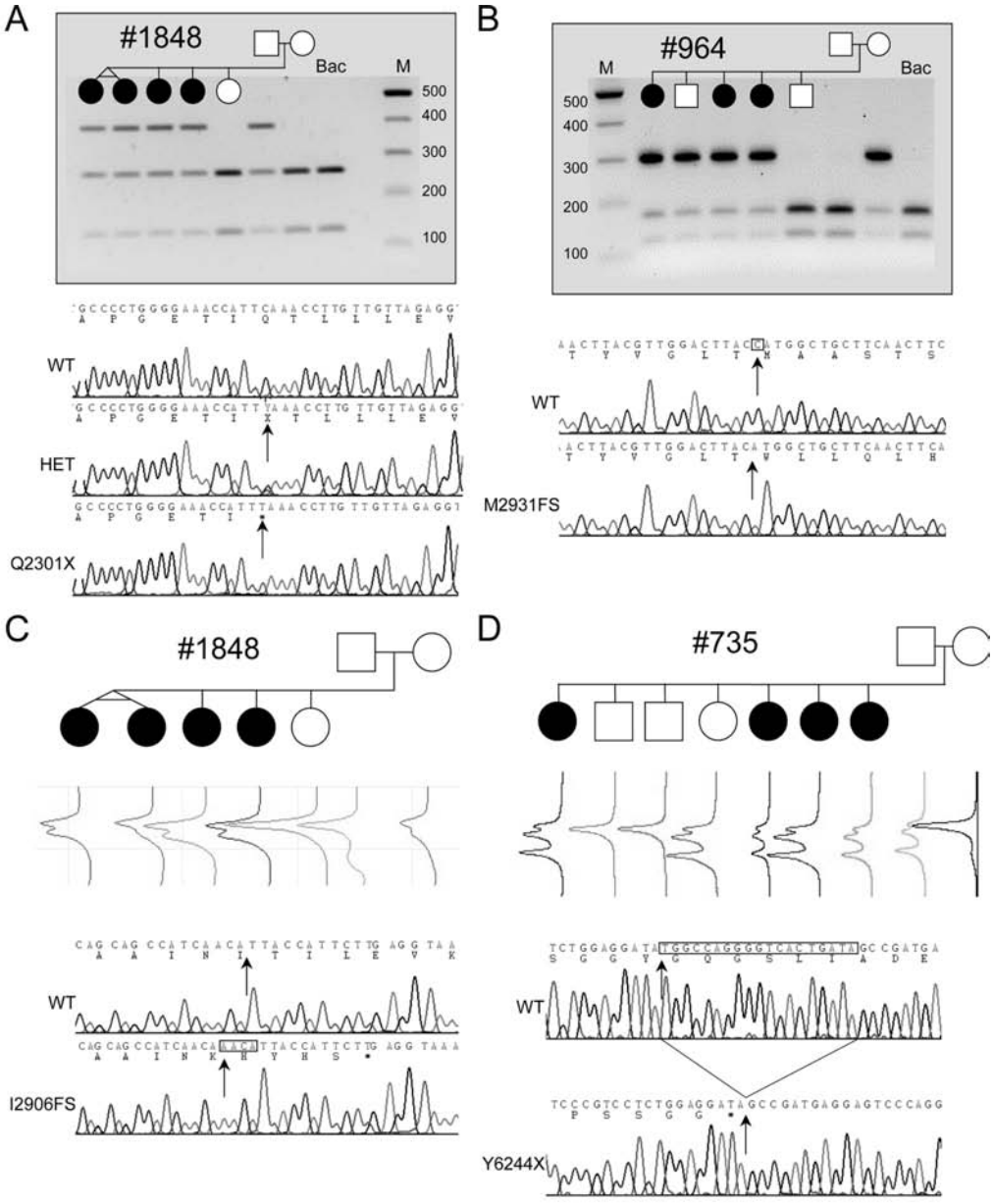

Figure 1. Segregation of *VLGR1* mutations Q2301X, M2931FS, I2906FS, and T6244X in families 735, 964, and 1848 (with USH2C). (A) Paternal inheritance of Q2301X in family 1848 is shown by agarose-gel electrophoresis of exon 31 PCR product *Xmn*I digests. Q2301X mutation is a 6901 C>T transition, 33 bp on the 3' end of the alternate exon 31 splice donor, affecting only the VLGR1b mRNA isoform (fig. 2a). Shown here are sequence electropherograms from the

heterozygous family 1848 proband (HET), an apparent Q2301X homozygote, and wild-type (WT) BAC clone RP11-29K14, with sequence and amino acid translation differences (*arrows*). The Q2301X homozygote was the result of a brother-sister incestuous union, whereas another singleton case was a Q2301X/occult heterozygote (data not shown; table 2). (B) Maternal inheritance of M2931FS in family 964 is shown by agarose-gel electrophoresis of exon 39 PCR product *Nco*I digests. Sequence electropherograms of the WT and the cloned M2931FS allele show 8790delC in exon 39 (*arrows*). This deletion causes a 10-codon frameshift. ending with a TAG stop encoded by the last 3 bases of exon 39, affecting VLGR1b. (C) Maternal inheritance of I2906FS in family 1848 by DHPLC of exon 38 PCR products. Sequence comparison of the cloned I2906FS mutation shows an 8716-17insAACA (*arrows*) causing a frameshift of 5 codons and ending with a TGA stop 1 bp short of the 3_end of exon 38, affecting VLGR1b. (D) Paternal inheritance of Y6244X detected by DHPLC of exon 89 PCR products. A 19-bp deletion brings a TAG stop codon immediately in-frame. Y6244X removes 63 amino acids from the COOH end of VLGR1a and VLGR1b. The putative maternal and paternal mutations in family 735 and family 964 have not been identified.

Table 2. Clinical summary of patients with USH2C harbouring *VLGR1* mutations

Family no.	*Individual no.*	*Severity of hearing loss*	*Age at RP diagnosis (years)*	*Sex*	*RP symptoms*	*VLGR mutation(s)*
735[a]	1	Moderate-severe	27[b]	Female	Typical	T62244X/occult
	5	Moderate-severe	25	Female	NA	T62244X/occult
	6	Moderate-severe	20	Female	NA	T62244X/occult
	7[c]	Moderate-severe	19	Female	NA	T62244X/occult
964[d]	1	Moderate-severe	24	Female	Typical	M2931FS/occult
	3	Moderate-severe	21	Female	Typical	M2931FS/occult
	4	Moderate-severe	33	Female	Mild	M2931FS/occult
1127	1	Moderate-severe	42	Female	Typical	Q2301X/occult
1848[a]	1	Moderate-severe	32[b]	Female	NA	Q2301X/I2906FS
	2	NA	29	Female	NA	Q2301X/I2906FS
	3	NA	29	Female	NA	Q2301X/I2906FS
	4	NA	21	Female	NA	Q2301X/I2906FS
2684[e]	1	Moderate-severe	17	Female	NA	Q2301X/Q2301X

NA: p not available.
[a] United States, country of origin.
[b] The RP diagnosis in the oldest child led to the earlier age at RP diagnosis in the other siblings.
[c] Reported that loud sounds caused nausea and, occasionally, dizziness.
[d] Sweden, country of origin.
[e] Consanguineous.

The VLGR1b and VLGR1c isoforms differ by 83 bp as a result of the alternative exon 31 donor splicing (Skradski et al. 2001, McMillan et al. 2002). A mouse *Vlgr1* mutation in exon 31 (7009delG; 2250FS) is responsible for the monogenic audiogenic seizure susceptible (MASS) phenotype (Skradski et al. 2001). The *Vlgr1*^{7009delG} (*Vlgr1*^{Mass1}) mouse allele mutates both mouse Vlgr1b and Vlgr1c splice isoforms, whereas the human exon 31 *VLGR1* mutation (Q2301X), in addition to the other three *USH2C* mutations, affects VLGR1b (fig. 2 and 3). To determine if species-specific differences in the VLGR1b and VLGR1c isoforms might help to explain the *VLGR1* mutant phenotypes,

RT-PCR of VLGR1 band VLGR1c isoforms from mouse and human fetal RNA was performed. For RT-PCR of the VLGR1b and VLGR1c isoforms, random-primed total mRNA from human and mouse fetal brain RNA (Clonetech) was reverse transcribed with Superscript III (Invitrogen), according to standard conditions, and PCR with AmpliTaq Gold (PE Biosystems) was as described for genomic PCR amplification, except that the amount of $MgCl_2$ was 3.0 mM. Amplification primers for the mouse Vlgr1b and Vlgr1c isoforms were as follows: sense 5'-CGAACTGGAGGAACATTTGCAG-3' and antisense 5'-GCAGACACGTTCACCCAAGTTC-3'. Cloning and sequencing of VLGR1b and VLGR1c RT-PCR products from both human and mouse confirm the evolutionarily conservation of the alternative exon 31 splice donor sites in both species (data not shown). It is not surprising that, although the VLGR1b messages of human and mouse share 81% sequence identity overall, the last 113 bp of exon 31 are 100% conserved at the DNA level, indicating that the sequence context of the mRNA in this region is critically important, perhaps defining a critical *cis* element necessary for alternative mRNA processing. A comparison of RT-PCR products from fetal human and mouse brain revealed a difference in the relative abundance of VLGR1b and VLGR1c isoforms, indicating a species-specific difference in mRNA processing through the alternative exon 31 donor sites (fig. 3c). These results suggest that isoform-specific mutations in *VLGR1,* either alone or in combination with a specific difference in mRNA processing, may underlie the manifestation of phenotype in these species.

In situ hybridisation of mouse embryo sections had shown *Vlgr1* expression concentrated in the ventricular zone where neural progenitor cells reside during embryonic neurogenesis, suggesting that the Vlgr1b and Vlgr1c isoforms play a role in the development of the murine CNS (McMillan et al. 2002). This idea is strengthened by the association of the MASS phenotype with the *Vlgr1* mutant allele (Skradski et al. 2001). The *Vlgr1* mouse ortholog includes in its open reading frame three additional and distinct mRNAs previously characterized as isoforms of the mouse *Mass1* gene (Mass1.1, Mass1.2, and Mass1.3) on mouse chromosome 13 (Skradski et al. 2001) (fig. 2). The *Frings* mouse has not been reported to have deficient hearing or vision; however, no histological or electrophysiological data have been published that explicitly rule out such possibilities. In addition to *Frings,* the BUB/BnJ inbred mouse was also found to be a $Vlgr1^{Mass1}$ homozygote, and it exhibits the MASS phenotype until a progressive age-related hearing loss phenotype manifests in this strain by 3 wk of age (Skradski et al. 2001). BUB/BnJ is one of several inbred mouse strains exhibiting AHL (Zheng et al. 1999). The variable severity and progression of hearing loss in many AHL mouse strains, including BUB/BnJ, is influenced by a major modifier locus on mouse chromosome 10 (*ahl*, also the modifier-of-deaf-waddler locus, *mdfw*). Both *ahl* and *mdfw* are caused by the $Cdh23^{753G>A}$ splicing mutation, a synonymous transition of the last nucleotide of exon 7 (Noben-Trauth et al. 2003). It remains to be determined if the early onset of hearing loss in BUB/BnJ is influenced by the $Vlgr1^{Mass1}$ mutation, as has been shown for other AHL "accelerating alleles" in combination with $Cdh23^{753A}$ (Noben-Trauth et al. 2003). It should be noted that BUB/BnJ is also homozygous for *rd1,* a mutation in the *Pde6b* gene that results in early photoreceptor-cell apoptosis because of a lack of cGMP phosphodiesterase activity. The fact that BUB/BnJ carries homozygous mutations in

Pde6b (rd1), Cdh23 (*ahl, mdfw*), and *Vlgr1* (*Mass1*) suggests caution should be used in interpreting the phenotypic effects of these genes in this mouse strain.

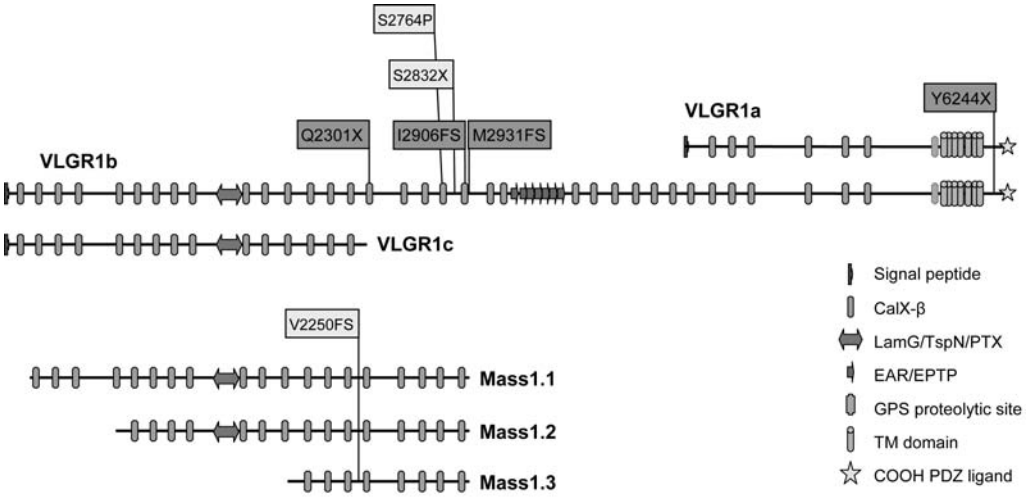

Figure 2. Domain structure of VLGR1/MASS1 isoforms. Conceptual translation of VLGR1b mRNA reveals a protein with a large ectodomain with 35 Calx-b domains, 1 LamG/TspN/PTX homology domain (Beckmann et al. 1998), 7 EAR/EPTP repeats forming a putative b-propeller folding domain (Scheel et al. 2002, Staub et al. 2002), a GPS, a B-family 7TM domain, a putative intracellular tail with multiple potential serine phosphorylation sites, and a putative PDZ-binding COOH-terminal end (McMillan et al. 2002). The PTX domains of VLGR1 and the *USH2A* protein usherin are most similar to one another, with a BLASTP score of 2e-09. The locations of human USH2C (grey) and febrile-seizure (FS)-associated mutations are shown on VLGR1a, VLGR1b, and VLGR1c isoforms. The mouse audiogenic reflex seizure model *Frings* and the age-related hearing loss model BUB/BnJ are both homozygous for the V2250FS mutation and are noted on Mass1.1, Mass1.2, and Mass1.3 isoforms (Skradski et al. 2001).

The VLGR1 protein belongs to a 33-member subgroup of the large N-terminal family B (LNB) seven transmembrane (7TM) receptors. Of the 33 LNB 7TM members, 32 are orphan receptors and only a few have demonstrated specific G-protein signaling (Foord et al. 2002). All LNB 7TM members, including VLGR1, have a G-protein-coupled proteolysis site (GPS); cleavage at this site is thought to be a requirement for the proper expression of this class of 7TM receptors on the cell surface (Krasnoperov et al. 2002). VLGR1 may function, like other LNB 7TM members, as a natural protein chimera, with an extracellular cell-adhesion subunit and a canonical G-protein-coupled receptor subunit that are linked by noncovalent interactions (Krasnoperov et al. 2002). The possible function of VLGR1 might be best explored by trying to predict the functions of the two putative subunits separately.

The C-terminal residues of VLGR1 correspond to the consensus motif that is recognized as a ligand for the class I subfamily of PDZ domains (PDZ-binding interface [PBI] [Nikkila et al. 2000, Hung and Sheng 2002]). Interestingly, the C-termini of cadherin 23, protocadherin 15, harmonin, and SANS, all proteins with mutations that cause the USH1 phenotype, have class I PBIs. An interaction through the 2nd PDZ domain of harmonin and the C-terminal PBI ligand of cadherin 23 has been independently

confirmed (Boëda et al. 2002, Siemens et al. 2002). Colocalisation of harmonin and SANS in transfected HeLa cells suggests that these proteins also interact, perhaps through a PDZ-PBI interaction (Weil et al. 2003). The fact that all USH1 protein mouse mutants, including the nonmuscle myosin VIIa, which also has a protein interaction with harmonin, phenotypically present with defects in hair cell stereocilia development suggests that these proteins function as a macromolecular complex necessary to shape and maintain the stereocilia as an organized cohesive unit (Boëda et al. 2002, Siemens et al. 2002, Weil et al. 2003). It remains to be determined whether one or more of the three PDZ domains of harmonin, or other PDZ domain-bearing protein, have a high-affinity interaction with the PBI of VLGR1.

The very large extracellular portion of VLGR1b has a total of 35 CalX-β modules (fig. 2), named for the homology shared between the regulatory domains of Na^+/Ca^{2+} exchanger proteins and the cytoplasmic portion of integrin-β4 (Schwarz and Benzer 1997, McMillan et al. 2002). Portions of the extracellular domain of VLGR1a that include a subset of the CalX-β domains bind Ca^{2+} and other cations (Nikkila et al. 2000). Because of the extensive CalX-β modules, one might postulate that the molecule acts as an extracellular Ca^{2+} sink, as an extracellular Ca^{2+} monitor sensitive to the regulation of intra- and extracellular Ca^{2+} trafficking, or in Ca^{2+}-dependent cell adhesion. Disruption of normal Ca^{2+} metabolism is known to affect both hearing and vision. For example, mutations in the plasma membrane Ca^{2+} ATPase pump Atp2b2 (PMCA2) cause the deaf waddler (*dfw*) phenotype in mice (Kozel et al. 1998, Street et al. 1998). It has been postulated that the murine *ahl* gene (*mdfw, Cdh23*^{753A}) acts epistatically to cause an age-dependent hearing loss through an interaction between the Ca^{2+}-extruding PMCA2 channel and the calcium-dependent homotypic cell-adhesion properties of the cadherin 23 protein (Noben-Trauth et al. 1997, 2003). Furthermore, a functional interaction has been postulated between PMCA2 and the sodium bicarbonate cotransporter, NBC3, at the photoreceptor synapse, as the loss of H^+ buffering by NBC3 causes retinal dystrophy (and hearing loss) in *NBC3* knock-out mice (Bok et al. 2003). The possibility that calcium homeostasis is involved in USH2C is especially intriguing in light of the observation that the Ca^{2+}-channel-blocking drug, diltiazem, is protective against noise-induced hearing loss (Maurer et al. 1998, Heinrich et al. 1999). However, there is conflicting evidence about whether diltiazem is neuroprotective for the retina, since none of the animal models tested had RP resulting from a calcium metabolism defect (Frasson et al. 1999, Pasantes-Morales et al. 2002, Pawlyk et al. 2002).

The large VLGR1b ectodomain has two recognized potential protein-interaction domains, LamG/TspN/PTX (Beckmann et al. 1998) and EAR/EPTP (Scheel et al. 2002, Staub et al. 2002) (fig. 2). It has been suggested that the multiple Ca^{2+}-binding CalX-β modules may mediate the protein-protein interactions of these two domains (McMillan et al. 2002). The EAR/EPTP motif occurs as a repeated set of domains that together are postulated to form a seven-bladed-propeller structure that, in other proteins, acts as a highly specific receptor (Pons et al. 2003). Probable ligands for the EAR/EPTP domain of VLGR1 would be extracellular or cell-adhesion proteins. Usherin, the product of the *USH2A* gene, is a known extracellular basement-membrane protein (Bhattacharya et al. 2002). When usherin is defective, the phenotype is remarkably similar to that seen

in patients with inactivated VLGR1. Immunolocalisation of usherin to the perinurium of the spiral ganglion cells of the cochlea (Bhattacharya et al. 2002) and the likely neuronal localization of the VLGR1 receptor indicates that VLGR1 and usherin may colocalise in specific subcellular compartments. Furthermore, the significant homology between the LamG/TspN/PTX motifs of VLGR1 (fig. 2) and usherin indicates that the two proteins may share an affinity for a common binding partner, reinforcing the hypothesis of an interaction between these proteins. Whether usherin is the extracellular ligand or another yet-to-be-identified USH2 protein remains to be established.

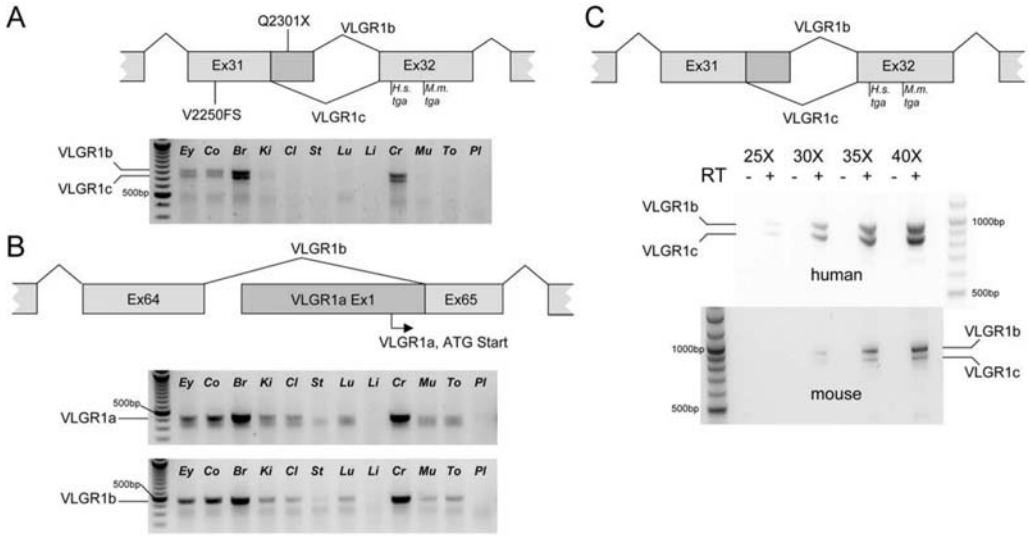

Figure 3. RT-PCR of VLGR1 mRNA splice forms from human and mouse fetal tissue. Human fetal tissues from left to right: eye (Ey), cochlea (Co), brain (Br), kidney (Ki), colon (Cl), stomach (St), lung (Lu), liver (Li), spinal cord (Cr), muscle (Mu), tongue (To), and adult placenta (Pl). (A) The relative locations of the human Q2301X and the *Frings* and BUB/BnJ mouse V2250FS mutations to the alternative donor site that differentiates the VLGR1b and VLGR1c splice isoforms. These isoforms differ by 83 bp because of the alternative use of a 5' splicedonor site in exon 31 (Skradski et al. 2001, McMillan et al. 2002). Expression from eye and cochlear tissue is less intense at 30 cycles of RT-PCR than from brain and spinal cord. At 40 cycles, all tissues but liver and placenta show VLGR1 expression of similar relative intensities for VLGR1c, compared with VLGR1b (fig. 2b; data not shown). (B) The location of the VLGR1a 5' start site, relative to the exon 65 3' splice acceptor of VLGR1b. RT-PCR results at 30 cycles for VLGR1a and VLGR1b splice forms show a similar tissue distribution to that in figure 2a, as well as similar relative intensities. All RNAs were positive for D-glyceraldehyde-3-phosphate dehydrogenase (GAPDH) (data not shown). (C) A comparison of VLGRb and VLGR1c concentration in human and mouse reveals a species-specific difference in the relative abundance of these isoforms, which were amplified from fetal brain mRNA, indicating a difference in the use of the alternate exon 31 donor sites between species.

Because *VLGR1* is expressed as at least three different isoforms in the human, questions arise as to which of the isoforms is responsible for USH2C and, as a corollary, whether mutations involving other isoforms cause a different phenotype, especially a seizure disorder. The *USH2C* mutations we have observed all involve isoform VLGR1b,

but not isoform VLGR1c. The *Frings* mutation affects both VLGR1b and VLGR1c. We specifically asked all of the patients with USH2C in our study about seizures of any type and received uniformly negative responses. It is plausible to hypothesize that the *Frings* seizure disorder is primarily due to mutations affecting the VLGR1c isoform. Whether a functional protein is encoded by VLGR1c will be important in helping to determine whether the disparity in phenotype between human and mouse *VLGR1* mutants are governed by species-specific differences in VLGR1 function, the inactivation of a subset of VLGR1 isoforms, or a combination of the two. The fact that the *VLGR1* S2832X and S2764P mutations (isoform VLGR1b) segregate in families with both febrile and afebrile seizures (FEB4 [MIM 604352]) suggests a causal relationship between human seizures and *VLGR1.* But the relative low frequency of FEB4-associated mutations, the lack of a significant association between *VLGR1* SNPs and FEB4, and the lack of any self-reported seizure-related phenotype in our USH2C patients suggest that VLGR1b is not a significant contributor to any seizure disorder (Nakayama et al. 2002).

All 13 patients with USH2C and *VLGR1* mutations are female, a highly significant deviation from expectation ($P < .002$, Fisher's exact test). The biologic significance, if any, of this observation can only be speculated on. Although some selection bias could conceivably play a role, it is difficult to understand why the shift in sex ratio is so extreme. A likely explanation is that males are being excluded from the sample: the male phenotype might be more severe, possibly lethal; it could be associated with some other hearing-/vision-loss syndrome; or the phenotype could be very mild or nonexistent. Nonetheless, the possibility that an endocrine-based component could influence the Usher syndrome phenotype as a modifier of *VLGR1* expression and/or protein function is intriguing. Mutations in *VLGR1* do not seem to be responsible for a large proportion of the USH2 cases in our sample, despite the fact that the gene is large and one might have expected otherwise. The possibility of male lethality could explain the apparently low contribution of *USH2C* mutations to the total USH2 mutational load.

The discovery of USH2C-associated *VLGR1* mutations poses several interesting and important questions regarding the etiology of USH2. Localization and functional studies, in addition to thorough genetic screening for additional *VLGR1* mutations, will be needed to elucidate the role of VLGR1 in the development, maintenance, and function of vision and hearing. Furthermore, its capacity as a putative G-coupled receptor makes it a legitimate target in the search for possible therapeutics that may have a broad impact on all types of Usher syndrome.

5.3 Acknowledgments

We thank the patients and their families for participating in the research, especially the Ralph and Justine Donnelly family for their patient support of this research. We want to acknowledge Sharon Kuo and Drs. Cynthia Morton, Peter Humphries, and Hannie Kremer for their interest and work in the identification and screening of other USH2C candidate genes. We thank Drs. Frans Cremers, Dana Orten, and Phillip Kelley for their critical reading of this manuscript. This work was supported by grant 5P01 DC01813-08 from the National Institutes of Health-National Institute on Deafness and

Other Communication Disorders (NIH-NIDCD) (to W.J.K.), a grant from the Foundation Fighting Blindness (to W.J.K.), a grant from the Morris J. and Betty Kaplun Foundation (to W.J.K), and the European Union commission project grant “GENDEAF Thematic Network” (to C.M.). The work of M.W.J.L. was sponsored by the Netherlands Organization of Scientific Research (NWO) grant 901-04-205.

5.4 Electronic database information

Accession numbers and URLs for data presented herein are as follows:National Eye Institute Gene Bank, http://neibank.nei.nih.gov/libs/NbLib0013/NbLib0013.shtml (for human retina) and http://neibank.nei.nih.gov/libs/NbLib0011/NbLib0011.shtml (for human fetal cochlea)

Online Mendelian Inheritance in Man (OMIM), http://www.ncbi.nlm.nih.gov/Omim/ (for USH2, USH1D, USH1F,USH2C, and FEB4)

UCSC Genome Browser, http://genome.cse.ucsc.edu/ (for human *VLGR1,* AF435925; mouse *Vlgr1,* AF435926; and *VLGR1* genomic DNA, NT_028179)

5.5 References

Ahmed Z.M., Riazuddin S., Bernstein S.L., et al., Mutations of the protocadherin gene *PCDH15* cause Usher syndrome type 1F. Am J Hum Genet 2001 69: 25-34.

Alagramam K.N., Yuan H., Kuehn M.H., et al., Mutations in the novel protocadherin *PCDH15* cause Usher syndrome type 1F. Hum Mol Genet 2001 10: 1709-1718.

Beckmann G., Hanke J., Bork P., et al., Merging extracellular domains: fold prediction for laminin G-like and amino-terminal thrombospondin-like modules based on homology to pentraxins. J Mol Biol 1998 275: 725-730.

Bhattacharya G., Miller C., Kimberling W.J., et al., Localization and expression of usherin: a novel basement membrane protein defective in people with Usher’s syndrome type IIa. Hear Res 2002 163: 1-11.

Bitner-Glindzicz M., Lindley K.J., Rutland P., et al., A recessive contiguous gene deletion causing infantile hyperinsulinism, enteropathy and deafness identifies the Usher type 1C gene. Nat Genet 2000 26: 56-60.

Boëda B., El Amraoui A., Bahloul A., et al., Myosin VIIa, harmonin and cadherin 23, three Usher I gene products that cooperate to shape the sensory hair cell bundle. EMBO J 2002 21: 6689-6699.

Bok D., Galbraith G., Lopez I., et al., Blindness and auditory impairment caused by loss of the sodium bicarbonate cotransporter NBC3. Nat Genet 2003 34: 313-319.

Bolz H., von Brederlow B., Ramirez A., et al., Mutation of *CDH23,* encoding a new member of the cadherin gene family, causes Usher syndrome type 1D. Nat Genet 2001 27: 108-112.

Bork J.M., Peters L.M., Riazuddin S., et al., Usher syndrome 1D and nonsyndromic autosomal recessive deafness DFNB12 are caused by allelic mutations of the novel cadherin-like gene *CDH23.* Am J Hum Genet 2001 68: 26-37.

Burgess D.L., Listen carefully: positional cloning of an audiogenic seizure mutation may yield Frings benefits. Neuron 2001 31: 507-508.

Chaib H., Kaplan J., Gerber S., et al. A newly identified locus for Usher syndrome type I, *USH1E,* maps to chromosome 21q21. Hum Mol Genet 1997 6: 27-31.

Eudy J.D., Weston M.D., Yao S., et al., Mutation of a gene encoding a protein with extracellular matrix motifs in Usher syndrome type IIa. Science 1998 280: 1753-1757.

Foord S.M., Jupe S., and Holbrook J., Bioinformatics and type II G-protein-coupled receptors. Biochem Soc Trans 2002 30: 473-479.

Frasson M., Sahel J.A., Fabre M., et al., Retinitis pigmentosa: rod photoreceptor rescue by a calcium-channel blocker in the rd mouse. Nat Med 1999 5: 1183-1187.

Geer L.Y., Domrachev M., Lipman D.J., et al., CDART: protein homology by domain architecture. Genome Res 2002 12: 1619-1623.

Heinrich U.R., Maurer J., and Mann W., Ultrastructural evidence for protection of the outer hair cells of the inner ear during intense noise exposure by application of the organic calcium channel blocker diltiazem. ORL J Otorhinolaryngol Relat Spec 1999 61: 321-327.

Hmani M., Ghorbel A., Boulila-Elgaied A., et al., A novel locus for Usher syndrome type II, *USH2B,* maps to chromosome 3 at p23-24.2. Eur J Hum Genet 1999 7: 363-367.

Hung A.Y. and Sheng M., PDZ domains: structural modules for protein complex assembly. J Biol Chem 2002 277: 5699-5702.
Joensuu T., Hamalainen R., Yuan B., et al., Mutations in a novel gene with transmembrane domains underlie Usher syndrome type 3. Am J Hum Genet 2001 69: 673-684.
Kaplan J., Gerber S., Bonneau D., et al., A gene for Usher syndrome type I (USH1A) maps to chromosome 14q. Genomics 1992 14: 979-987.
Kimberling W.J., Weston M.D., Moller C., et al., Localization of Usher syndrome type II to chromosome 1q. Genomics 1990 7: 245-249.
Kimberling W.J., Möller C.G., Davenport S., et al., Linkage of Usher syndrome type I gene (USH1B) to the long arm of chromosome 11. Genomics 1992 14: 988-994.
Kozel P.J., Friedman R.A., Erway L.C., et al., Balance and hearing deficits in mice with a null mutation in the gene encoding plasma membrane Ca2_-ATPase isoform 2. J Biol Chem 1998 273: 18693-18696.
Krasnoperov V., Lu Y., Buryanovsky L., et al., Post-translational proteolytic processing of the calcium-independent receptor of a-latrotoxin (CIRL), a natural chimera of the cell adhesion protein and the G protein-coupled receptor: role of the G protein-coupled receptor proteolysis site (GPS) motif. J Biol Chem 2002 277: 46518-46526.
Maurer J., Mann W.J., and Amedee R.G., Calcium channel blockers for prevention of noise trauma in otologic surgery. J La State Med Soc 1998 150: 400-405.
McMillan D.R., Kayes-Wandover K.M., Richardson J.A., et al., Very large G protein-coupled receptor-1, the largest known cell surface protein, is highly expressed in the developing central nervous system. J Biol Chem 2002 277: 785-792.
Mustapha M., Chouery E., Torchard-Pagnez D., et al. A novel locus for Usher syndrome type I, USH1G, maps to chromosome 17q24-25. HumGenet 2002 110: 348-350.
Nakayama J., Fu Y.H., Clark A.M., et al., A nonsense mutation of the *MASS1* gene in a family with febrile and afebrile seizures. Ann Neurol 2002 52: 654-657.
Nikkila H., McMillan D.R., Nunez B.S., et al., Sequence similarities between a novel putative G protein-coupled receptor and Na^{+}/Ca^{2+} exchangers define a cation binding domain. Mol Endocrinol 2000 14: 1351-1364.
Noben-Trauth K., Zheng Q.Y., Johnson K.R., et al., *mdfw:* a deafness susceptibility locus that interacts with deaf waddler (*dfw*). Genomics 1997 44: 266-272.
Noben-Trauth K., Zheng Q.Y., and Johnson K.R., Association of cadherin 23 with polygenic inheritance and genetic modification of sensorineural hearing loss. Nat Genet 2003 35: 21-23.
Pasantes-Morales H., Quiroz H., and Quesada O., Treatment with taurine, diltiazem, and vitamin E retards the progressive visual field reduction in retinitis pigmentosa: a 3-year follow-up study. Metab Brain Dis 2002 17: 183-197.
Pawlyk B.S., Li T., Scimeca M.S., et al., Absence of photoreceptor rescue with D-*cis*-diltiazem in the rd mouse. Invest Ophthalmol Vis Sci 2002 43: 1912-1915.
Pieke-Dahl S., Moller C.G., Kelley P.M., et al., Genetic heterogeneity of Usher syndrome type II: localisation to chromosome 5q. J Med Genet 2000 37: 256-262.
Pons T., Gomez R., Chinea G., et al., Beta-propellers: associated functions and their role in human diseases. Curr Med Chem 2003 10: 505-524.
Sankila E.M., Pakarinen L., Kaariainen H., et al., Assignment of an Usher syndrome type III (USH3) gene to chromosome 3q. Hum Mol Genet 1995 4: 93-98.
Scheel H., Tomiuk S., and Hofmann K., A common protein interaction domain links two recently identified epilepsy genes. Hum Mol Genet 2002 11: 1757-1762.
Schwarz E.M. and Benzer S., *Calx,* a Na-Ca exchanger gene of *Drosophila melanogaster.* Proc Natl Acad Sci USA 1997 94: 10249-10254.
Siemens J., Kazmierczak P., Reynolds A., et al., The Usher syndrome proteins cadherin 23 and harmonin form a complex by means of PDZ-domain interactions. Proc Natl Acad Sci USA 2002 99: 14946-14951.
Skradski S.L., Clark A.M., Jiang H., et al., A novel gene causing a Mendelian audiogenic mouse epilepsy. Neuron 2001 31: 537-544.
Smith R.J., Lee E.C., Kimberling W.J., et al., Localization of two genes for Usher syndrome type I to chromosome 11. Genomics 1992 14: 995-1002.
Staub E., Perez-Tur J., Siebert R., et al., The novel EPTP repeat defines a superfamily of proteins implicated in epileptic disorders. Trends Biochem Sci 2002 27: 441-444.
Street V.A., McKee-Johnson J.W., Fonseca R.C., et al., Mutations in a plasma membrane Ca^{2+}-ATPase gene cause deafness in deaf waddler mice. Nat Genet 1998 19:390-394.
Verpy E., Leibovici M., Zwaenepoel I., et al., A defect in harmonin, a PDZ domain-containing protein expressed in the inner ear sensory hair cells, underlies Usher syndrome type 1C. Nat Genet 2000 26: 51-55.
Wayne S., Der Kaloustian V.M., Schloss M., et al., Localization of the Usher syndrome type ID gene (Ush1D) to chromosome 10. Hum Mol Genet 1996 5: 1689-1692.
Wayne S., Lowry E.B., McLeod D.R., et al., Localization of the Usher syndrome type 1F (Ush1F) to chromosome 10. Am J Hum Genet Suppl 1997 61: A300.
Weil D., Blanchard S., Kaplan J., et al., Defective myosin VIIA gene responsible for Usher syndrome type 1B. Nature 1995 374: 60-61.
Weil D., El Amraoui A., Masmoudi S., et al., Usher

syndrome type I G (USH1G) is caused by mutations in the gene encoding SANS, a protein that associates with the USH1C protein, harmonin. Hum Mol Genet 2003 12: 463-471.
Zheng Q.Y., Johnson K.R., and Erway L.C., Assessment of hearing in 80 inbred strains of mice by ABR threshold analyses. Hear Res 1999 130: 94-107.

Chapter 6

General discussion

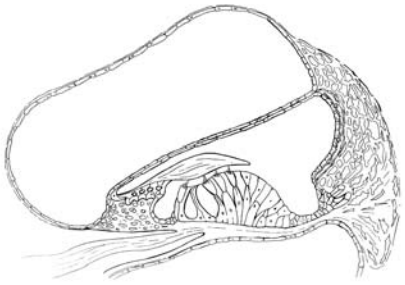

6.1 The value of a subtracted cochlea cDNA library

In chapter two the construction of a human fetal cochlea cDNA library with a subtraction suppressive hybridisation technique and the analysis of this cDNA library was described. In view of recent publications, some aspects of this study will be discussed.

Several cDNA libraries of the inner ear were constructed either with or without subtraction and/or enrichment. A comparison was made of the 46 most frequently represented known genes in the present library (table 2, chapter 2) with the known genes represented in the human foetal cochlea cDNA library analysed by Robertson et al. (1994) (http://hearing.bwh.harvard.edu/cochleacdnalibrary.htm), the organ of Corti cDNA library analysed by Pompeia et al. (2004) (http://neibank.nei.nih.gov), and the complete collection of inner ear derived ESTs in dbEST (http://neibank.nei.nih.gov). Thirty-five of these 46 genes were found to be represented in the Morton cDNA library, 31 were found to be represented in the Pompeia organ of Corti cDNA library, 31 genes were found in the dbEST inner ear collection, and 21 genes were found to be represented in all of these libraries. Recently, the analysis of a cDNA library prepared with RNA from cartilage of 18 to 20 week old human foetuses was published (Krakow et al. 2003, Pogue et al. 2004). Of the 21 genes found in all cDNA collections described above five are also found in the cartilage cDNA library (Pogue et al. 2004). Only three genes from the cDNA library described in chapter 2, *SNCA*, *PSEN1* and *AS3*, were not found in any of the above-mentioned cDNA collections. Whether the presence of these genes in our cDNA library has any functional significance is not clear. We can however conclude that the cochlea cDNA library that we constructed contains unique sequences that are not found in the other inner ear cDNA libraries. The frequency with which known genes were represented varies greatly between the different cDNA libraries which, among other reasons, is due to the different subtraction and/or enrichment procedures used to construct the libraries.

The RNA that we used for the construction of the cDNA library was extracted from 16 to 22 week old foetal cochleas. At this stage the cochlea is still developing (table 1, chapter 1) and as expected, among the known genes represented there are several, e.g. *DIO2*, *FGFR2*, *IGF1*, and *SOX9* that are involved in cochlear development as described in chapter one. Genes involved in nonsyndromic hearing loss that are found in the library include *ACTG1*, *COCH*, *CRYM*, *MYO6*, and *POU3F4*. In addition, genes were found that have not been implicated in hearing loss or inner ear development, but are good candidate genes because of their function and presence in the library (*CDH11*, *EYA2*, *FGF13*, *OTOR*, *PCDH9*, *PCDH18* and *SOX4*). Not all known nonsyndromic deafness genes are found in our library, which is due to the method used to construct the library, subtraction suppressive hybridisation. Genes that are expressed in any of the tissues used to prepare the driver cDNA pool were selected against. However, some genes that are known to be specifically expressed in the cochlear hair cells, for example *STRC*, were not found either. This could be due to the developmental time window in which these genes are expressed, but more likely they were not identified in this study because they are expressed in a specific type of cells. The amount of for example hair cells is very low when compared to the whole cochlea, less than 1%. As a result, the

mass of mRNAs encoded by hair cell specific genes may be too low in the large pool of RNAs derived from the whole cochlea.

In chapter two *SIX1* is suggested to be a good candidate gene for DFNA23. The involvement of *SIX1* in the development in the inner ear, as part of the *SIX-PAX-EYA-DACH* genetic network, was suggested. Ruf et al. (2004) have indeed found three different mutations in *SIX1* in patients suffering from branchio-oto-renal (BOR) syndrome type 3. BOR syndrome is characterised by hearing loss and malformations of the kidney or urinary tract. It was demonstrated that the mutations in *SIX1* disturb EYA1-SIX1 interaction and DNA binding (Ruf et al. 2004).

As mentioned in chapter two many collagen genes were represented in our cDNA library. An explanation is that the cochleas used for preparing the RNA samples were embedded in cartilage, which cannot be completely removed by microdissection. Due to the absence of RNA derived from a bony tissue in the driver cDNA pool, genes expressed in cartilage were not selected against during the subtraction procedure. The publication of a human foetal cartilage cDNA library (Krakow et al. 2003, Pogue et al. 2004) enabled a comparison and estimation to what extent our cDNA library contains cartilage-derived cDNAs. As expected, collagen cDNAs were highly represented in the cartilage library (*COL2A1*, *COL9A1*, *COL9A2, COL11A1*), but interestingly not all collagens, e.g. *COL1A1*, *COL1A2*, *COL3A1*, were found. Other genes that were found to be highly represented in the cartilage and cochlea cDNA libraries were; *ACTG1* (actin gamma 1), *HSPA8* (heat shock 70kD protein), *SPARC* (osteonectin), and *VIM* (vimentin). In total, nine out of the 46 most highly represented genes in our cDNA library were found in the cartilage cDNA library.

In the cochlea cDNA library a large number of clones were found to be located 3' to or in introns of known or predicted genes and generally lacked an open reading frame. It was assumed that they were derived from the 3'-untranslated regions of those genes or from alternatively spliced isoforms. However, recent publications by Cawley et al. (2004) and Numata et al. (2004) have provided an alternative explanation. Numata et al. (2004) show that a significant fraction of the RIKEN mouse full-length cDNA collection (>14%), consists of noncoding RNAs (ncRNAs). NcRNAs are encoded by highly regulated, in most cases multi-exon, transcriptional units, are processed like typical protein-coding mRNAs and are increasingly implicated in the regulation of many cellular functions in eukaryotes. NcRNAs have been identified in plants and animals and are expressed in a tissue-specific manner (Erdmann et al. 2001). In addition, Cawley et al. (2004) have found that the human genome contains many more transcription factor binding sites than can be expected based on predictions of open reading frames. Only 22% of the transcription binding site regions is located at the 5'-end of protein coding genes while 36% lie within or immediately 3' to well characterised genes and are significantly correlated with ncRNAs. Many reports demonstrate that naturally occurring antisense transcription regulates prokaryotic gene expression (Wagner and Simons 1994), and there has been an increasing appreciation that antisense transcription plays an important role in eukaryotic cells (Yelin et al. 2003). Examples of this include X-chromosome inactivation (Brockdorff et al. 1992, Brown et al. 1992), small ncRNA-mediated control of gene silencing in *C.elegans* (Ashrafi et al. 2003, Kamath et al. 2003)

and plants (Hamilton and Baulcombe 1999), gene imprinting (Sleutels and Barlow 2002), and more recently elucidated individual gene regulation (Solymar et al. 2002, Kramer et al. 2003). In view of this data, we believe that a number of the cDNAs from the cochlea cDNA library are ncRNAs and that they may be functional.

Four of the 38 genes known to cause nonsyndromic hearing loss have been found using inner ear specific cDNA libraries. Although the construction and analysis of tissue specific cDNA libraries is time consuming and expensive, these studies provide gene expression information, which can help to elucidate the developmental processes and homeostasis of the inner ear. It is also important that data generated with the analysis of cDNA libraries is deposited in publicly available databases so it can be used in comparative analysis as shown by Pompeia et al. (2004) and the website of the national eye institute (http://neibank.nei.nih.gov). Among the 46 most highly represented genes in our cDNA library, three genes were previously implicated in nonsyndromic hearing loss and seven were previously implicated in syndromic hearing loss. Thus far, our cDNA library did not yield novel nonsyndromic hearing loss genes. However, since the majority of nonsyndromic hearing loss genes remains to be identified, a systematic mutation analysis approach of the most promising candidate genes in the future, e.g. using capillary DGGE analysis, can lead to the identification of novel disease genes.

6.2 Molecular mechanisms underlying DFNA5

DFNA5 was first identified in a large Dutch family (Van Laer et al. 1998). In chapter three a second Dutch family is described, and in 2003 Yu et al. described a novel Chinese DFNA5 family. The hearing loss in all three families is similar: nonsyndromic, progressive, sensorineural and starting in the high frequencies. The *DFNA5*-associated mutations are different in each family, a complex insertion-deletion mutation in intron 7 in the first Dutch family (a 1,189 bp fragment is deleted from intron 7, 127 bp from intron 8 are inserted into intron 7 in the opposite direction, followed by a GCCCA-stretch of unknown origin), a nucleotide substitution in the splice acceptor site of intron 7 in the second Dutch family described in chapter three (c.991-6C>G), and a three nucleotide deletion in the polypyrimidine tract of the 3' splicing site of intron 7 (c.991-17_19del). Interestingly, at the mRNA level all three mutations have the same affect; skipping of exon 8. This leads to a frameshift starting after amino acid 330, which introduces an aberrant stretch of 41 amino acids followed by a stop codon that prematurely truncates the protein (p.Cys331_Glu395>LysfsX41).

Morpholino antisense nucleotide knock-down of *dfna5* function in zebrafish leads to disorganisation of the developing semicircular canals and reduction of the pharyngeal cartilage (Bunsch-Nentwich et al. 2003). This phenotype closely resembles previously isolated zebrafish craniofacial mutants including the mutant *jekyll* (Neuhauss et al. 1996). The *jekyll* zebrafish has a homozygous mutation in Ugdh (uridine 5'-diphosphate (UDP)-glucose dehydrogenase), an enzyme that is required for the synthesis of proteoglycans including the extracellular matrix component hyaluronic acid (Walsh and Stainier 2001). In many areas of the developing human inner ear hyaluronic acid is highly abundant and it is suggested to serve as a friction reducing lubricant and molecular filter in the inner

ear (Anniko and Arnold 1995). In zebrafish treated with *dfna5* morpholinos, expression of *ugdh* is absent in the developing ear and pharyngeal arches, and hyaluronic acid levels are strongly reduced in the outgrowing protrusions of the developing semicircular canals (Bunsch-Nentwich et al. 2003). If hyaluronic acid biosynthesis is reduced or lost in the human inner ear, it is possible that this disruption of extracellular matrix causes increased mechanical stress on hair cells and thus disfunction and/or degeneration of the hair cells.

The striking similarity of the functional effect of the three different DFNA5 mutations, i.e. the skipping of exon 8, strongly suggests that this is a “gain of function” mutation, resulting in a truncated protein with a deleterious new function. Gregan et al. (2003) showed the first evidence of this deleterious new function. They describe a CCCH domain as a domain that is shared between DFNA5 and the Mcm10 family of DNA replication proteins. Mcm10 is required for efficient initiation of DNA replication (Wohlschlegel et al. 2002). Interestingly, yeast cells with mutant mcm10 (Merchant et al. 1997) have the same phenotype as yeast cells carrying DFNA5 containing the mutation described in humans by van Laer et al. (1998). Both are blocked in G1 or early S phase of the cell cycle. The truncated proteins both lack the CCCH domain and the expression of wild-type DFNA5 did not affect the yeast cells. In addition, van Laer et al. (2004) presented evidence for the involvement of the truncated DFNA5 protein in cell cycle dysregulation. The percentage of dead HEK293T cells was significantly higher when the cells were transfected with mutant *DFNA5* compared to cells transfected with wild-type *DFNA5*. The number of necrotic cells was also significantly higher when the cells were transfected with mutant *DFNA5*, while the number of apoptotic cells remained stable. Van Laer et al. (2004) also show that wild-type DFNA5 was distributed evenly in the cytoplasm, while mutant DFNA5 was localised in the cytoplasm in a granular manner. Mutant DFNA5 seemed to be associated with the plasma membrane especially in cells with an unhealthy appearance. The localisation of mutant DFNA5 at the plasma membrane might indicate that a predicted transmembrane region in the aberrant tail of the protein is functional or that mutant DFNA5 interacts with a membrane protein.

Expression of *DFNA5* was detected at low levels in every tissue investigated so far (Van Laer et al. 1998). If cell death would occur in every tissue that expresses *DFNA5*, a lethal phenotype would be expected in mutation carriers. However, affected individuals show progressive hearing loss as the only recognisable clinical characteristic. It is possible that cochlear cells are much more sensitive to the deleterious actions of mutant DFNA5 because DFNA5 might interact with cellular components that are expressed specifically in cochlear cells.

6.3 The DFNA11 phenotype is caused by mutations in different functional domains of myosin VIIa

In 1997 Liu et al. described a Japanese family with autosomal dominant hearing impairment caused by a mutation in *MYO7A* (DFNA11). Patients suffered from sensorineural hearing loss with gradual progression at all frequencies and minor vestibular problems. This phenotype was similar to the phenotype found in patients

from a Dutch family and, as described in chapter three, indeed a mutation was found in *MYO7A*. At the same time, mutations in *MYO7A* were found in an American and a German family with DFNA11 (Bolz et al. 2004, Street et al. 2004). The patients from the American family showed progressive sensorineural hearing loss at all frequencies with the greatest progression at the high frequencies, but the clinical phenotype varied between patients from different branches of the family. In the German family, patients were found to have slowly progressing hearing loss and mild vestibular dysfunction. The American family was the only family in which vestibular problems were not found. In none of the families there was evidence for retinitis pigmentosa.

Different mutations in *MYO7A* segregate with the hearing loss in the four families; in the Japanese family a 9-bp deletion in exon 22 lead to a 3 amino acid deletion in the coiled-coil domain of the protein (c.2656_2664del [p.Ala886_Lys888del]), in the Dutch family a nucleotide change in exon 13 is predicted to result in an amino acid substitution in the motor head domain of the protein (c.1373A>T [p.Asn458Ile]), in the American family a nucleotide substitution in exon 17 is predicted to cause an amino acid substitution in the motor head domain of the protein (c.2164G>C [p.Gly722Arg]) and in the German family a missense mutation in exon 21 changes the fourth evolutionary conserved residue of the consensus sequence of the fifth IQ motif, a putative calmodulin binding domain (c.2557C>T [Arg853Cys]). Even though all four mutations are different and have a different predicted effect on protein function, the disease mechanism seems to be the same because in all cases a similar phenotype and mode of inheritance is found. To be able to understand how these different mutations lead to a similar phenotype in humans, the effect of these mutations on protein function can be studied in a model system.

Recently, a mouse model for DFNA11 with low frequency autosomal dominant hearing loss was published by Rhodes et al. (2004). In an ENU screening the heterozygote *headbanger* mutant that displays classic behaviour indicative of vestibular dysfunction including hyperactivity and head bobbing was found. The mice show a Preyer reflex in response to sound but have raised cochlear thresholds especially at low frequencies. Scanning electron microscopy of the surface of the organ of Corti revealed abnormal stereocilia bundle development from an early age that was more severe in the apex than the base. Mutation screening of *Myo7a* revealed a nucleotide transversion (c.532A>T) that is predicted to cause an amino acid substitution in a conserved region of the motor head domain of the protein (p.Ile178Phe). Studying the mouse model further might reveal in which way the protein function is impaired in the *headbanger* mouse and how different mutations in myosin VIIa relate to the phenotype found in humans.

The use of another model system, *Dictyostelium discoideum,* was illustrated by Sato et al. (2004). A mutation in the myosin VI gene responsible for DFNA22 in humans (c.1325G>A [p.Cys442Tyr]) (Melchionda et al. 2001) was studied in *Dictyostelium*. Sato et al. (2004) found three major changes in mechanoenzymatic functions of the myosin VI protein that are altered by the DFNA22 mutation. First, the ADP dissociation rate is markedly increased by the mutation. Second, the mutation markedly increased the basal ATPase activity of myosin VI. Thirdly, the actin-activated ATPase activity of mutant myosin is Ca^{2+} sensitive. These results indicate that *Dictyostelium* is a good model

system for studying the effect of mutations on the biochemical properties of myosin proteins.

6.4 VLGR1 involvement in Usher syndrome type II

In chapter five mutations in *VLGR1* are described that are causative for Usher syndrome type IIc. Other mutations in *VLGR1* are known to cause febrile and afebrile seizures in humans (Nakayama et al. 2002), and audiogenic seizures in mice (Skradski et al. 2001, McMillan and White 2003). Three VLGR1 isoforms are found in humans and these and three additional isoforms are found in mice. The function of full length VLGR1 or any of the isoforms is not clear. Therefore, it is also difficult to speculate on the phenotype of mutations in different isoforms. As described in chapter five, in some patients only in one allele a mutation was found. It is important that the mutation in the other allele is also found in these cases to exclude the involvement of other genes in these cases, but considering the size of the *VLGR1* gene (>19 kb) and the multiple splice variants this will not be easy. Alternatively, the use of a model system is important to study the effect of the mutations on protein function. Two mouse models, with a natural mutation (*Frings*) (Skradiske et al. 2001) and an introduced deletion (McMillan and White 2003) have already been published. It would be interesting to study the effect of USHIIc mutations on the phenotype in mice.

Putative protein-protein interaction domains found in VLGR1 seem to imply that VLGR1 is part of a protein complex that also includes cadherin 23, SANS and USH2A. Recent evidence indeed suggests the existence of a large macromolecular protein complex including both USH1 and USH2 proteins that is necessary to shape and maintain the stereocilia as an organised cohesive unit (Boëda et al. 2002, Siemens et al. 2002, Weil et al. 2003, and personal communications).

6.5 General conclusion

This thesis describes several strategies to identify the molecular defects underlying hereditary hearing loss. Results described in this thesis and table 6 of the introduction suggest that positional cloning is the most successful strategy to identify these genes. However, especially when studying small families and isolated patients where positional cloning cannot be used, other strategies are also needed to identify additional hearing loss genes. In general, a combination of different strategies is expected to be the most successful.

6.6 References

Anniko M. and Arnold W., Hyaluronic acid as a molecular filter and friction-reducing lubricant in the human inner ear. ORL J Otorhinolaryngol Relat Spec 1995 57: 82-86.

Ashrafi K., Chang F.Y., Watts J.L., et al., Genome-wide RNAi analysis of Caenorhabditis elegans fat regulatory genes. Nature 2003 421: 268-272.

Boëda B., El-Amraoui A., Bahloul, et al., Myosin VIIa, harmonin and cadherin 23, three Usher I gene products that cooperate to shape the sensory hair cell bundle. EMBO J 2002 21: 6689-6699.

Bolz H., Bolz S.S., Schade G., et al., Impaired calmodulin binding of myosin-7A causes autosomal dominant hearing loss (DFNA11). Hum Mut 2004 24: 274-275

Brockdorff N., Ashworth A., Kay G.F., et al., The

product of the mouse Xist gene is a 15 kb inactive X-specific transcript containing no conserved ORF and located in the nucleus. Cell 1992 71: 515-526.
Brown C.J., Hendrich B.D., Rupert J.L., et al., The human XIST gene: analysis of a 17 kb inactive X-specific RNA that contains conserved repeats and is highly localized within the nucleus. Cell 71: 527-542.
Bunsch-Nentwich E., Söllner C., Roehl H., et al., The deafness gene dfna5 is crucial for ugdh expression and HA production in the developing ear in zebrafish. Development 2003 131: 943-951.
Cawley S., Bekiranov S., Ng H.H., et al., Unbiased mapping of transcription factor binding sites along human chromosomes 21 and 22 points to widespread regulation of noncoding RNAs. Cell 2004 116: 499-509.
Erdmann V.A., Barciszewska M.Z., Hochberg A., et al., Regulatory RNAs. 2001 Cell Mol Life Sci 2001 58: 960-977.
Gregan J., Van Laer L., Lieto L.D., et al., A yeast model for the study of human DFNA5, a gene mutated in nonsyndromic hearing impairment. Biochin Biophys Acta 2003 1638: 179-186.
Hamilton and Baulcombe, A species of small antisense RNA in posttranscriptional gene silencing in plants. Science 1999 286: 950-952.
Kamath R.S., Fraser A.G., Dong Y., et al., Systematic functional analysis of the Caenorhabditis elegans genome using RNAi. Nature 2003 421: 231-237.
Krakow D., Sebald E.T., Pogue R., et al., Analysis of clones from a human cartilage cDNA library provides insight into chondrocyte gene expression and identifies novel candidate genes for the osteochondrodysplasias. Mol Genet Metab 2003 79: 34-42.
Kramer C., Loros J.J., Dunlap J.C., et al., Role for antisense RNA in regulating circadian clock function in Neurospora crassa. Nature 2003 421: 948-52.
Liu X.Z., Walsh J., Mburu P., et al., Mutations in the myosin VIIA gene cause non-syndromic recessive deafness. Nat Genet 1997 17: 268-269.
McMillan D.R. and White P.C., Loss of the transmembrane and cytoplasmic domains of the very large G-protein-coupled receptor-1 (VLGR1 or Mass1) causes audiogenic seizures in mice. Mol Cell Neurosci 2003 26: 322-329.
Melchionda S., Ahituv N., Bisceglia L., et al., MYO6, the human homologue of the gene responsible for deafness in Snell's waltzer mice, is mutated in autosomal dominant nonsyndromic hearing loss. Am J Hum Genet 2001 69: 635-640.
Merchant A.M., Kawasaki Y., Chen Y., et al., A lesion in the DNA replication initiation factor Mcm10 induces pausing of elongation forks through chromosomal replication origins in Saccharomyces cerevisiae. Mol Cell Biol 1997 17: 3261-3271.
Nakayama J., Fu Y.H., Clark A.M., et al., A nonsense mutation of the MASS1 gene in a family with febrile and afebrile seizures. 2002 Ann Neurol 52: 654-657.
Neuhauss S.C., Solnica-Krezel L., Schrier A.F., et al., Mutations affecting craniofacial development in zebrafish. Development 1996 123: 357-367.
Numata K., Kanai A., Saito R., et al., Identification of putative noncoding RNAs among the RIKEN mouse full- length cDNA collection. Genome Res 2004 13: 1301-1306.
Pogue R., Sebald E., King L., et al., A transcriptional profile of human fetal cartilage. Matrix Biol 2004 23: 299-307.
Pompeia C., Hurle B., Belyantseva I.A., et al., Gene expression profile of the mouse organ of Corti at the onset of hearing. Genomics 2004 83: 1000-1011.
Rhodes C.R., Hertzano R., Fuchs H., et al., A Myo7a mutation cosegregates with stereocilia defects and low-frequency hearing impairment. Mamm Genome 2004 15: 686-697.
Robertson N.G., Khetarpal U., Gutierrez-Espeleta G.A., et al., Isolation of novel and known genes from a human fetal cochlear cDNA library using subtractive hybridization and differential screening. Genomics 1994 23: 42-50.
Ruf R.G., Xu P.X., Silvius D., et al., SIX1 mutations cause branchio-oto-renal syndrome by disruption of EYA1-SIX1-DNA complexes. PNAS 2004 101: 8090-8095.
Sato O., White H.D., Inoue A., et al., Human deafness mutation of myosin VI (C442Y) accelerates the ADP dissociation rate. JBC 2004 279: 28844-28854.
Siemens J., Kazmierczak P., Reynolds A., et al., The Usher syndrome proteins cadherin 23 and harmonin form a complex by means of PDZ-domain interactions. PNAS 2002 99: 14946-14951.
Skradski S.L., Clark A.M., Jiang H., et al., A novel gene causing a mendelian audiogenic mouse epilepsy. Neuron 2001 31: 537-544.
Sleutels F. and Barlow D.P., The origins of genomic imprinting in mammals. Adv Genet 2002 46: 119-164.
Solymar D.C., Argawal S., Bassing C.H., et al., A 3' enhancer in the IL-4 gene regulates cytokine production by Th2 cells and mast cells. Immunity 2002 17: 41-50.
Street V.A., Kallman J.C., and Kiemele K.L., Modifier controls severity of a novel dominant low-frequency MyosinVIIA (MYO7A) auditory mutation. J Med Genet 2004 41: e62.
Van Laer L., Huizing E.H., Verstreken M., et al., Nonsyndromic hearing impairment is associated with a mutation in DFNA5. Nat Genet 1998 20: 194-197.
Van Laer L., Vrijens K., Thys S, et al., DFNA5: hearing impairment eon instead of hearing impairment gene. J Med Genet 2004 41: 401-406
Wagner E.G. and Simons R.W., Antisense RNA control in bacteria, phages, and plasmids. Annu Rev Microbiol 1994 48: 713-742.
Walsh E.C. and Stainier D.Y., UDP-glucose dehydrogenase required for cardiac valve formation in zebrafish. Science 2001 293: 1670-1673.

Weil D., El-Amraoui A., Masmoudi S., et al., Usher syndrome type I G (USH1G) is caused by mutations in the gene encoding SANS, a protein that associates with the USH1C protein, harmonin. Hum Mol Genet 2003 12: 463-471.
Wohlschlegel J.A., Dahr S.K., Prokhorova T.A., et al., Xenopus Mcm10 binds to origins of DNA replication after Mcm2-7 and stimulates origin binding of Cdc45. Mol Cell 2002 9: 233-240.
Yelin R., Dahary D., Sorek R., et al., Widespread occurrence of antisense transcription in the human genome. Nat Biotechnol 2003 21: 379-386.
Yu C., Meng X., Zhang S., et al., A 3-nucleotide deletion in the polypyrimidine tract of intron 7 of the DFNA5 gene causes nonsyndromic hearing impairment in a Chinese family. Genomics 2003 83: 575-579.

Chapter 7

Summary

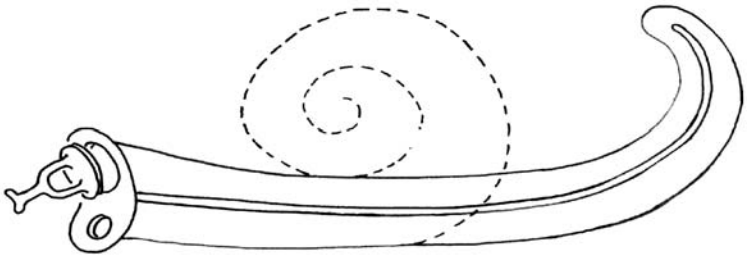

7.1 Summary

Hearing loss is the most common sensory disorder in the human population. It affects 0.1% of all young children and by the age of 70, 30% of the population suffers from hearing loss greater than 40 dB. When early onset hearing loss is inherited, 70% is classified as nonsyndromic and 30% as syndromic. Nonsyndromic hearing loss is further subdivided by its mode of inheritance; ~77% of the cases are autosomal recessive (DFNB), ~22% are autosomal dominant (DFNA) and ~1% are X-linked (DFN). Eighty nonsyndromic hearing loss loci have been described so far, but new loci are continuously found. For approximately half of the loci the genetic defect responsible for the hearing loss has been identified. Several strategies are being used to elucidate the genetic defect for the remaining loci. The method most commonly used employs linkage analysis in affected families followed by positional cloning of the gene involved.

Although positional cloning has been very successful in identifying hereditary hearing loss genes in the past, several new strategies have been developed recently for identifying candidate genes. One of these strategies, the construction and analysis of a cDNA library, is described in chapter two. Using a suppression subtractive hybridisation technique a human fetal cochlea cDNA library was constructed. By using sequence and BLAST analysis 2640 clones were characterised. Approximately 150 cDNA clones were found to map in nonsyndromic hearing loss loci for which the causative gene had not been identified yet. The expression of these cDNA clones and some additional interesting clones was analysed by RT-PCR. None of the analysed cDNAs were exclusively expressed in the cochlea, however, the expression data showed that about 25% of the novel cDNAs from the library were preferentially expressed in the cochlea. Although the characterisation of the cDNA library did not yield any new nonsyndromic hearing loss genes yet, it did generate a large number of candidate genes for hereditary hearing loss and inner ear development.

The use of clinical data (e.g ARTAs) can greatly facilitate the elucidation of the cause of hearing loss in specific families (chapter three and four) exemplifying the synergism that occurs upon a close collaboration between clinicians and researchers.

The fifth dominant nonsyndromic locus that has been described, DFNA5, is characterised by high frequency hearing loss caused by a mutation in the *DFNA5* gene. The second Dutch family with DFNA5 is described in chapter three. The hearing loss segregating in this family is sensorineural and symmetric. In the high frequencies, hearing impairment amounted to 30 dB at young age. Progression of hearing loss was most pronounced at 1 kHz. A nucleotide change in the splice acceptor site of intron 7, c.991-6C>G, leading to skipping of exon 8 in part of the transcripts, was found to be responsible for the hearing loss segregating in this family. The skipping of exon 8 leads to a prematurely truncated protein with an aberrant stretch of amino acids that likely results in a deleterious gain of function of the protein in the inner ear.

Another form of dominantly inherited high frequency hearing loss is DFNA11. The hearing impairment is characterized by flat audiograms at young ages and mild progression most prominent at the high frequencies. DFNA11 is associated with a mutation in the *MYO7A* gene. In chapter 4 a Dutch family with DFNA11 is described.

The hearing loss in this family segregates with a c.1373A>T transversion in *MYO7A* that is heterozygously present in all affected family members. The nucleotide change is predicted to lead to an p.Asn458Ile amino acid change in the motor domain of the myosin VIIA protein. A molecular model of the protein was built based on the myosin II heavy chain of *Dictyostelium discoideum*. In the model, the amino acid substitution predicts conformational changes with severe effects on the function of the myosin VIIA protein.

As mentioned above, 30% of prelingual inherited hearing loss is classified as syndromic. Usher syndrome is a form of syndromic hearing loss that is characterized by various degrees of congenital hearing loss and of loss of eyesight through progressive retinitis pigmentosa and is the most common form of deaf-blindness (50%). Its prevalence is currently estimated in developed countries at 3.8-4.4 per 100,000 live births. Usher syndrome is a genetically heterogeneous autosomal recessive disorder, for which at least twelve loci account for subtypes of the syndrome. For Usher syndrome type II there are at least three genetic subtypes (USH2A, USH2B, and USH2C). Chapter 5 describes the identification of mutations in *VLGR1* in patients suffering from Usher syndrome type IIC. Three human *VLGR1* mRNA isoforms are expressed (*VLGR1a*, *VLGR1b*, and *VLGR1c*) and four isoform-specific mutations were found in the patients. On the basis of its potential extracellular and intracellular protein-protein interaction domains and its wide mRNA expression profile, it is probable that VLGR1 serves diverse cellular and signalling processes.

7.2 Samenvatting

Gehoorsverlies is de meest voorkomende sensorische aandoening in de humane populatie. Ongeveer 0.1% van alle jonge kinderen en 30% van alle volwassenen boven de 70 hebben een gehoorsverlies groter dan 40 dB. Gehoorsverlies wat optreedt op jonge leeftijd en mendeliaans overerft kan worden onderverdeeld in syndromaal gehoorsverlies (70% van alle gevallen) en niet-syndromaal gehoorsverlies (30% van de gevallen). Niet-syndromaal gehoorsverlies wordt geclassificeerd op basis van de vorm van overerving; in ~77% van de gevallen is de overerving autosomaal recessief (DFNB), in ~22% autosomaal dominant (DFNA), en in ~1% X-gebonden (DFN). Tot nu toe zijn 80 niet-syndromale doofheidloci beschreven, maar nieuwe loci worden nog steeds gevonden. Voor ongeveer de helft van alle doofheidloci is het oorzakelijke gendefect geïdentificeerd.

Verschillende methoden worden gebruikt om nieuwe “doofheid-genen” te vinden, maar de meest gebruikte methode is koppelingsonderzoek in aangedane families gevolgd door het positioneel kloneren van het betrokken gen. In het verleden is deze methode erg succesvol gebleken, desondanks zijn recentelijk enkele nieuwe strategieën ontwikkeld. Een van deze strategieën, het construeren en analyseren van een cDNA-bank, wordt beschreven in hoofdstuk twee. Een suppressie-subtractie-hybridisatie-techniek werd gebruikt om een humane foetale cochlea cDNA-bank te construeren en met behulp van sequentie- en BLAST-analyse werden 2640 klonen gekarakteriseerd. Ongeveer 150 cDNA klonen werden gelokaliseerd in loci betrokken bij vormen van niet-syndromaal gehoorsverlies waar het oorzakelijke gen nog niet voor gevonden is. De expressie van deze en andere interessante klonen werd geanalyseerd met behulp van RT-PCR. Geen van de geanalyseerde klonen kwam uitsluitend tot expressie in de cochlea, maar op basis van de expressie data kan worden geconcludeerd dat ongeveer 25% van de nieuwe klonen preferentieel tot expressie komt in de cochlea. Ondanks dat de analyse van de cDNA-bank nog niet heeft geleidt tot de identificatie van nieuwe genen betrokken bij niet-syndromaal gehoorsverlies, heeft de analyse wel een groot aantal kandidaat genen voor vormen van erfelijk gehoorsverlies en binnenoor ontwikkeling opgeleverd.

Het gebruik van klinische data (b.v. ARTAs) kan het ophelderen van de oorzaken van erfelijk gehoorsverlies in specifieke families ten goede komen. De resultaten die in hoofdstuk 3 en 4 van dit proefschrift worden beschreven zijn het gevolg van een goede samenwerking tussen wetenschappers en clinici.

Het doofheidlocus dat als vijfde werd beschreven, DFNA5, wordt gekarakteriseerd door hoge tonen gehoorsverlies veroorzaakt door een mutatie in het *DFNA5* gen. In hoofdstuk 3 wordt de tweede Nederlandse familie met DFNA5 beschreven. Het gehoorsverlies in deze familie is sensorineuraal en symmetrisch. Op jonge leeftijd kan het gehoorsverlies in de hoge tonen oplopen tot 30 dB en bij 1 kHz is de progressie van het gehoorsverlies het grootst. Een nucleotideverandering in de splice-acceptor-site van intron 7, c.991-6C>G, die het overslaan van exon 8 in een deel van de transcripten veroorzaakt, is verantwoordelijk voor het gehoorsverlies in deze familie. Het overslaan van exon 8 resulteert waarschijnlijk in een prematuur beëindigd eiwit met een aantal

afwijkende aminozuren. Deze verandering van de samenstelling van het eiwit leidt waarschijnlijk tot en verandering van de functie van het eiwit. Mogelijk is deze nieuwe functie nadelig voor het functioneren van het binnenoor.

Een andere vorm van dominant overervend hoge tonen gehoorsverlies is DFNA11. DFNA11 wordt gekarakteriseerd door een vlak audiogram op jonge leeftijd en milde progressie die het grootst is in de hoge tonen. Deze vorm van gehoorsverlies is geassocieerd met een mutatie in het *MYO7A* gen. In hoofdstuk vier wordt een Nederlandse familie met DFNA11 beschreven. In deze familie erft het gehoorsverlies over met een c.1373A>T nucleotideverandering in *MYO7A* die heterozygoot aanwezig is in alle aangedane familieleden. De gevonden nucleotide verandering leidt waarschijnlijk tot een p.Asn458Ile aminozuur-verandering in het motor domein van het myosine VIIA eiwit. Een moleculair model van myosine VIIA werd geconstrueerd gebaseerd op de myosine II heavy chain van *Dictyostelium discoideum*. Het model voorspelt een conformatieverandering van het eiwit als gevolg de aminozuurverandering. De conformatie verandering van het eiwit zal de functie van het myosine VIIA eiwit waarschijnlijk verstoren.

Zoals hierboven al werd aangegeven, is 30% van het prelinguaal erfelijk gehoorsverlies syndromaal. Usher syndroom is een vorm van syndromaal gehoorsverlies die wordt gekenmerkt door een variërende mate van congenitaal gehoorsverlies in combinatie met gezichtsverlies door progressieve retina dystrofie (retinitis pigmentosa). Usher syndroom is de meest voorkomende vorm van doof-blindheid (50%) en volgens schattingen lijden er in westerse landen 3.8-4.4 per 100.000 levend geboren kinderen aan Usher syndroom. Usher syndroom is een genetisch heterogene autosomaal recessieve aandoening. Ten minste 12 loci zijn verantwoordelijk voor de drie verschillende typen van het syndroom (USH1, USH2 en USH3). Voor Usher syndroom type II zijn tot nu toe drie verschillende subtypen (USH2A, USH2B en USH2C) beschreven. In hoofdstuk vijf wordt de identificatie van mutaties in het *VLGR1* gen in patiënten met Usher syndroom type IIC beschreven. Drie verschillende *VLGR1* mRNA isovormen komen tot expressie (*VLGR1a*, *VLGR1b*, *VLGR1c*) in de mens. Vier isovorm-specifieke mutaties werden gevonden in de USH2C-patiënten. Op basis van de voorspelde extracellulaire en intracellulaire eiwit-eiwit interactie-domeinen van het VLGR1 eiwit, wordt aangenomen dat VLGR1 een rol speelt in diverse cellulaire en signaaltransductieprocessen.

Chapter 8

Appendices

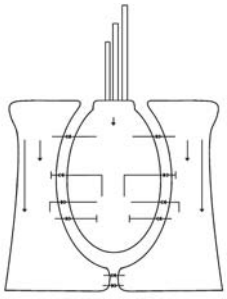

8.1 Appendix 1: Table of gene expression in the developing inner ear

m: mouse, c: chick, z: zebrafish, x: xenopus, r: rat

human gene	*gene other species*	*expression during otic placode stage*	*expression during otic vesicle stage*	*expression during differentiation stage*	*phenotype mutant*	*remarks*
BMP4	*Bmp4* (m,c)		in mouse in the developing otocyst epithelium in two patches corresponding to the primordia of the anterior and posterior sensory cristae (Morsli et al. 1998) and in the developing statoacoustic ganglion (Liu et al. 2003)	in mouse in the periotic mesenchyme,themesenchyme of the developing otic capsule, and in the nerve fibers emerging from the acoustic and vestibular ganglion (Liu et al. 2003), in chick in supporting cells of the vestibular system and in sensory hair cells in the cochlea (Oh et al. 1996)		bone morphogenic protein
BMP7	*Bmp7* (m,c)	in chick in the otic placode (Oh et al. 1996)	in chick in the posterior portions of the otic cup (Oh et al. 196)	in the vestibular system of chick segregated from the main sensory tissue areas at the onset of differentiation, in the cochlea restricted to the sensory tissues and later supporting cells (Oh et al. 1996)	a Bmp7 knockout mouse has no ear phenotype (Dudley et al. 1995, Luo et al. 1995)	bone morphogenic protein
C-JUN	*c-jun* (c)	in the otic placode and the dorsal area of the otic pit (Sanz et al. 1999)	in the dorsal otic vesicle and cochleovestibular ganglion (Sanz et al. 1999), coincides with the proliferative period of growth of the otic vesicle (Leon et al. 1998)			proto-oncogene
DACH1	*Dach1* (m,c)		in mice in the medial wall of the otic vesicle, in chick in the dorsal part of the otic vesicle (Heannue et al. 2002)		a *Dach1* knockout mouse does not show any obvious ear defects (Davis et al. 2001)	
DLX2	*Dlx2* (m,c)		low level restricted to the vestibular part as the otic vesicle begins to elongate and the vestibular labyrinth and cochlea become distinguishable (Robinson and Mahon 1994)	in the epithelium of the semicircular canals in mice (Robinson and Mahon 1994), in chick also in the non neuronal cells of the cochleavestibular ganglion and nerves (Brown et al. 2005)		homeodomain transcription factor

human gene	*gene other species*	*expression in otic placode stage*	*expression in otic vesicle stage*	*expression during differentiation stage*	*phenotype mutant*	*remarks*
DLX3	*Dlx3* (m,c), *Dlx3b* (z), *x-Dll2* (x)	marks the otic placode in chick and becomes limited to epithelium adjacent to the hindbrain as invagination of the otic placode begins (Brown et al. 2005)	low level in the dorsal part of the otic vesicle (Brown et a. 2005) restricted to the vestibular part as the otic vesicle begins to elongate and the vestibular labyrinth and cochlea become distinguishable (Robinson and Mahon 1994)	in the epithelium of the utricle and the semicircular canals (Robinson and Mahon 1994)		homeodomain transcription factor
DLX5	*Dlx5* (m,c) *x-Dll3* (x)	at the rim of the otic pit in chick (Brown et al. 2005)	spreads throughout the dorsal otocyst in chick and mouse (Brown et al. 2005)	thoughout formation of the semicircular canals and endolymphatic structures and cochlear and vestibular nerves in chick (Brown et al. 2005)	mouse mutants have severe vestibular malformations, no formation of the anterior and posterior semicircular canals; defects in the lateral semicircular canal, cochlea and vestibular maculae (Acampora et al. 1999, Depew et al. 1999)	homeodomain transcription factor
DLX6	*Dlx6* (m,c) *x-Dll3* (x)	at the rim of the otic pit overlap with Dlx5 expression in chick (Brown et al. 2005)	spreads throughout the dorsal otocyst overlap with Dlx5 expression in chick and mouse (Brown et al. 2005)	throughout the formation of the semicircular canals and endolymphatic structures in chick (Brown et al. 2005)	Dlx5/Dlx6 double knockout mouse has unrecognizable inner ear structures (Robleno et al. 2002)	homeodomain transcription factor
EYA1	*Eya1* (m,z)	in zebrafish already in a patch that later develops into the otic placode, also in the otic placode (Sahly et al. 1999)	in mice in the ventromedial wall of the otic vesicle and in the statoacoustic ganglion and the periotic mesenchyme (Kalatzis et al. 1998); in zebrafish also in the ventral half of the otic vesicle, this including the region in which the acoustic ganglion forming neuroblasts originate and the hair and supporting cells begin to develop (Sahly et al. 1999)	in mice in the hair and supporting cells of the sensory epithelia as well as in the associated ganglia; persists after differentiation has taken place (Kalatzis et al. 1998)	heterozygous *Eya1* knockout mice have conductive hearing loss and renal abnormalities, homozygous knockouts lack ears and kidneys, the inner ear development is arrested at the otic vesicle stage (Xu et al. 1999); the *Drosophila Eya1* mutant dog-eared shows abnormal development of semicircular canals and lack cristae the sensory patches show abnormal development, macular hair cells show decreased numbers and defective arrangement (Whitfield et al. 1996)	transcription factor; in humans mutations in *EYA1* cause BOR syndrome (Abdelhak et al. 1997), in zebrafish *Eya1* seems to be primarily required for survival of sensory hair cells in the developing ear (Kozlowski et al. 2005)

EYA4	*Eya4* (m,r)		in mouse in the otic vesicle (Borsani et al. 1999)	in rat in neuroepithelia, primarily in the upper epithelium of the cochlear duct which gives rise to Reisner's membrane and the stria vascularis, and also in the mesenchyme surrounding the duct, also in areas of the cochlear duct that are destined to become the spiral limbus, organ of Corti, and spiral prominence in the developing vestibular system and in the sensory epithelium (Wayne et al. 2001)		transcription factor; in humans mutations in *EYA4* cause postlingual, progressive, autosomal dominant nonsyndromic hearing loss at the DFNA10 locus (Wayne et al. 2001)
FGF10	*Fgf10* (m,c)	mesodermal signal for induction of the otic placode in mice (Ladher et al. 2005)	in the ventral half of the otic vesicle (Wilkinson et al. 1989, Pirvola et al. 2000, Pickles et al. 2001)	in sensory epithelia: in hair cells, supporting cells, nerve tissues, and other cells (Pirvola et al. 2000) abundant expression in delaminating neuroblasts (Pirvola et al. 2000)	mouse mutants have inner ear defects, but milder than in *Fgf3* knockout (Ohuchi et al. 2000, Pirvola et al. 2000) *Fgf10* and *Fgf3* double knockout otic vesicle formation severely reduced (Alvarez et al. 2003, Wright and Mansour 2003)	growth factor
FGF19	*Fgf15* (m) *Fgf19* (c)	mesodermal signal for induction of the neuroectoderm, which in turn induces expression of Wnt8c and Fgf3 in chick (Pickles and Chir 2002, Ladher et al 2005) in mice expressed in the neuroectoderm not in the mesoderm (Wright et al. 2004)			no otic abnormalities (Wright et al. 2004)	growth factor
FGF2	*Fgf2* (m,c)	early (Frenz et al. 1994, Vendrell et al. 2000)	medial ventral (Frenz et al. 1994)	in hair cells, supporting cells and nerve tissues of the cochlea and vestibular system (Pickles and Heumen 1997, Carnicero et al. 2004)	mutant mice haveno abnormalities at adult stage, normal hearing thresholds before and after noise damage (Carnicero et al. 2004 and references therein)	growth factor

human gene	*gene other species*	*expression in otic placode stage*	*expression in otic vesicle stage*	*expression during differentiation stage*	*phenotype mutant*	*remarks*
FGF3	*Fgf3* (m,c)	in mice in the developing hindbrain next to the otic placode and vesicle (Wilkinson et al. 1989, McKay et al. 1996, Alvarez et al. 2003)	protein is required for pattern formation in the otic vesicle, is expressed in the adjacent hindbrain in mice (Wilkinson et al. 1989, Pirvola et al. 2000, Pickles et al. 2001) and necesarry for formation of the otic vesicle in chick (Represa et al. 1991, Vendrell et al. 2000)	in the sensory patches of the inner ear (Wilkinson et al. 1989, Mckay et al. 1996)	mutant mice have severe ear malformations; the endolymphatic duct fails to form correctly but the otic vesicles are still formed (Mansour et al. 1993), these results are questioned by Pickles and Chir (2002) because these mice often do not survive, therefore only the survivors, the least affected, are investigated. Knockout mice show no apparent inner ear defects (Alvarez et al. 2003)	growth factor; role is thought to be in chondrogenesis, whereby mesenchymal cells around the vesicle are recruited to form cartilage-producing chondrocytes (Frenz and Liu 1998)
FGF8	*Fgf8* (m,c)	endodermal in chick and mice, necessary and sufficient for Fgf19 expression in chick (Ladher et al. 2005)	low in some cells of the ventromedial region of the otic vesicle in chick (Hidalgo-Sanchez et al. 2000)	in sensory neural region in neonatal mouse cochlea (Pickles 2001)	*Fgf8* and *Fgf3* double knockout mice fail to form otic vesicles and show no expression of early otic placode markers (Maroon et al. 2002)	growth factor
FGF9	*Fgf9* (m)		in specific nonsensory domains of the otic epithelium (Colvin et al. 1999, Pirvola et al. 2004)		mutant mice have hypoplastic vestibular component of the otic capsule, caused by reduced proliferation of the chondrogenic mesenchyme, absence of the epithelial semicircular ducts, malformation of the scala vestibuli caused by defects in the interaction between Reissner´s membrane and the mesenchymal cells (Pivola et al. 2004)	growth factor

FGFR2-IIIb	*Fgfr2-IIIb* (m)		high in the dorsal part of the otic vesicle in mouse (Pirvola et al. 2000)	in the nonsensory epithelium of the otocyst that gives rise to structures such as the endolymhatic and semicircular ducts in mouse (Pirvola et al. 2000)	mouse mutants have severe dysgenesis of the cochleovestibular membranous labyrinth, caused by failure in morphogenesis at the otic vesicle stage (Pirvola et al. 2000, De Moerlooze et al. 2000)	growth factor receptor; with the highest expression in the inner ear, receptor for FGF3 and FGF10 and possibly for FGF19 (reviewed by Pickles and Chir 2002)
GATA3	*Gata3* (m)	in mouse in the whole otic placode and the invaginating otic cup (Lawoko-Kerali et al. 2002)	in mice in the dorsolateral and ventral otic vesicle (Lawoko-Kerali et al. 2002) and the surrounding mesenchyme (Lillevali et al. 2004)	in mouse in the spiral ganglion and the sensory epithelium, progressive decrease in the hair cells as they differentiate, and subsequently decrease in the supporting cells, also in the sensory areas and the surrounding mesenchyme of the vestibule (Lillevali et al. 2004), no expression in the adult sensory epithelium (Rivolta and Holley 1998)	ears of knock-out mice remain cystic with a single extension of the endolymphatic duct, the semicircular canals or saccular and utricular recesses are not formed, there high variability in the degree of ear formation (Karis et al. 2001), heterozygotes show a hearing loss but no outer or middle ear abnormalities, the cochlea shows progressive morphological degeneration starting with the OHCs at the apex, ultimately affecting all hair cells and supporting cells (van der Wees et al. 2004)	zinc finger transcription factor; in humans patients with HDR syndrome suffer from hypothyroidism, deafness and renal dysplasia due to a heterozygous deletion of *GATA3* (van Esch et al. 2000)
GBX2	*Gbx2* (m,c)	in chick in the medial region of the invaginating otic placode (Hidalgo-Sanchez et al. 2000)	in chick in the medial region of the otocyst (Hidalgo-Sanchez et al. 2000)	in chick in the dorsomedial wall in the proximal part of the cochlear duct (Sanchez-Calderon et al. 2002)	a knockout mouse shows absence of the endolyphatic duct and swelling of the membranous labyrinth, absence of the anterior and posterior semicircular canals and a malformed saccule and cochlear duct (Lin et al. 2005)	homeobox transcription factor

human gene	*gene other species*	*expression in otic placode stage*	*expression in otic vesicle stage*	*expression during differentiation stage*	*phenotype mutant*	*remarks*
HMX2	*Hmx2* (m)		in mouse in the dorsolateral wall of the otic vesicle, later in the entire dorsal otic vesicle (reviewed by Wang and Lufkin 2005)	in mouse resticted to the vestibular part of the membranous labyrinth, where only found in the nonsensory epithelium, in the cochlea only in the stria vascularis (Rinkwitz-Brandt et al. 1996)	a knockout mouse shows reduced cell proliferation in epithelial cells, which includes the vestibular sensory patches and semicircular canal fusion plates, as well as in the adjacent mesenchyme, no semicircular canals are formed, significant loss of the three cristae occurs and the macula utriculus and sacculus are fused into one utriculosaccular chamber (Wang et al. 2001)	homeobox transcription factor
HMX3	*Hmx3* (m)	in mouse uniform through the otic placode (Rinkwitz-Brandt et al. 1995)	in mouse first in the anterior and posterior margin, later at the dorsal side (Rinkwitz-Brandt et al. 1995)	in mouse restricted to the vestibular part of the membranous labyrinth, where only in the non-sensory epithelium, in the cochlea only in the stria vascularis (Rinkwitz-Brandt et al. 1996)	a knockout mouse shows depletion of sensory cells in the saccule and utricule and complete loss of horizontal semicircular canal crista, as well as fusion of the utricule and saccule endolymphatic spaces into a common utriculosaccular cavity (Wang et al. 1998)	homeobox transcription factor
IGF-I	*Igf-1* (m)		in the mouse otic vesicle and the cochleovestibular ganglion (Leon et al. 1995)		knockout mice show reduction in size of the cochlea and cochlear ganglion, an immature tectorial membrane and a significant decrease in the number and size of the auditory neurons, delayed maturation and innervation of the organ of Corti (Camarero et al. 2001) an altered myelin sheeth in ganglion cells associated with	growth factor; in humans a homozygous inactivation of IGF-I causes growth failure, sensorineural deafness, and mental retardation (Woods et al. 1996)

					a decrease in number and a general delayed of auditory neurons (Camarero et al. 2002)	
NEUROD	*NeuroD* (m)		in the ventral otic vesicle, the adjacent mesenchyme and the developing auditory ganglion (Lawoko-Kerali et al. 2004)		in null mutant mice migration of both auditory and vestibular neuroblasts is compomised, these mice are profoundly deaf due to a severe loss of inner ear sensory neurons during development (Kim et al. 2001)	basic helix loop helix transcription factor
NGN1	*Ngn1* (m)		in mice in the otocyst and delaminating neurons (Fritzsch 2003)		knockout mice fail to generate the proximal subset of cranial sensory neurons (Ma et al. 1998), neither afferent, efferent nor autonomic nerve fibres are detected in the ears of null mice, these mice also develop smaller sensory epithelia with normal hair cells (Ma et al. 2000)	basic helix loop helix transcription factor
OTX1	*Otx1* (m)		in mouse in the posteroventral quadrant of the lateral part of the otic vesicle (Morsli et al. 1999)	in mouse in the lateral canal and ampulla as well as part of the utricule, in the lateral wall of the cochlea, only in the nonsensory regions of the developing inner ear (Morsli et al. 1999)	an *Otx1* knockout mouse has no lateral semicircular canal, lateral ampulla, utriculosaccular duct and cochleosaccular duct, and a poorly defined proximal part of the cochlea (Morsli et al 1999)	homeobox transcription factor
OTX2	*Otx2* (m)	in mouse in the lateral region of the invaginating otic placode (Hidalgo-Sanchez et al. 2000)	in mouse in the ventrolateral part of the otic vesicle (Morsli et al. 1999)	in mouse in the macula utriculi, the lateral wall of the saccule and Reissner´s membrane of the cochlea (Morsli et al. 1999)	*Otx2* knockout mice are eary embryonic lethal and develop without heads (Acampora et al. 1995), heterozygous mutants display cranofacial malformation known as otocephaly (Hide et al. 2002)	homeobox transcription factor

human gene	*gene other species*	*expression in otic placode stage*	*expression in otic vesicle stage*	*expression during differentiation stage*	*phenotype mutant*	*remarks*
PAX2	*Pax2* (m,c,x)	in chick very early in the development of the otic placode, in the placodal ectoderm and otic placode (Groves and Bronner-Fraser 2000)	in mouse, medial in the otocyst (Lawoko-Kerali et al. 202)	in mouse in all sensory and some nonsensory epithelia, within the sensory epithelia resticted to the hair cells (Lawoko-Kerali et al. 2002), in the cochlea seen in the stria vasularis (Burton et al. 2004)	mouse mutants lack a distinct saccule, and the endolymphatic duct and common crus, cochlear outgrowth in the mutants is arrested at an early stage. Tissue specification in the cochlear duct is affected, particularly in regions between the sensory tissue and the stria vascularis (Burton et al. 2004)	paired box transcription factor; in humans mutations in the *PAX2* gene cause renal coloboma syndrome that is characterized by kidney abnormalities, optic nerve colobomas and mild sensorineural hearing loss (Sanyanusin et al. 1995, Schimmenti et al. 1997)
PAX5	*Pax5* (m,c,x,z)	not in mouse otic system; in xenopus in the otic placode transient and restricted to the invaginating otic vesicle (Heller and Brandli 1999)	in zebrafish in the anterior part of the otic vesicle (Pfeffer et al. 1998)		knockout mice have no ear phenotype but B-cell development is arrested at an early stage and morphogenesis of the posterior midbrain is affected (Urbánek et al. 1994 and Nutt et al. 1997)	paired box transcription factor; deregulation of *PAX5* in humans may contribute to the pathogenesis of Hodgkin's lymphomas (Busslinger et al. 1996)
PAX8	*Pax8* (m,c,x,z)	in the primordium of the otic placode of mouse, zebrafish and xenopus (Pfeffer et al. 1998, Heller and Brandli 1999)	the otic vesicle of mouse but not of zebrafish (Pfeffer et al. 1998), in xenopus in the invaginating otic vesicle (Heller an Brandli 1999)		knockout mice have no ear phenotype (Mansouri et al. 1998)	paired box transcription factor; in humans heterozygosity for *PAX8* is associated with congenital hypothyroidism

					(Macchia et al. 1998)
RALDH2	*Raldh2* (m)	in a V-shaped medio-dorsal region of the otocyst outer epithelium, which evolves as two separate domains upon otic vesicle morphogenesis (Romand et al. 2001)	in the stria vascularis and Reissner´s membrane in the cells that face the perilymph, in the vestibular region in two areas of the utricular epithelium, specific regions of the saccule, the mesenchyme, in epithelial regions adjacent to the cristae ampullaris and in nonsensory membranes (Romand et al. 2001, 2004)		enzyme involved in the generation of retinoic acid
RALDH3	*Raldh3* (m)		in the cochlear region strong in the cochlear nerve and stria vascularis, in the vestibular part restricted to the lateral semicircular canal and the endolymphatic duct, in the baso-lateral region of the crista and the lateral regions of the saccular and utricular sensory epithelia (Romand et al. 2004)		enzyme involved in the generation of retinoic acid
SHH	*Shh* (m)	in the mouse in the lateral wall of the otocyst and in the cells bordering the developing statoacoustic ganglion complex and the periotic mesenchyme (Liu et al. 2002)	in the mouse in the ventromedial aspect of the forming cochlear duct, in the epithelium of the developing utricle, saccule, cochlear duct, semicircular canals, and the vestibular and acoustic ganglia (Liu et al. 2002)	in a knockout mouse ventral otic derivatives including the cochlear duct, semicircular canals and the cochleavestibular ganglion fails to develop (Liu et al. 2002, Riccomagno et al. 2002)	a secreted protein that acts as an inductive signal during development

human gene	*gene other species*	*expression in otic placode stage*	*expression in otic vesicle stage*	*expression during differentiation stage*	*phenotype mutant*	*remarks*
SIX1	*Six1* (m,z)	in the ventral region of the otic pit in mice (Zheng et al. 2003), in zebrafish in the otic placode (Bessarab et al. 2004)	in mice and zebrafish in the middle and ventral region of the otic vesicle within which respectively, the vestibular and auditory epithelia form (Zheng et al. 2003, Ozaki et al. 2004, Bessarab et al. 2004)	in mice and zebrafish in all sensory epithelia of the inner ear (Zheng et al. 2003, Bessarab et al. 2004)	knockout mice display malformations of the outer, middle and inner ear, arrest at the otic vesicle stage, increased cell death and reduced cell proliferation in the otic epithelium, enlarged endolymphatic sac (Zheng et al. 2003, Ozaki et al. 2004)	homeobox transcription factor; *Six1* functions as a key regulator of otic vesicle patterning at early embryogenesis and controls the expression domain of downstream otic genes responsible for inner ear structures (Ozaki et al. 2004). In humans mutations in *SIX1* are associated with BOR and BO syndrome (Ruf et al. 2004)
TBX1	*Tbx1* (m,z)		in mice early in the lateral-ventral wall of the posterior otocyst and the periotic mesenchyme (Vitell et al. 2003) in zebrafish in the otocyst (Piotrowski et al. 2003)	in mice in the otic epithelium where it precisely defines the entire vestibular apparatus and the developing cochlea (Vitelli et al. 2003); in zebrafish in the otic epithelium, in the apical poles of the cells within the sensory patches and semicircular canals (Piotrowski et al. 2003)	mouse knockout has severe abnormalities of the outer, middle, and inner ear, the otocyst is smaller than normal, expands minimally, and does not undergo the morpgogenic changes required to form the cochlea and semicircular canals (Jerome and Papaioannou 2001), loss of function blocks inner ear development at the early otocyststage and after neurogeneis and the cochleovstibular ganglion is abnormally positioned	T-box transcription factor; in humans *TBX-1* is involved in the DiGeorge/ velocardiofacial syndrome (Jerome and Papaioannou 2001)

				(Vitelli et al. 2003) a zebrafish mutant van gogh has a mutation in *Tbx1* and small otic vesicles (Piotrowski et al. 2003)
WNT8c	*Wnt8c* (m,c)	induced by FGF19 in the neural ectoderm; FGF19 and WNT8c synergize to induce the otic placde (Ladher et al. 2000)		

8.2 References

Abdelhak S., Kalatzis V., Heilig R., et al., A human homologue of the Drosophila eyes absent gene underlies branchio-oto-renal (BOR) syndrome and identifies a novel gene family. Nature Genet 1997 15: 157-164.

Acampora D., Mazan S., Lallemand Y., et al., Forebrain and midbrain regions are deleted in Otx2 -/ - mutants due to a defective anterior neuroectoderm specification during gastrulation. Development 1995 121: 3279-3290.

Acampora D., Merlo G.R., Paleari L., et al. Craniofacial, vestibular and bone defects in mice lacking the Distal-lessrelated gene Dlx5. Development 1999 126: 3795-3809.

Alvarez Y., Alonso M.T., Vendrell V., et al., Requirements for FGF3 and FGF10 during inner ear formation. Development 2003 130: 6329-6338

Bessarab D.A., Chong S.-W., and Korzh V., Expression of zebrafish six1 during sensory organ development and myogenesis. Dev Dyn 2004 230: 781–786.

Borsani G., DeGrandi A., Ballabio A., et al., EYA4, a novel vertebrate gene related to Drosophila eyes absent. Hum Mol Genet 1999 8: 11-23.

Brown S.T., Wang J., and Groves A.K., Dlx gene expression during chick inner ear development. J Comp Neur 2005 483: 48–65

Burton Q., Cole L.K., Mulheisen M., et al., The role of Pax2 in mouse inner ear development. Dev Biol 2004 272: 161– 175.

Busslinger M., Klix N., Pfeffer P., et al., Deregulation of PAX-5 by translocation of the Eμ enhancer of the IgH locus adjacent to two alternative PAX-5 promotors in a diffuse large-cell lymphoma. Proc Natl Acad Sci USA 1996 93: 6129–6134.

Camarero G., Avendano C., Fernandez-Moreno C., et al., Delayed inner ear maturation and neuronal loss in postnatal Igf-1-deficient mice. J Neurosci 2001 21: 7630–7641.

Camarero G., Villar M.A., Contreras J., et al., Cochlear abnormalities in insulin-like growth factor-1 mouse mutants. Hear Res 2002 170: 2-11.

Carnicero E., Zelarayan L.C. Rüttiger L., et al., Differential roles of fibroblast growth factor-2 during development and maintenance of auditory sensory epithelia. J Neurosci Res 2004 77: 787-797

Colvin J.S., Feldman B., Nadeau J.H., et al., Genomic organization and embryonic expression of the mouse fibroblast growth factor 9 gene. Dev Dyn 1999 216: 72-88.

Davis R.J., Shen W., Sandler Y.I., et al., Dach1 mutant mice bear no gross abnormalities in eye, limb, and brain development and exhibit postnatal lethality. Mol Cell Biol 2001 21: 1484-1490.

De Moerlooze L., Spencer-Dene B., Revest J.-M., et al., An important role for the IIIb isoform of fibroblast growth factor receptor 2 (FGFR2) in mesenchymal-epithelial signalling during mouse organogenesis. Development 2000 127: 483-492.

Depew M.J., Liu J.K., Long J.E., et al., Dlx5 regulates regional development of the branchial arches and sensory capsules. Development 1999 126: 3831-3846.

Dudley A.T., Lyons K.M. and Robertson E.J., A requirement for bone morphogenetic protein-7 during development of the mouse mammalian kidney and eye. Genes Dev 1995 9: 2795-2807.

Frenz D.A., Liu W., Williams J.D., et al., Induction of chondrogenesis: requirement for synergistic interaction of basic fibroblast growth factor and transforming growth factor-beta. Development 1994 120: 415-24.

Frenz D.A. and Liu W., Role for FGF3 in otic capsule chondrogenesis in vitro: An antisense oligonucleotide approach. Growth Factors 1998 15: 173-182

Fritzsch B., Development of inner ear afferent connections: forming primary neurons and connecting them to the developing sensory epithelia. Brain Research Bulletin 2003 60: 423–433.

Groves A.K. and Bronner-Fraser M., Competence, specification and commitment in otic placode induction. Development 2000 127: 3489-3499

Heanue T.A., Davis R.J., Rowitch D.H., et al., Dach1, a vertebrate homologue of Drosophila dachshund, is expressed in the developing eye and ear of both chick and mouse and is regulated independently of Pax and Eya genes. Mech Dev 2002 111: 75-87.

Heller N. and Bandli A.W., Xenopus Pax-2/5/8 orthologues: Novel insights into Pax gene evolution and identification of Pax-8 as the earliest marker for otic and pronephric cell lineages Dev Genet 1999 24: 208–219.

Hidalgo-Sanchez M., Alvarado-Mallart R., and Alvarez I.S., Pax2, Otx2, Gbx2 and Fgf8 expression in early otic vesicle development. Mech Dev 2000 95: 225-229.

Hide T., HatakeyamaJ., Kimura-Yoshida C., et al., Genetic modifiers of otocephalic phenotypes in Otx2 heterozygous mutant mice. Development 2002 129: 4347-4357.

Jerome L.A. and Papaioannou V.E., DiGeorge syndrome phenotype in mice mutant for the T-box gene, Tbx1. Nat Genet 2001 27: 286-91.

Kalatzis V., Sahly I., El-Amraoui A., et al., Eya1 expression in the developing ear and kidney: towards the understanding of the pathogenesis of Branchio-Oto-Renal (BOR) syndrome. Dev Dyn 1998 213: 486-99.

Karis A., Pata I., van Doorninck J.H., et al., Transcription factor GATA-3 alters pathway selection of olivocochlear neurons and affects morphogenesis of the ear. J Comp Nurol 2001 429: 615–630.

Kim W.Y., Fritzsch B., Serls A., et al., NeuroD-null mice are deaf due to a severe loss of the inner ear sensory neurons during development. Development 2001 128: 417–426.

Kozlowski D.J., Whitfield T.T., Hukriede N.A., et al.,

The zebrafish dog-eared mutation disrupts eya1, a gene required for cell survival and differentiation in the inner ear and lateral line. Dev Biol 2005 277: 27-41.
Ladher R.K., Anakwe K.U., Gurney A.L., et al., Identifcation of synergistic signals initiating inner ear development. Science 2000 290: 1965-1967
Ladher R.K., Wright T.J., Moon A.M., et al., FGF8 initiates inner ear induction in chick and mouse. Genes Dev 2005 19: 603–613
Lawoko-Kerali G., Rivolta M.N., and Holley M., Expression of the transcription factors GATA3 and Pax2 during development of the mammalian inner ear. J Comp Neurol 2002 442: 378–391
Lawoko-Kerali G., Rivolta M.N., Lawlor P., et al., GATA3 and NeuroD distinguish auditory and vestibular neurons during development of the mammalian inner ear. Mech Dev 2004 121: 287–299.
Leon Y., Vazquez E., Sanz C., et al., Insulin-like growth factor-I regulates cell proliferation in the developing ear, activating glycosyl-phosphatidlyinositol hydrolysis and Fos expression. Endocinology 1995 136: 3494-3503.
Leon Y., Sanz C., Giraldez F., et al., Induction of cell growth by insulin and insulin-like growth factor-I is associated with Jun expression in the otic vesicle. J Comp Neurol 1998 398: 323-332.
Lillevali K.,Matilainen T., Karis A., et al., Partially overlapping expression of Gata2 and Gata3 during inner ear development. Dev Dyn 2004 231: 775–781.
Lin Z., Cantos R., Patente M., et al., Gbx2 is required for the morphogenesis of the mouse inner ear: a downstream candidate of hindbrain signaling. Development 2005 132: 2309-2318.
Liu W., Li G., Chien J.S., et al., Sonic hedgehog regulates otic capsule chondrogenesis and inner ear development in the mouse embryo. Dev Biol 2002 248: 240–250.
Liu W., Oh S.A., Kang Y.K., et al., Bone morphogenetic protein 4 (BMP4): A regulator of capsule chondrogenesis in the developing mouse inner ear. Dev Dyn 2003 226: 427–438.
Luo G., Hofmann C., Bronckers A.L.J.J., et al., BMP-7 is an inducer of nephrogenesis, and is also required for eye development and skeletal patterning. Genes Dev 1995 9: 2808-2820.
Ma Q., Chen Z., del Barco Barrantes I., et al., Neurogenin1 is essential for the determination of neuronal precursors for proximal cranial sensory ganglia. Neuron 1998 20: 469-82.
Ma Q., Anderson D.J., and Fritzsch B., Neurogenin 1 null mutant ears develop fewer, morphologically normal hair cells in smaller sensory epithelia devoid of innervation. J Assoc Res Otolaryngol 2000 1: 129-43.
Macchia P.E., Lapi P., Krude H., et al., PAX8 mutations associated with congenital hypothyroidism caused by thyroid dysgenesis. Nature 1998 Genet 19: 83–86.
Mansour S.L., Goddard J.M., and Capecchi M.R., Mice homozygous for a targeted disruption in the proto-oncogene int-2 have developmental defects in the tail and inner ear. Development 1993 117: 13-28
Mansouri A., Chowdhury K., and Gruss P., Follicular cells of the thyroid gland require Pax8 gene function. Nature Genet 1998 19: 87–90.
Maroon H., Walshe J., Mahmood R., et al., Fgf3 and Fgf8 are required together for formation of the otic placode and vesicle. Development 2002 129: 2099-2108
McKay I.J., Lewis J., and Lumsden A., The role of FGF-3 in early inner ear devlopment: An analysis in normal and Kreisler mutant mice. Dev Biol 1996 174: 370-378.
Morsli H., Choo D., Ryan A., et al., Development of the mouse inner ear and origin of its sensory organs. J Neurosci 1998 18: 3327-3335.
Morsli H., Tuorto F., Choo D., et al., Otx1 and Otx2 activities are required for the normal development of the mouse inner ear Development 1999 126: 2335-2343.
Nutt S.L., Urbánek P., Rolink A., et al., Essential functions of Pax5 (BSAP) in pro-B cell development: difference between fetal and adult B lymphopoiesis and reduced V-to-DJ recombination at the IgH locus. Genes Dev 1997 11: 476-491.
Oh S.H., Johnson R., and Wu D.K., Differential expression of bone morphogenetic proteins in the developing vestibular and auditory sensory organs. J Neurosci 1996 16: 6463-6475.
Ohuchi H., Hori Y., Yamasaki M., et al., FGF10 acts as a major ligand for FGF receptor 2 IIIb in mouse multi-organ development. Biochem Biophys Res Commun 2000 277: 643-9.
Ozaki H., Nakamura K., Funahashi J.-I., et al., Six1 controls patterning of the mouse otic vesicle. Development 2004 131: 551-562.
Pfeffer P.L., Gerster T., Lun K., et al., Characterization of three novel members of the zebrafish Pax2/5/8family: dependency of Pax5and Pax8expression on the Pax2.1(noi) function. Development 1998 125: 3063-3074.
Pickles J.O., The expression of fibroblast growth factors and their receptors in the embryonic and neonatal mouse inner ear. Hear Res 2001 155: 54-62
Pickles J.O. and van Heumen W.R., The expression of messenger RNAs coding for growth factors, their receptors, and eph-class receptor tyrosine kinases in normal and ototoxically damaged chick cochleae. Dev Neurosci 1997 19: 476-87.
Pickles J.O. and Chir B., Roles of fibroblast growth factors in the inner ear. Aidiol Neurootol 2002 7: 36-39
Piotrowski T., Ahn D.-G., Schilling T.F., et al., The zebrafish van goghmutation disrupts tbx1, which is involved in the DiGeorge deletion syndrome in

humans. Development 2003 130: 5043-5052.
Pirvola U., Spencer-Dene B., Xing-Qun L., et al., FGF/FGFR-2(IIIb) signaling is essential for inner ear morphogenesis. J Neurosci 2000 20: 6125-34.
Pirvola U., Zhang X., Mantela J., et al., Fgf9 signaling regulates inner ear morphogenesis through epithelial–mesenchymal interactions. Dev Biol 2004 273: 350–360
Represa J., Leon Y., Miner C., et al., The int-2 proto-oncogene is responsible for induction of the inner ear. Nature 1991 353: 561-563
Riccomagno M.M., Martinu L., Mulheisen M., et al., Specification of the mammalian cochlea is dependent on Sonic hedgehog. Genes Dev 2002 16: 2365–2378.
Rinkwitz-Brand S., Justus M., Oldenettel I., et al., Distinct temporal expression of mouse Nkx-5.1 and Nkx-5.2 homeobox genes during brain and ear development. Mech Dev 1995 52: 371-381.
Rinkwitz-Brand S., Arnold H.-H., and Bober E., Regionalized expression of Nkx5-1, Nkx5-2, Pax2 and sek genes during mouse inner ear development. Hear Res 1996 99: 129-138.
Rivolta M.N. and Holley M.C., GATA3 is downregulated during hair cell differentiation in the mouse cochlea. J Neurocytol 1998 27: 637–647.
Robinson G.W. and Mahon K.A., Differential and suggest distinct overlapping expression domains of Dlx-2 and Dlx-3 roles for Distal-less homeobox genes in craniofacial development. Mech Dev 1994 48: 199-215.
Robledo R.F., Rajan L., Li X., et al., The Dlx5 and Dlx6 homeobox genes are essential for craniofacial, axial, and appendicular skeletal development. Genes Dev 2002 16: 1089–1101.
Romand R., Albuisson E., Niederreither K., et al., Specific expression of the retinoic acid-synthesizing enzyme RALDH2 during mouse inner ear development. Mech Dev 2001 106: 185-189.
Romand R., Niederreither K., Abu-Abed S., et al., Complementary expression patterns of retinoid acid-synthesizing and -metabolizing enzymes in pre-natal mouse inner ear structures. Gene Expr Patt 2004 4: 123–133.
Ruf R.G., Xu P.-X., Silvius D., et al., SIX1 mutations cause branchio-oto-renal syndrome by disruption of EYA1–SIX1–DNA complexes. Proc Natl Acad Sci USA 2004 101: 8090–8095
Sahly I., Andermann P., and Petit C., The zebrafish eya1 gene and its expression pattern during embryogenesis. Dev Genes Evol 1999 209: 399-410.
Sanchez-Calderon H., Martin-Partido G., and Hidalgo-Sanchez M., Differential expression of Otx2, Gbx2, Pax2, and Fgf8 in the developing vestibular and auditory sensory organs. Br Res Bull 2002 57: 321–323.
Sanyanusin P., Schimmenti L.A., McNoe L.A., et al., Mutation of the PAX2 gene in a family with optic nerve colobomas, renal anomalies and vesicoureteral reflux. Nat Genet 1995 9: 358– 364.
Sanz C., Leon Y., Canon S., et al., Pattern of expression of the jun family of transcription factors during the early development of the inner ear: implications in apoptosis. J Cell Sci 1999 112: 3967-3974.
Schimmenti L.A., Cunliffe H.E., McNoe L.A., et al., Further delineation of renal-coloboma syndrome in patients with extreme variability of phenotype and identical PAX2 mutations. Am J Hum Genet 1997 60: 869– 878.
Urbánek P., Wang Z.-Q., Fetka I., et al., Complete block of early B cell differentiation and altered patterning of the posterior midbrain in mice lacking Pax5/BSAP. Cell 1994 79: 901-912.
van der Wees J., van Looij M.A.J., de Ruiter M.M., et al., Hearing loss following Gata3 haploinsufficiency is caused by cochlear disorder. Neurobiol Dis 2004 16: 169–178.
Van Esch H., Groenen P., Nesbit M.A., et al., GATA3 haplo-insufficiency causes human HDR syndrome. Nature 2000 406: 419– 422.
Vendrell V., Carnicero E., Giraldez F., et al., Induction of inner ear fate by FGF3. Development 2000 127: 2011-2019.
Vitelli F., Viola A., Morishima M., et al., TBX1 is required for inner ear morphogenesis. Hum Mol Gen 2003 12: 2041–2048.
Wang W. and Lufkin T., Hmx homeobox gene function in inner ear and nervous system cell-type specification and development. Exp Cell Res 2005 306: 373-379.
Wang W., Van De Water T., and Lufkin T., Inner ear and maternal reproductive defects in mice lacking the Hmx3 homeobox gene. Development 1998 125: 621-634.
Wang W., Chan E.K., Baron S., et al., Hmx2 homeobox gene control of murine vestibular morphogenesis. Development 2001 128: 5017-5029.
Wayne S., Robertson N.G., DeClau F., et al., Mutations in the transcriptional activator EYA4 cause late-onset deafness at the DFNA10 locus. Hum Mol Genet 2001 10: 195-200.
Whitfield T.T., Granato M., van Eeden F.J.M., et al., Mutations affecting development of the zebrafish inner ear and lateral line Development 1996 123: 241-254.
Wilkinson D.G., Bhatt S., and McMahon A.P. Expression patterns of the FGF-related proto-oncogene int-2 suggests multiple roles in fetal development. Development 1989 105: 131-136
Woods K.A., Camacho-Hubner C., Savage M.O., et al., Intrauterine growth retardation and postnatal growth failure associated with deletion of the insulin-like growth factor I gene. N Engl J Med 1996 335: 1363–1367.
Wright T.J. and Mansour S.L., Fgf3 and Fgf10 are required for mouse otic placode induction.

Development 2003 130: 3379-3390
Wright T.J., Ladher R., McWhirter J., et al., Mouse FGF15 is the ortholog of human and chick FGF19, but is not uniquely required for otic induction. Dev Biol 2004 269: 264–275
Xu P.X., Adams J., Peters H., et al., Eya1-deficient mice lack ears and kidneys and show abnormal apoptosis of organ primordia. Nat Genet 1999 23: 113-117.
Zheng W., Huang L., Wei Z.-B., et al., The role of Six1 in mammalian auditory system development. Development 2003 130: 3989-4000.

8.3 Appendix 2: Full colour figures

Chapter 4

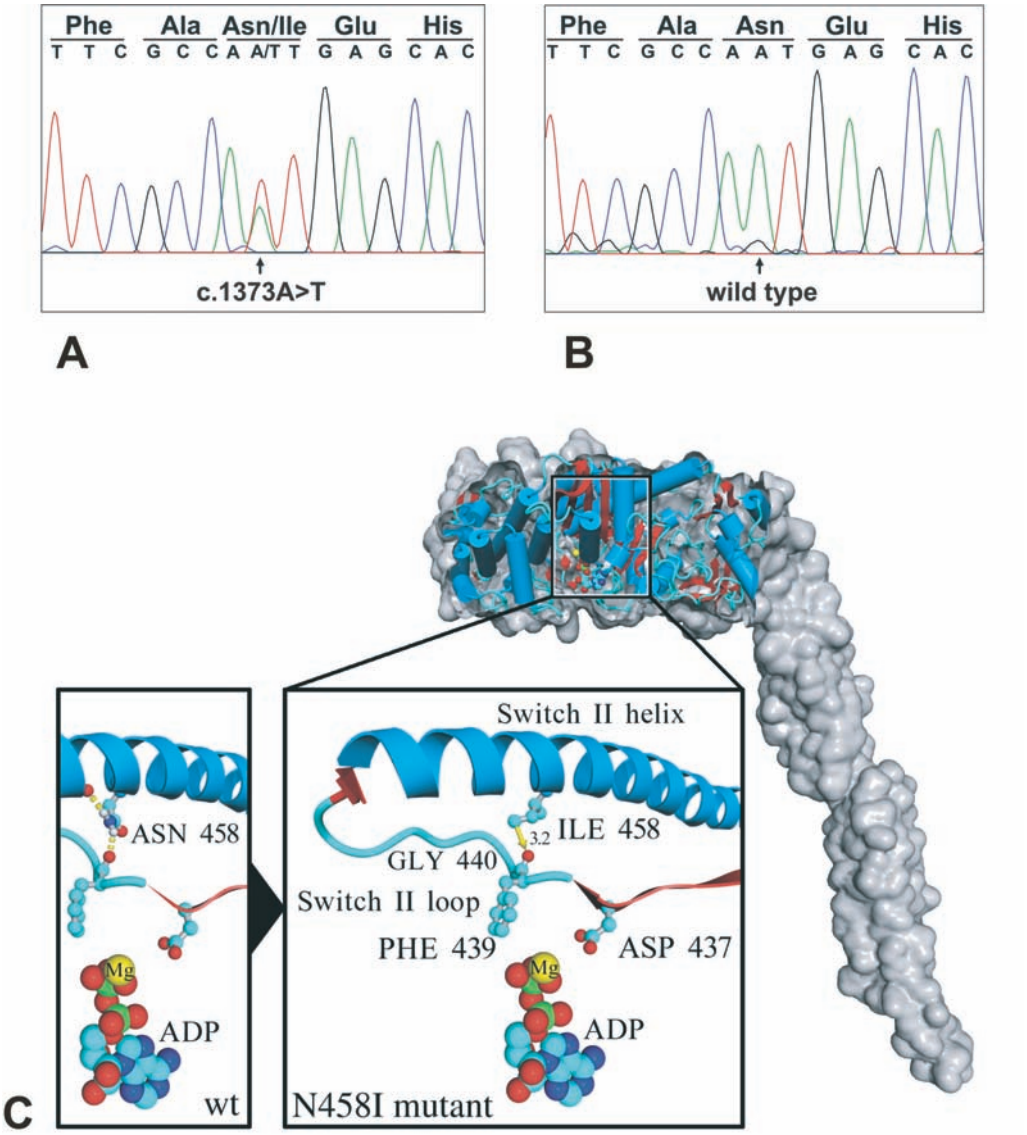

Figure 3. Identification of the Asn458Ile mutation and the predicted functional effect in the myosin VIIA model. (A) Sequence analysis of exon 13 of MYO7A reveals a heterozygous c.1373A>T (Asn458Ile) substitution. (B) Sequence analysis of exon 13 of MYO7A of an unaffected individual. (C) Molecular modelling of myosin VIIA. If isoleucine replaces asparagine at position 458, its larger side-chain collides with the backbone oxygen of phenylalanine 439 in the switch II loop (arrow), pushing the loop towards the ATPase pocket. This is assumed to negatively influence the sensing of the active site state (involving Asp437) and the reorientation in the switch II loop hinge region (Ile438 and Gly440, not shown).

Chapter 5

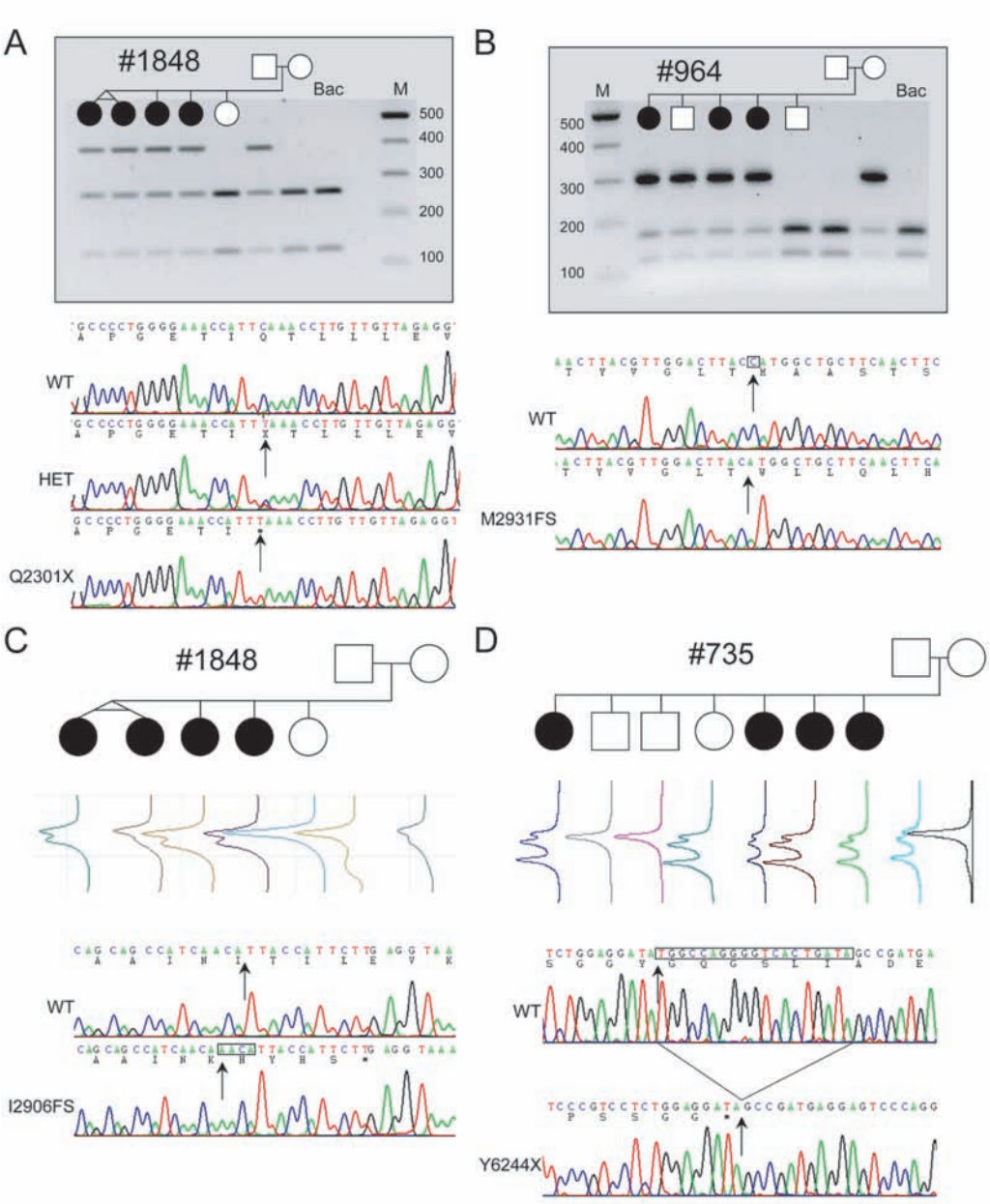

Figure 1. Segregation of *VLGR1* mutations Q2301X, M2931FS, I2906FS, and T6244X in families 735, 964, and 1848 (with USH2C). (A) Paternal inheritance of Q2301X in family 1848 is shown by agarose-gel electrophoresis of exon 31 PCR product *Xmn*I digests. Q2301X mutation is a 6901 C>T transition, 33 bp on the 3' end of the alternate exon 31 splice donor, affecting only the VLGR1b mRNA isoform (fig. 2a). Shown here are sequence electropherograms from the heterozygous family 1848 proband (HET), an apparent Q2301X homozygote, and wild-type (WT) BAC clone RP11-29K14, with sequence and amino acid translation differences (*arrows*).

The Q2301X homozygote was the result of a brother-sister incestuous union, whereas another singleton case was a Q2301X/occult heterozygote (data not shown; table 2). (B) Maternal inheritance of M2931FS in family 964 is shown by agarose-gel electrophoresis of exon 39 PCR product *Nco*I digests. Sequence electropherograms of the WT and the cloned M2931FS allele show 8790delC in exon 39 (*arrows*). This deletion causes a 10-codon frameshift. ending with a TAG stop encoded by the last 3 bases of exon 39, affecting VLGR1b. (C) Maternal inheritance of I2906FS in family 1848 by DHPLC of exon 38 PCR products. Sequence comparison of the cloned I2906FS mutation shows an 8716-17insAACA (*arrows*) causing a frameshift of 5 codons and ending with a TGA stop 1 bp short of the 3_ end of exon 38, affecting VLGR1b. (D) Paternal inheritance of Y6244X detected by DHPLC of exon 89 PCR products. A 19-bp deletion brings a TAG stop codon immediately in-frame. Y6244X removes 63 amino acids from the COOH end of VLGR1a and VLGR1b. The putative maternal and paternal mutations in family 735 and family 964 have not been identified.

Dankwoord

Dankwoord

Eindelijk, mijn proefschrift is klaar. En aan het einde van een proefschrift is er gelukkig ruimte om de mensen te bedanken zonder wie er geen proefschrift was geweest.

Als eerste Frans, jij was het die dit project schreef en mij de kans gaf om in jou groep mijn promotie onderzoek te doen. Ik heb aan jou enorm veel te danken. Ondanks dat er momenten zijn geweest dat ik heb getwijfeld over het slagen van dit project was jij altijd vol vertrouwen. De snelheid waarmee jij altijd mijn manuscripten hebt nagekeken, jou enorme kennis en betrokkenheid bij je personeel zijn uniek. Ik ben dan ook trots dat je naast mijn begeleider ook mijn promotor bent geworden.

Toen ik begon aan mijn promotieonderzoek was ik de enige op ons lab die aan doofheid werkte. Maar nadat jij, Hannie, het doofheidonderzoek ging leiden groeide het “doofheidgroepje” gestaag. Jou inbreng in dit project is ontzettend belangrijk geweest en ook nadat ik uit Nijmegen weg was gegaan was jij het die steeds het contact hebt gehouden en mij hebt gemotiveerd om het allemaal af te maken. Ik weet zeker dat er met jou aan het hoofd van het dffheidonderzoek er nog vele successen in het verschiet liggen.

Han, bedankt dat ook jij me destijds de kans hebt gegeven om binnen de afdeling antropogenetica aan de slag te gaan. Jou aanwijzingen en verbeteringen hebben mijn publicaties zeker verbeterd.

Het al eerder genoemde “doofheidgroepje” wil ik bedanken voor de leerzame werkbesprekingen, de inhoudelijke discussies en de goede samenwerking binnen “ons” groepje.

Graag wil ik iedereen waar ik mee heb samengewerkt op het lab van moleculaire genetica bedanken voor de gezelligheid tijdens lunch en koffie pauzes en de keren dat we gingen eten en dansen in de stad. Maar zeker ook bedankt voor alle hulp en het goede advies dat ik gedurende de tijd op het lab heb gekregen, en niet in de laatste plaats voor al die keren dat ik tegen jullie mocht klagen en zeuren, bedankt voor het aanhoren, zonder jullie was het allemaal een stuk minder leuk geweest. In het bijzonder geldt dit voor mijn kamergenootjes.

Speciaal wil ik Dorien, Gerard en Erwin bedanken voor hun bijdrage aan respectievelijk hoofdstuk twee, drie en vier van dit proefschrift. Zonder jullie had dit proefschrift er heel anders uitgezien. Erwin wil ik natuurlijk in het bijzonder bedanken, omdat hij mijn paranimf wil zijn.

De samenwerking met de afdeling KNO heeft een belangrijke rol gespeeld bij de totstandkoming van dit proefschrift. Ik wil iedereen van de afdeling KNO die heeft bijgedragen aan met name hoofdstuk drie en vier van dit proefschrift bedanken. Dit

proefschrift is mede het resultaat van deze goede samenwerking.

In Nijmegen heb ik niet alleen tijdens werktijd mensen leren kennen die een belangrijke rol hebben gespeeld voor mijn promotie. Ernie bedankt voor de broodnodige ontspanning in de vorm van sport- en eetafspraken, Yvette bedankt voor je hulp in mijn eerste tijd op het lab en de gezelligheid buiten het lab en natuurlijk de meisjes van de Sint Annastraat 26, door jullie was het altijd prettig thuis komen.

Natuurlijk moet ik mijn ouders bedanken die het voor mij mogelijk hebben gemaakt om te gaan studeren en mij altijd hebben gesteund in de keuzes die ik heb gemaakt. Jullie onvoorwaardelijke vertrouwen in een goede afloop is altijd een enorme steun geweest.

Jolanda, je bent niet alleen mijn zus maar ook mijn beste vriendin en bovendien mijn paranimf, bedankt voor alles.

Alle familie, schoonfamilie en vrienden die altijd meegeleefd hebben, bedankt voor jullie interesse en bemoedigende woorden als het even niet zo mee zat.

Als laatste Tanno, zonder jou had ik dit niet kunnen doen. Je was enthousiast en geïnteresseerd als het goed ging, maar ook begripvol en een grote steun als het niet zo goed ging. Bovendien heb je jou stempel op dit proefschrift gedrukt door het tekenen van verschillende figuren en het ontwerpen van de kaft van dit proefschrift. Ik ben blij dat ik jou vrouw ben.

Zonder alle mensen die ik hierboven genoemd heb en nog veel meer mensen die ik niet genoemd heb, was dit proefschrift er nooit gekomen, dus bij deze allemaal bedankt!

List of Publications

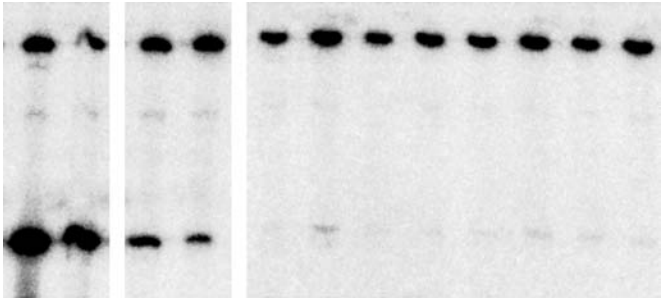

List of publications

Luijendijk M.W.J., Van Wijk E., Bischoff A.M.L.C., Krieger E., Huygen P.L.M., Pennings R.J.E., Brunner H.G., Cremers C.W.R.J., Cremers F.P.M., and Kremer H., Identification and molecular modelling of a mutation in the motor head domain of myosin VIIA in a family with autosomal dominant hearing impairment (DFNA11). Hum Genet 2004 115: 149-56.

Weston M.D., Luijendijk M.W.J., Humphrey K.D., Moller C., Kimberling W.J. Mutations in the VLGR1 gene implicate G-protein signaling in the pathogenesis of Usher syndrome type II. Am J Hum Genet 2004 74: 357-66.

Bischoff A.M.L.C., Luijendijk M.W.J., Huygen P.L.M., van Duijnhoven G., De Leenheer E.M.R., Oudesluijs G.G., Van Laer L., Cremers F.P.M., Cremers C.W.R.J., and Kremer H., A novel mutation identified in the DFNA5 gene in a Dutch family: a clinical and genetic evaluation. Audiol Neurootol 2004 9: 34-46.

Luijendijk M.W.J., van de Pol T.J.R., van Duijnhoven G., den Hollander A.I., ten Caat J., van Limpt V., Brunner H.G., Kremer H., and Cremers F.P.M., Cloning, characterization, and mRNA expression analysis of novel human fetal cochlear cDNAs. Genomics 2003 82: 480-90.

Bom S.J.H., Kemperman M.H., Huygen P.L.M., Luijendijk M.W.J., and Cremers C.W.R.J., Cross-sectional analysis of hearing threshold in relation to age in a large family with cochleovestibular impairment thoroughly genotyped for DFNA9/COCH. Ann Otol Rhinol Laryngol 2003 112: 280-6.

van Wees S.C.M., Luijendijk M.W.J., Smoorenburg I., van Loon L.C., and Pieterse C.M.J., Rhizobacteria-mediated induced systemic resistance (ISR) in Arabidopsis is not associated with a direct effect on expression of known defense-related genes but stimulates the expression of the jasmonate-inducible gene Atvsp upon challenge. Plant Mol Biol 1999 41: 537-49.

Curriculum Vitae

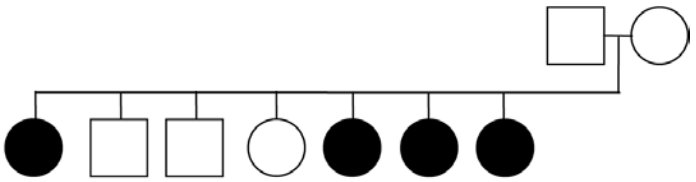

Curriculum vitae

Mirjam Luijendijk werd op 22 mei 1976 geboren te Bleiswijk. In 1994 behaalde zij haar VWO diploma aan het Sint-Laurens College in Rotterdam waarna aansluitend werd begonnen aan een studie biologie aan de Universiteit Utrecht. Tijdens deze studie biologie werden twee afstudeerstages voltooid. De eerste stage werd uitgevoerd bij de projectgroep fytopatholgie aan de Universiteit Utrecht onder begeleiding van Saskia van Wees. Het onderwerp van deze stage was het bestuderen van de expressie van door jasmonzuur gereguleerde genen in *Arabidopsis thaliana* geïnduceerd door biocontrole bacteriën en signaalmoleculen. De tweede stage werd uitgevoerd bij het Unilever Research and Development Laboratorium Colworth in Sharnbrook, Engeland, onder begeleiding van dr. Bill Parish. Het onderwerp van deze stage was bescherming van de humane huid tegen UVA straling. In maart 1999 studeerde zij af aan de Universiteit Utrecht. Op 1 mei 1999 werd begonnen aan een promotie project bij de afdeling antropogenetica, sectie moleculaire genetica van het Universitair Medisch Centrum Sint Radboud te Nijmegen. Het project, kloneren van genen betrokken bij niet-syndromaal gehoorsverlies, werd begeleid door Prof. dr. Frans Cremers en dr. Hannie Kremer. Sinds 1 december 2004 is zij werkzaam voor de afdeling Pathologie aan het Erasmus Medisch Centrum te Rotterdam in de groep van dr. Ellen Zwarthoff.